DOE/ET/27111-1

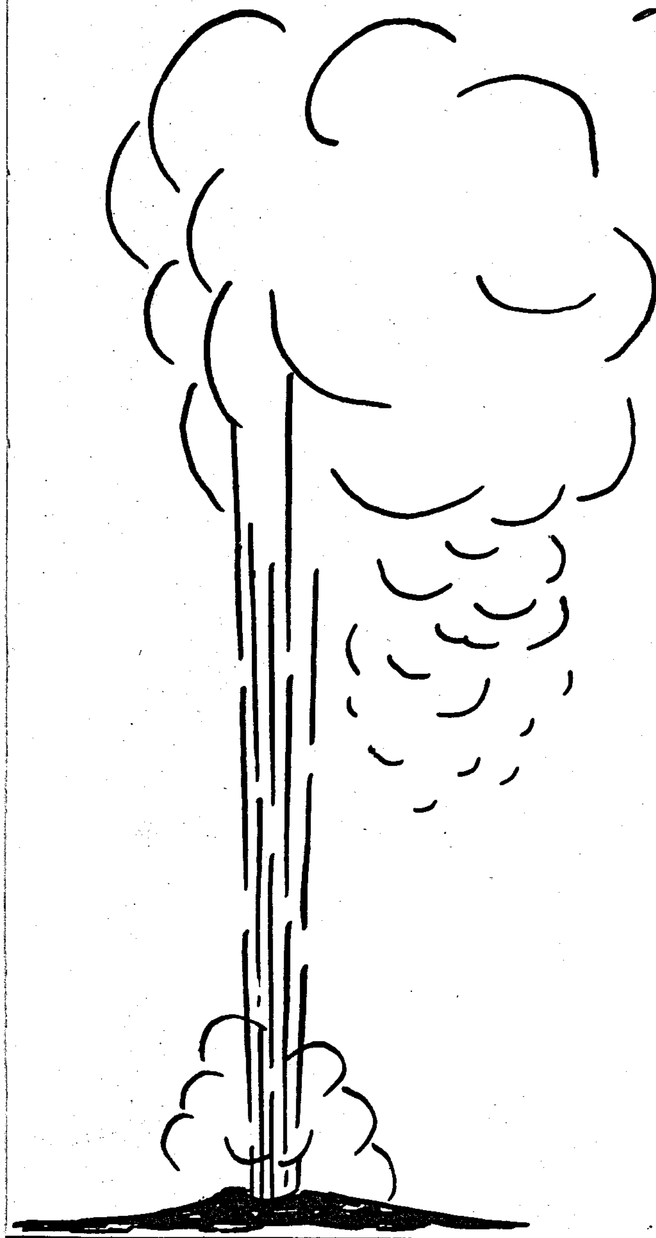

FACTORS CONTROLLING RESERVOIR QUALITY IN TERTIARY SANDSTONES AND THEIR SIGNIFICANCE TO GEOPRESSURED GEOTHERMAL PRODUCTION

Annual Report, May 1, 1979—May 31, 1980

By

R. G. Loucks
D. L. Richmann
K. L. Milliken
M. M. Elliot
J. L. Forman
L. A. Jirik
C. L. McCall
J. R. Suter
L. S. Underwood

July 1980

Work Performed Under Contract No. AC08-79ET27111

Bureau of Economic Geology
The University of Texas
Austin, Texas

U. S. DEPARTMENT OF ENERGY

Geothermal Energy

DISCLAIMER

DISCLAIMER

Available from the National Technical Information Service, U. S. Department of Commerce, Springfield, Virginia 22161.

Price: Printed Copy A09
Microfiche A01

DOE/ET/27111-1

Distribution Category UC-66

FACTORS CONTROLLING RESERVOIR QUALITY IN TERTIARY SANDSTONES AND THEIR SIGNIFICANCE TO GEOPRESSURED GEOTHERMAL PRODUCTION

Annual Report
for the period
May 1, 1979 - May 31, 1980

by

R. G. Loucks, D. L. Richmann, and K. L. Milliken

Assisted by

M. M. Elliot
J. L. Forman
L. A. Jirik
C. L. McCall
J. R. Suter
L. S. Underwood

Prepared for

The Division of Geothermal Energy, U.S. Department of Energy
in partial fulfillment of
Contract No. DE-AC08-79ET27111

July, 1980

Bureau of Economic Geology
The University of Texas at Austin

W. L. Fisher, Director

CONTENTS

Figures

Text figures

Appendix figures

Tables

Text tables

Appendix tables

ABSTRACT

Differing extents of diagenetic modification is the factor primarily responsible for contrasting regional reservoir quality of Tertiary sandstones from the Upper and Lower Texas Gulf Coast. Detailed comparison of Frio sandstones from the Chocolate Bayou/Danbury Dome area, Brazoria County, and Vicksburg sandstones from the McAllen Ranch Field area, Hidalgo County, reveals that extent of diagenetic modification is most strongly influenced by (1) detrital mineralogy and (2) regional geothermal gradients.

Vicksburg sandstones from the McAllen Ranch Field area are less stable, chemically and mechanically, than Frio sandstones from the Chocolate Bayou/Danbury dome area. Vicksburg sandstones are mineralogically immature and contain greater proportions of feldspars and rock fragments than do Frio sandstones. The reactive detrital assemblage of Vicksburg sandstones is highly susceptible to diagenetic modification. Susceptibility is enhanced by higher than normal geothermal gradients in the McAllen Ranch Field area. Thus, consolidation of Vicksburg sandstones began at shallower depth of burial and precipitation of authigenic phases (especially calcite) was more pervasive than in Frio sandstones. Moreover, the late-stage episode of ferroan calcite precipitation that occluded most secondary porosity in Vicksburg sandstones did not occur significantly in Frio sandstones. Therefore, regional reservoir quality of Frio sandstones from Brazoria County is far better than that characterizing Vicksburg sandstones from Hidalgo County, especially at depths suitable for geopressured geothermal energy production.

However, in predicting reservoir quality on a site-specific basis, locally variable factors such as relative proportions of porosity types, pore geometry as related to permeability, and local depositional environment must also be considered. Even in an area of regionally favorable reservoir quality, such local factors can significantly affect reservoir quality and, hence, geothermal production potential of a specific sandstone unit.

INTRODUCTION

Two deep subsurface areas of greatly contrasting reservoir quality were identified by Loucks and others (1979) (fig. 1). Deep Frio sandstones in Brazoria County (Upper Texas Gulf Coast) are characterized by abundant secondary porosity and high permeability. In contrast, Vicksburg sandstones in Hidalgo County (Lower Texas Gulf Coast) are characterized by abundant authigenic calcite at all depths examined and contain only minor secondary porosity. Distribution of sandstone samples from both areas is shown in figure 2. This study identifies the factors responsible for differences in the sequences and intensities of diagenetic events that produced such extreme variations in reservoir quality in these two areas.

A major factor contributing to differences in regional reservoir quality in the two study areas is the difference in detrital mineralogies of the sandstones. The detrital constituents of Vicksburg sandstones in Hidalgo County are chemically and mechanically less stable than those of Frio sandstones in Brazoria County. Superposed upon these contrasting detrital assemblages are differences in regional temperature gradients and depths to the transition from the hydropressured to the geopressured regime. The McAllen Ranch Field area is characterized by a higher geothermal gradient and shallower depth to the top of the geopressured zone than is the Chocolate Bayou/Danbury Dome area. Potential differences in bulk mineralogy of associated shales in the two areas may also influence diagenesis, and hence, reservoir quality.

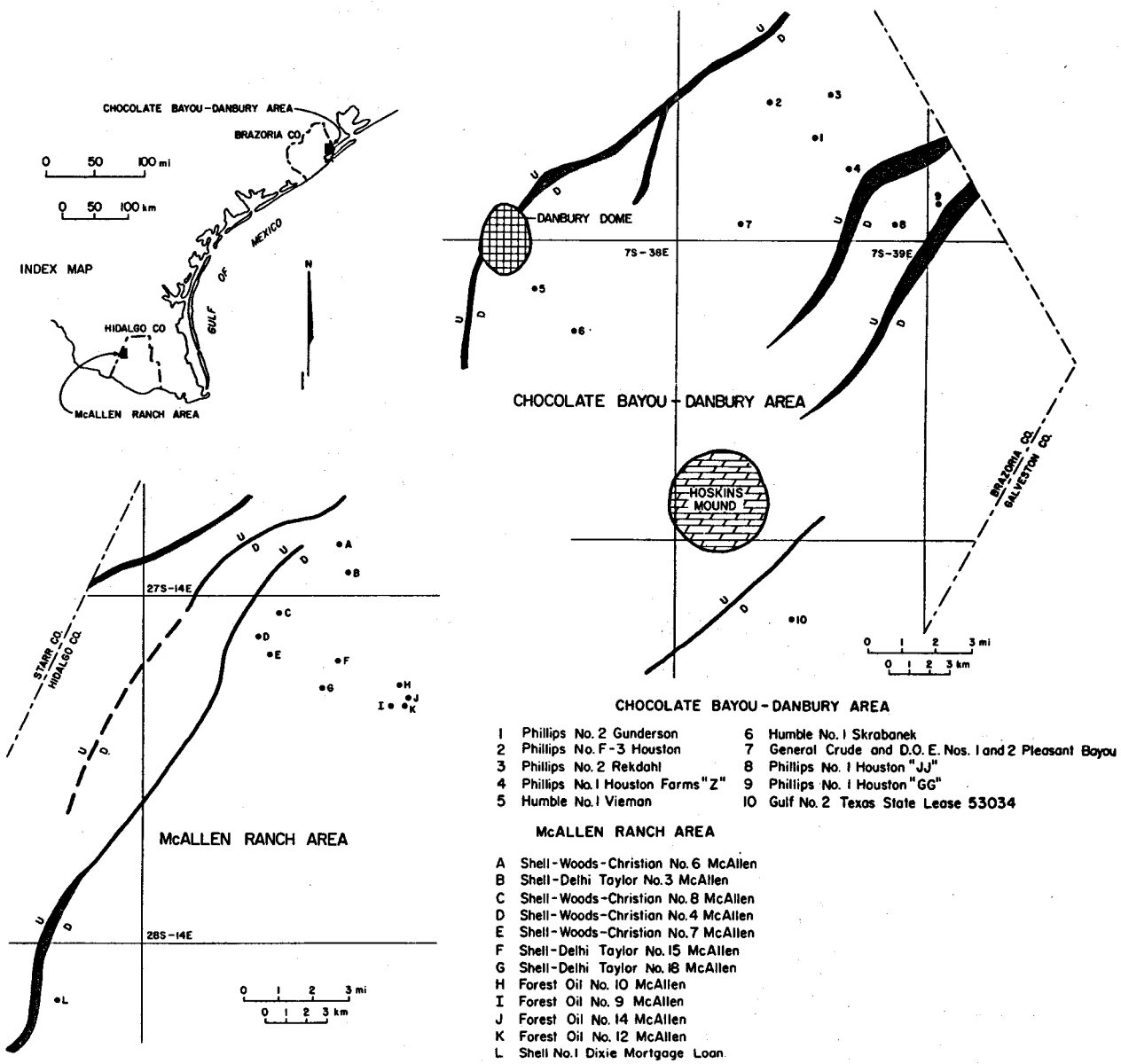

CHOCOLATE BAYOU - DANBURY AREA

1	Phillips No. 2 Gunderson	6	Humble No. 1 Skrabanek
2	Phillips No. F-3 Houston	7	General Crude and D.O.E. Nos. 1 and 2 Pleasant Bayou
3	Phillips No. 2 Rekdahl	8	Phillips No. 1 Houston "JJ"
4	Phillips No. 1 Houston Farms "Z"	9	Phillips No. 1 Houston "GG"
5	Humble No. 1 Vieman	10	Gulf No. 2 Texas State Lease 53034

McALLEN RANCH AREA

A	Shell-Woods-Christian No. 6 McAllen
B	Shell-Delhi Taylor No. 3 McAllen
C	Shell-Woods-Christian No. 8 McAllen
D	Shell-Woods-Christian No. 4 McAllen
E	Shell-Woods-Christian No. 7 McAllen
F	Shell-Delhi Taylor No. 15 McAllen
G	Shell-Delhi Taylor No. 18 McAllen
H	Forest Oil No. 10 McAllen
I	Forest Oil No. 9 McAllen
J	Forest Oil No. 14 McAllen
K	Forest Oil No. 12 McAllen
L	Shell No. 1 Dixie Mortgage Loan

Figure 1. Location of samples used in this study. Map of Chocolate Bayou-Danbury Dome area from Bebout and others (1978). Map of McAllen Ranch area modified from Berg and others (1979).

CORE DISTRIBUTION BY DEPTH AND WELL

((n) indicates number of samples in well)

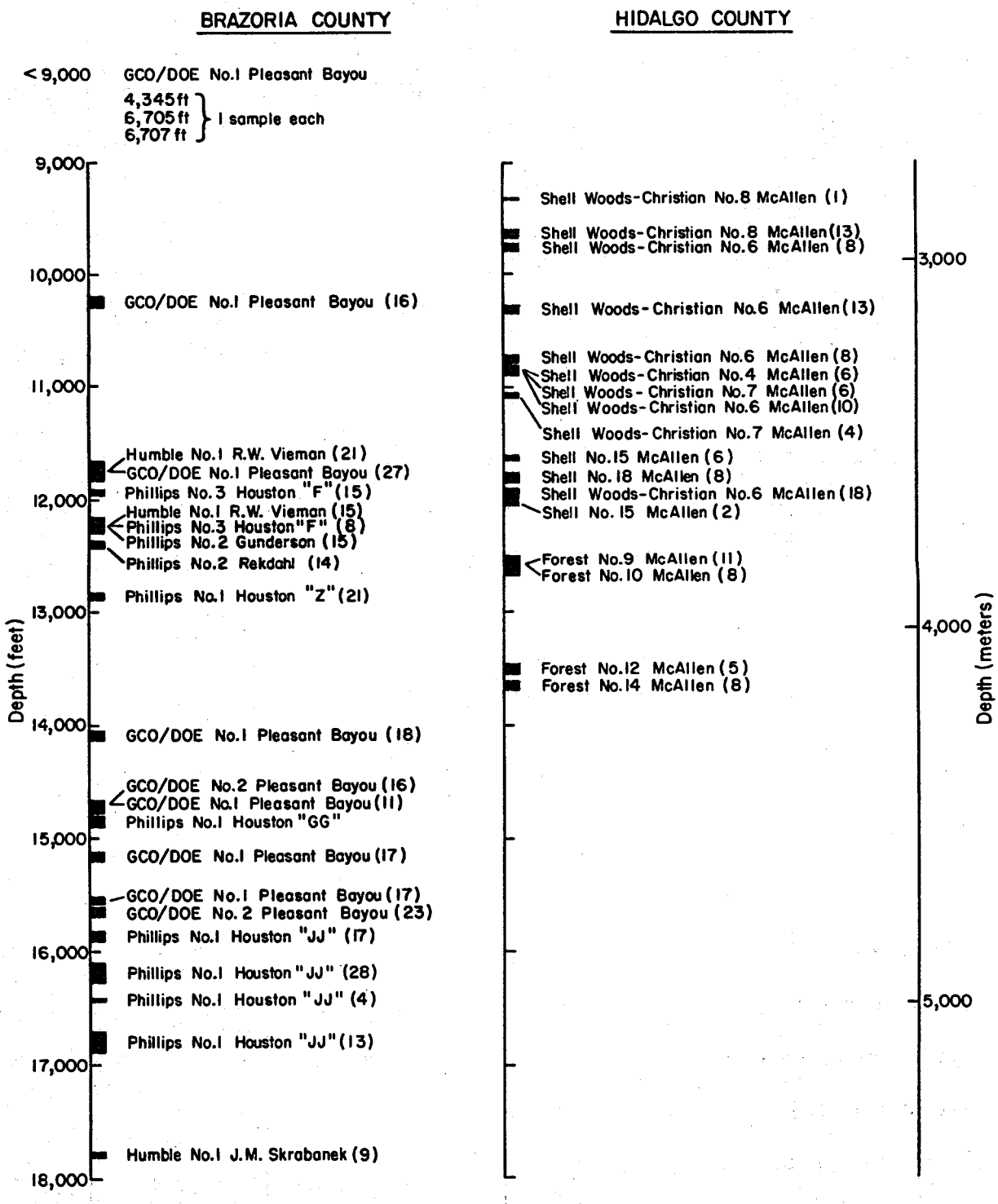

Figure 2. Sample distribution with depth.

OBJECTIVES

The overall goal of this study is to expand our understanding of the occurrence and distribution of deep subsurface geothermal reservoirs. Specific objectives are to:

(1) Determine the origin of porosity, with emphasis on secondary leached porosity.

(2) Define relationships among porosity, permeability, and mineralogy.

(3) Relate effects of concomitant shale diagenesis to cementation and leaching in adjacent sandstones.

(4) Integrate conclusions from objectives 1 through 3 into geothermal resource assessment studies in Texas to aid in identification of areas favorable for geopressured geothermal exploration.

ANALYSIS OF FRIO SANDSTONES, CHOCOLATE BAYOU/DANBURY DOME AREA, BRAZORIA COUNTY

Depositional Systems and Structure

Frio sediments in the Chocolate Bayou/Danbury Dome area were deposited as a series of slightly elongate deltas on the downdip side of a large growth fault in a salt withdrawal basin (Bebout and others, 1978). Major sand depocenters in the upper Frio migrated updip, resulting in mud-dominated distal delta and shelf deposits overlying the older deltaic sandstones. Thus, sandstones are most abundant in the lower part of the section, although overall they are volumetrically minor, relative to the surrounding shales (Bebout and others, 1978).

Sediments of the ancestral Gulf of Mexico Basin were deposited on a trailing plate margin during Tertiary time. The ancestral Gulf of Mexico Basin subsided

rapidly, and uplift was restricted to areas of upward-moving salt domes and ridges. Salt domes, growth faults with offsets ranging from a few feet to over 4,000 ft (1,220 m) (fig. 3), and associated rollover anticlines constitute the major geologic structures. Faulting was contemporaneous with deposition; growth faults formed partly in response to loading of sand units on soft, water-saturated muds (Bruce, 1973). Sands subsided along the faults, resulting in thick sand sections on the downthrown sides. Salt dome growth in the Upper Texas Gulf Coast area was synchronous with deposition of the lower part of the section and with faulting (Bebout and others, 1978).

External Controls on Reservoir Quality

The external parameters that influence regional reservoir quality are fluid pressure gradient and resultant basinal hydrology, geothermal gradient, and pore fluid chemistry.

Fluid Pressure Gradient

The influence of pressure on diagenesis is related to the concept of geopressure. Pore fluids in the Gulf Coast are divided into two hydrologic regimes, hydropressured and geopressured. In the hydropressured zone, the pressure gradient is 0.465 psi/ft (normal hydrostatic) and rocks are under lithostatic pressure of approximately 1.0 psi/ft. In the "soft" geopressured zone (pressure gradient 0.465 to 0.7 psi/ft) the pore fluid supports part of the overburden load. Thus, the effective pressure on the rocks is less than the lithostatic pressure. At a pressure gradient of 0.7 psi/ft, the zone of "hard" geopressure is encountered. The 0.7 psi/ft value was chosen to define the top of the "hard" geopressured regime because it is at this value that resistivities increase dramatically. Thus, this zone can easily be picked from electric logs. In the Chocolate Bayou/Danbury Dome area the top of the "hard" geopressured zone occurs between 8,000 and 12,000 ft (2,440 and 3,660 m).

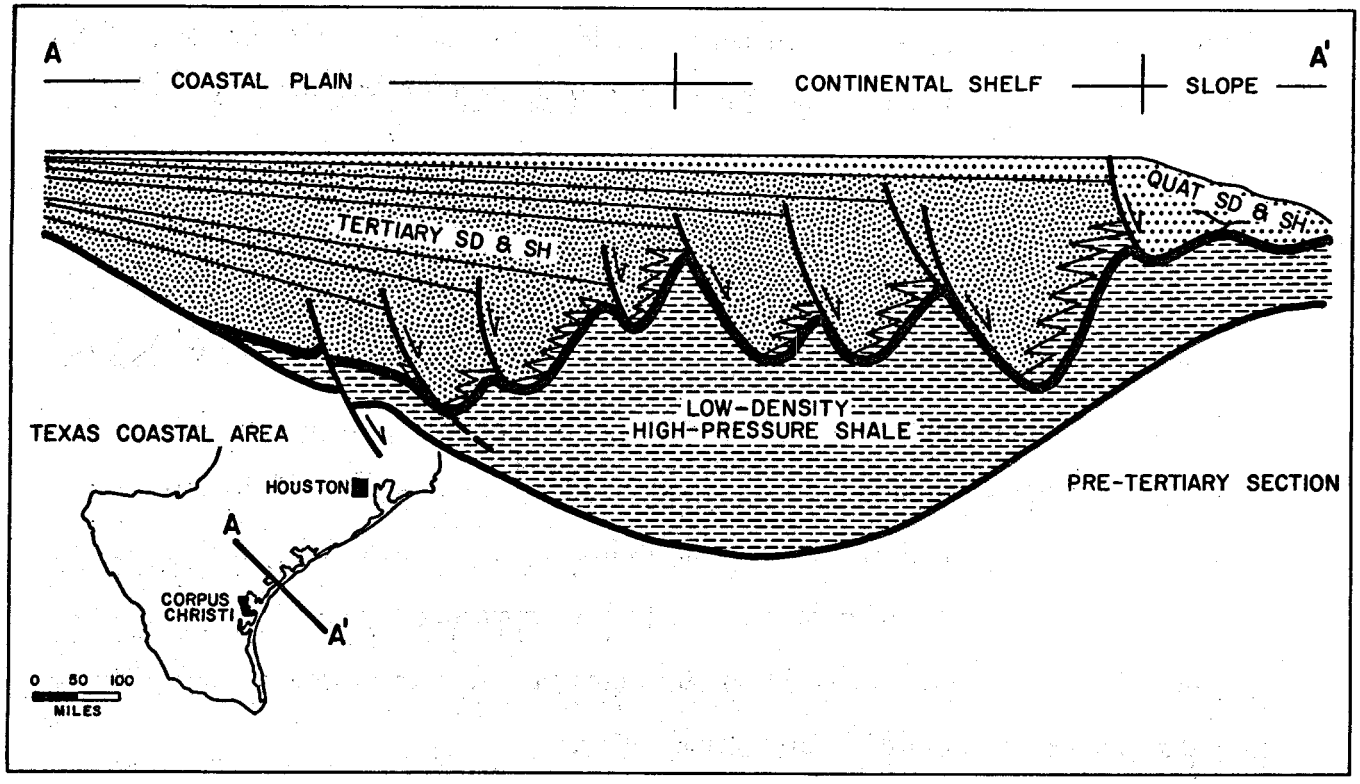

Figure 3. Depositional style of Tertiary strata along the Texas Gulf Coast. (From Bruce, 1973.)

Geopressuring effects may influence the fluid flow system. As the near-surface sediments compact, water is squeezed from the muds and sands and will ordinarily migrate updip out of the system. However, if the migration path is blocked, fluid escape is impeded. Over long periods of time, however, fluid will migrate from the geopressured zone to lower pressured areas because no sedimentary rock is totally impervious. Also, fluids may flow out of the geopressured zone along faults (Jones, 1975). The faults may be areas of persistent local leakage or they may periodically expel fluids as pressure builds up. In the Gulf Coast area, geopressuring can occur within a few thousand feet of the surface (Schmidt, 1973; Magara, 1975). Once geopressured, sediments tend to remain so throughout their burial history (Bonham, 1980).

Fluids flow most readily through permeable units to areas of lower pressure, which are generally shallower in the section. Therefore, the distribution of sands and sandstones defines the major fluid flow path in the section. However, fluids also flow through shales but at diminished rates due to low permeabilities (10^{-6} mD; figs. 9 and 10 in Magara, 1978). Significant volumes of fluid may migrate through shales, given geologically significant periods. Also, if shales are hydrofractured at depth, fluids may flow through them more easily (Sharp, 1980).

Thermal Gradient

The temperature gradient for Brazoria County is not constant with depth (fig. 4). Changes in the gradient are related to the top of geopressure and possibly to lithologic discontinuities (Lewis and Rose, 1970). Heat flow within a finite area can be considered constant and is defined as,

$$Q = (K_h/Z)A\,\Delta T,$$

where: K_h = thermal conductivity,

A = cross-sectional area perpendicular to heat flow, and

ΔT = temperature change across thickness Z.

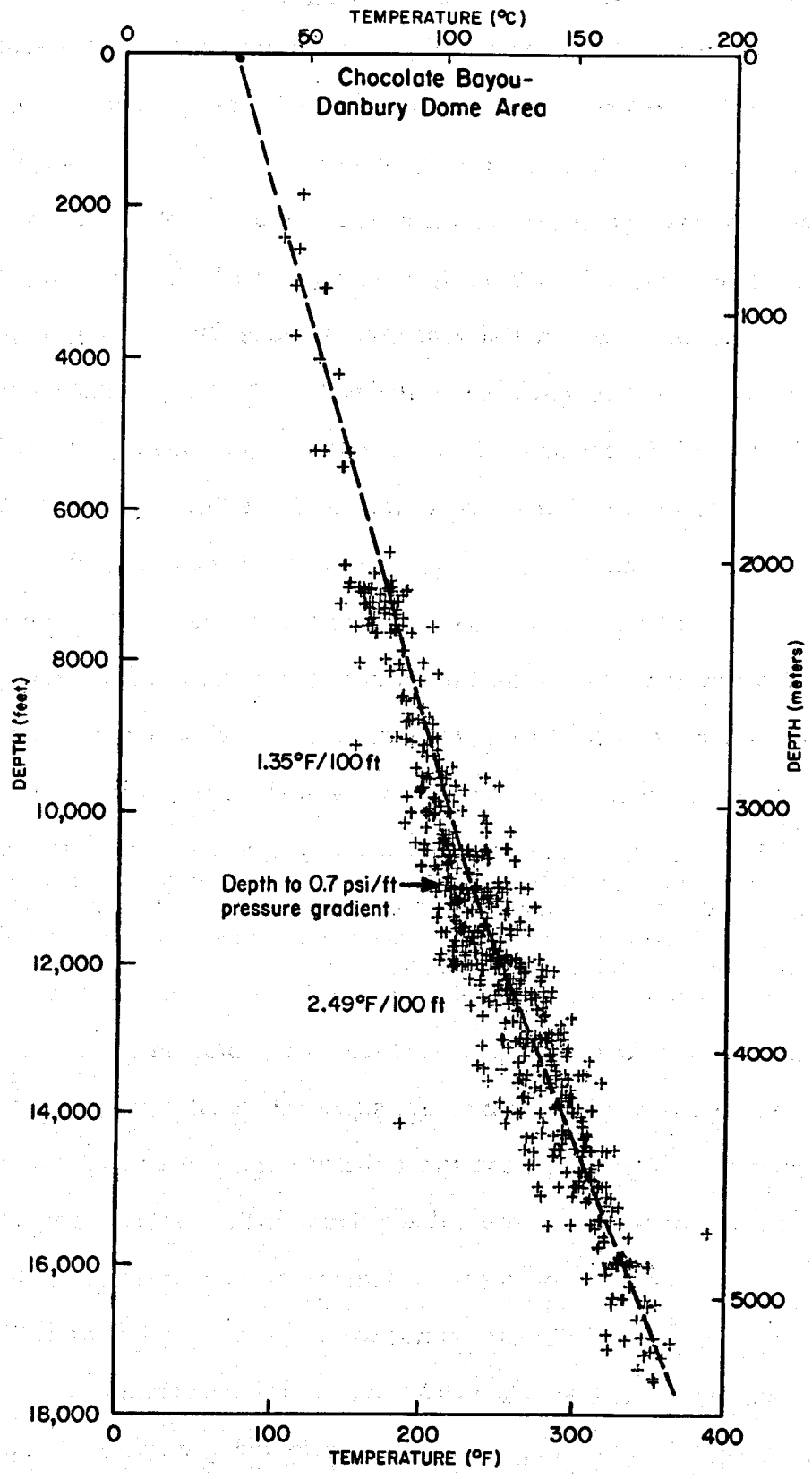

Figure 4. Temperature versus depth, Brazoria County, Texas.

From this relationship it is apparent that K_h and ΔT are inversely related, that is, if K_h decreases, ΔT must increase proportionally to maintain constant Q. Within the geopressured zone, rocks are under less than lithostatic pressure, and unless totally cemented, are more porous (undercompacted) than equivalent rocks in the hydropressured section. Because they are more porous, geopressured units contain more water with a thermal conductivity that is only about one-third that of the average sedimentary rock. Therefore, within the geopressured zone, thermal conductivity is lower than in the hydropressured zone, so the thermal gradient (ΔT) must increase to keep heat flow constant. The temperature gradient plot for the Chocolate Bayou/ Danbury Dome area shows a break in slope at the top of the "hard" geopressured zone (0.7 psi/ft). Above "hard" geopressure, the geothermal gradient is 1.35°F/100 ft, and it increases to 2.49°F/100 ft within the "hard" geopressured regime. This temperature gradient inflection also coincides with the lithologic boundary between Oligocene sands and overlying Miocene shales.

Pore Fluid Chemistry

Controls on pore fluid chemistry in Brazoria County are not well understood. Kharaka and others (1977b, 1980) believe that waters contained in Gulf Coast Tertiary sediments represent connate waters trapped by rapid subsidence. Subsidence in the Gulf Coast, especially immediately after deposition, was rapid. In addition, the low-lying coastal topography of the region generally precludes significant meteoric recharge. Thus, a connate-water hypothesis for these rocks is plausible. In any case, the pore waters of the sand-bearing intervals of the study area were highly modified after burial by reaction with the enclosing sediments at temperatures up to 180°C (360°F) and possibly by filtering through micropore systems in shales, as outlined for other basins by Graf and others (1965) and Hitchon and Friedman (1969).

Several investigators have compared salinities in the geopressured and hydropressured zones. Most have reported that salinities decrease below the top of

geopressure (Dickey and others, 1972; Schmidt, 1973). Gregory and Backus (1980) report from well log data that salinities in Brazoria County initially decrease below the top of geopressure and then become erratic, the values in the deeper waters being both above and below salinities in the hydropressured zone (fig. 5). Kharaka and others (1980) report from analyses of waters in Chocolate Bayou Field that salinities increase in the geopressured zone.

Detrital Mineralogy and Texture

Three hundred fifty-four Frio thin sections from Brazoria County, Texas, were point counted (200 points per section) to determine detrital and authigenic compositions of the sandstones. Of the total thin sections, 145 are samples from the two Pleasant Bayou geothermal test wells. Data from these samples are included in the Brazoria County data base from which generalizations regarding Frio sandstones were drawn. However, the Pleasant Bayou test well sites were selected based on their particularly favorable geothermal potential. Therefore, certain physical characteristics of samples from these wells are predictably atypical. A later section will address significant differences in Pleasant Bayou samples relative to typical Frio sandstones from Brazoria County.

Samples selected for petrographic study are typically medium to very fine grained, moderately to well-sorted sandstones. Minor lithologies include muddy, very fine grained sandstones and siltstones. Although the detrital mineralogy is quite simple (most framework grains are either quartz, plagioclase, or volcanic rock fragments) the relative proportions of these constituents, especially quartz, vary widely. Sandstones are classified according to Folk (1974) (fig. 6). Most sandstones are lithic arkoses and feldspathic litharenites; however, a significant number contain sufficient quartz to be subarkoses and sublitharenites (fig. 7). Detailed descriptions of the various detrital constituents follow.

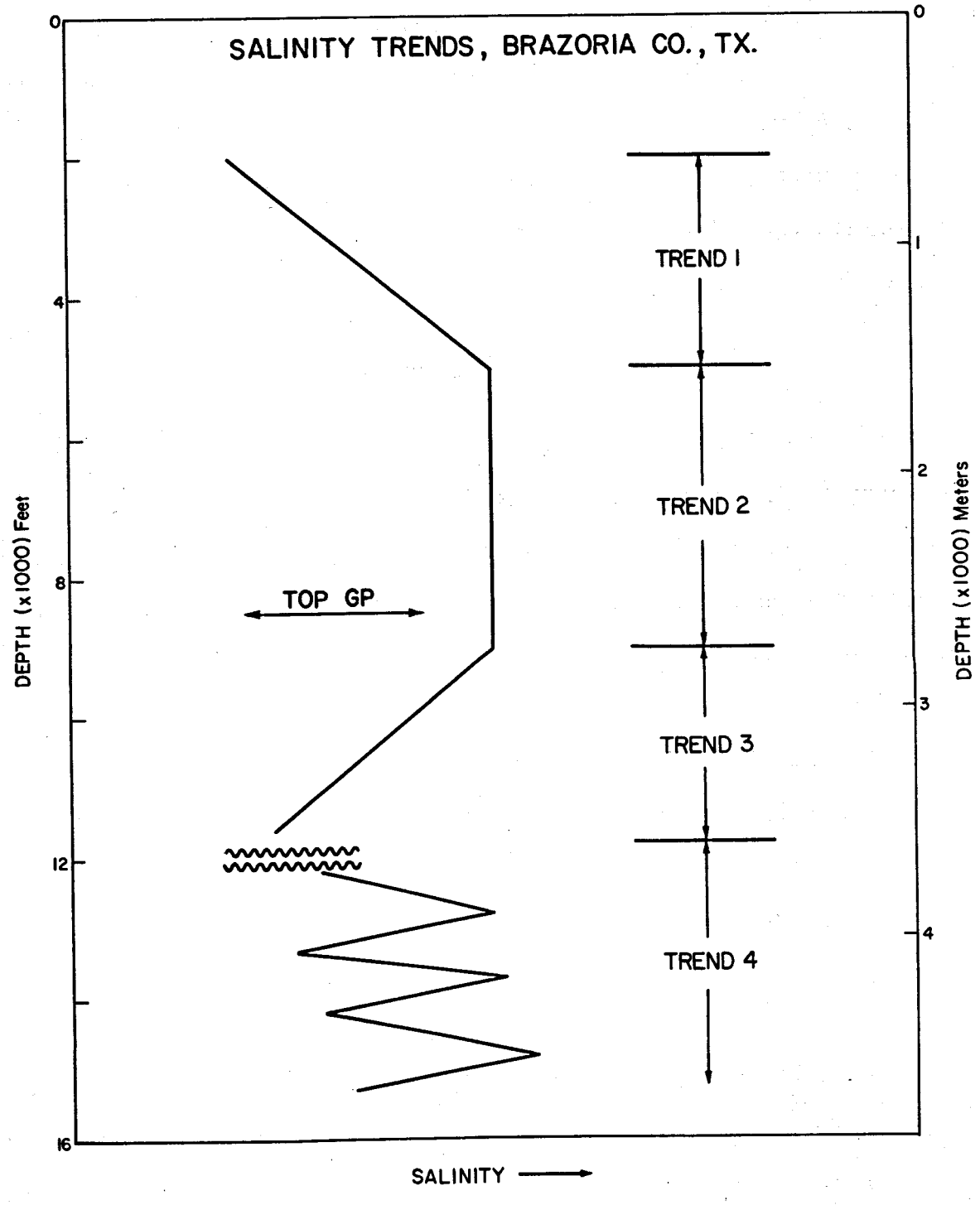

Figure 5. Generalized salinity trends, Brazoria County, Texas. (From Gregory and Backus, 1980.)

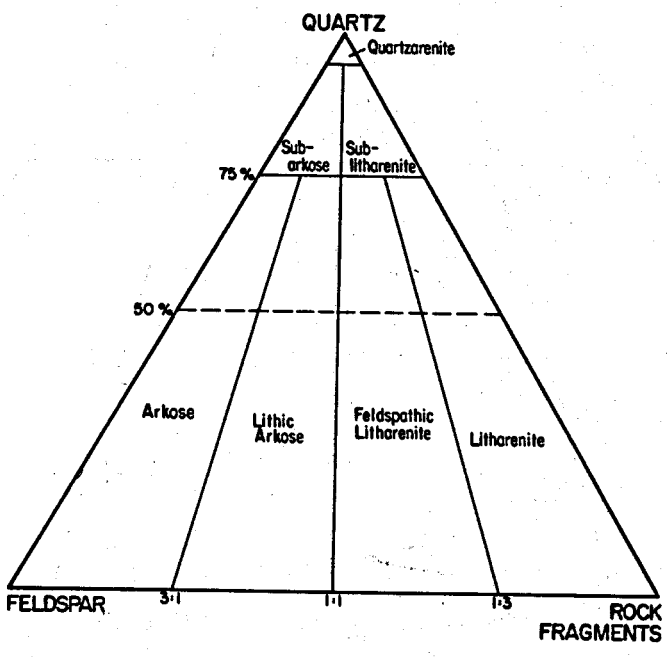

Figure 6. Sandstone classification of Folk (1974).

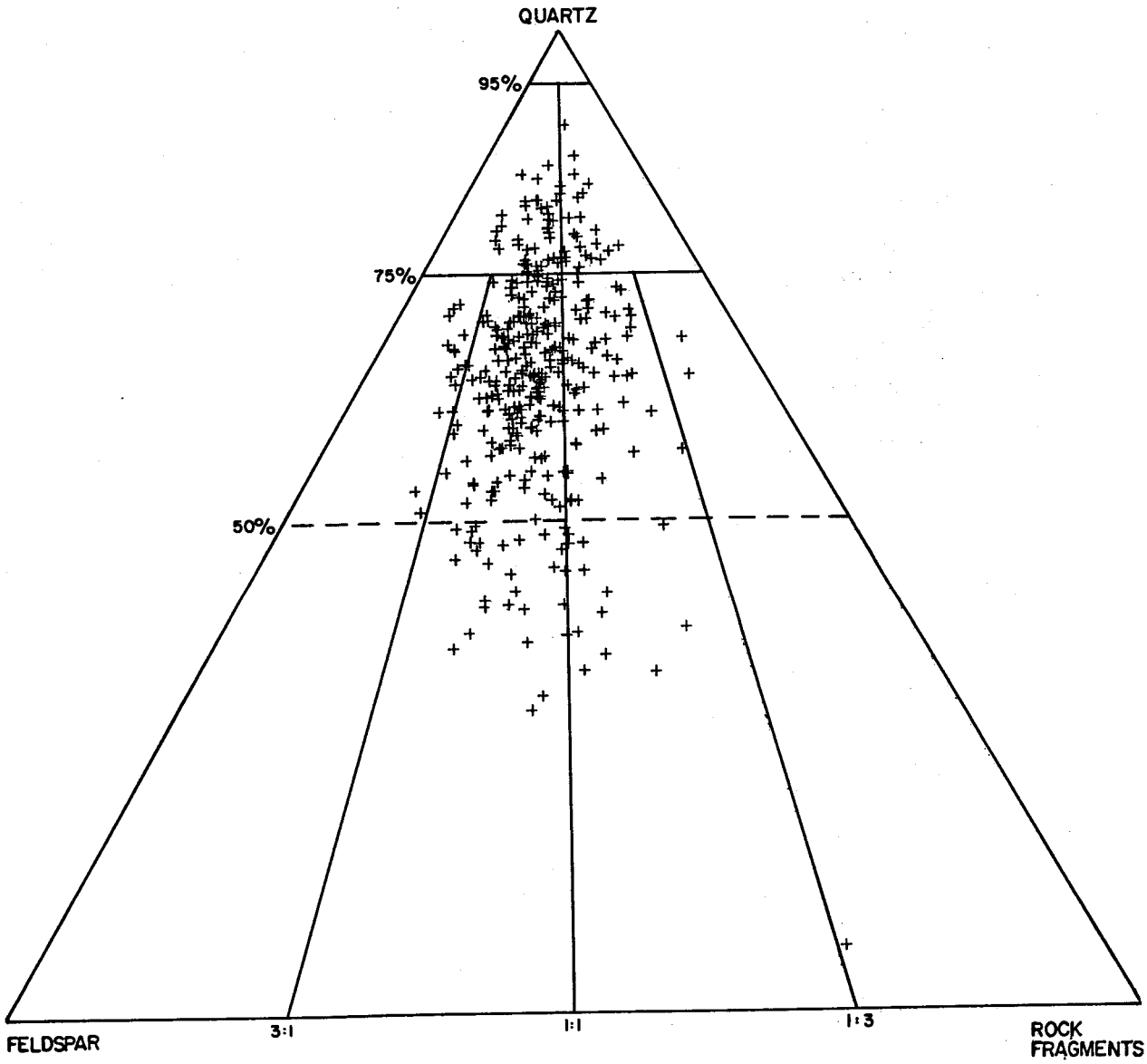

Figure 7. Primary detrital mineralogy, Chocolate Bayou-Danbury Dome area.

Quartz

Volcanic, metamorphic, reworked sedimentary, and "common" quartz are all present in Frio sandstones. "Common" (unstrained) quartz is by far the most important volumetrically. Unfortunately, this variety has no unique genetic association. Volcanic quartz, with straight extinction and well developed crystal faces, occurs in minor amounts and was most likely derived from volcanic terrain in West Texas. Stretched metamorphic quartz grains and reworked sedimentary quartz, identified by transported overgrowths, are also present in minor quantities; the source of these grains is unclear.

Feldspar

Plagioclase is the dominant feldspar variety. Most grains are untwinned and show varying degrees and types of alteration, including vacuolization, sericitization, replacement by calcite or kaolinite, and leaching. Amaranth stain, used to aid in plagioclase identification (Laniz and others, 1964), does not react well with the typical plagioclase of these samples, which indicates low calcium content. Electron microprobe analysis of a number of detrital plagioclase grains from Pleasant Bayou samples (Appendix D) confirms that they are albite. However, polysynthetic twinning is rarely absent in primary albite. It seems reasonable to assume that the plagioclase originally had an intermediate composition that was modified subsequently through extensive albitization. Boles (1979) suggests that such albitization in Frio sandstones may occur over the temperature range of 100° to 120°C (212° to 250°F). This corresponds to burial depth of approximately 10,000 to 12,000 ft (3,050 to 3,660 m) in the Pleasant Bayou/Danbury Dome area.

Minor quantities of detrital potassium feldspar are present in Frio sandstones. Many grains are microcline, characterized by grid twinning and a relatively fresh appearance compared to detrital plagioclase. Other grains exhibit textures suggestive of albitization (fig. 8). Both plagioclase and potassium feldspar are susceptible to

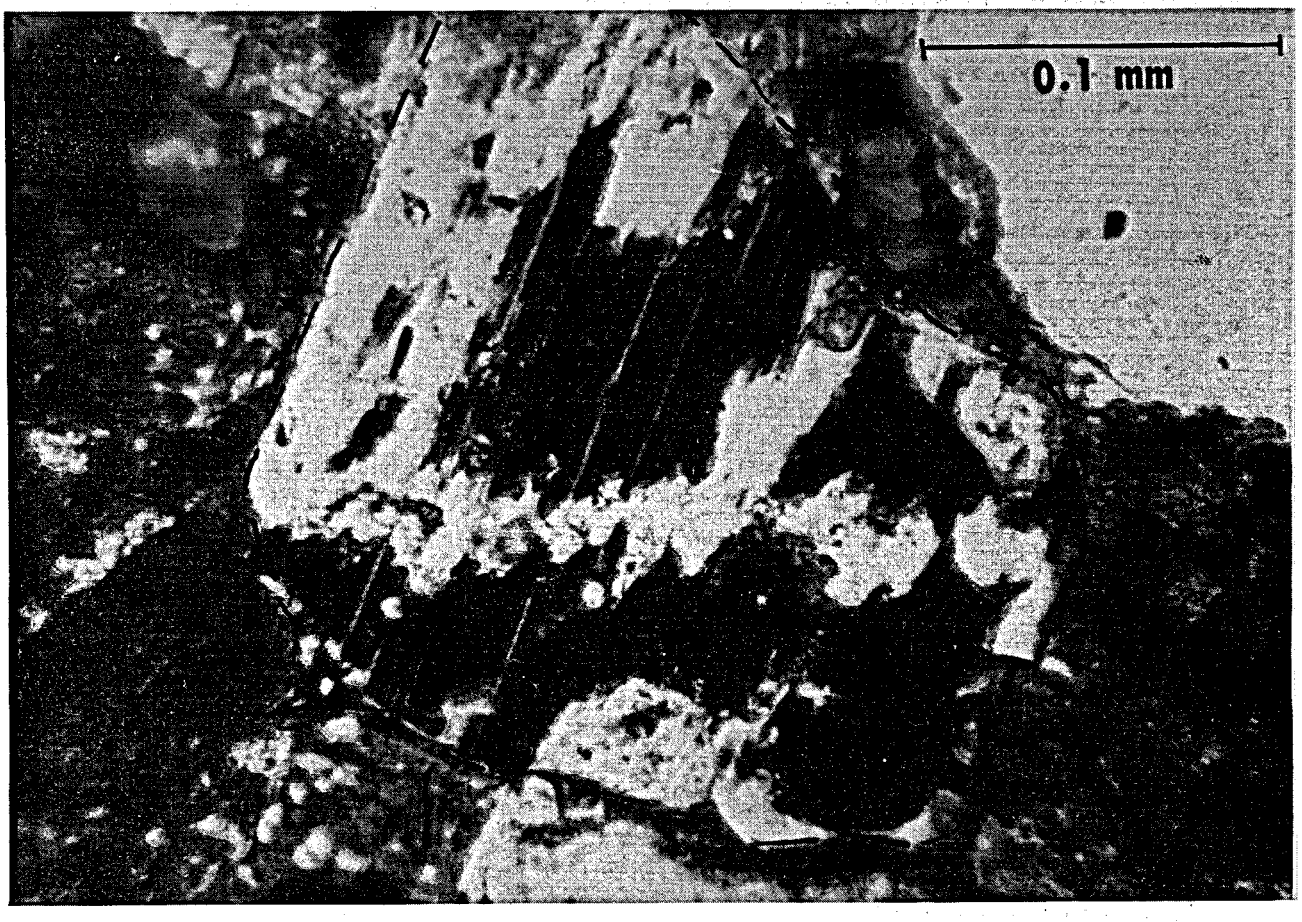

Figure 8. Chessboard twinning resulting from albitization of potassium feldspar (outlined). Crossed polars.

leaching and abundant leached grains contribute substantially to secondary porosity (fig. 9). Whether this intragranular porosity results directly from leaching of feldspars or from dissolution of grain-replacement carbonate is unknown, as is the relative importance of these mechanisms.

Rock Fragments

Volcanic rock fragments (VRF's) are the dominant variety (fig. 10). Compositionally, they reflect a felsic to intermediate volcanic source; VRF's are primarily rhyolites and trachytes (Lindquist, 1977). Some fragments exhibit distinctive igneous features such as easily recognizable plagioclase phenocrysts, while others have altered to clays to such an extent as to be almost unidentifiable. Still other VRF's have altered to microcrystalline quartz. In those fragments where relict phenocrysts are identifiable, a volcanic source can be assigned with certainty (fig. 11). However, many clasts are virtually identical to chert fragments eroded from carbonate source rocks. We infer a volcanic source for these silicified fragments.

Sedimentary mudstone and shale clasts occur less commonly than VRF's in Frio sandstones. However, these argillaceous rock fragments, along with clay-altered VRF's, are significant because during compaction they can be extensively deformed to form "pseudomatrix" (fig. 12) (Dickinson, 1970). Pseudomatrix, where abundant, is an important inhibitor of permeability, and thus interferes with the normal diagenetic sequence. Other sedimentary rock fragment types, low-grade metamorphic and plutonic rock fragments, are encountered only rarely.

Miscellaneous Framework Grains

Glauconite, micas, heavy minerals, shell fragments, and organics are present in trace quantities. Of the heavy minerals, zircon is dominant.

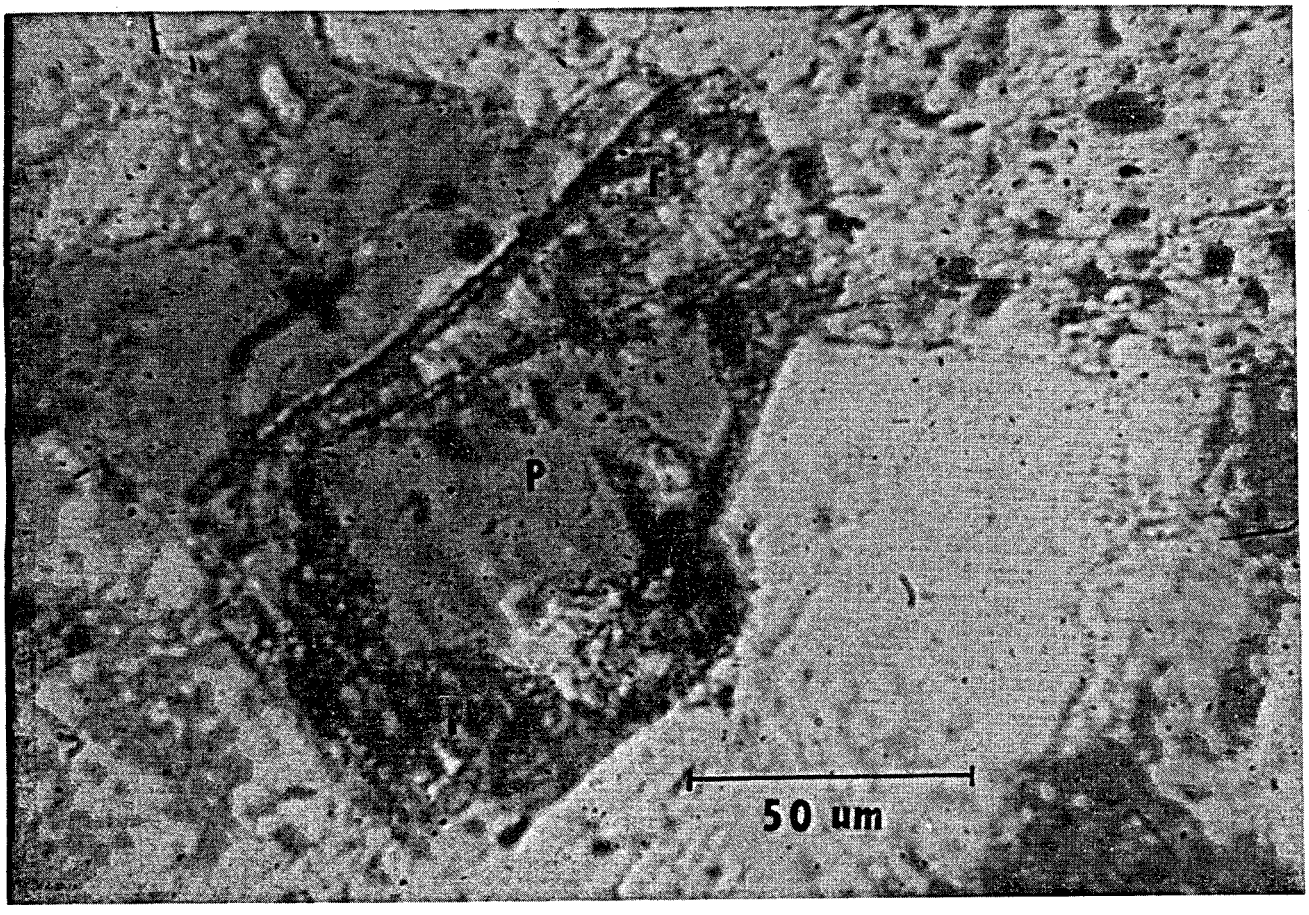

Figure 9. Secondary porosity (P) within leached feldspar (F). Plane polarized light.

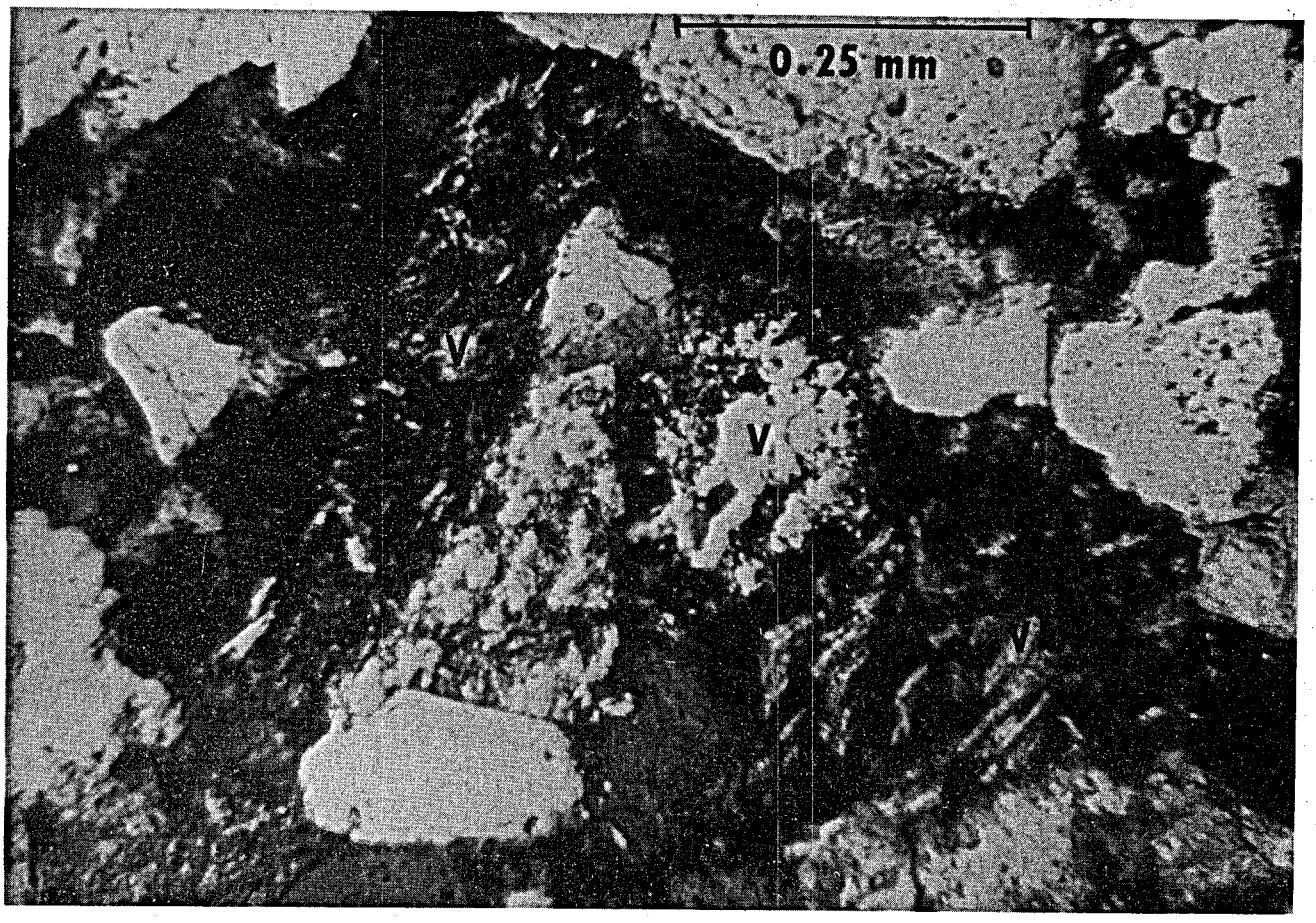

Figure 10. Volcanic rock fragments (V) of several types. Crossed polars.

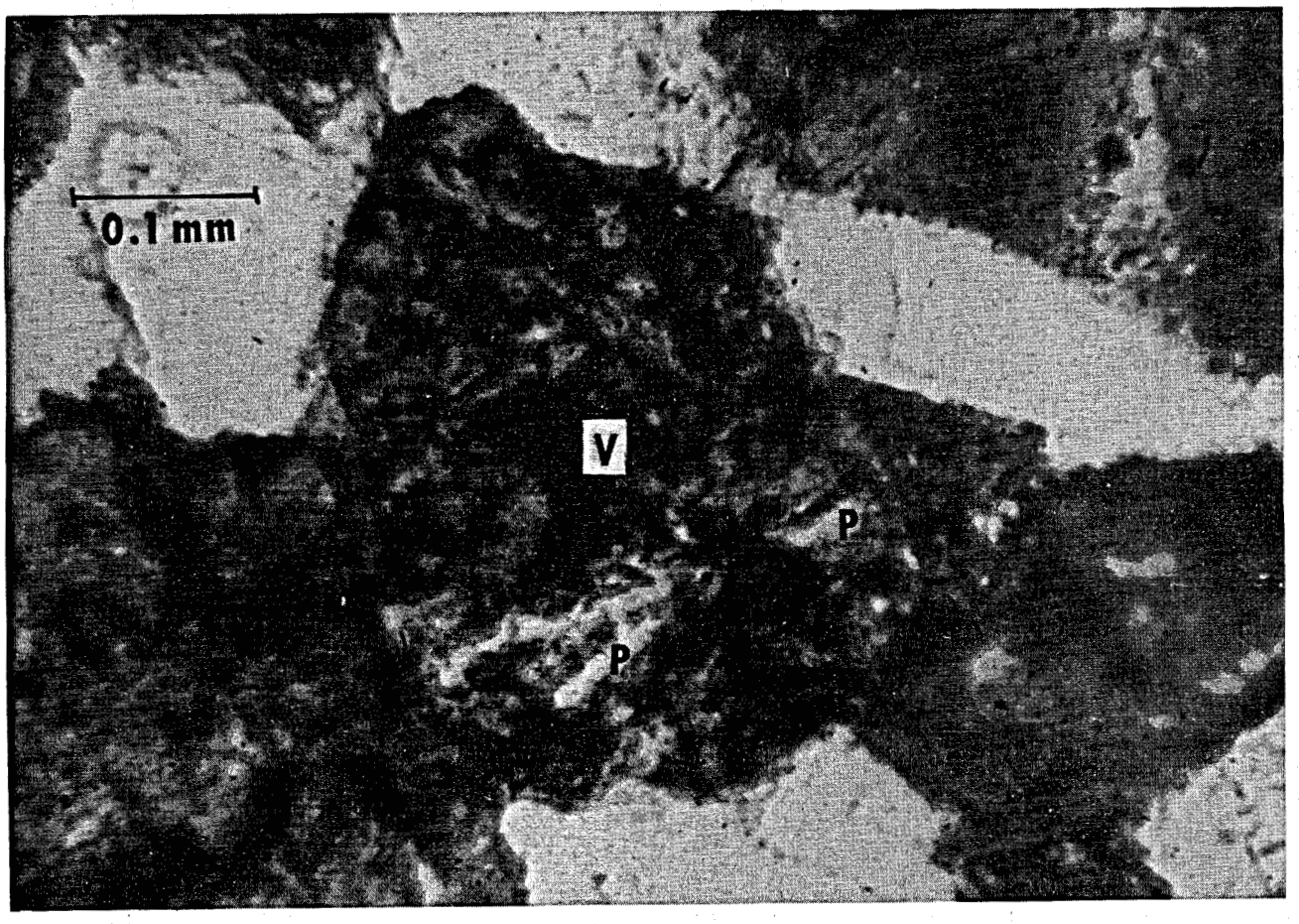

Figure 11. Silicified volcanic rock fragment containing relict phenocrysts. Crossed polars.

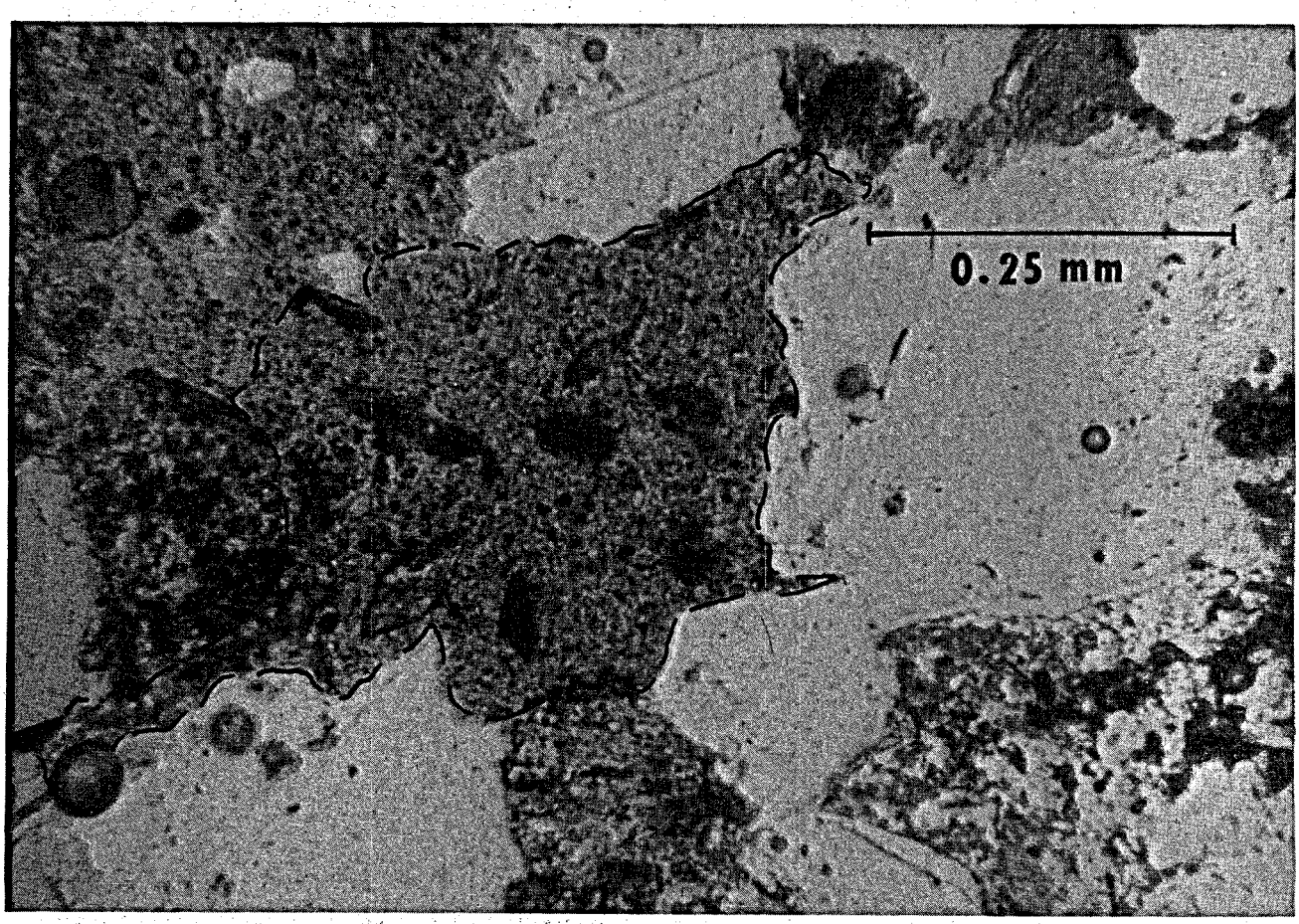

Figure 12. Mudstone clast (outlined) deformed by compaction to make pseudomatrix. Plane polarized light.

Matrix

Depositional matrix is common in Frio sandstones (fig. 13). This detrital material, finer than 20 μm, is composed largely of clays that obstruct permeability. As in rocks containing abundant pseudomatrix, diagenesis in matrix-rich rocks is severely restricted. Figure 14 shows the relative proportions of secondary porosity, cements, and matrix in Frio samples from Brazoria County. The two areas of highest data concentration are at the matrix apex and on the line connecting the cement and secondary porosity apices. Thus, while matrix tends to inhibit both cementation and development of secondary porosity, cements and secondary porosity are not mutually exclusive and commonly occur together. Many of the data points on the interior of the triangle may represent samples containing abundant argillaceous rock fragments. When intensely deformed to form pseudomatrix, these grains often become indistinguishable from true depositional matrix and may have been misinterpreted in the point counts. In addition to the more commonly observed clay matrix, some samples contain a "cherty matrix" believed to be composed of diagenetically modified detrital material and authigenic quartz (fig. 15). A similar material was described by Dapples (1972), who also interpreted it as a highly altered and recrystallized depositional matrix.

Diagenetic Modification

Diagenesis includes precipitation of cements, chemical alteration of existing minerals, and dissolution of existing grains.

Authigenic minerals

Major authigenic phases identified in Frio samples from Brazoria County include multiple varieties of carbonate, quartz, and kaolinite. Minor phases are feldspars, chlorite, zeolite, and unidentified authigenic clays as rims and coats on detrital grains.

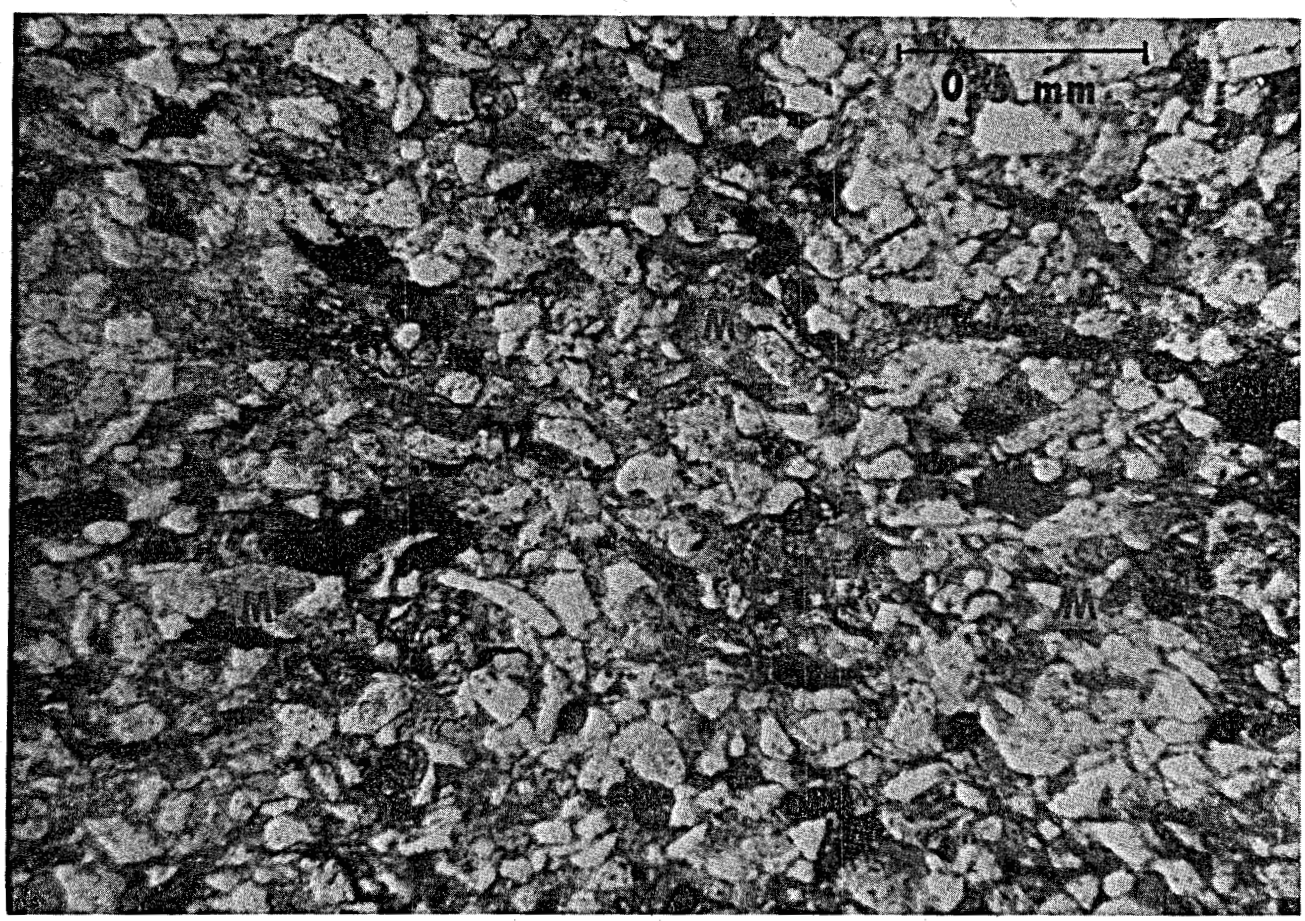

Figure 13. Matrix-rich sandstone (M = matrix). Plane polarized light.

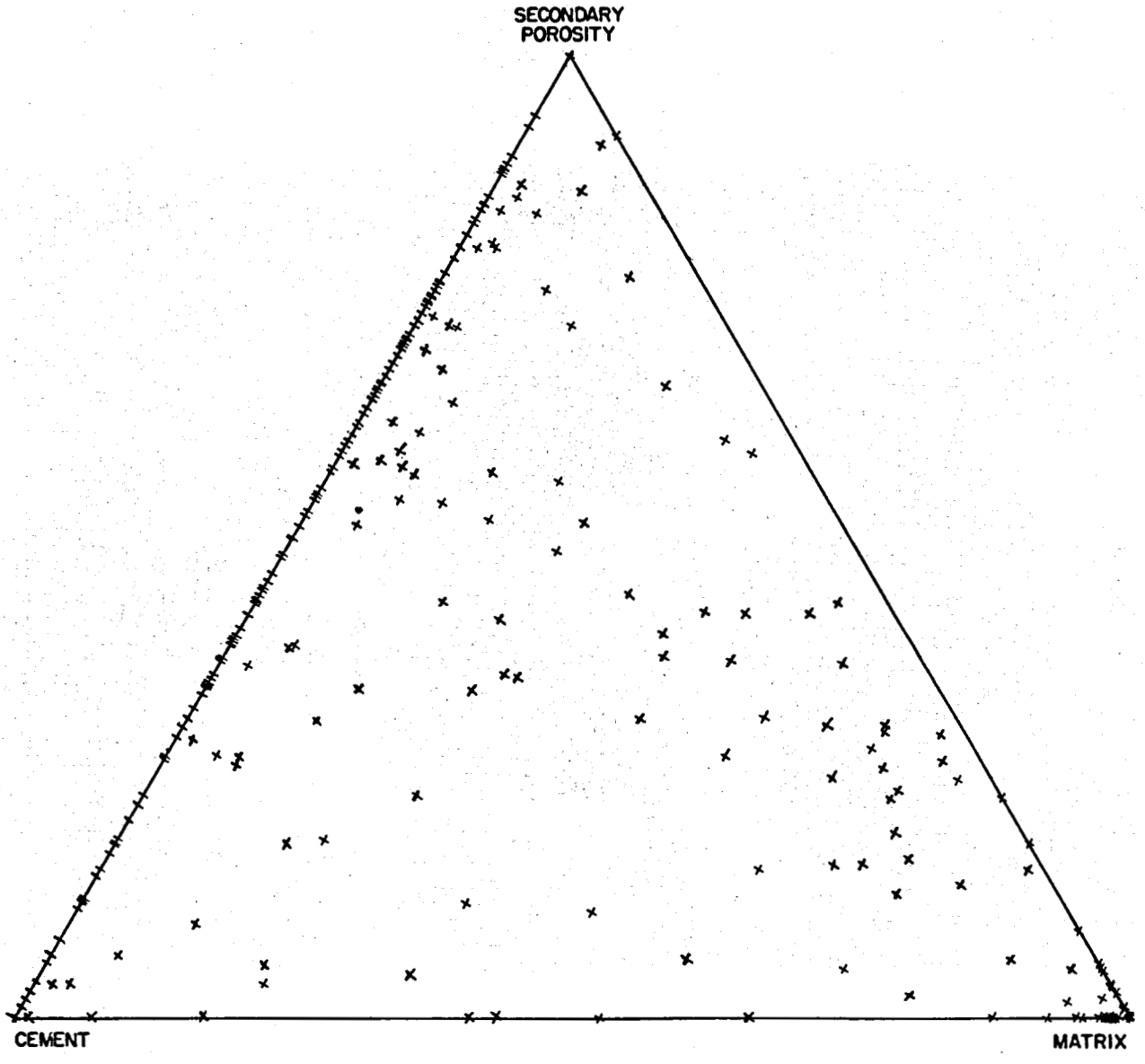

Figure 14. Cement-matrix - secondary porosity triangle. Note: concentrations of data points along the cement-secondary porosity join near the matrix apex. This distribution suggests that while cement and secondary porosity are not mutually exclusive, samples containing abundant matrix exhibit neither abundant cement nor secondary porosity.

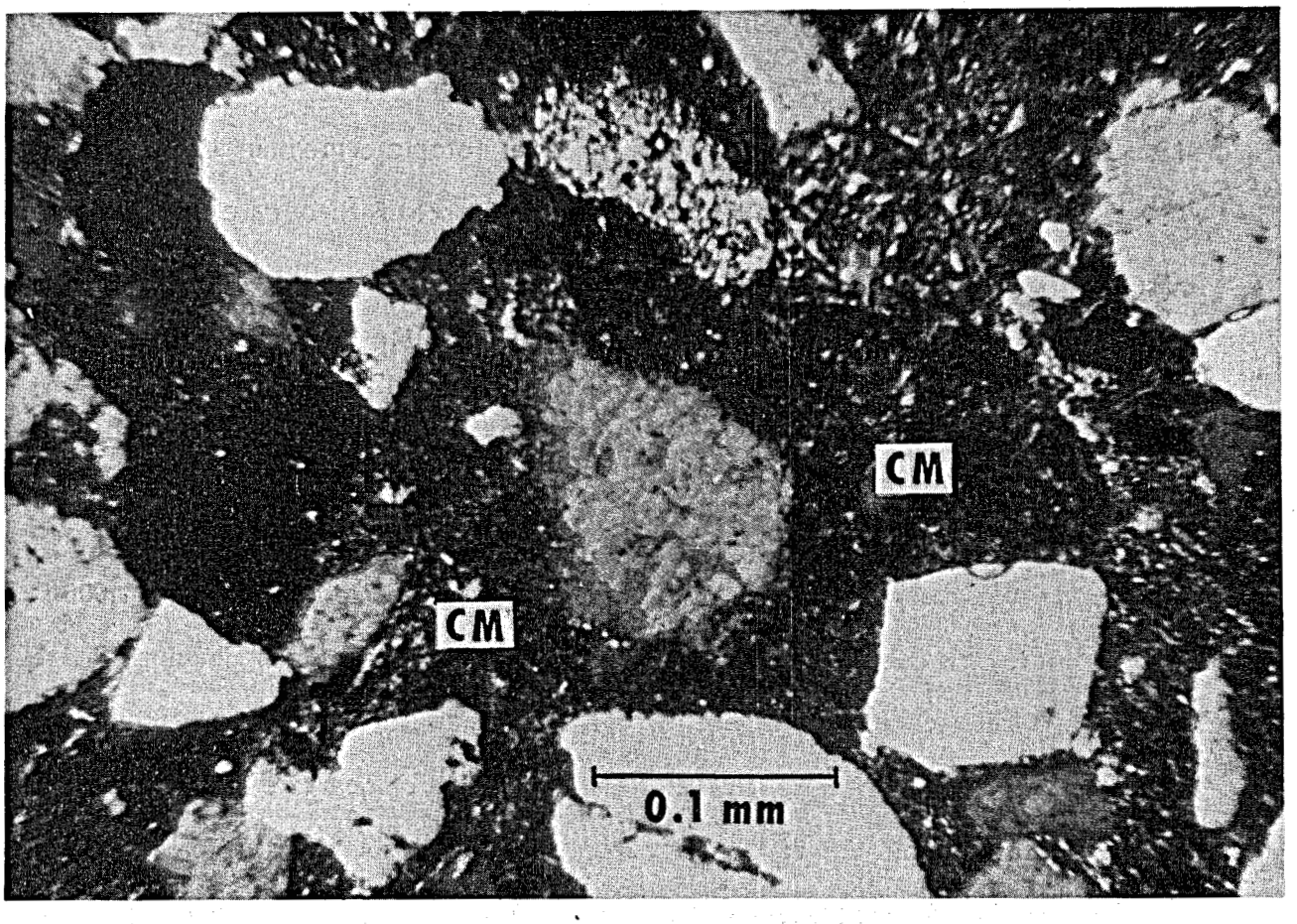

Figure 15. Diagenetic "cherty matrix" (CM). Crossed polars.

Carbonates

The dominant carbonate variety is calcite, some of which is ferroan. Both ferroan and non-ferroan calcite occur as sparry and poikilotopic cement and the non-ferroan variety also replaces grains (especially plagioclase and VRF's) (fig. 16). Calcite cements are present in samples from all depths studied. Dolomite, characterized by undulose extinction and curved crystal faces ("baroque" dolomite, after Folk and Assereto, 1974) is also present as sparry and poikilotopic cement in a few samples; however, it is considerably less abundant and widespread than calcite. Euhedral ferroan dolomite (or ankerite) rhombs were also observed in a small number of samples (fig. 17). Leaching of authigenic carbonates is responsible for a large part of the secondary porosity developed in Frio sandstones.

Quartz

Authigenic quartz formed as overgrowths on detrital quartz grains. Such overgrowths are abundant in samples from the deep burial interval (>11,000 ft; 3,350 m) defined by Loucks and others (1979). Quartz overgrowths developed after early formed calcite cement; where overgrowths grew into pores, they commonly developed euhedral terminations (fig. 18). The abundance of quartz overgrowths shows a weak correlation with detrital quartz abundance. The source of silica for quartz overgrowth formation continues to be a subject of speculation. Several proposed sources include: (1) pressure solution between detrital quartz grains (Thomson, 1959); (2) silica derived from the smectite/illite transition in associated shales (Towe, 1962; Boles and Franks, 1979; Land and Dutton, 1978); and (3) in situ leaching of detrital feldspars and rock fragments. We saw little petrographic evidence to support the first mechanism; however, the second and third proposed sources are reasonable possibilities that deserve further investigation, and they will be discussed in the section comparing diagenetic sequences in the Frio and Vicksburg sandstones.

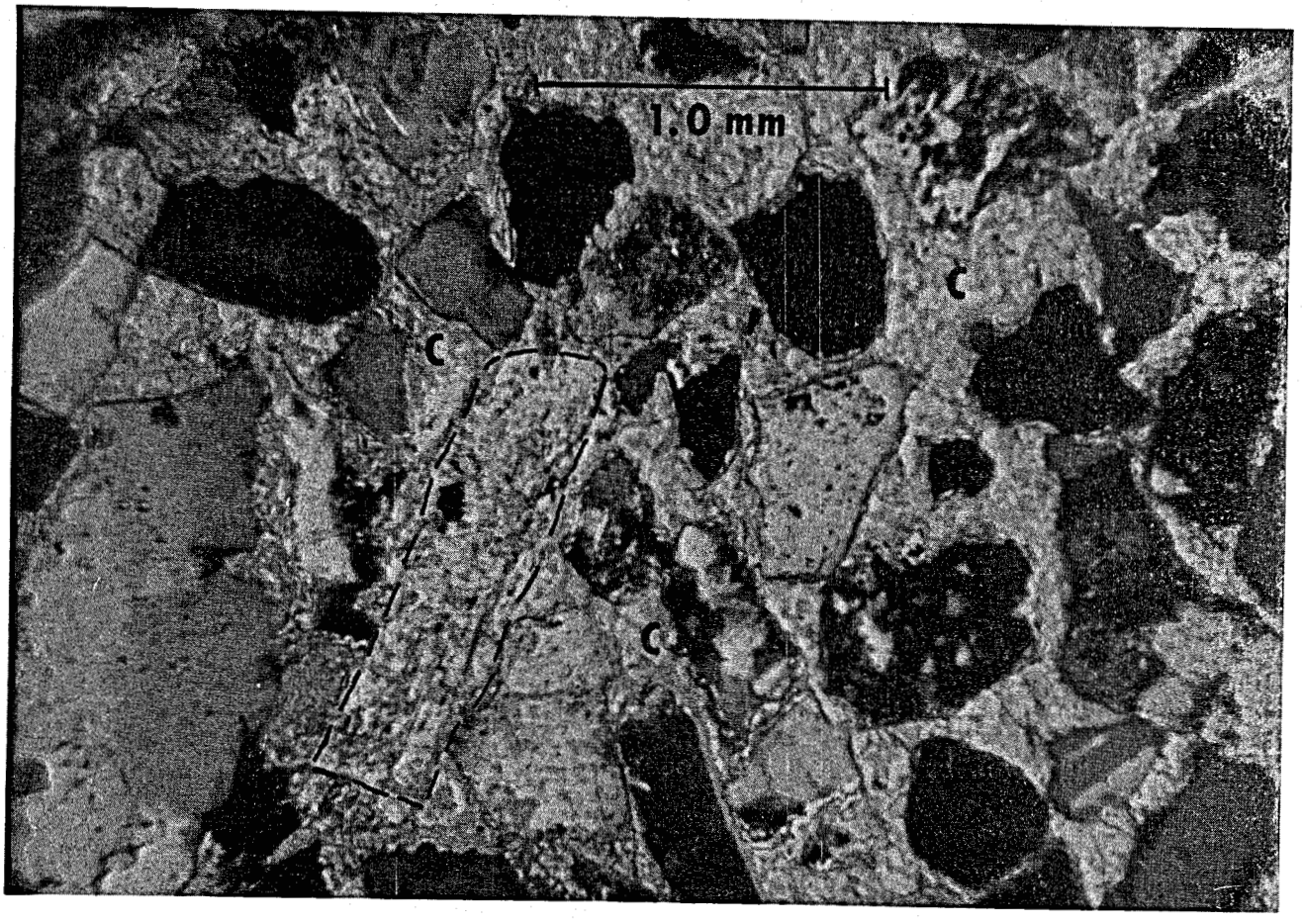

Figure 16. Poikilotopic calcite cement (C) and calcite grain replacement (outlined). Crossed polars.

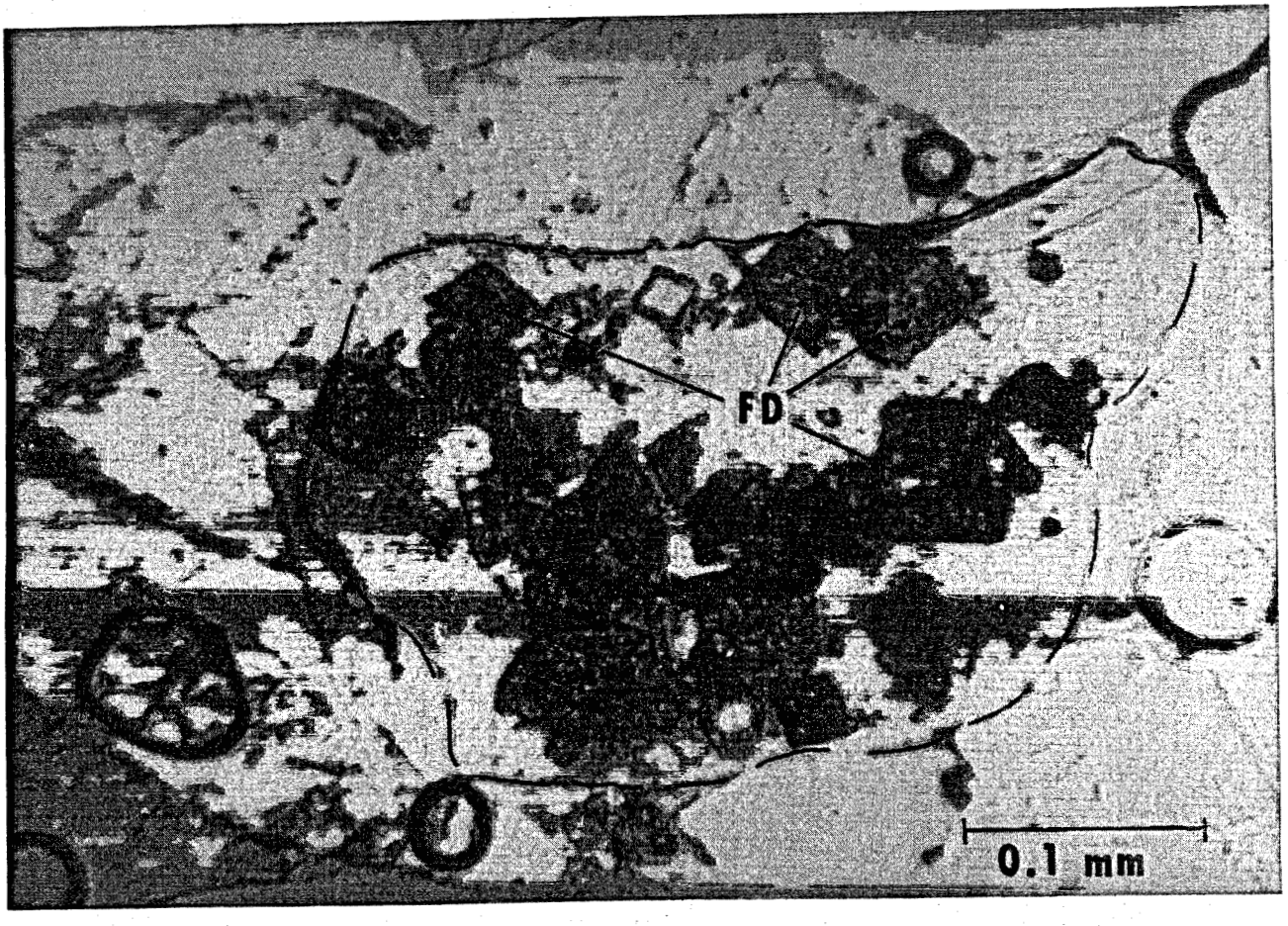

Figure 17. Euhedral ferroan dolomite (FD) replacing a rock fragment (outlined). Plane polarized light.

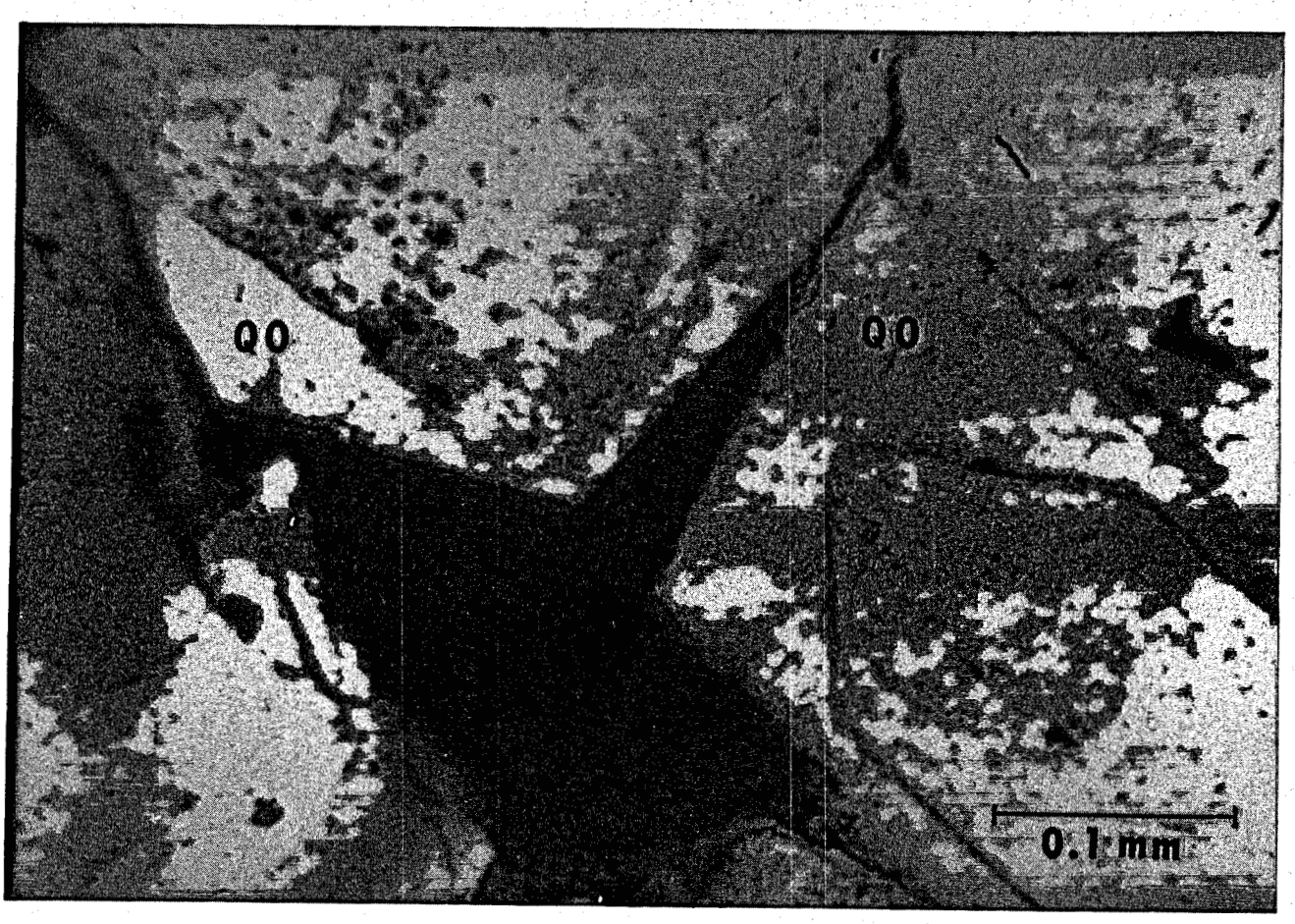

Figure 18. Euhedral quartz overgrowth cement (QO). Plane polarized light.

Kaolinite

Authigenic kaolinite is abundant in sandstones to depths in excess of 17,700 ft (5,395 m). Most kaolinite occurs as a pore-filling cement with a vermicular habit (fig. 19). Individual booklets have grown up to several hundred microns in length. Kaolinite has also been observed as a replacement mineral, especially associated with plagioclase. Some detrital grains have been totally replaced, and in these instances the kaolinite commonly grew outward from the grain surface into available pore space. The persistence of pristine authigenic kaolinite in the deepest samples (at temperatures approaching 205°C [400°F]) at first seems anomalous, as observations by Boles and Franks (1979) suggest that kaolinite abundance generally decreases with increasing depth of burial. We observed no petrographic evidence to suggest that degradation was occurring at these depths. However, at shallower depths, several zones that are devoid of kaolinite alternate with kaolinite-bearing zones. In addition, Boles and Franks (1979) suggested that kaolinite reacts with ankerite and dolomite in the presence of excess silica to form chlorite. Neither the carbonate reactants nor authigenic chlorite were observed in significant quantities in these samples. Rocks containing abundant authigenic kaolinite are generally not of reservoir quality. They are characterized by moderate porosities but very low permeabilities. The porosity present is largely microporosity (pore aperture radii less than 0.5 μm) existing between individual clay flakes. This type of porosity does not contribute significantly to permeability. Additionally, the presence of authigenic kaolinite can create production problems because the delicate structure of authigenic kaolinite makes it highly susceptible to breakage (Pittman, 1979). Dislodged clay flakes can further obstruct permeability.

Minor Authigenic Minerals

Authigenic feldspars, chlorite, zeolite, and clay rims and coats were identified in trace amounts in some Frio sandstone samples. Authigenic feldspars formed as

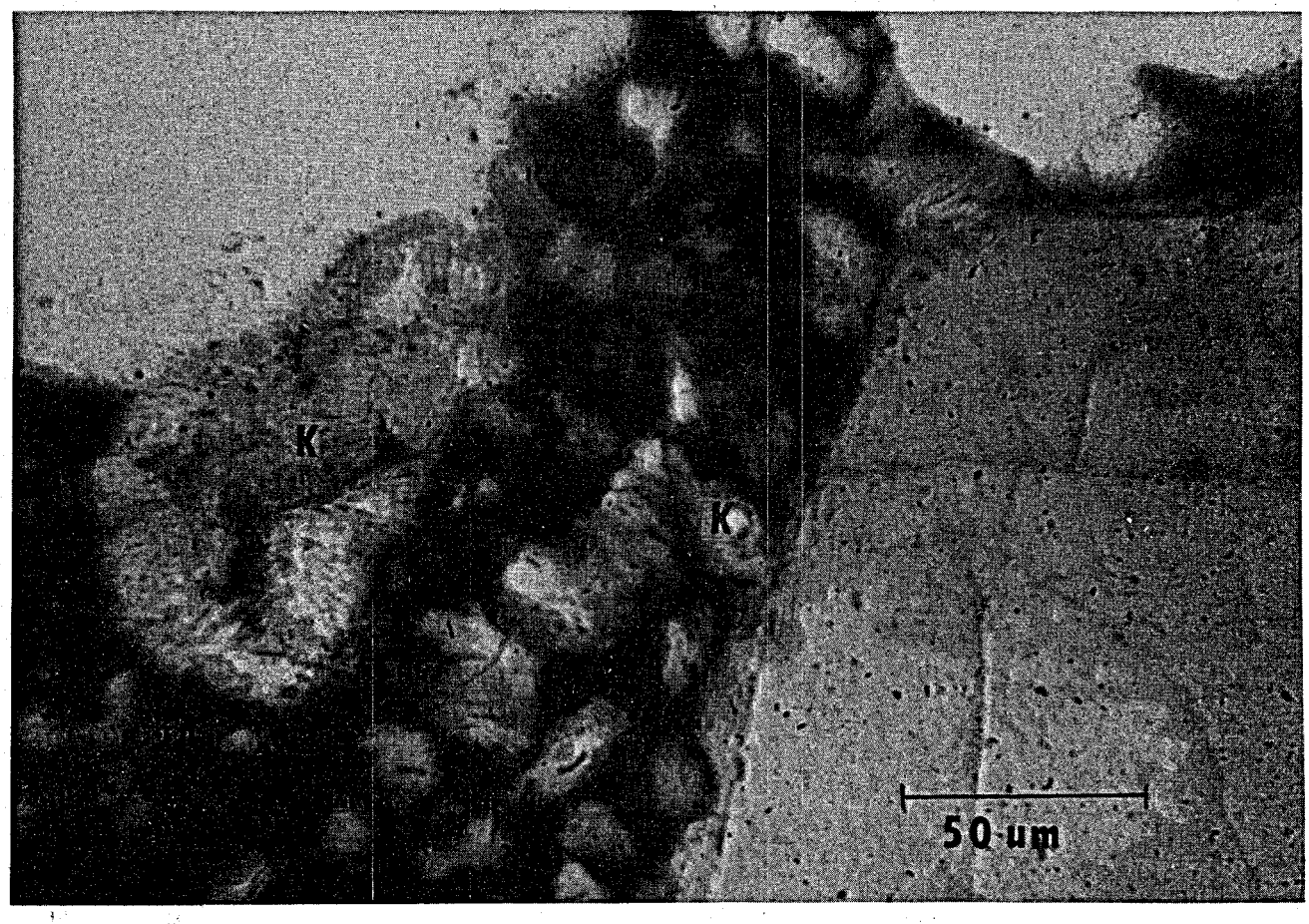

Figure 19. Pore-filling kaolinite (K). Crossed polars.

overgrowths on detrital feldspar grains (fig. 20). Overgrowths are most commonly albite, although rare potassium feldspar overgrowths are also present. Albite overgrowths are occasionally twinned. Frequently, fresh feldspar overgrowths rim leached detrital grains and where leaching was extensive the overgrowth may outline the moldic porosity (fig. 21) Authigenic feldspars are more chemically stable than their detrital counterparts and thus have greater resistance to leaching because they formed under conditions more closely approximating the environment in which they are found today.

Chlorite is another trace authigenic constituent in Frio samples. It is occasionally found as an alteration product of VRF's, and, rarely, as a minor cement. Likewise, the zeolite, laumontite, was identified in a few samples. Laumontite apparently formed a poikilotopic cement; however, only a few fragmental patches survived leaching.

Clay coats and rims are diagenetic features formed on detrital grains very early in the sandstone consolidation sequence. In clay rims, the individual clay flakes are oriented perpendicular to the grain surface, whereas clay coats are formed by clay flakes oriented tangential to the grain surface. Clay coats are more prevalent than clay rims and often form the boundary between detrital quartz grains and quartz overgrowths.

Porosity Types

Porosity may be broadly subdivided into two categories based primarily on average pore-throat diameter. "Microporosity" has an average pore-throat diameter of less than 1.0 µm, whereas the average pore-throat diameter of "macroporosity" is greater than 1.0 µm.

Microporosity is difficult to quantify petrographically because of its small size and its intimate association with authigenic clays, clay matrix, and fine-grained, argillaceous rock fragments. This porosity type is dominant in lithologies containing

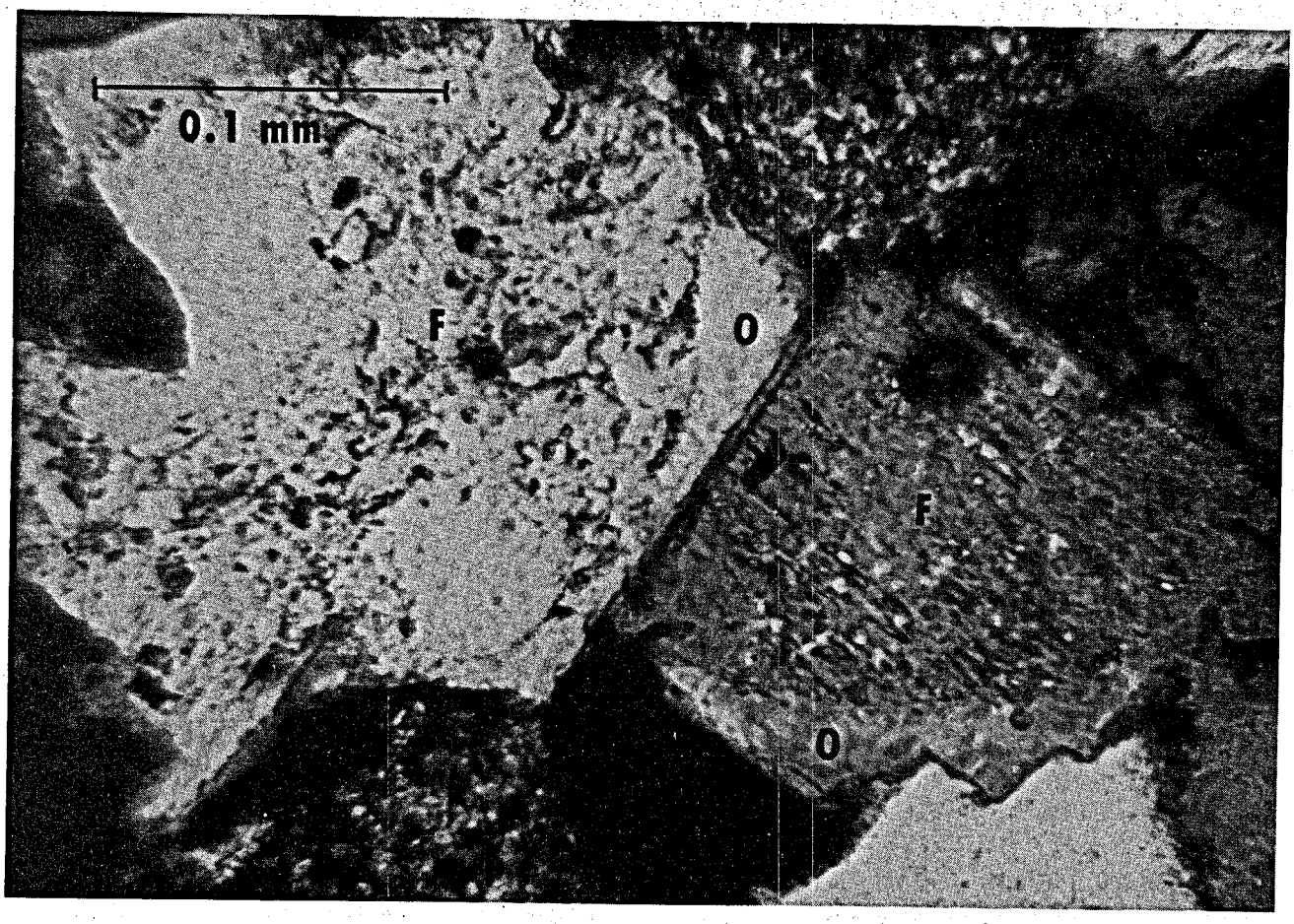

Figure 20. Feldspar overgrowths (O) on detrital feldspar (F). Crossed polars.

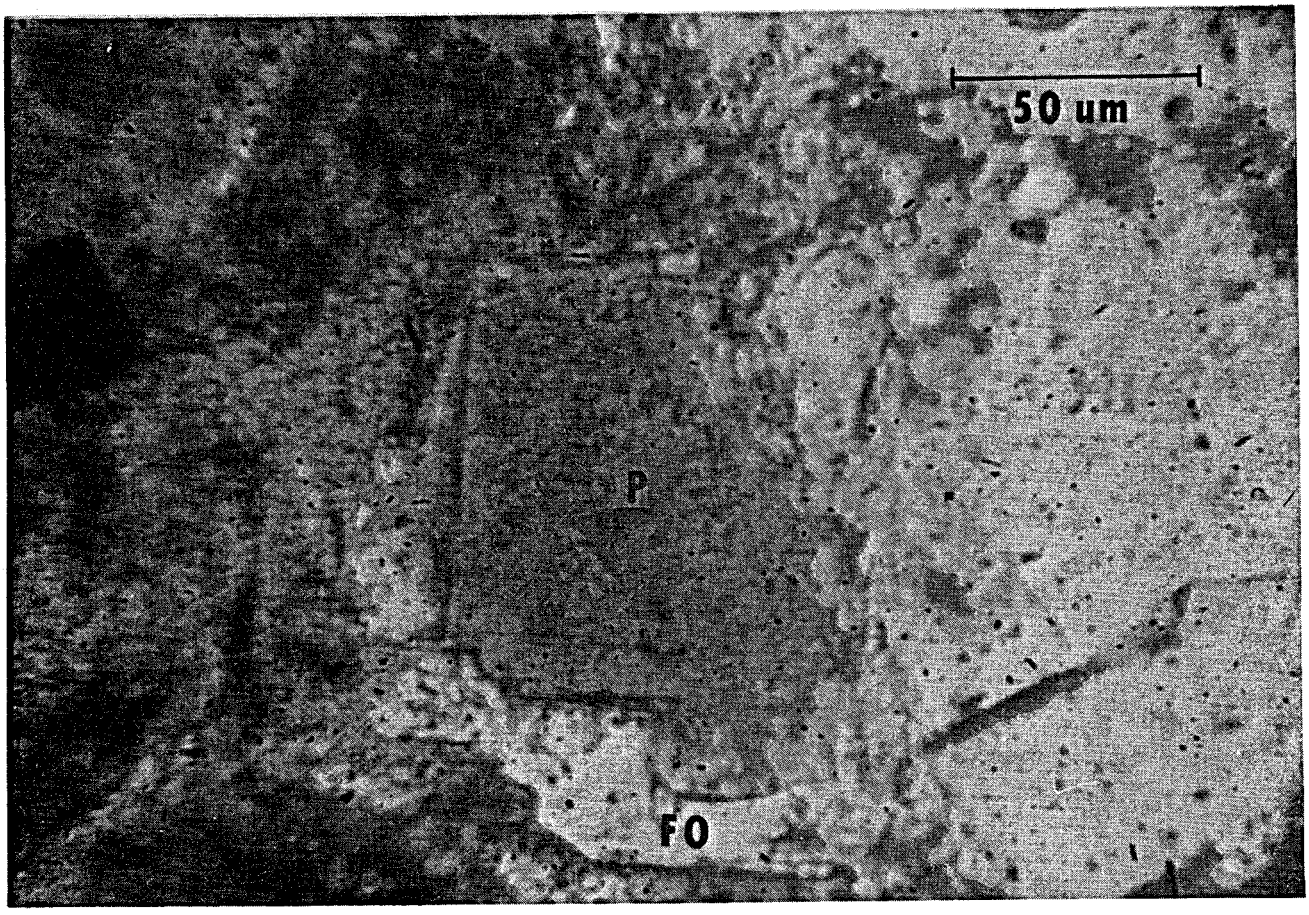

Figure 21. Feldspar overgrowth (FO) outlining moldic porosity (P).

these constituents. Microporosity does not contribute measurably to permeability but is responsible for much of the irreducible water saturation in sandstones (Pittman, 1979).

In contrast, macroporosity is easily recognized in thin section, and it contributes most significantly to permeability. This porosity type is dominant in the coarser grained, matrix-poor sandstones examined. Macroporosity may be present in sandstones in one or more of the following forms:

(1) Primary intergranular: that part of the depositional porosity between detrital grains remaining at any subsequent stage of diagenesis.

(2) Secondary (dissolution):

   (a) Intergranular - porosity resulting from dissolution of cements.

   (b) Intragranular - porosity resulting from dissolution of framework grains and/or intragranular replacement minerals.

(3) Hybrid: porosity that cannot be unequivocally classified as completely primary or secondary. Many oversized pores are probably hybrid, that is, they are primary pores that have been enlarged by the secondary process of dissolution.

The dominant type of porosity occurring in matrix-free sandstones of the shallow subsurface (to depths of approximately 6,000 ft [1,830 m] in Brazoria County) is primary intergranular porosity. However, the major types of porosity encountered at depths suitable for geopressured-geothermal energy production are microporosity and secondary porosity. Secondary porosity is most extensively developed in matrix-poor sandstones. These rocks are the best potential geothermal reservoirs. Most primary intergranular porosity was occluded by cement before the sandstones reached the "soft" geopressured zone (0.465 psi/ft) (Loucks and others, 1979); therefore, permeability in the geopressured zone is most dependent on dissolution porosity.

Minor Element Chemistry

Electron microprobe analyses were conducted on selected samples from GCO/DOE Nos. 1 and 2 Pleasant Bayou, Brazoria County, in order to supplement petrographic data. Our major objectives were preliminary quantification of variations in the minor element chemistry of authigenic carbonate phases, and determination of detrital feldspar compositions. Appendix D presents microprobe data as weight percent of oxides for carbonates and feldspars from Pleasant Bayou.

The minor element chemistries of authigenic carbonates present in selected samples from GCO/DOE Nos. 1 and 2 Pleasant Bayou were investigated. Although we were not able to analyze enough samples to identify potentially systematic variations in composition with depth, these analyses are valuable in bracketing the range of possible compositional variations and in confirming the existence of multiple generations of authigenic carbonate in the two areas.

Authigenic carbonates in samples from the following depths were analyzed for MgO, SrO, CaO, MnO, and FeO by electron microprobe:

GCO/DOE Nos. 1 and 2

4,345 ft (1,324 m)

11,773 ft (3,589 m)

14,685 ft (4,476 m)

15,162 ft (4,621 m)

15,173 ft (4,625 m)

All authigenic carbonates analyzed are calcite; however, in some samples, the poikilotopic cement contains variable amounts of FeO, up to approximately 3 percent. MnO content of cements is also variable, ranging from <0.1 to approximately 1.5 percent. MgO content is somewhat less variable than either FeO or MnO and does not exceed 0.6 percent in any analysis. SrO is a minor component in the calcite cements.

Microprobe traverses across several areas of sparry and poikilotopic calcite detected no trace element zoning within the cements. The probe analyses do, however, confirm the existence of multiple, compositionally distinct, generations of calcite. The presence of ferroan and non-ferroan calcite was known from petrographic analysis of thin sections stained with alizarin red-S and potassium ferricyanide (technique of Lindholm and Finkelman, 1972). Unfortunately, such staining does not quantitatively reflect subtle variations in iron concentrations, nor does it indicate the presence of other ions substituting for calcium (for example, Mn^{+2}, Mg^{+2}, and so on). For example, the shallowest Pleasant Bayou sample analyzed (from 4,345 ft; 1,324 m) contains a highly ferroan (up to approximately 3 percent) poikilotopic calcite cement and non-ferroan calcite grain replacements and foraminifers. In a deeper sample (from 11,773 ft [3,589 m]) the poikilotopic cement and grain replacements share a common chemical composition distinctly different from either of the calcite compositions in the 4,345 ft (1,324 m) sample; these deeper calcites contain only about one-third the FeO, but are substantially enriched in MnO (containing up to approximately 1.4 percent) relative to the shallower calcites. Although the deeper calcites are compositionally distinct from the shallow ferroan calcite, their slight chemical differences could not have been detected in stained thin sections.

Another distinctive poikilotopic calcite composition occurs in the sample from 14,685 ft (4,476 m). This calcite contains MgO and FeO in proportions similar to the poikilotopic calcite in the shallowest sample, but it is also enriched in MnO. Grain replacements have compositions only slightly depleted in FeO and enriched in MnO, relative to the cement

Two samples were taken from below 15,000 ft (4,572 m). Calcite cement in the sample from 15,162 ft (4,621 m) is essentially pure, while cements and grain replacements at 15,173 ft (4,625 m) are compositionally similar to those occurring in the sample from 11,773 ft (3,589 m).

In all, at least four unique calcite cement and grain replacement compositions were distinguished, twice the number that could be identified using carbonate staining techniques in conjunction with standard petrographic analysis. The existence of such a variety of calcite compositions within so limited a set of samples strongly supports our views on the sequence of diagenetic events occurring in Tertiary Gulf Coast sandstones. Apparently, calcite precipitation, leaching, and reprecipitation went on almost continuously throughout the sandstones' burial history, resulting in multiple, distinctive calcite compositions at various depths (Loucks and others, 1980; Richmann and others, 1980).

A further problem concerning carbonate genesis in Tertiary sandstones is the source of calcium. Various sources have been proposed, most notably migration of compaction waters from associated pelitic sediments carrying dissolved Ca^{+2}, which is precipitated as calcite in the sandstones (Boles and Franks, 1979), and albitization of detrital plagioclase within the sandstones, which contributes calcium to form the calcite cements (Boles, 1980). The first model requires that the shale-sandstone system be open to chemical exchange, a situation that is not necessarily requisite to the second model.

Microprobe analyses of detrital feldspars were run on six samples from GCO/DOE Nos. 1 and 2 Pleasant Bayou to evaluate the possibility that albitization is a major source of the calcium needed to form the authigenic calcite. With only one exception, all of the detrital plagioclase analyzed is albite (An_{0-10}). Furthermore, core-to-rim zoning of both leached and intact grains was not observed. Original zoning of plagioclase might be expected as the plagioclase is believed to have been derived primarily from a volcanic source. Leaching of detrital plagioclase appears to be preferential; that is, some factor appears to have controlled the sites of leaching within a particular grain. Compositional variations within individual grains most likely provided such control. However, any such original variations have been obliterated.

Assuming that detrital plagioclase originally had an intermediate composition and that albitization occurred at some time after deposition, albitization could have supplied calcium for calcite cementation. Verification of this hypothesis requires more specific information on original feldspar compositions and analysis of detrital plagioclase from shallower, updip samples in order to define the depth range over which albitization could have occurred. Boles (1980) believes that albitization is a significant calcium source in Frio sandstones and that the process occurs over a temperature range of 100° to 120°C (212° to 250°F).

Isotopic Composition of Authigenic Phases

Five authigenic minerals were analyzed isotopically: calcite, dolomite, quartz, kaolinite, and albite. Two samples of skeletal aragonite enclosed in shales were also analyzed. The authigenic minerals were selected because of their volumetric importance in the sandstones. Results of the analyses are consistent with the possible range of temperatures and water isotopic compositions that have affected Frio sandstones in Brazoria County. A brief discussion in Appendix B outlines the relationship between the isotopic composition of a mineral, the isotopic composition of water, and temperature. The following two sections summarize what is known about the variation of $\delta^{18}O_{H_2O}$ and temperature in the subsurface of the Chocolate Bayou/Danbury Dome area.

Temperature and $\delta^{18}O_{H_2O}$

Brazoria County has been characterized by net subsidence through the Quaternary (Winker, 1979); thus, it is reasonable to assume that subsurface rocks in Brazoria County have never experienced significant uplift and are presently very near their maximum temperature.

Bonham (1980) postulates that subsurface temperatures of some Gulf Coast rocks may have been slightly hotter in the past because of progressive burial of the higher temperature gradient found below the top of geopressure. Isotopic data for sandstones

in Brazoria County, however, show no evidence of former higher temperatures, unless subsurface waters were at some time much heavier. Perhaps by the time sediments now characterized by higher gradients reached an equilibrium temperature profile, they were already buried many thousands of feet because of high subsidence rates.

Frio rocks in Brazoria County were deposited in marine or near-marine settings (Bebout and others, 1978), so water buried with Frio sediments had an isotopic composition similar to sea water or slightly lighter if the water were brackish. Interstitial water can become heavier through time by reaction with the enclosing sediment (Craig, 1966; Clayton and others, 1972; Hitchon and Friedman, 1969; Kharaka and others, 1977b; Land, in press). Kharaka and others (1977a, 1980) have reported a number of isotopic analyses for subsurface waters in Brazoria County (table 1). All the waters are heavy relative to standard mean ocean water (SMOW).

Carbonate Minerals

Whole rock samples were powdered in a tungsten carbide ball mill and reacted with anhydrous phosphoric acid to produce CO_2 gas from the carbonates (McCrea, 1950). All samples were routinely X-rayed, and gases from those samples containing significant quantities of dolomite in addition to calcite were separated using the double extraction technique outlined by Epstein and others (1963).

Grain replacements and cements made of the same mineral cannot be separated chemically, and the smallness and intricacy of these features preclude mechanical separation. Instead, detailed petrographic study was used to determine the nature of isotopic variability between different forms of authigenic carbonate. All isotope samples were examined in thin section. Many of the samples from GCO/DOE Nos. 1 and 2 Pleasant Bayou were sliced from core plugs and thin-sectioned immediately adjacent (1 to 2 mm away) to the material actually ground in the ball mill. These samples were then point-counted to 500 points to determine the relative proportions of different types of authigenic carbonate. Appendix C gives the results of isotopic analyses of carbonates together with information from petrographic study.

Table 1. $\delta^{18}O$ values for subsurface waters in the Chocolate Bayou Field, Brazoria County, Texas. From Kharaka and others, 1977a, 1980.

Depth (m)	Temperature (°C)	$\delta^{18}O$(‰)
2,626	96	4.6
2,681	99	4.1
2,696	98	4.9
2,981	103	3.5
3,259	117	4.9
3,440	122	3.5
3,463	118	5.7
3,574	127	5.6
3,892	138	4.6
4,161	150	7.5
4,462	138	5.4
4,740	150	4.9

Oxygen Isotopic Data -- A plot of oxygen isotope values for calcium carbonates with depth reveals a trend toward lighter values at greater depths (fig. 22). The considerable scatter of values found at any particular depth can be explained at least partly by the variability of calcite types as seen in thin section. The two aragonite samples plot to the far right and represent mollusk fragments that have remained virtually unaltered since deposition. Samples dominated by grain replacements and early calcite cement, formed prior to quartz overgrowth, also plot to the right side of the scatter. Samples comprised mainly of pore-filling cement plot mostly on the left of the point distribution (fig. 23).

Thus, a history of cementation is preserved in the isotopic composition of authigenic carbonates. Samples formed at shallow depth may be buried to higher temperatures without subsequent crystallization. If continuous crystallization occurred during burial, variability among closely associated samples would not exist and the points in figures 22 and 23 would show little scatter. It seems plausible, then, that samples farthest left on figure 22 represent those samples most nearly in equilibrium with present conditions at depth. Those on the right are samples that are farthest from equilibrium, probably having been buried farthest from their point of precipitation without subsequent recrystallization.

Dolomite samples show a similar trend toward lighter $\delta^{18}O$ values with depth (fig. 24). The lesser amount of scatter in figure 24 compared to figure 22 probably reflects the smaller number of dolomite samples. Dolomite, in all but one anomalous sample taken immediately adjacent to a salt dome, is 2 to 3 per mil heavier than associated calcite. This is consistent with other observations on differences in fractionations of calcite and dolomite (Land, in press) and suggests that where these minerals are associated they formed under similar conditions.

In spite of considerable scatter due to preservation of burial history, a clear trend toward lighter $\delta^{18}O$ values for carbonates with depth remains. Thus, while a

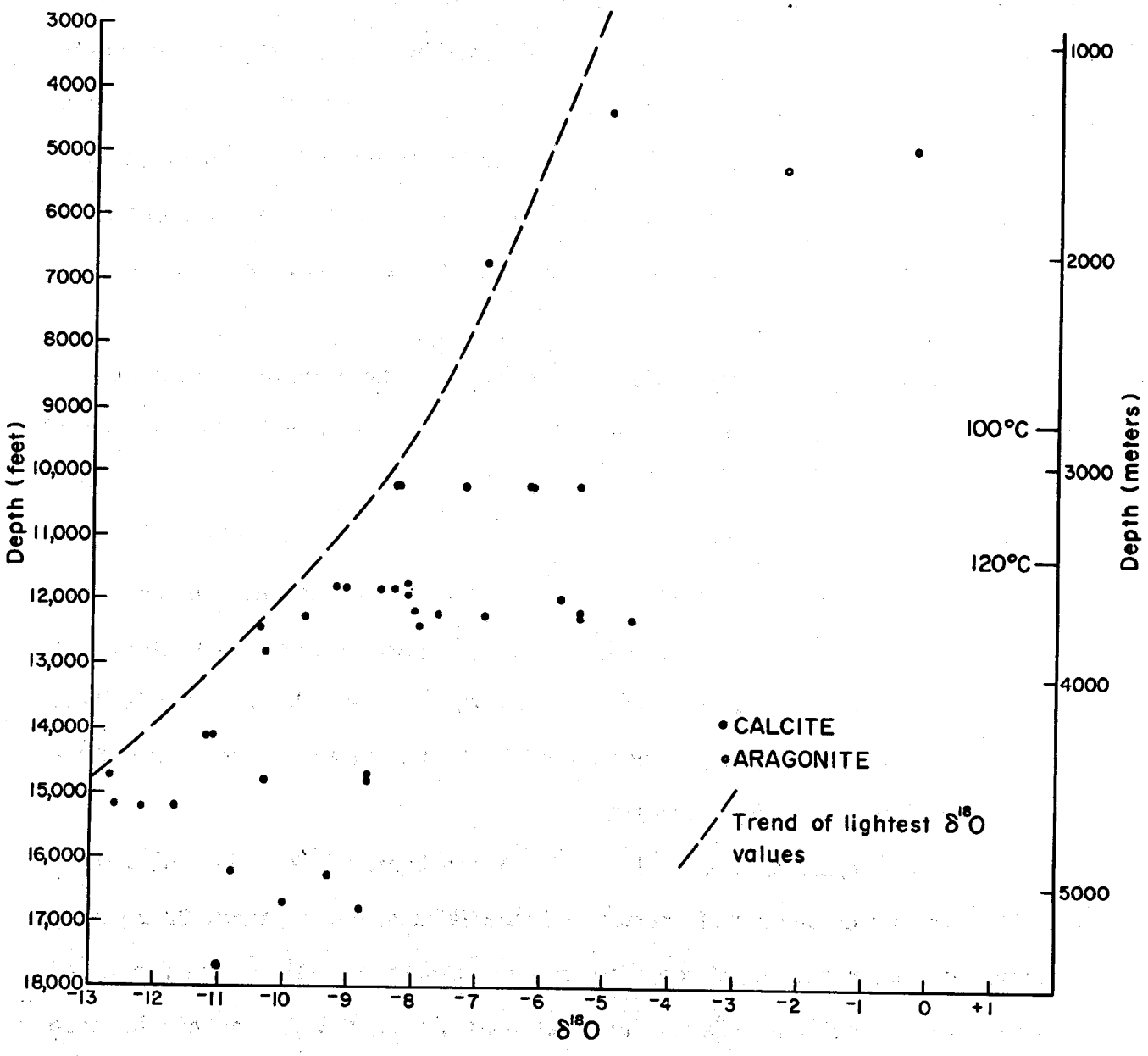

Figure 22. $\delta^{18}O$ of calcium carbonate versus depth in Brazoria County (reported relative to PDB).

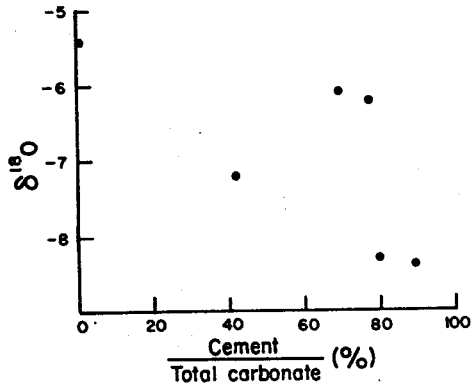

Figure 23. $\delta^{18}O$ versus percent calcite cement in total carbonate (cement + grain replacements) for six samples in the Pleasant Bayou No. 1 well.

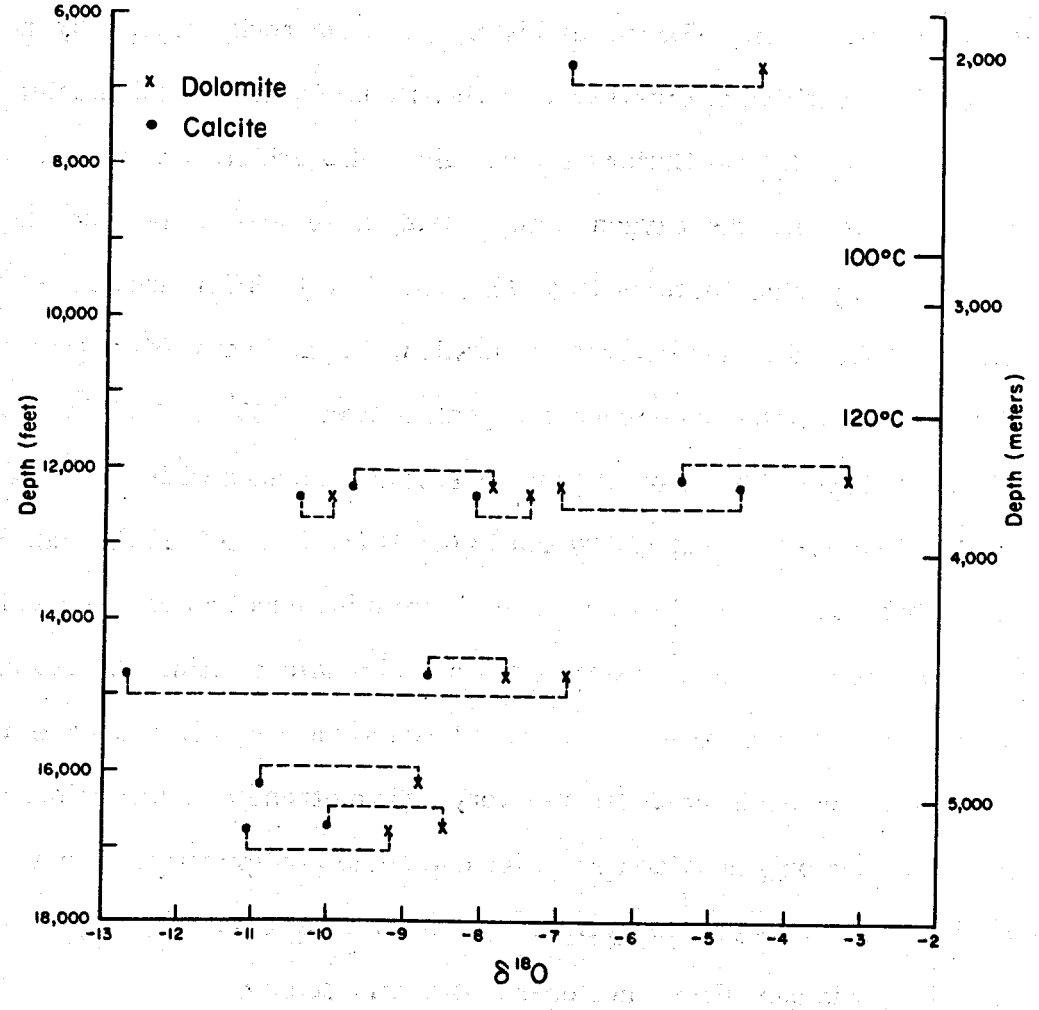

Figure 24. $\delta^{18}O$ versus depth for dolomites and associated calcites (reported relative to PDB).

carbonate crystal may survive a large amount of burial, the chance of a particular crystal surviving more than 5,000 ft (1,525 m) of burial is slight. The occurrence of abundant secondary porosity in the Frio of Brazoria County (Bebout and others, 1978) explains this phenomenon. The burial history of these rocks apparently has been characterized by repetitive alternations of carbonate precipitation and dissolution.

Carbon Isotopic Data — Carbon isotope values also exhibit a distinct trend with depth (fig. 25). As with the oxygen isotope data, some scatter in figure 25 can be explained by petrographic features (fig. 26). The overall differences in $\delta^{13}C$ with depth can be attributed to hydrocarbon maturation. Liquid hydrocarbon generation in the Gulf Coast is initiated and reaches a peak between 100° and 120°C (212° and 250°F) (Bonham, 1980). This zone of peak generation coincides with the marked shift to lighter $\delta^{13}C$ values between 10,000 and 13,000 ft (3,050 to 3,960 m). Lighter $\delta^{13}C$ values for carbonates formed in this zone result from introduction of isotopically light organic carbon from organic reactions into the carbonate system. At depths above this zone, carbon is derived from isotopically heavier sources, perhaps skeletal debris in shales. Below this zone, production of very light methane may utilize much of the light carbon, leaving only heavier carbon for carbonate precipitation. The absence of the very light $\delta^{13}C$ values to greater depths also reflects the large amount of secondary porosity in deep Frio sandstones in Brazoria County.

Quartz

All samples for analysis of quartz were broken by gentle pounding and further disaggregated ultrasonically. The sediment fraction smaller than 62 µm was decanted to remove fine-grained quartz not accounted for during point counts. Quartz was then isolated using the technique described by Syers and others (1968). All samples were checked for purity by X-ray analysis. Detailed point counts to determine the relative proportions of different quartz types were made on thin sections 1 to 2 mm away from the samples analyzed.

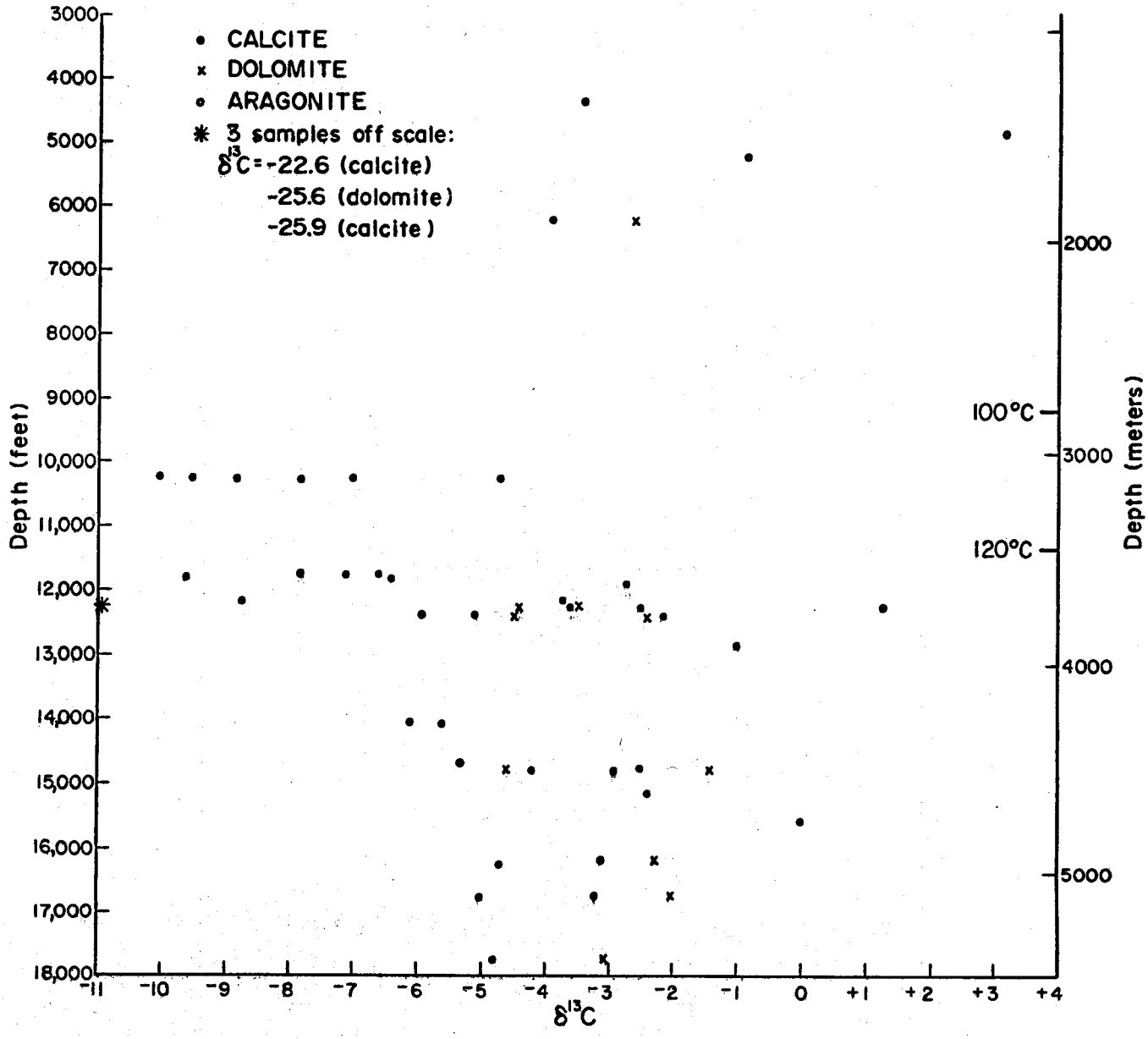

Figure 25. $\delta^{13}C$ versus depth for carbonate minerals (reported relative to PDB).

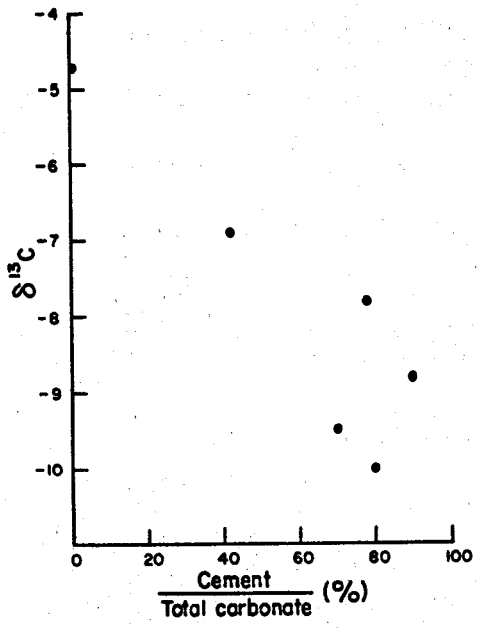

Figure 26. $\delta^{13}C$ versus percent calcite cement in total carbonate (cement + grain replacement) for samples depicted in figure 23. As with the oxygen data, samples dominated by cements are depleted relative to samples with larger proportions of grain replacements.

Oxygen isotope analysis of Frio quartz overgrowths is complicated by two factors: (1) the presence of silicified volcanic rock fragments in addition to detrital igneous quartz and authigenic quartz, and (2) an apparent 3-to-4 per mil variation in $\delta^{18}O$ of detrital quartz at different depths.

Volcanic rock fragments (VRF's) were separated from one sample (2069) by picking. These fragments were treated to isolate quartz. Little weight loss resulted from the quartz isolation process, confirming that these rock fragments are primarily quartz and not zeolites. $\delta^{18}O$ for the rock fragment quartz was determined to be 29.6. This value is consistent for silicification of rocks by near-surface water in the Trans-Pecos volcanic source to the west ($\delta^{18}O_{H_2O} \simeq 6.0‰$).

Using this value, corrections were made for each $\delta^{18}O$ according to the abundance of silicified rock fragments determined from thin section. A plot of these corrected values versus the percent quartz cement in total quartz, however, does not show a trend that can be extrapolated to give a $\delta^{18}O$ value for overgrowths. Variation in $\delta^{18}O$ of detrital quartz and possible differences in $\delta^{18}O$ of quartz cement at different depths make such a plot meaningless. Plotting together only those samples that are closely spaced gives a somewhat better trend and suggests that $\delta^{18}O$ for quartz overgrowths is around 30 per mil (fig. 27).

To define $\delta^{18}O$ for quartz cement more accurately, two quartz samples with relatively large amounts of quartz overgrowths were etched repeatedly in concentrated hydrofluoric acid. Three samples were removed at different times during the etching process in order to determine $\delta^{18}O$ variation as the quartz overgrowths were progressively removed. A part of each aliquot was used to make a grain mount for point counting. Results are shown in table 2. When $\delta^{18}O$ values corrected for rock fragments are plotted versus percent cement in total quartz, a much better trend results (fig. 28). Both samples of quartz cement are quite heavy relative to detrital igneous quartz.

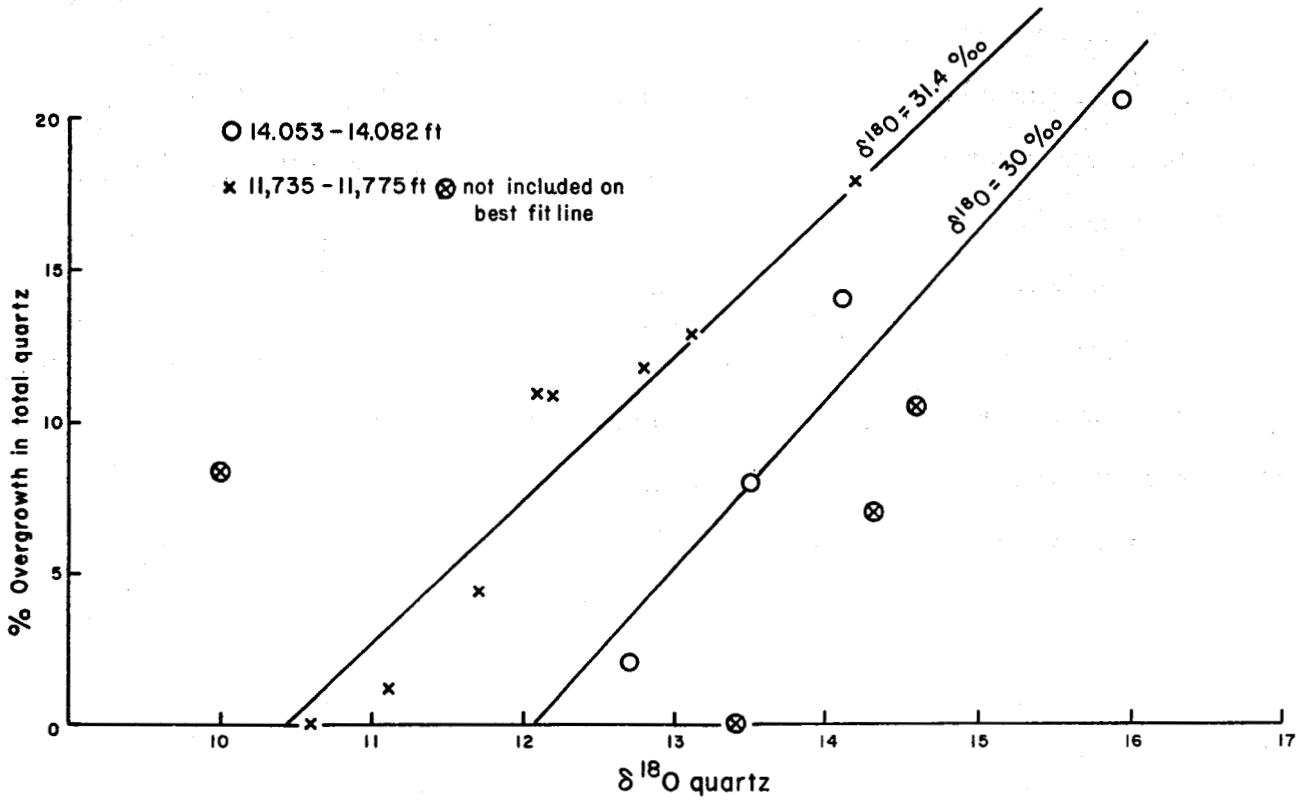

Figure 27. $\delta^{18}O$ quartz, corrected for rock fragments, versus percent overgrowth in total quartz. Linear regression lines are drawn for two groups of closely spaced samples and indicate a $\delta^{18}O$ for overgrowths of about 30‰. Samples omitted from the left line contain abundant fine-grained quartz suspected to be authigenic, or represent analyses that are suspect.

Table 2. Results of etching experiment.

Sample Number		Quartz Types			$\delta^{18}O$	$\delta^{18}O$ corrected for VRF's
		Grains (%)	Overgrowths (%)	VRF (%)		
2012	A	82.5	10.5	7.0	15.94	14.91
	B	85.5	9.0	5.5	15.15	14.31
	C	95.25	4.75	0	13.16	13.16
	D	99.5	0.5	0	12.60	12.60
(Depth = 14,082 ft [4,292 m])						
2093	A	84.0	11.5	4.5	13.56	12.80
	B	85.0	10.0	5.0	13.45	12.60
	C	92.0	8.0	0	12.05	12.05
	D	100.0	0	0	10.62	10.62
(Depth = 15,641 ft [4,767 m])						

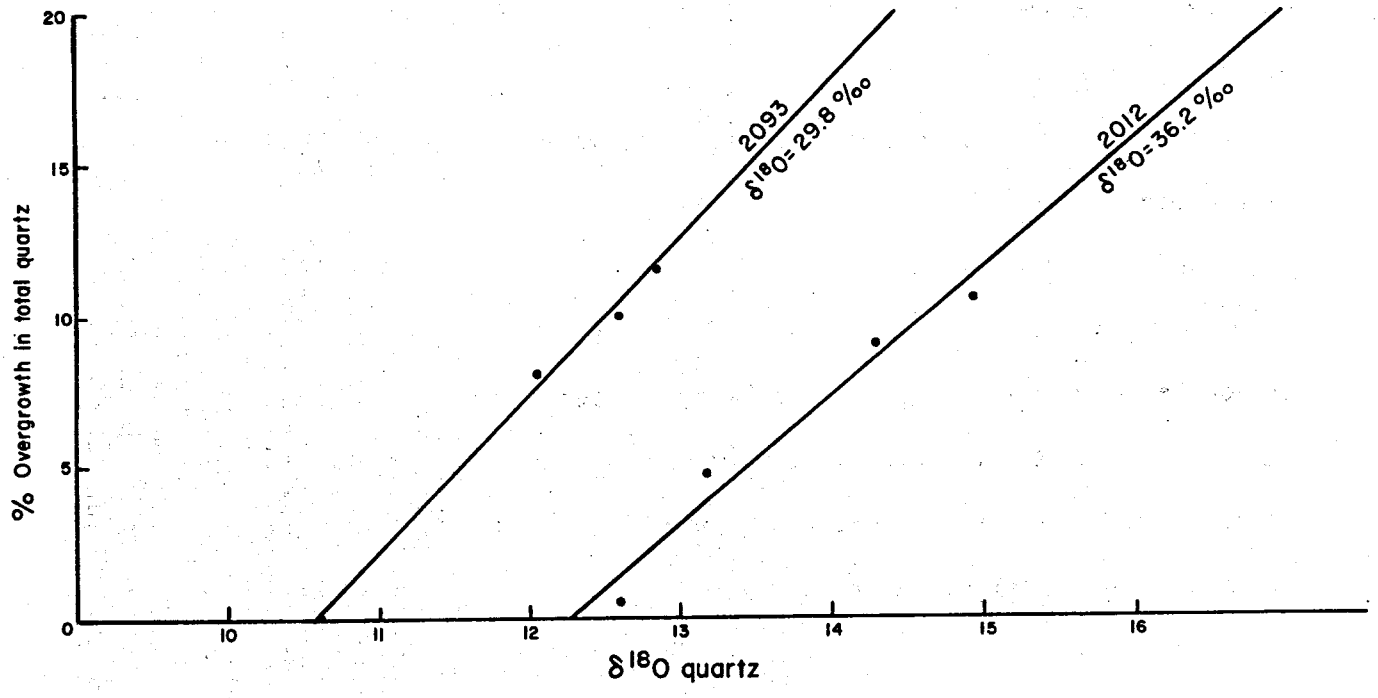

Figure 28. Plot of data from table 2. Values for detrital quartz differ by 2‰. The correlation coefficient for 2093 is 0.997; for 2012 is 0.981.

Kaolinite

Authigenic kaolinite was size-separated from six samples by settling. Abundant quartz in the same size fraction as kaolinite precluded complete separation. Ratios of kaolinite to quartz were determined from X-ray patterns, and the mixtures were analyzed for $\delta^{18}O$. Kaolinite was then removed from four samples by heating at 600°C (1112°F) for four hours. $\delta^{18}O$ was determined for the combined quartz of these four samples, and this value was used to calculate $\delta^{18}O$ for kaolinite in the original mixtures. $\delta^{18}O$ for kaolinite is around 20 per mil.

Albite

Albite was separated from one sample (2069) by picking. $\delta^{18}O$ for this sample was determined to be 17.2‰.

Given the range of $\delta^{18}O_{H_2O}$ values observed in Brazoria County (Kharaka and others, 1977a, 1980), temperatures of precipitation for various cements can be established. Isotopic data, as related to temperatures, for carbonates, kaolinite, quartz, albite, and waters are summarized in figure 29. Quartz probably formed at 75° to 80°C (167° to 176°F), kaolinite at around 100°C (212°F), and carbonates over temperatures spanning the entire range of depths examined. Albitization took place primarily below 12,000 ft (3,660 m), at temperatures greater than 120°C (250°F). Relative sequences of events determined in this way largely corroborate paragenetic sequences determined for the cements by petrographic study.

Reservoir Quality

Most of the porosity present in the sampled Frio sandstones is secondary porosity, that is, porosity formed by dissolution of detrital grains and/or cements (fig. 30). Loucks and others (1979) demonstrated that in Upper Texas Gulf Coast Tertiary sandstones large volumes of primary porosity, occluded by carbonate cements early in the diagenetic sequence, are frequently resurrected in the zone of "soft"

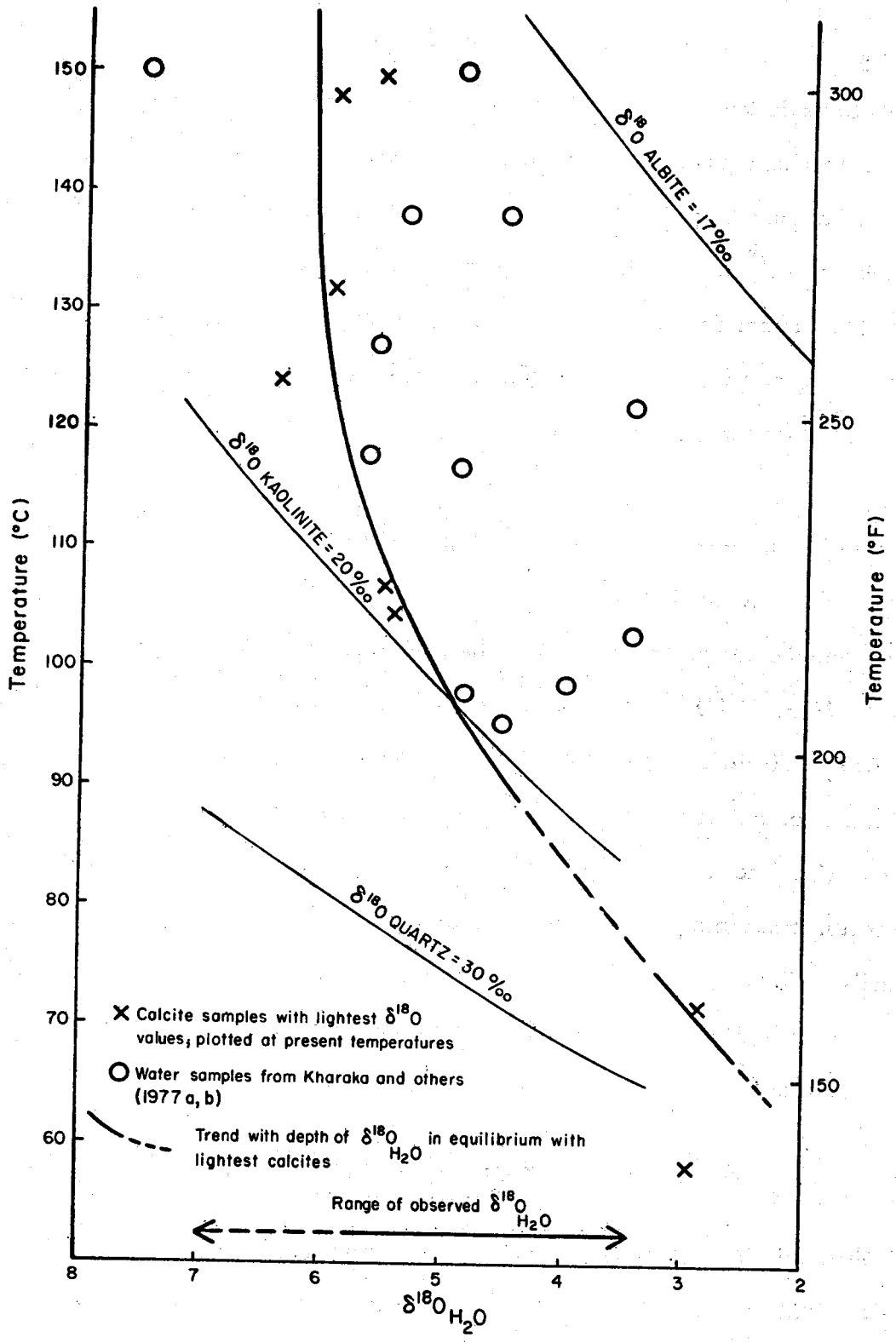

Figure 29. Summary of isotopic data. Equations relating temperature, $\delta^{18}O_{H_2O}$, and $\delta^{18}O_{min}$ for quartz ($10^3 \ln\alpha = 3.38(10^6 T^{-2}) - 3.4$), calcite ($10^3 \ln\alpha = 2.78\ (10^6 T^{-2}) - 2.89$), albite ($10^3 \ln\alpha = 2.91(10^6 T^{-2}) - 3.41$) are listed by Friedman and O'Neil (1977). The equation for kaolinite ($10^3 \ln\alpha = 2.5(10^6 T^{-2}) - 2.87$) is modified from Eslinger (1971).

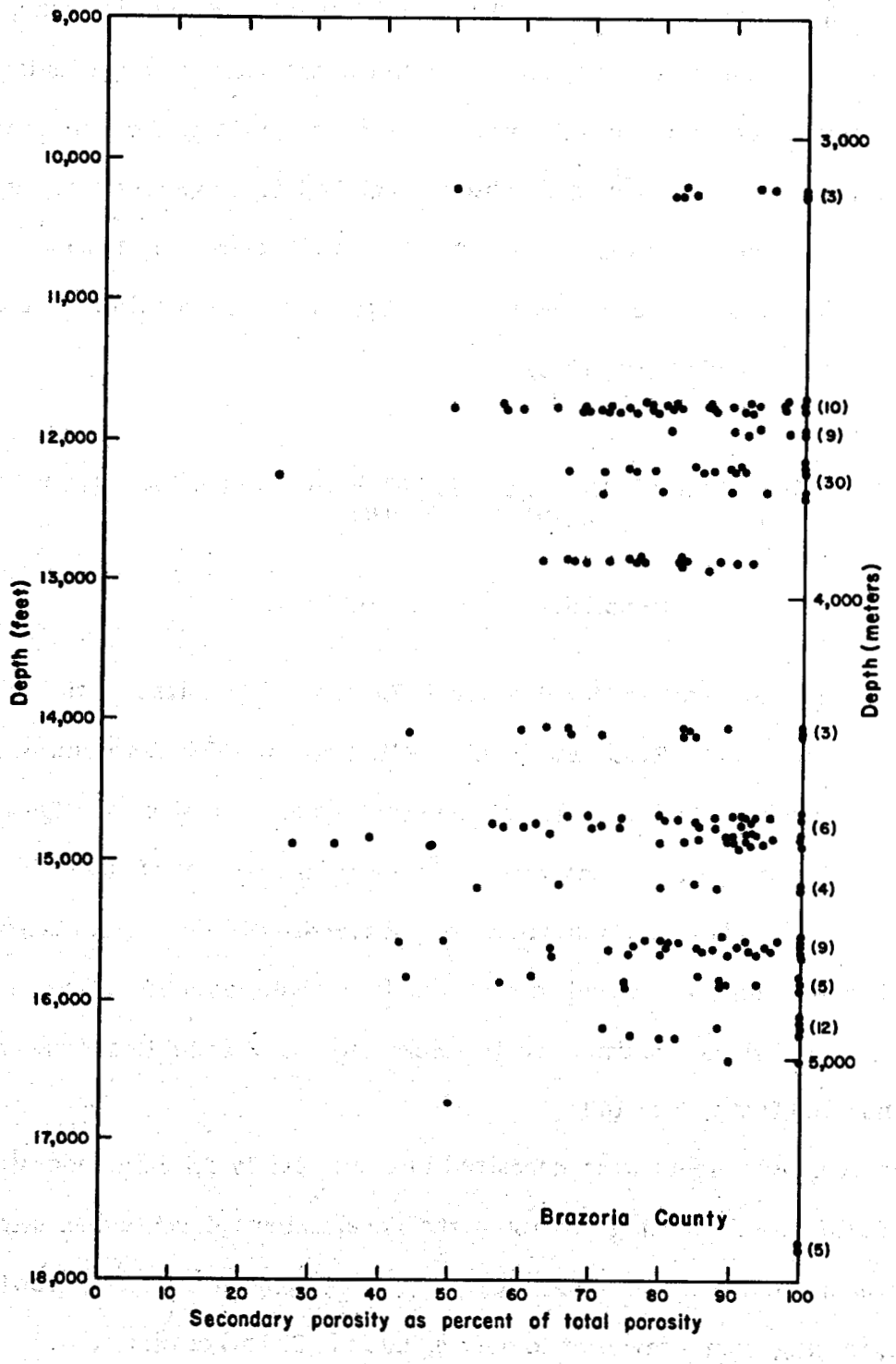

Figure 30. Secondary porosity as percent of total porosity versus depth for Brazoria County samples. Numbers in parentheses represent samples containing only secondary porosity.

geopressure (pressure gradients from 0.465 to 0.7 psi/ft). Within this zone, under the appropriate chemical conditions, formation fluids can dissolve pre-existing cements and may also directly leach feldspars and rock fragments. Where the resulting secondary porosity is not occluded subsequently by late-stage cements, high-quality geothermal reservoirs may exist at depth. Frio sandstones of Brazoria County have the highest potential for deep reservoir quality of all Texas Gulf Coast Tertiary sandstones (Bebout and others, 1978).

ANALYSIS OF VICKSBURG SANDSTONES, MC ALLEN RANCH FIELD, HIDALGO COUNTY

Depositional Systems and Structure

Vicksburg sediments in McAllen Ranch Field were deposited on the downdip side of a large growth fault (Ritch and Kozik, 1971; Loucks, 1978; Berg and others, 1979; Han, 1980). Sands in the lower part of the section were deposited as slightly elongate deltas. A major marine transgression followed deposition of the Vicksburg and deposited a mud-rich shelf to slope section above the deltaic sands. Volumetrically, sand bodies are minor compared to shales and the shale units effectively enclose the sandstones. Individual sandstone unit thicknesses vary from less than one foot to several hundred feet (0.3 to 100 m).

Vicksburg sediments were deposited into the rapidly subsiding ancestral Gulf of Mexico Basin. Rapid loading promoted the development of contemporaneous growth faults, which are the major structures present. Displacement along growth faults is variable, ranging from a few feet to over 4,000 ft (1,220 m) of offset.

External Controls on Reservoir Quality

Depth to the top of the geopressured zone, geothermal gradient, basinal hydrology, and pore fluid chemistry are the most important external variables influencing reservoir quality on a regional scale.

In McAllen Ranch Field, the top of the "hard" geopressured zone (0.7 psi/ft) is encountered at approximately 8,500 ft (2,590 m). Above the "hard" geopressured zone, the temperature increases with depth at a rate of 1.64°F/100 ft; the geothermal gradient increases to 2.92°F/100 ft within the "hard" geopressured regime (fig. 31).

Similarities in depositional and structural histories between Hidalgo County Vicksburg and Brazoria County Frio sandstones dictate similar basinal hydrologies.

Pore fluid data applicable to McAllen Ranch Field are not available. The corresponding section in the discussion of Frio sandstones from Brazoria County contains a summary of currently available information on pore fluids in Tertiary Gulf Coast sandstones.

Some studies have addressed the problem of water chemistry variations relative to depth, lithology, and structure, but few patterns have emerged. Kharaka and others (1977a) reported analyses that show generally decreasing subsurface salinities from the Louisiana Gulf Coast southward to Hidalgo County, Texas. They attribute the highest salinities to dissolution of salt domes.

Detrital Mineralogy and Texture

One-hundred-one stained Vicksburg thin sections from Hidalgo County, Texas, were point-counted (200 points per section). Sample selection was purposely biased toward coarsest grain size and lowest matrix content because a greater degree of diagenetic alteration typically characterizes coarser, more porous rocks.

Most Vicksburg sandstones examined are poorly to moderately sorted, fine-grained feldspathic volcanic arenites and lithic arkoses (classification of Folk, 1974), all with less than 30 percent quartz (fig. 32). The rock fragments consist of abundant caliche and volcanic rock fragments (VRF's). Sodium-rich plagioclase and VRF's constitute the majority of framework grains and occur in subequal amounts. The chemically unstable mineralogy of these sandstones contributed significantly to the

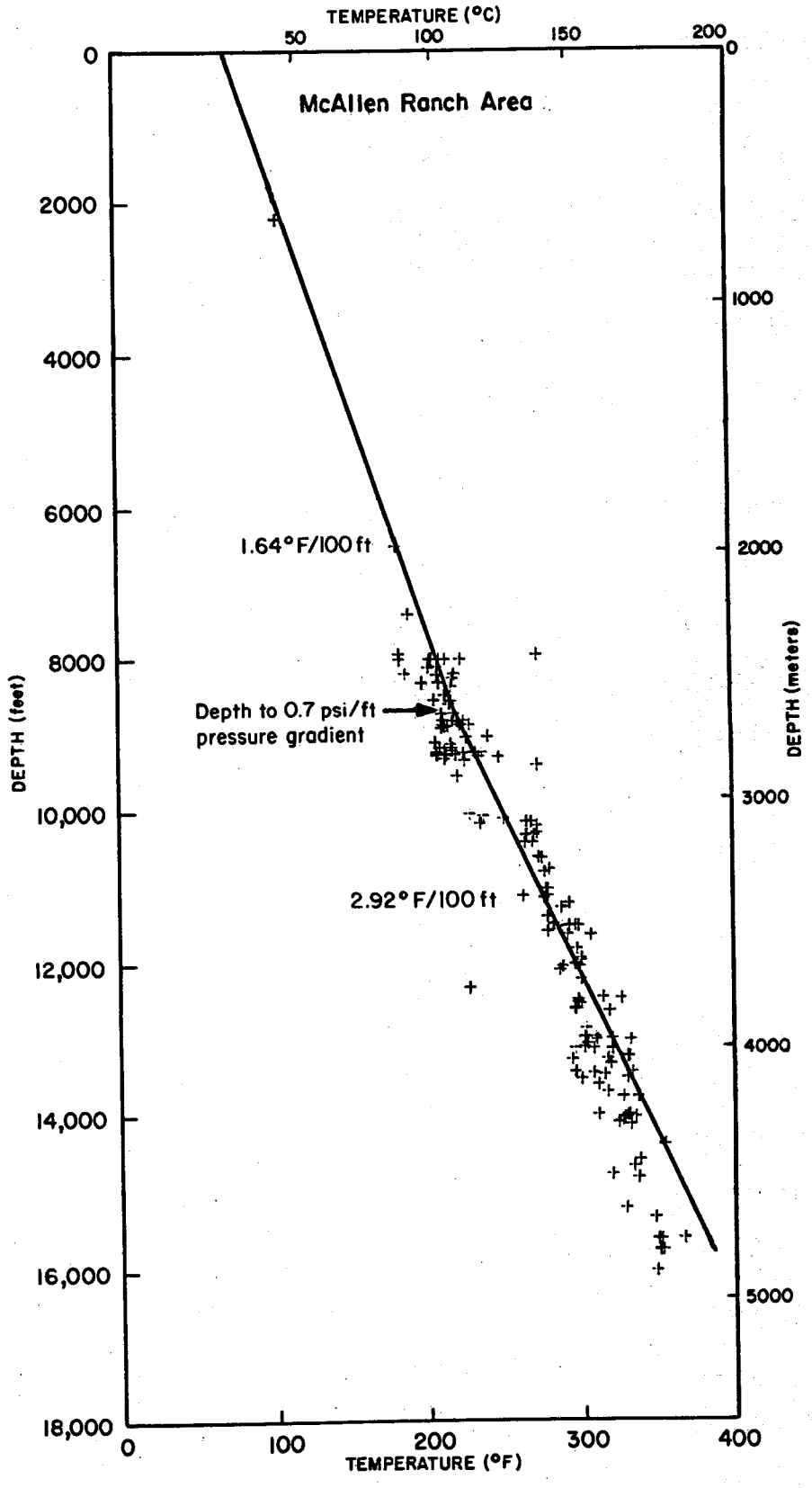

Figure 31. Temperature versus depth, McAllen Ranch area.

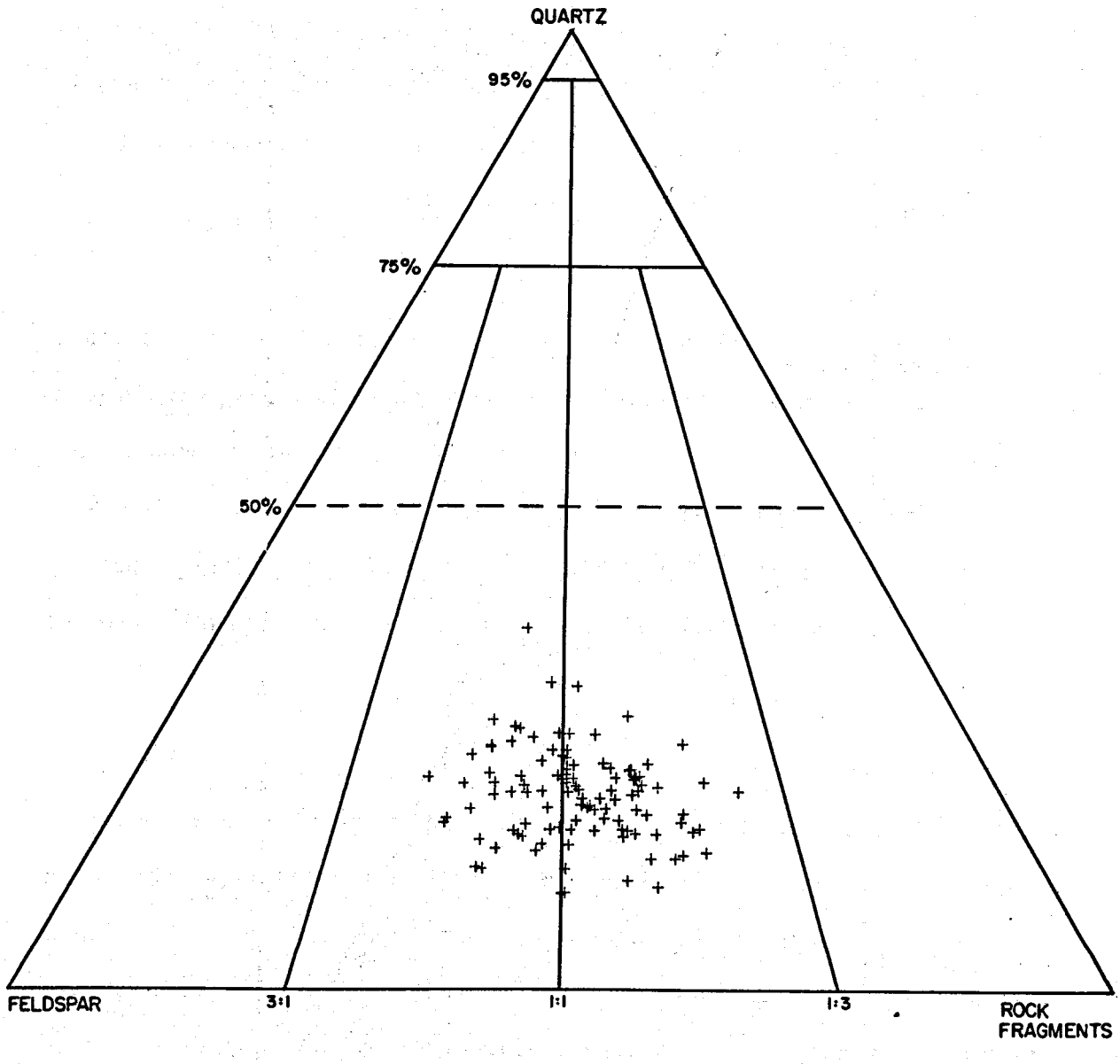

Figure 32. Primary detrital mineralogy, McAllen Ranch area.

extensive diagenetic modifications which occurred in this area. Detailed descriptions of the various detrital constituents follow.

Quartz

Detrital quartz content is less than 30 percent and averages approximately 15 percent. Volcanic quartz is the dominant variety, although common quartz is also abundant and a few metamorphic quartz grains were identified.

Feldspar

Plagioclase is the most abundant feldspar variety; detrital potassium feldspar grains were rarely encountered. As in Frio sandstones from Brazoria County, most of the plagioclase is albite. However, grains rarely exhibit typical albite twinning, and we suggest that the present compositions resulted from postdepositional albitization. Vacuolization and sericitization of plagioclase are the most common feldspar alterations; calcite-replaced and leached feldspars are additional, less frequently observed alteration types.

Rock Fragments

Volcanic rock fragments (VRF's) are the most abundant type occurring in Vicksburg sandstones (fig. 33). The abundance of VRF's in the Vicksburg reflects the extensive Tertiary volcanism that occurred in West Texas and Mexico. Original volcanic textures are generally well preserved in VRF's, and feldspar phenocrysts are easily recognized in many fragments. A few glassy rock fragments appear relatively fresh, although silicification of very fine grained VRF's is common. Other observed alterations of volcanic rock fragments include replacement by calcite and chlorite, leaching and alteration to clays. Pseudomatrix in Vicksburg sandstones is composed largely of clay-altered VRF's.

Carbonate rock fragments (CRF's), which are dominantly microspar, are present in variable amounts up to 12 percent. Lindquist (1977) suggested that these clasts

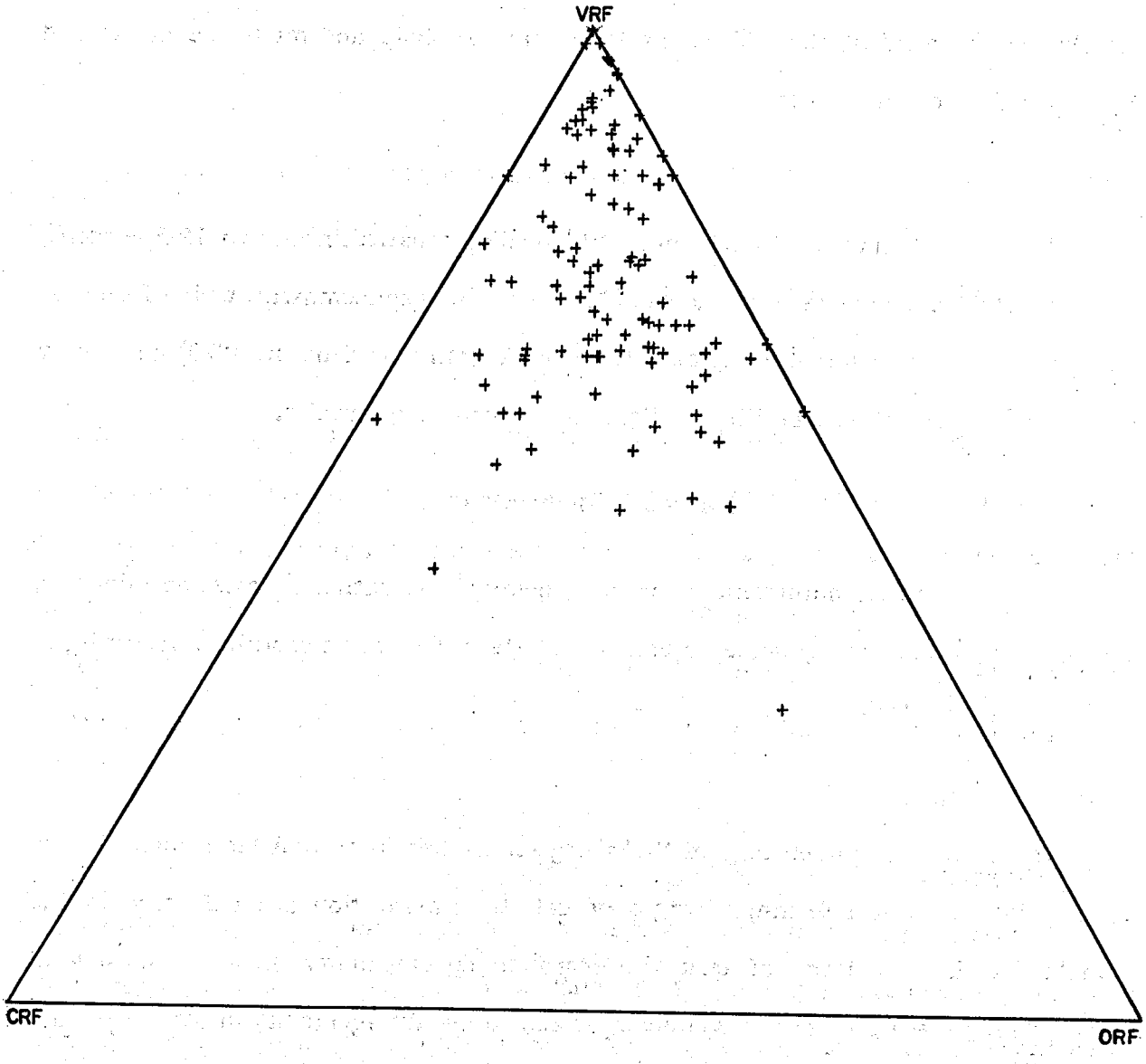

Figure 33. Rock fragment types, McAllen Ranch area. (VRF=volcanic rock fragment; CRF=carbonate rock fragment; ORF=other rock fragments.) VRF's are the dominant rock fragment type and contribute to the overall chemical and mechanical instability of Vicksburg sandstones.

were derived from calichified Oligocene soils rather than from a Cretaceous carbonate source. Less abundant rock fragment types include shale and mudstone clasts and metamorphic rock fragments.

Matrix

Depositional matrix can be important locally, constituting up to 18.5 percent, but it is a minor constituent in the samples selected. Pseudomatrix, which forms by deformation of mechanically unstable framework grains (Dickinson, 1970) commonly reduces porosity and permeability of Vicksburg sandstone reservoirs.

Diagenetic Modification

Development of authigenic minerals, chemical alteration of existing minerals, and leaching of chemically unstable grains constitute diagenetic reactions occurring in Vicksburg sandstones.

Authigenic Minerals

The authigenic mineralogy of Vicksburg sandstones from McAllen Ranch Field is highly diverse. Multiple major stages of calcite cementation are reflected in the samples, as is an episode of quartz overgrowth development. In addition, several minor cements are preserved. Kaolinite, which forms authigenically in other Tertiary sandstones of the Texas Gulf Coast (Loucks and others, 1979), is conspicuously absent from all sandstones examined. The absence of kaolinite is one line of evidence suggesting that the chemistry of formation waters in the Vicksburg of McAllen Ranch Field was distinctly different from that of waters in other Tertiary sandstones where good quality deep reservoirs developed (for example, Frio sandstone reservoirs in Brazoria County, Texas).

Calcite

Calcite is the most abundant authigenic constituent in Vicksburg sandstones. The presence of several calcite phases reflects a multistage diagenetic history. Both

ferroan and non-ferroan calcite are present as poikilotopic and sparry cements and as grain replacements. However, temporal relationships between coexisting phases are unclear and in some cases cannot be deciphered unequivocally by petrographic means. Ferroan and non-ferroan calcite grain replacements and cements can all be present within a single thin section.

Quartz

Authigenic quartz is present as overgrowths on detrital quartz grains. Although these overgrowths are ubiquitous in the Vicksburg samples, they form a volumetrically minor part of the cements and therefore do not occlude porosity significantly.

Minor Authigenic Minerals

A minor authigenic constituent has been identified as aluminum-bearing sphene on the basis of microprobe analysis. Comprising up to 2 percent of some sandstones, sphene occurs as a replacement of VRF's and plagioclase as well as a pore-filling mineral. The optical properties are abnormal for sphene. Birefringence is only upper second order, and characteristic rhombic cross sections are rare. It occurs mainly as granular aggregates of anhedral crystals, although a few euhedral crystals were observed in secondary pores (fig. 34).

Feldspar (albite) overgrowths, chlorite rims, and poikilotopic zeolite cement are other minor authigenic components present in Vicksburg sandstones. In general, distribution of these authigenic constituents is sporadic; concentrations of a particular constituent occur in distinct zones and, in some cases, may be restricted to certain wells. Well-developed albite overgrowths are prominent in a number of Vicksburg sandstone samples from the eastern section of McAllen Ranch Field. Overgrowths are seldom in optical continuity with host grains but are occasionally twinned (fig. 35). Chlorite rims and pore-filling cement are present in several samples below 10,000 ft (3,050 m) and are exceptionally well developed in a number of samples taken below 12,500 ft (3,810 m) in Forest Oil Nos. 9 and 10 McAllen wells. The delicate structure

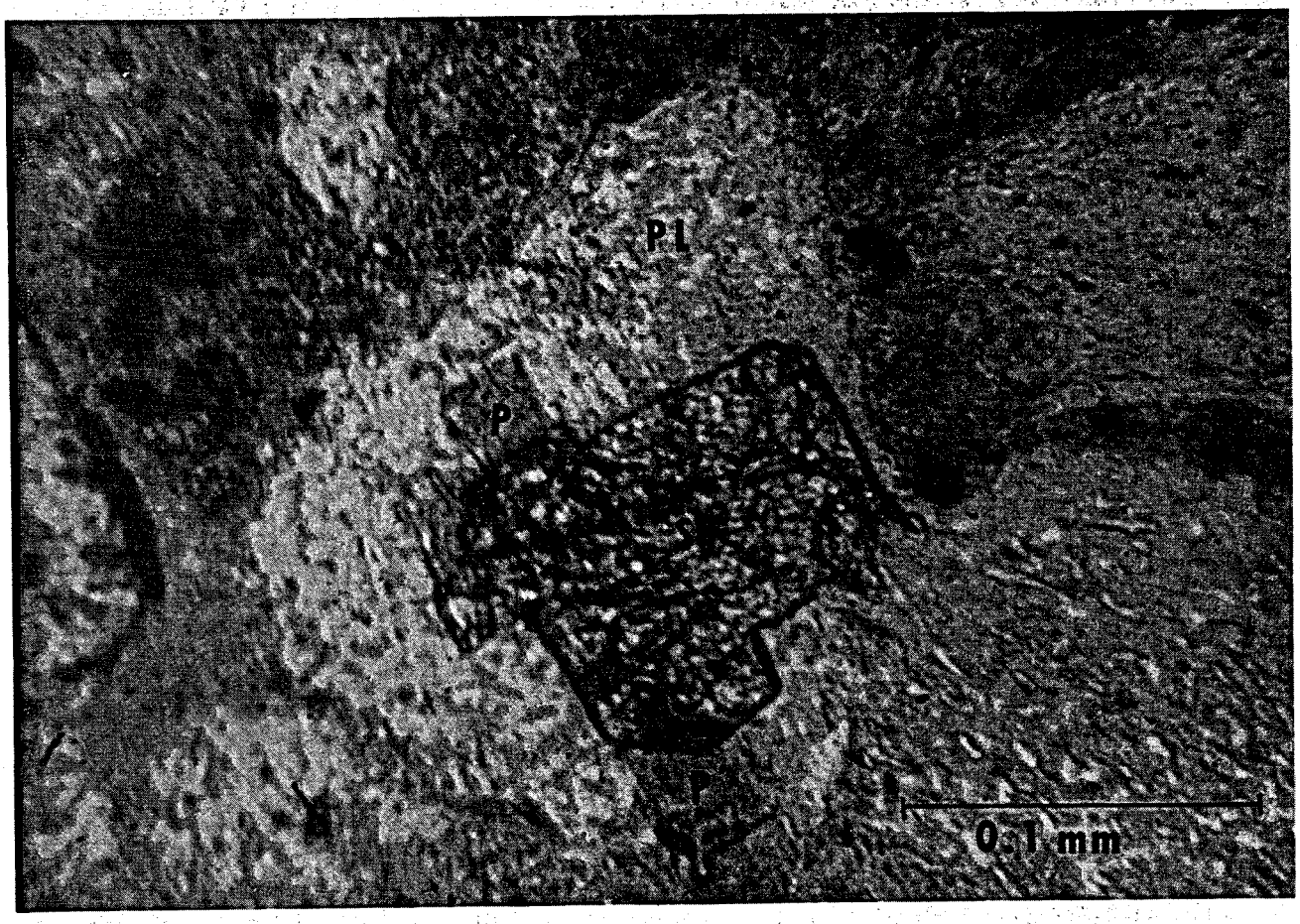

Figure 34. Authigenic sphene (S) in plagioclase (PL) partly filling a secondary pore (P). Plane polarized light.

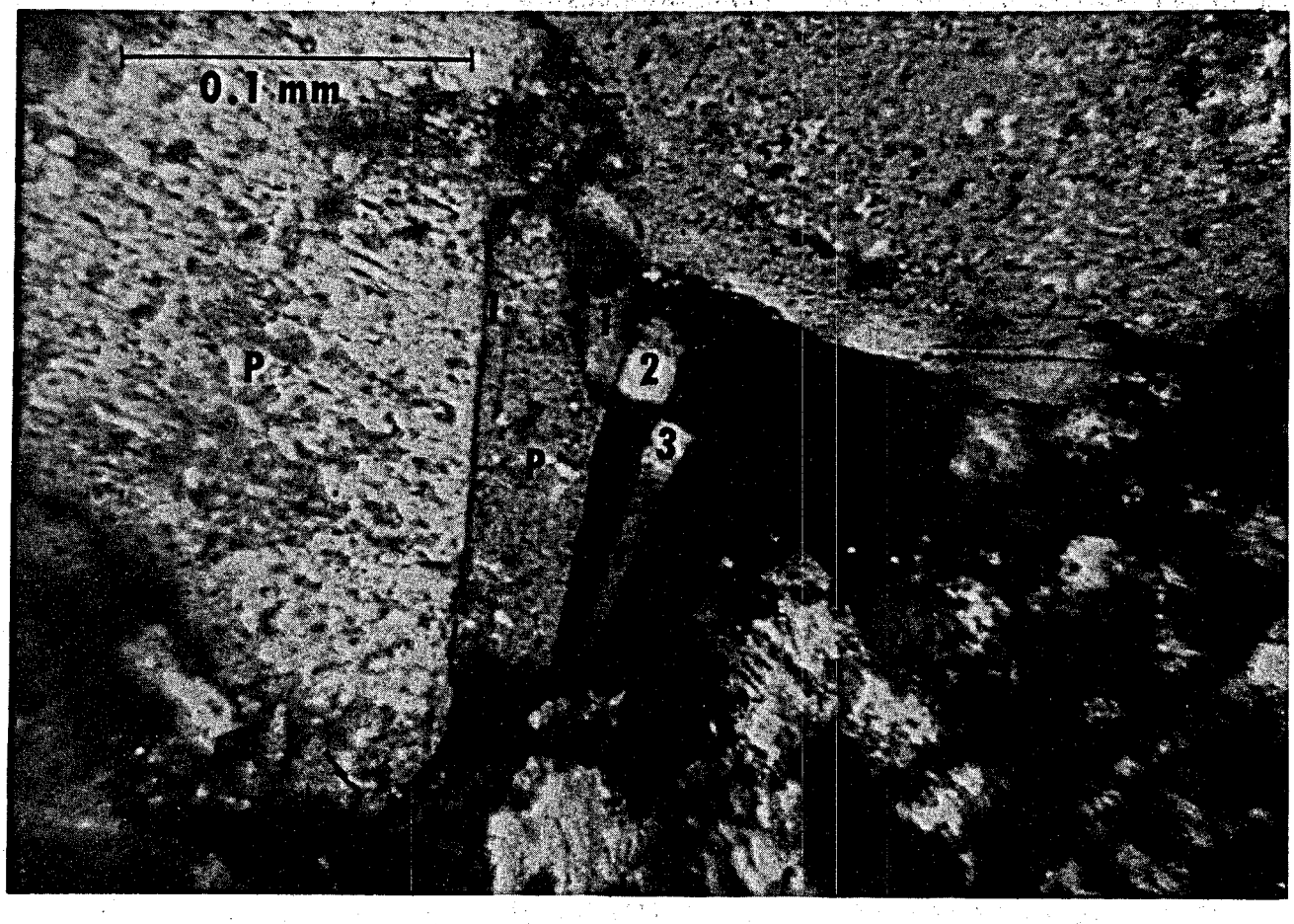

Figure 35. Multiple twinned plagioclase overgrowths on detrital plagioclase (P). Crossed polars.

of the chlorite rims attests to their authigenic nature (figs. 36 and 37). Poikilotopic zeolite cement and grain replacements occur in samples from four of the wells studied (figs. 38 and 39). This zeolite was first identified as laumontite by X-ray analysis and identification was subsequently confirmed by SEM equipped with an energy dispersive analyzer. Particularly good examples are preserved in samples from 9,600 to 9,700 ft (2,925 to 2,955 m) in Shell Nos. 6 and 8 Woods-Christian wells and from approximately 11,060 ft (3,370 m) in the Shell No. 7 Woods-Christian well. Overall, laumontite cementation is volumetrically insignificant, but in the restricted zones where it occurs, it is a major inhibitor of porosity and it may constitute as much as 17 percent of the sample.

Porosity Types

Primary porosity may be significant at depths less than 3,000 ft (900 m). However, in deeper samples, interval transit times decrease sharply, suggesting extensive cementation. Thus, in matrix-free sandstones below 3,000 ft (900 m), secondary porosity is the dominant porosity type (fig. 40). At depths suitable for geopressured geothermal energy production, however, most of this secondary porosity has been occluded by late-stage carbonate cements.

Minor Element Chemistry

Authigenic calcite cement and grain replacements in three Vicksburg samples from McAllen Ranch Field were analyzed for MgO, SrO, CaO, MnO, and FeO by electron microprobe. The results are tabulated in Appendix D. A review of these data reveals the existence of at least three distinctive calcite generations and supports our views on the near continuous nature of alternate precipitation and leaching episodes. Detrital feldspars were analyzed in five Vicksburg samples. As in Frio samples from Brazoria County, their present compositions are albite. The major source of detrital plagioclase in Vicksburg sandstones in South Texas is the area of Tertiary volcanics in

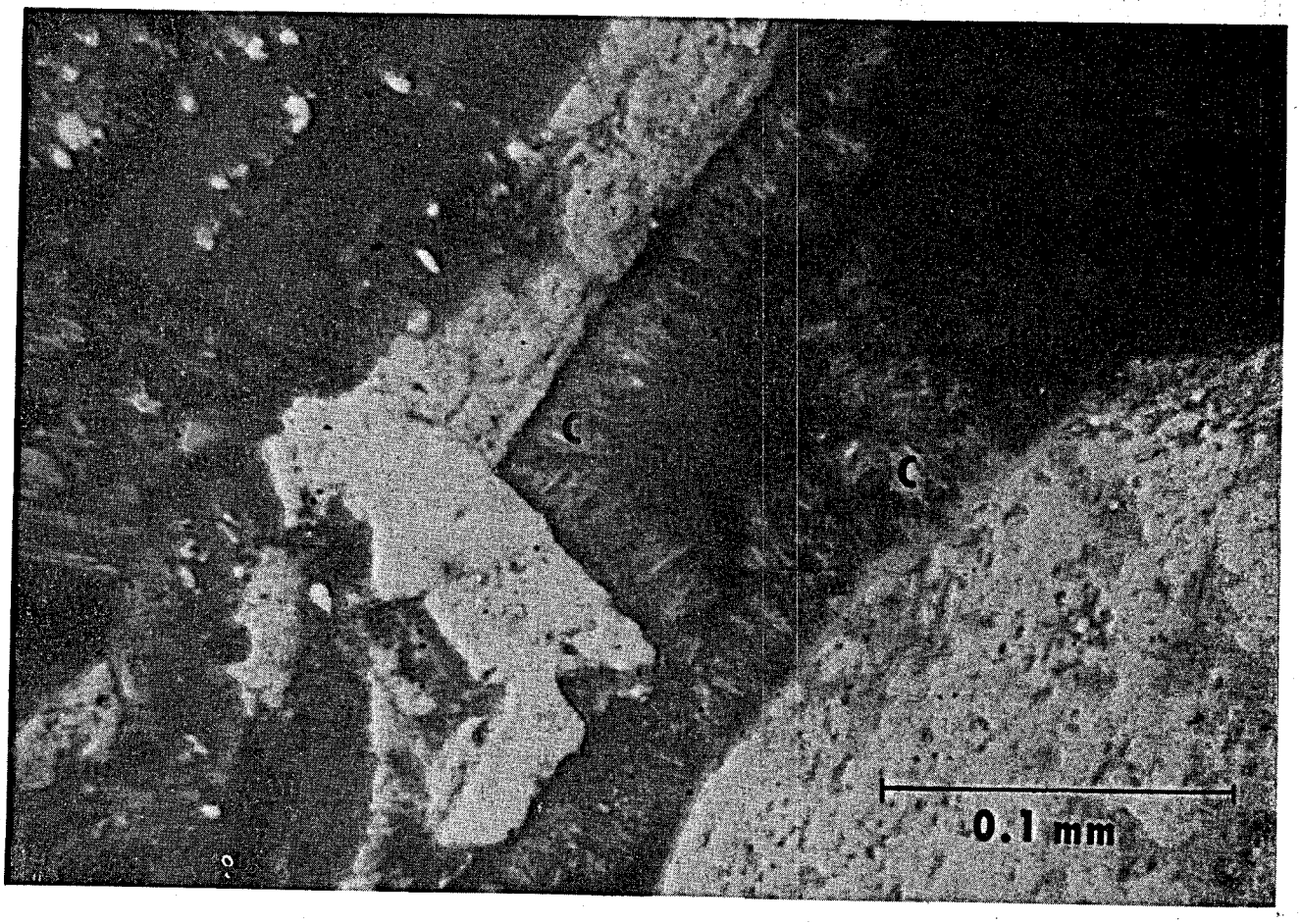

Figure 36. Authigenic chlorite (C) as rims on detrital grains. Crossed polars.

Figure 37. SEM photograph of chlorite cement (C).

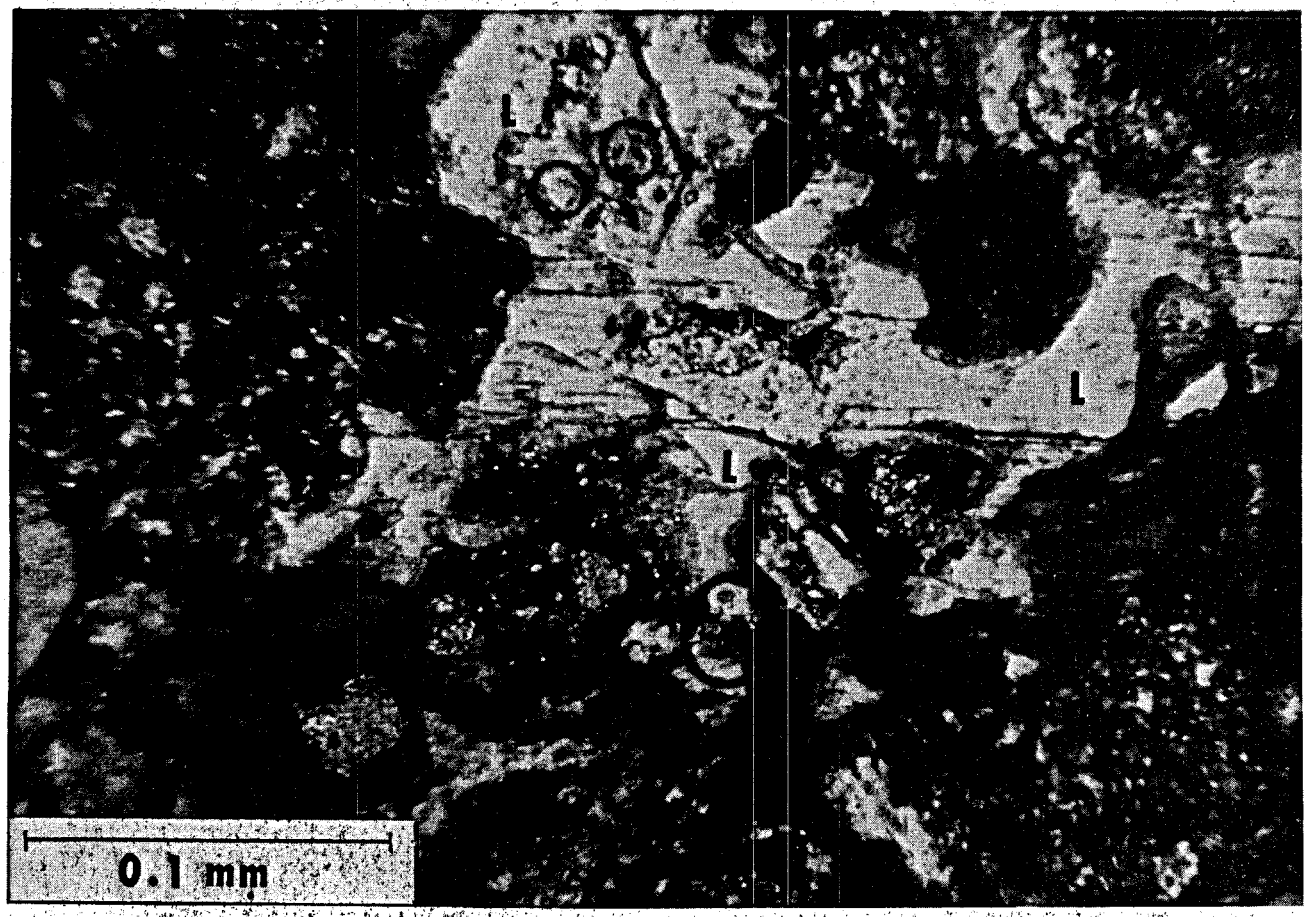

Figure 38. Poikilotopic laumontite cement (L). Crossed polars.

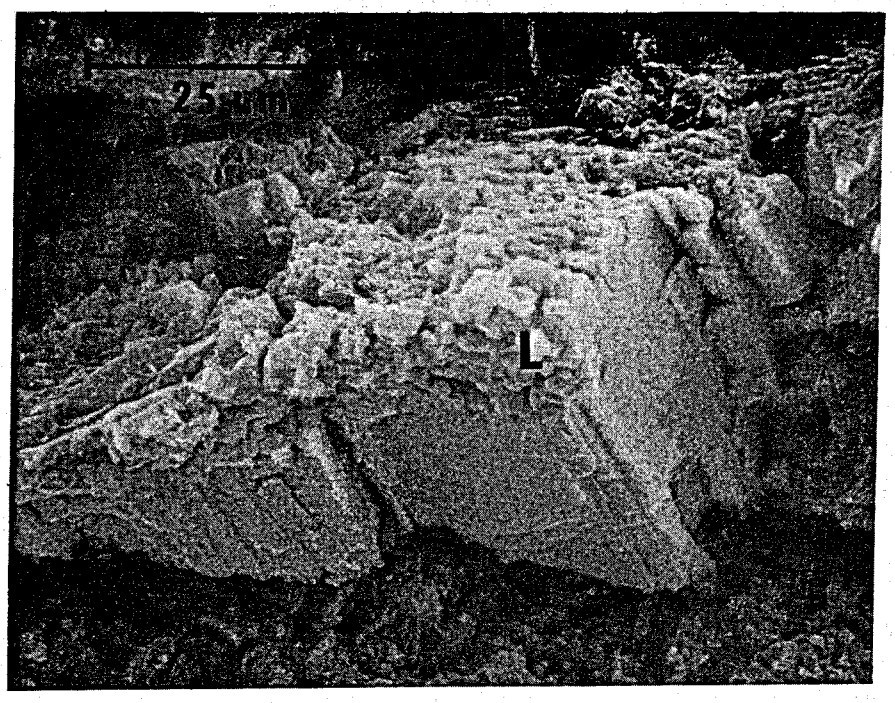

Figure 39. SEM photograph of laumontite (L).

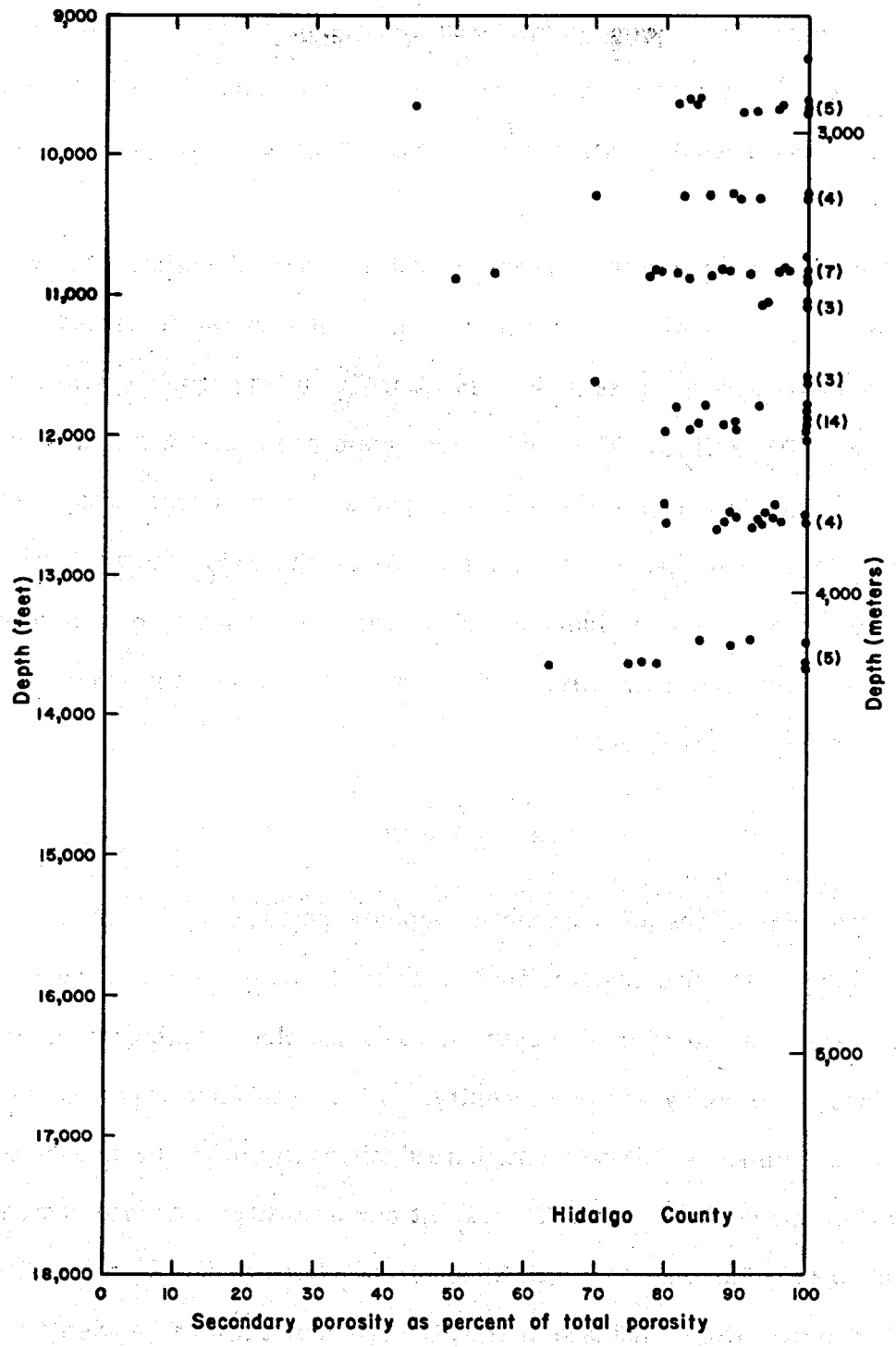

Figure 40. Secondary porosity as percent of total porosity versus depth for Hidalgo County samples. Numbers in parentheses represent samples containing only secondary porosity.

West Texas. Plagioclase in the source area generally has compositions in the range An_{20} - An_{40} (C. D. Henry, oral communication, 1979). Thus, it seems certain that extensive postdepositional albitization is responsible for the present plagioclase compositions.

In addition to analyzing the carbonates and feldspars, the microprobe was used to identify positively two authigenic minerals. The first mineral occurs as poikilotopic cement in some Vicksburg samples and was identified as laumontite, with the formula $Ca_{0.9}(Al_{1.9}Si_{4.1}O_{12})\cdot 4H_2O$. The second authigenic phase exhibits optical properties that are somewhat unusual for this mineral species. The mineral was identified by microprobe as aluminous sphene with the formula $Ca(Ti_{0.7}Al_{0.3})\ SiO_3$. Such varieties of sphene containing abundant aluminum substituting for titanium are characterized by lower birefringence and refractive indices than the more common pure titanium varieties (Deer and others, 1966).

Reservoir Quality

Multiple generations of carbonate cement are represented in the sandstone samples examined. Calcite cements formed early in the diagenetic sequence and are present in variable amounts in all depth intervals sampled. Authigenic calcite is the major inhibitor of porosity and permeability. Other authigenic replacement minerals and cements are minor and do not contribute significantly to the poor reservoir quality of the McAllen Ranch Field wells. The extent and intensity of calcite cementation do not appear to be related to the abundance of carbonate rock fragments (CRF's), and petrographic observations indicate that CRF's did not serve as nucleation sites for incipient calcite precipitation. The abundance of CRF's (caliche clasts) does, however, indicate that the chemical environment was rich in carbonate at the time of Vicksburg sandstone deposition. Apparently, the formation waters remained carbonate-rich throughout most of the sandstones' burial history. Calcite-cemented zones interfinger

with discrete zones containing abundant secondary porosity. We believe that with increasing depth of burial, the sandstone bodies moved through a succession of geochemical environments where some preexisting calcites were leached and new calcites were precipitated. Unfortunately, from a reservoir quality standpoint, calcite precipitation and preservation were far more extensive than calcite leaching, and ferroan calcite cement formed late in the diagenetic sequence occluded most deep secondary porosity Considerable secondary porosity is preserved in zones that were not affected by this late calcite. However, these zones are isolated and do not appear to be volumetrically significant. Even where calcite cements are absent or minimally developed, the chemically unstable detrital mineralogy of the McAllen Ranch Field sandstones contributes significantly to occlusion of porosity and permeability through the formation of pseudomatrix.

PHYSICAL FACTORS CONTROLLING RESERVOIR QUALITY

McAllen Ranch and Chocolate Bayou/Danbury Dome areas have similar structural and depositional styles as well as fluid flow histories. Differences between the two areas are mineralogy, depth to geopressure, and temperature gradient. These differences are responsible for the contrasting reservoir quality in the two areas.

Detrital mineralogy is determined primarily by the mineralogy of the source area. Differences in detrital compositions of sandstones may simply be due to different source areas. Alternatively, different detrital mineral assemblages can be produced from a common source, given sufficiently different climatic conditions and distance along alternate paths of transport from the source.

Climates during Oligocene Vicksburg and Frio deposition were similar to climates along the Texas coast today (Galloway, 1977; Loucks and others, 1979). The Lower Texas Gulf Coast area was arid; the Upper Texas Gulf Coast area was humid.

The arid climate in the Lower Texas Gulf Coast produced soil caliches (Lindquist, 1977; Galloway, 1977) and favored preservation of volcanic rock fragments (VFR's) during transport. Hence, the lower Texas Vicksburg contains a large proportion of chemically unstable rock fragments. Soil caliches could not form in the more humid climate of the Upper Texas Gulf Coast and detrital grains underwent more extensive chemical degradation during transport. Therefore, Frio sandstones in the Upper Texas Gulf Coast are characterized by a more chemically stable mineral assemblage.

The major source area of Vicksburg sediments in McAllen Ranch Field was the Trans-Pecos region of West Texas and Mexico (Loucks and others, 1979). Extensive volcanism during Vicksburg time contributed volcanic rock fragments, volcanic quartz, feldspars, and glass shards to the sandstones. Glass shards and volcanic ash altered to smectite, which is the major clay component in the system. The Rocky Mountain area may have been the source of some metamorphic rock fragments. Soil caliche local to the area of deposition was the source of carbonate rock fragments.

The Rocky Mountain area may have been a source for the Frio sandstones in the Chocolate Bayou/Danbury Dome area. This area contains a variety of sedimentary, metamorphic, and probably some volcanic rock types. Some volcanic rock fragments (VRF's) were probably derived from the West Texas area, and abundant volcanic ash from West Texas contributed to the formation of smectite clays.

The greater chemical and mechanical instability of the grain assemblage in the Lower Texas Gulf Coast as compared to the Upper Texas Gulf Coast contributed to extensive cementation of Vicksburg sediments, resulting in poor reservoir quality, especially at depths necessary for geothermal reservoirs. As pointed out by Loucks and others (1979), a relatively stable mineral assemblage is necessary to preserve high quality reservoirs in the deep subsurface. Twenty to thirty percent unstable components favors the development of secondary reservoirs. Unstable grains such as

feldspars dissolve, creating secondary porosity. However, if the percentage of unstable grains is too high, as in the Lower Texas Gulf Coast, the system becomes choked with cement and secondary porosity is destroyed.

Depth to the top of geopressure, and hence to the inflection in geothermal gradient, differs in the two study areas. In the Chocolate Bayou/Danbury Dome area the occurrence of "hard" geopressure is deeper (11,000 ft or 3,350 m, approximately) than in the McAllen Ranch area (8,500 ft or 2,590 m, approximately). In addition, geothermal gradients in the Chocolate Bayou/Danbury Dome area are less than in the McAllen Ranch area. Together, these two factors (depth to top of geopressure and geothermal gradients) result in overall higher temperatures at any particular depth in the Lower Texas Gulf Coast area. This in turn influences the depth at which the temperature-dependent smectite/illite transformation occurs (Appendix A).

EFFECTS OF DIAGENESIS AND BULK CHEMISTRY OF PELITIC SEDIMENTS

Tertiary sediments along the Texas Gulf Coast are mainly pelitic (mudstones and shales). Sandstones are common but are only locally abundant. Sandstones were emphasized in past geothermal studies because they are the potential reservoir rocks. To understand the diagenetic system, however, both sandstones and associated pelitic rocks must be studied.

A major question in the study of Gulf Coast diagenesis is whether pelitic rocks represent an open or a closed chemical system relative to associated sandstones. In other words, do chemical reactions within the shales produce ions that subsequently precipitate as authigenic phases in the sandstones? Published findings pertinent to this question are contradictory. Hower and others (1976) found that authigenic products in shales could account for most ions released by clay mineral transitions, requiring no transport of these materials into sandstones. Land and Dutton (1978), however, documented the quantities of silica required for sandstone cementation and concluded

that the large amounts required can only come from shales. Boles and Franks (1979) suggested that quantities of materials released from shales are small relative to amounts produced by clay reactions and that the material loss from shales is therefore not readily detected.

Argillaceous sediments from two wells in each of Brazoria and Hidalgo Counties were analyzed for this study. We outlined depth-related changes in mineralogy and bulk chemistry of the pelitic sediments and attempted to correlate these changes with diagenetic features in associated sandstones. Other studies along the Gulf Coast (Burst, 1969; Perry and Hower, 1970; Hower and others, 1976; Yeh and Savin, 1977), have included similar analyses of pelitic sediments but their conclusions were based solely on the pelitic system. They did not postulate the effects of clay diagenesis on the sandstone system. An exception is the study by Boles and Franks (1979) of the effects of clay diagenesis on cementation in Wilcox sandstones in the Lower Texas Gulf Coast. However, the argillaceous system in the Wilcox Group is different from the systems in Vicksburg and Frio Formations (Perry and Hower, 1970; this study) and results should be extrapolated with caution.

Our discussion will be confined to the major aspects of diagenesis in pelitic sediments as they relate to observed diagenetic features in associated sandstones. A material balance calculation within the pelitic sediments or between the pelitic sediments and the sandstones will not be attempted because our data are not sufficiently quantitative.

Smectite/Illite Transformation

Chemical Reaction

Mixed-layer smectite undergoes transformation to mixed-layer illite as temperatures and pressures increase with burial (Weaver, 1958; Burst, 1969; de Segonzac, 1970; Perry and Hower, 1970; Weaver and Beck, 1971; Schmidt, 1973; Hower and others,

1976; Boles and Franks, 1979). The transformation of smectite to illite is potentially important if water and ions released by this reaction migrate into the sandstones where they may affect diagenesis.

Boles and Franks (1979) discussed the role of aluminum in the smectite-illite transition. Using clay mineral formulas from Hower and others (1976) they show that reactions with aluminum as an immobile component release significantly greater amounts of cations (most notably, silica release increases more than five times) relative to reactions in which aluminum is considered a mobile component.

Burst (1969) calculated the amount of interlayer water expelled during clay diagenesis as 10 to 15 percent of the compacted bulk volume of the argillaceous sediments. This is a large volume of water, given the high ratio of argillaceous sediment to permeable sand beds in the Gulf Coast Basin. This water is thought to be less saline than the normal brines within the sandstone units. Expulsion of compaction waters transports cations released in the smectite-illite transition into the sandstones where they may precipitate as authigenic phases.

Timing and Depth of Occurrence

The transformation of randomly interlayered smectite to ordered mixed-layered illite is mainly temperature controlled (Burst, 1969; Perry and Hower, 1970; Hower and others, 1976; this study). In the Lower Texas Gulf Coast where the geothermal gradient is higher, the transformation to strongly ordered interlayering occurs at a lesser depth (7,500 to 9,000 ft; 2,290 to 2,740 m) than in the Upper Texas Gulf Coast (11,200 to 11,750 ft; 3,415 to 3,580 m) where the geothermal gradient is lower. However, other factors also influence the transformation because it occurs at temperatures 25° to 30°C higher in Brazoria County than in Hidalgo County (Appendix A). The variation in the temperature of transformation in these two areas may result from differences in pore fluid pressure or differences in primary detrital mineralogy (that is, original ratio of smectite to illite). Another possibility is that the

geothermal gradients in the two areas have not been constant throughout geologic history (see Bonham, 1980).

In the Gulf Coast area, an empirical relationship exists between the occurrence of illite/smectite transformation and the top of "hard" geopressure (geopressure as defined by resistivity plots) (Burst, 1969; Schmidt, 1973; this study). Some workers feel that clay transformation creates geopressure (Powers, 1967; Foster and Custard, 1980), whereas others feel that the relationship is coincidental (Magara, 1975). Our data indicate that the transformation is related to the top of geopressure. This relationship is likely due to a thermal seal created by undercompacted shale in the geopressured zone. The temperature-dependent smectite to illite transformation occurs near the zone of increased thermal gradient produced by this thermal seal (Magara, 1975).

Van Olphen (1963) has shown that lithostatic pressure alone cannot be responsible for removal of interlayer water from clays, but rather, it must act with temperature to expel water. However, in a geopressured system lithostatic pressure is reduced and fluid pressure increases. Fluid pressure inhibits the expulsion of interlayer water. The quantitative effects of pressure on clay transformation are not well understood and deserve more study.

Another possible control on the smectite-illite transformation is the original ratio of smectite to illite layers in the mixed layered clays and/or other differences in detrital mineralogy. Ordering in the clay does not occur until the mixture is 60 percent or more illite (Appendix A). It is probable that the higher the percentage of illite in the pelitic sediment at the time of deposition the lower the temperature needed for the transformation to occur.

Oxide Analyses of Pelitic Rocks

Pelitic rocks were analyzed for CaO, K_2O, Al_2O_3, Na_2O, MgO, and Fe_2O_3 to determine whether shales behave as open or closed systems relative to associated

sandstones. The samples analyzed were composed of the less than 177 micron size fraction. Subdivision into narrower size fractions was not attempted because we were interested only in general trends. Unfortunately, the silica analysis techniques we used did not yield reproducible results. Therefore, trends with depth shown in figures 41 through 44 are based on ratios of the various oxides to Al_2O_3. Because we assume that aluminum behaves as an immobile constituent in the smectite-illite transition, and is therefore confined to the pelitic system, oxide ratios normalized to Al_2O_3 should give trends with depth that are actually related to losses and gains in the shales. In addition to the observation that assuming aluminum immobility maximizes the number of cations released (Boles and Franks, 1979) the fact that Al_2O_3 varies directly with the amount of clay (Perry and Hower, 1970) supports the contention that aluminum is relatively immobile. Any significant trends with depth will bear on the question of open or closed sandstone/shale systems.

CaO

The ratio of the CaO to Al_2O_3 shows the most variable trend with depth. In the two Brazoria County wells the maximum absolute values and the maximum range of values are found above 10,000 ft (3,050 m). Below this depth both the CaO content and its variability decrease. Three explanations for this trend can be offered.

1. The shale system is open with respect to calcium and loses calcium to the sandstones below 10,000 ft (3,050 m). Petrographic analyses of sandstones from corresponding depths do not support this possibility because calcite cements decrease with depth.
2. The shale system is open with respect to calcium, and above 10,000 ft (3,050 m) receives calcium that is recycled from the leached sandstones lower in the section (leaching is extensive in Frio sandstones from Brazoria County).

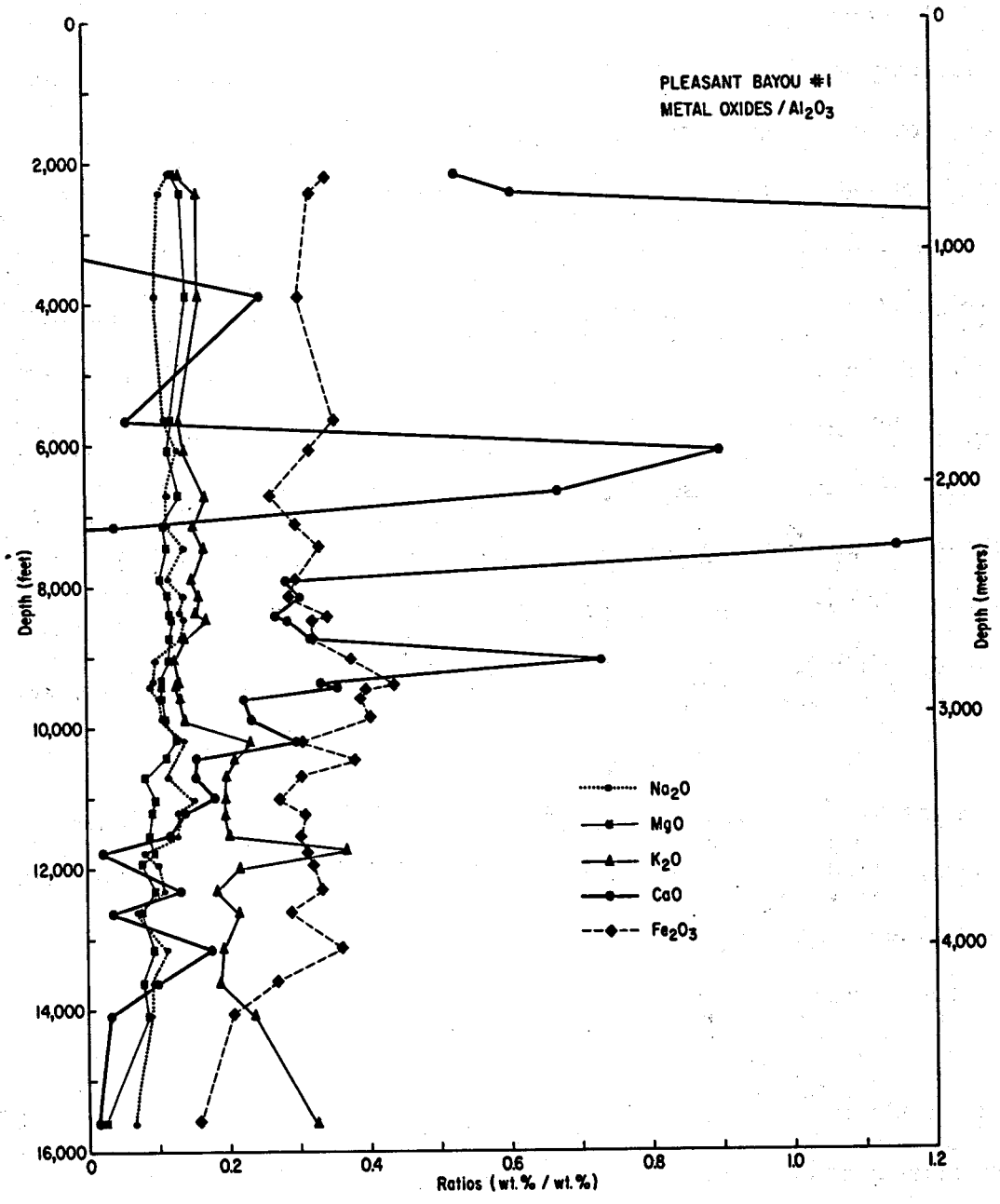

Figure 41. Oxide trends with depth, Pleasant Bayou No. 1, Brazoria County.

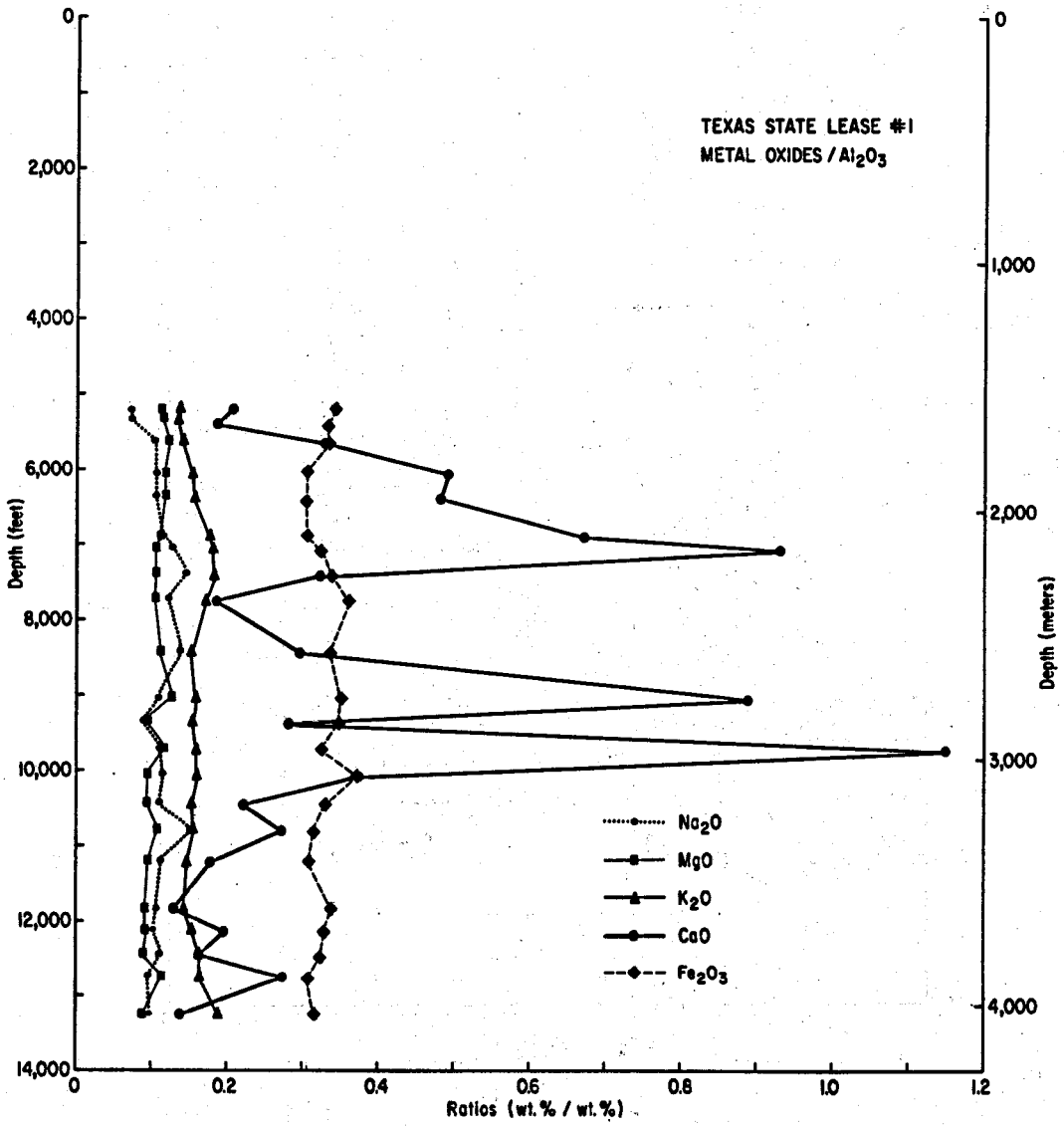

Figure 42. Oxide trends with depth, Texas State Lease No. 1, Brazoria County.

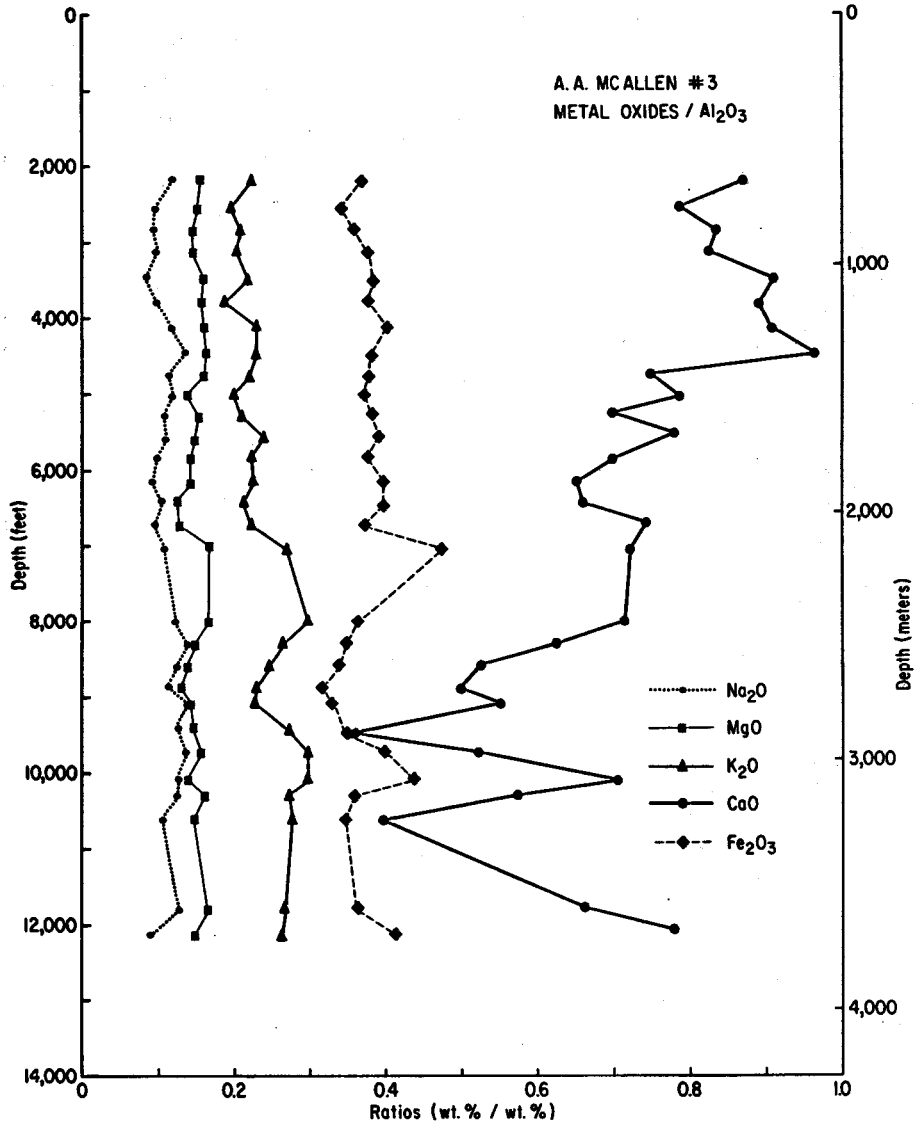

Figure 43. Oxide trends with depth, A. A. McAllen No. 3, Hidalgo County.

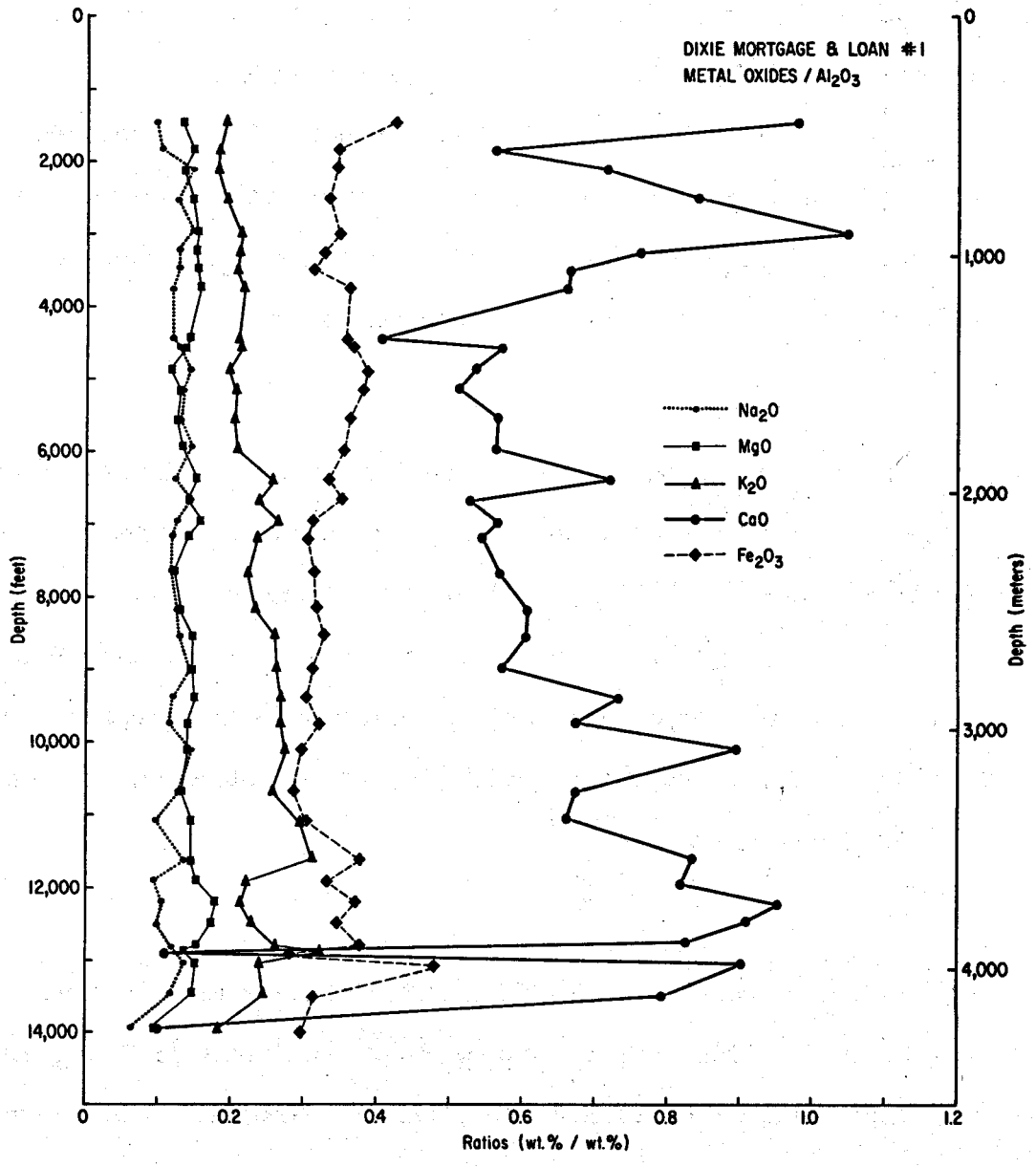

Figure 44. Oxide trends with depth, Dixie Mortgage and Loan No. 1, Hidalgo County.

3. The shales are closed systems with respect to calcium, and differences in CaO reflect primary differences in shale mineralogy (for example, sporadic concentrations of shell debris). This explanation is supported by the sporadic occurrence of the high CaO/Al_2O_3 values above 10,000 ft (3,050 m).

Overwhelming evidence in support of either explanation 2 or 3 is not found in the data. No trends in CaO are observed in the Hidalgo County wells. This indicates that either Hidalgo County shales are closed systems or loss of calcium from these shales cannot be detected due to the high total calcite concentration.

K_2O

A slight increase in K_2O was observed in one well in Brazoria County. A plot of K_2O versus percent expandable layers in the clays for the same well shows that K_2O varies directly with the amount of illite. Two of the three remaining wells show a similar trend. This suggests that potassium must be added to the system. Potassium may be derived from the coarse fraction of the pelitic rocks that was not analyzed, thus making the shales closed systems with respect to potassium, or from the sandstones if the shales are open.

Fe_2O_3

Fe_2O_3 decreases slightly below 13,000 ft (3,960 m) in one Brazoria County well. The other wells show no trend with this oxide. Boles and Franks (1979) suggest that iron derived from smectite is responsible for high iron contents in late carbonate cements. However the most recent authigenic carbonates in the well that shows loss of Fe_2O_3 are iron poor. A few other wells in the Brazoria area have minor amounts of iron-rich carbonates, but the timing of precipitation of these phases is obscure and these phases are mostly associated with iron-rich grains such as glauconite. Thus differences in Fe_2O_3 in the one well which shows a trend are probably due to original differences in mineralogy and there is no evidence in these data that the shales are open with respect to iron.

MgO and Na_2O

No trends with depth for these oxides were observed in any of the four wells studied. Internal recycling of these components seems likely.

Summary

There is little evidence in the oxide data to support the contention that the shales are open systems with respect to the sandstones. Data for CaO and K_2O are the most suggestive of an open pelitic system, but trends in these data are open to multiple interpretations. The large quantities of cations required for sandstone diagenesis, however, seemingly must come from shales (Land and Dutton, 1978; Boles and Franks, 1979). The absence of trends in our data does not exclude the possibility suggested by Boles and Franks (1979) that the relative volume of shales to sandstones is so great that material loss too small to be detected in oxide analyses of pelitic rocks may still be significant in sandstone diagenesis. In fact, X-ray data obtained by Freed (Appendix A) on shale samples from the same wells in Brazoria County suggest that mixed-layer clays release silica, carbonate, iron, and magnesium during transformation to the ordered illite-rich structure. In Hidalgo County, however, exchange was more limited, probably restricted to silica. Iron and magnesium released by the clay transformation were used in situ to form authigenic chlorite (Appendix A). Until sufficient data are generated on both sandstones and shales to permit mass balance calculations of a highly quantitative nature (including oxide analyses complete with silica data and mineral phase distribution data), this problem cannot be resolved.

COMPARISON OF DIAGENETIC SEQUENCES

Differences in diagenetic history are largely responsible for the differences in reservoir quality between the two study areas. Combined isotopic and petrographic techniques were used to interpret the sequence of diagenetic events in Frio sandstones

in the Chocolate Bayou/Danbury Dome area. Sequences of events in Vicksburg sandstone of the McAllen Ranch area were interpreted from petrographic data alone, because carbonate phases in these rocks are too complex to permit separation for isotopic analysis. Information on clay mineral transformations (Appendix A) was also integrated into our interpretations of diagenetic history.

Diagenetic History of Chocolate Bayou/Danbury Dome Area

Figure 45 summarizes the sequence of diagenetic events in the Frio Formation of the Chocolate Bayou/Danbury Dome area. In a regional petrographic study of the Frio, Loucks and others (1979) observed carbonates from near surface to the deepest occurrence of the Frio, suggesting that carbonate precipitation must occur in several stages. In thin sections from the geothermal wells, carbonates both preceded and post-dated formation of quartz overgrowths. Secondary porosity largely post-dates formation of quartz but occurred both before and after carbonate precipitation. Isotopic data are consistent with these observations. Alternate leaching and precipitation of carbonate minerals must have occurred over the entire range of depths examined and under much shallower conditions as well.

Quartz cements in Brazoria County do not become important until nearly 12,000 ft (3,660 m). Rocks immediately overlying the Frio in Brazoria County are Miocene shales. The sandstones above these shales contain no quartz overgrowths and are mostly unconsolidated. On a regional scale, however, overgrowths appear at much shallower depths, at 5,000 to 6,000 ft (1,525 to 1 830 m) (Loucks and others, 1979). In thin section, quartz in Brazoria County appears mainly to pre-date formation of secondary porosity, suggesting that it formed at shallower depths than it is presently found. The very heavy $\delta^{18}O$ values for quartz overgrowths in Brazoria County are consistent with formation at shallower depths.

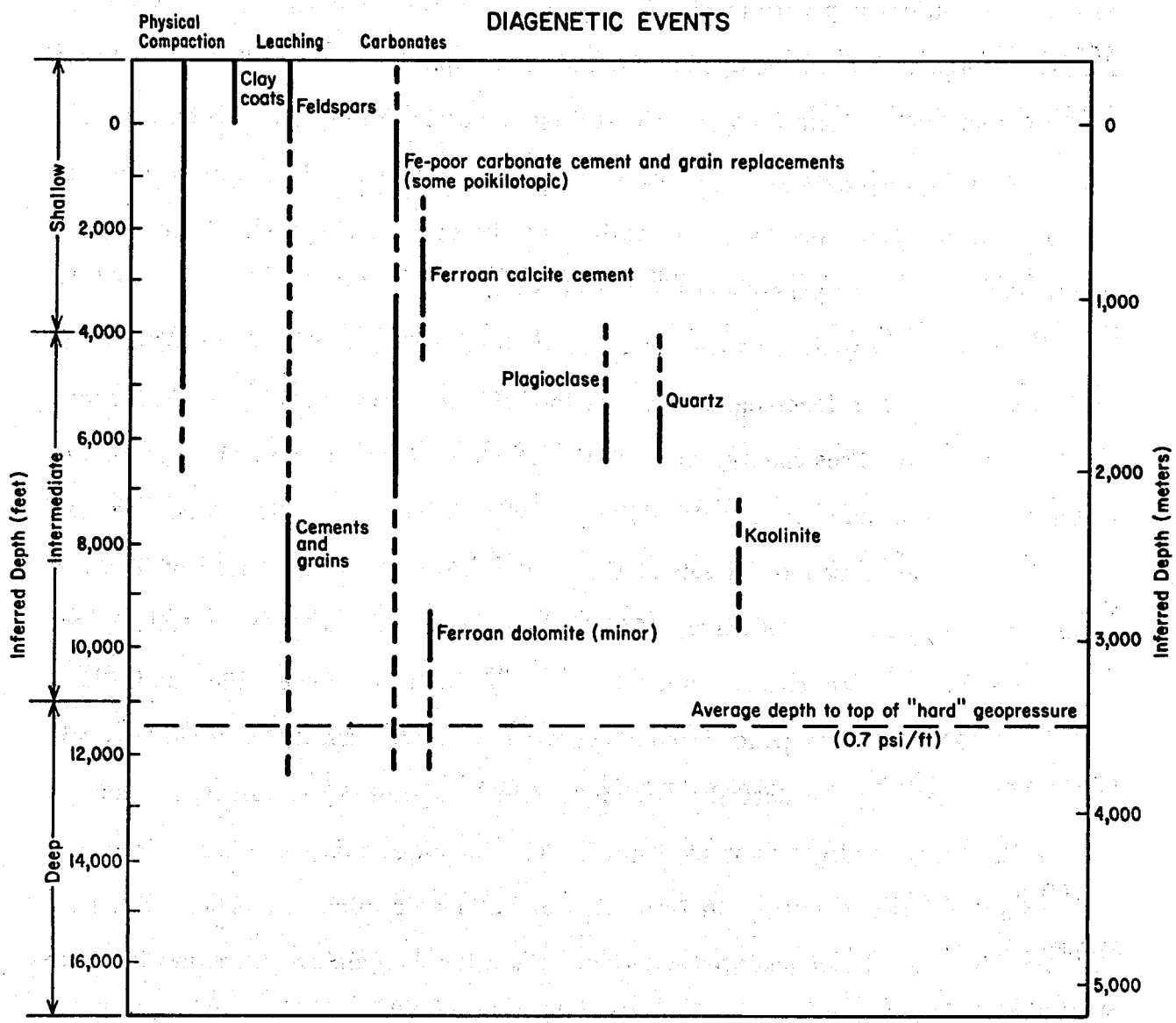

Figure 45. History of diagenetic events, Chocolate Bayou/Danbury Dome area.

Kaolinite occurs mainly as a filling in secondary pores and as a feldspar replacement. It definitely post-dates quartz and much of the leaching, but its paragenetic relationship with much of the late carbonate is unclear. It appears to be the last authigenic phase developed in most of the samples.

In addition to formation of pore-filling minerals, three other processes are important to Frio diagenesis in Brazoria County. One of these is the maturation of organic matter. The other two, albitization and the smectite/illite transition, involve reaction of detrital components with the pore fluid.

Reaction of organic components at some stage during burial is said to produce acids responsible for leaching and formation of secondary porosity (Schmidt and MacDonald, 1979). Presumably, much of this leaching involves removal of carbonate minerals (Schmidt and MacDonald, 1979). Hydrocarbon maturation processes are known to be one source of dissolved $CO_3^=$ in subsurface fluids, based on isotopic evidence (Carothers and Kharaka, 1980). Bonham (1980) states that Gulf Coast Tertiary sediments are characterized by peak generation between 100° and 120°C (212° and 250°F). Authigenic carbonates within this temperature zone in Brazoria County are the ones characterized by an extreme range of $\delta^{13}C$ values, including a number of extremely light samples (fig. 25). This indicates that some carbon released by organic maturation is used in formation of authigenic minerals. Thus, carbonate diagenesis in the zone of peak hydrocarbon generation is complex, encompassing both precipitation and leaching.

Albitization of feldspars, both alkali-feldspars and plagioclase, occurs with depth in Brazoria County and in other Tertiary rocks along the Gulf Coast (Garbarini and Carpenter, 1978; Boles, 1979). Isotopic data and trends in feldspar composition with depth suggest that albitization in Brazoria County occurs slightly deeper than the illite/smectite transition.

Textures in calcitized feldspar grains suggest that complete albitization was preceded by most of the grain replacement. This is deduced from the observation that many incompletely calcitized grains consist of calcite in the middle surrounded by a rim of albite. If complete albitization had occurred prior to calcitization, there would have been no compositional zoning in the grain to cause the differential replacement. The remaining rims may in some cases represent feldspar overgrowths. If this is the case, formation of feldspar cement may also have preceded albitization. Again, if developed on an albite core, the albite rim itself would have been equally subject to replacement.

Diagenetic History of McAllen Ranch Field Area

Calcite is the earliest and the most pervasive authigenic component. Interval transit time data from acoustic logs suggest that cements, which are assumed to be carbonate, are extensively developed by the time the sandstones are buried approximately 5,000 ft (1,525 m). In our shallowest thin section sample, framework grains (especially plagioclase) have already undergone extensive replacement by calcite. Petrographic analysis cannot definitively reveal whether grains were directly replaced by calcite or whether calcite precipitated in secondary intragranular pores. Poikilotopic ferroan calcite precipitated next in most intergranular pore spaces, resulting in a well-indurated rock with almost no porosity (fig. 46). We have observed no evidence of earlier non-carbonate cementation, thus supporting our conclusions based on petrophysical data and on the observations of Frio sandstones from the Lower Texas Gulf Coast (Loucks and others, 1979) that the pervasive cements occurring at shallow depths are carbonate.

Precipitation of poikilotopic ferroan calcite was followed by a major leaching episode which destroyed much of the preexisting calcite cement in certain intervals. Where abundant secondary porosity developed, quartz overgrowths formed with

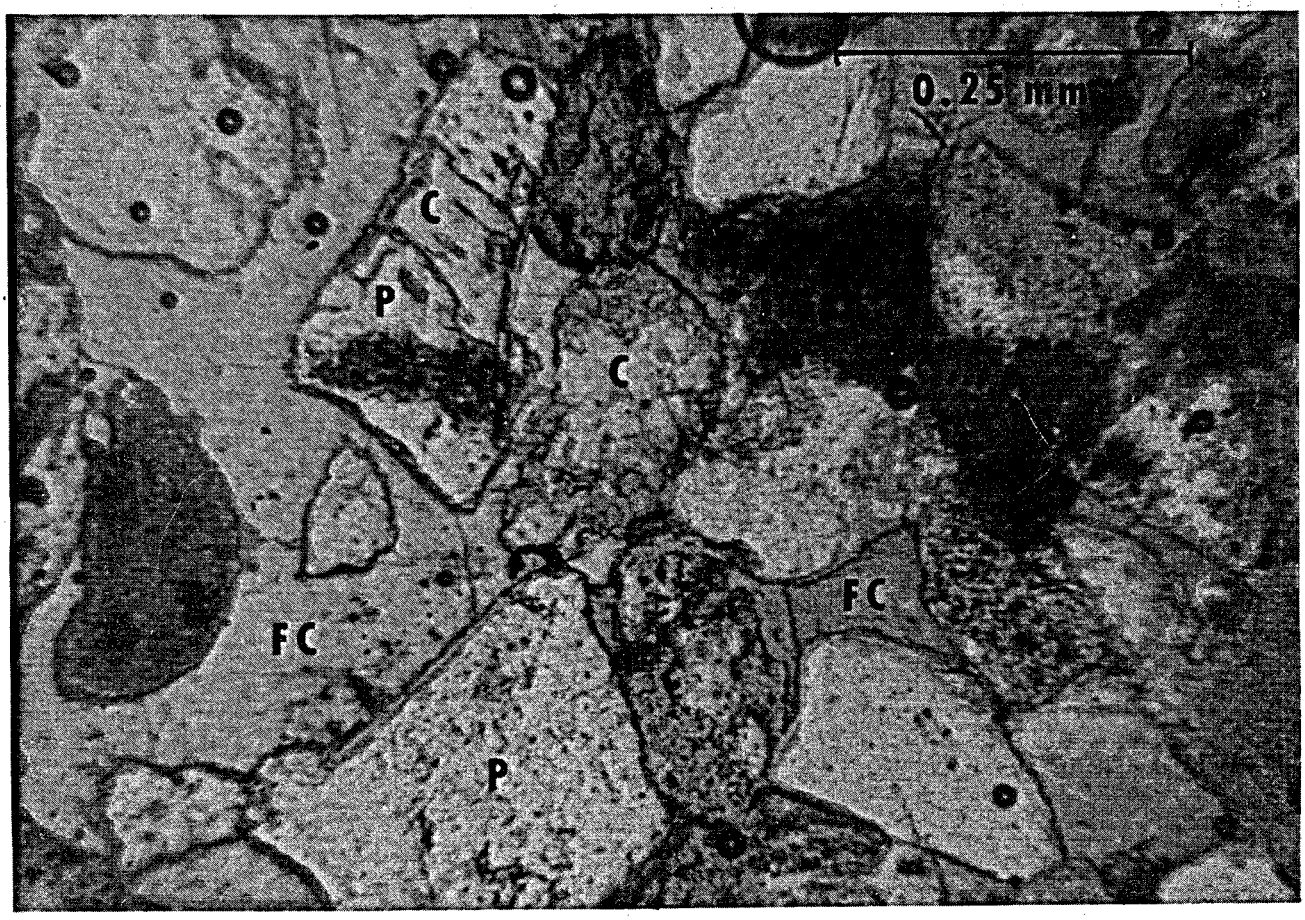

Figure 46. Low porosity sandstone resulting from pervasive calcite cementation, McAllen Ranch area. P = detrital plagioclase; C = calcite grain replacement; FC = ferroan calcite cement. Plane polarized light.

euhedral crystal faces where their growth was unobstructed (fig. 47). Similarly, plagioclase overgrowths grew into secondary pores. Temporal relationships between quartz and plagioclase overgrowth development are difficult to discern because of the chance occurrence of authigenic quartz and feldspar in contact and because there appear to have been multiple pulses of plagioclase overgrowth development (fig. 35). Plagioclase overgrowths may have begun to form slightly earlier than quartz overgrowths, but their major periods of development appear to coincide.

In samples from depths of approximately 10,800 ft (3,290 m), where chlorite rims and pore-filing cement are well developed, quartz overgrowths are rare. However, authigenic chlorite appears to have formed in secondary pores. This suggests that much of the chlorite formed after the period of carbonate leaching but prior to quartz cementation, thereby preventing silica-rich fluids from nucleating on detrital quartz grains. There is some evidence from samples below 12,000 ft (3,660 m) that minor chlorite precipitation may have persisted after the initiation of quartz cementation, as a small number of grains have chlorite rims developed on quartz overgrowths.

Paragenetic relationships indicate that laumontite precipitation occurred after development of quartz overgrowths (fig. 48). Poikilotopic grains grew into secondary pores and were later partially leached. Additional observations of paragenetic relationships indicate that sphene also formed after quartz overgrowths but prior to the second major episode of iron-poor sparry calcite precipitation.

Another major episode of calcite precipitation occurred following development of quartz overgrowths and the minor cements discussed above. Most of this calcite is present as non-ferroan grain replacements; however, it also occurs with a sparry, pore-filling morphology (fig. 49).

The final stage of calcite precipitation recorded in samples studied occurred prior to burial of sandstones to 10,600 ft (3,230 m). This calcite also occurs as sparry pore-fill and, to a lesser extent, as grain replacements; but in contrast to the

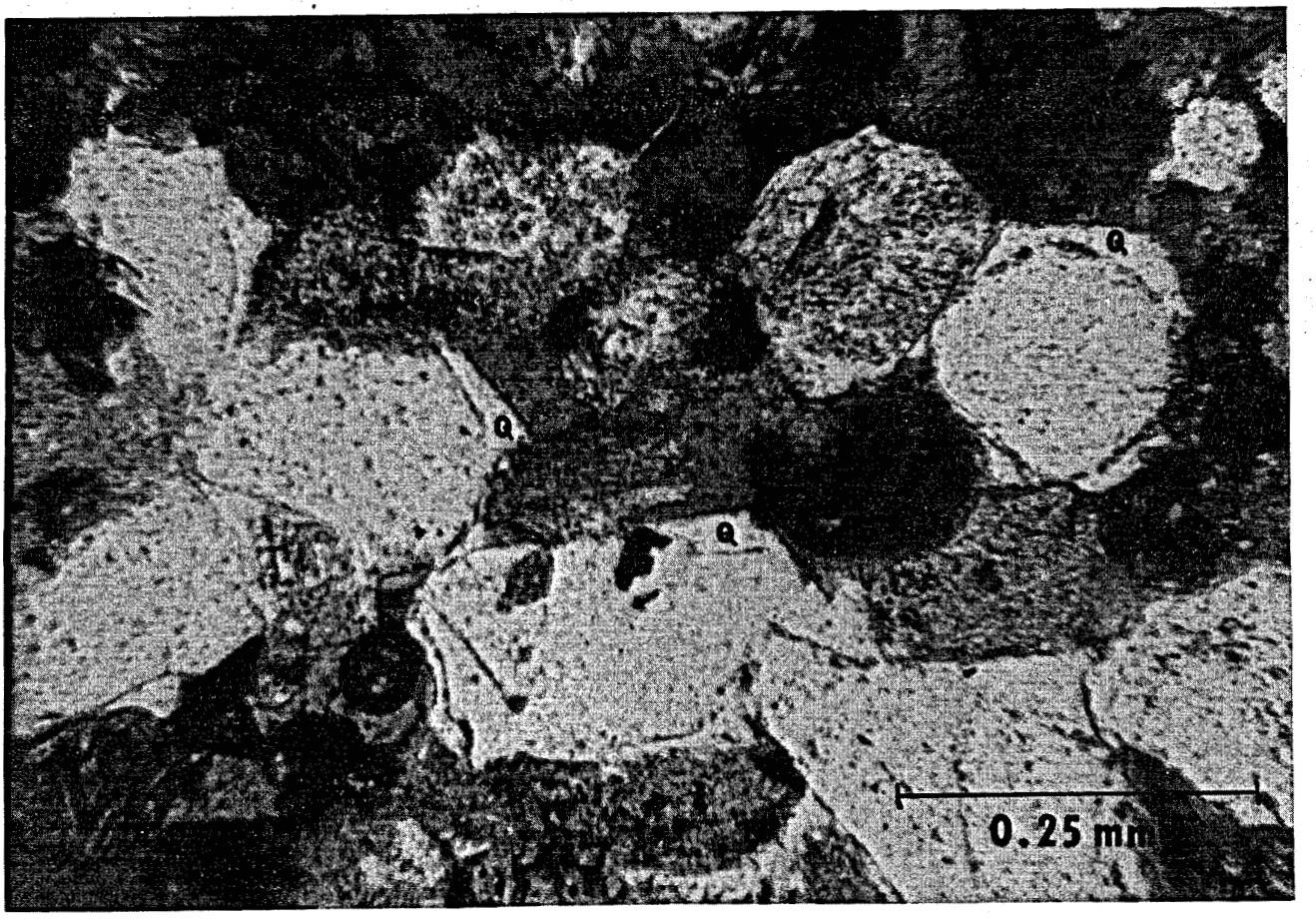

Figure 47. Euhedral quartz overgrowths (Q), McAllen Ranch area. Plane polarized light.

Figure 48. Post-quartz overgrowth (Q) laumontite cement (L). Dashed line indicates the boundary between detrital quartz and its overgrowth. Crossed polars.

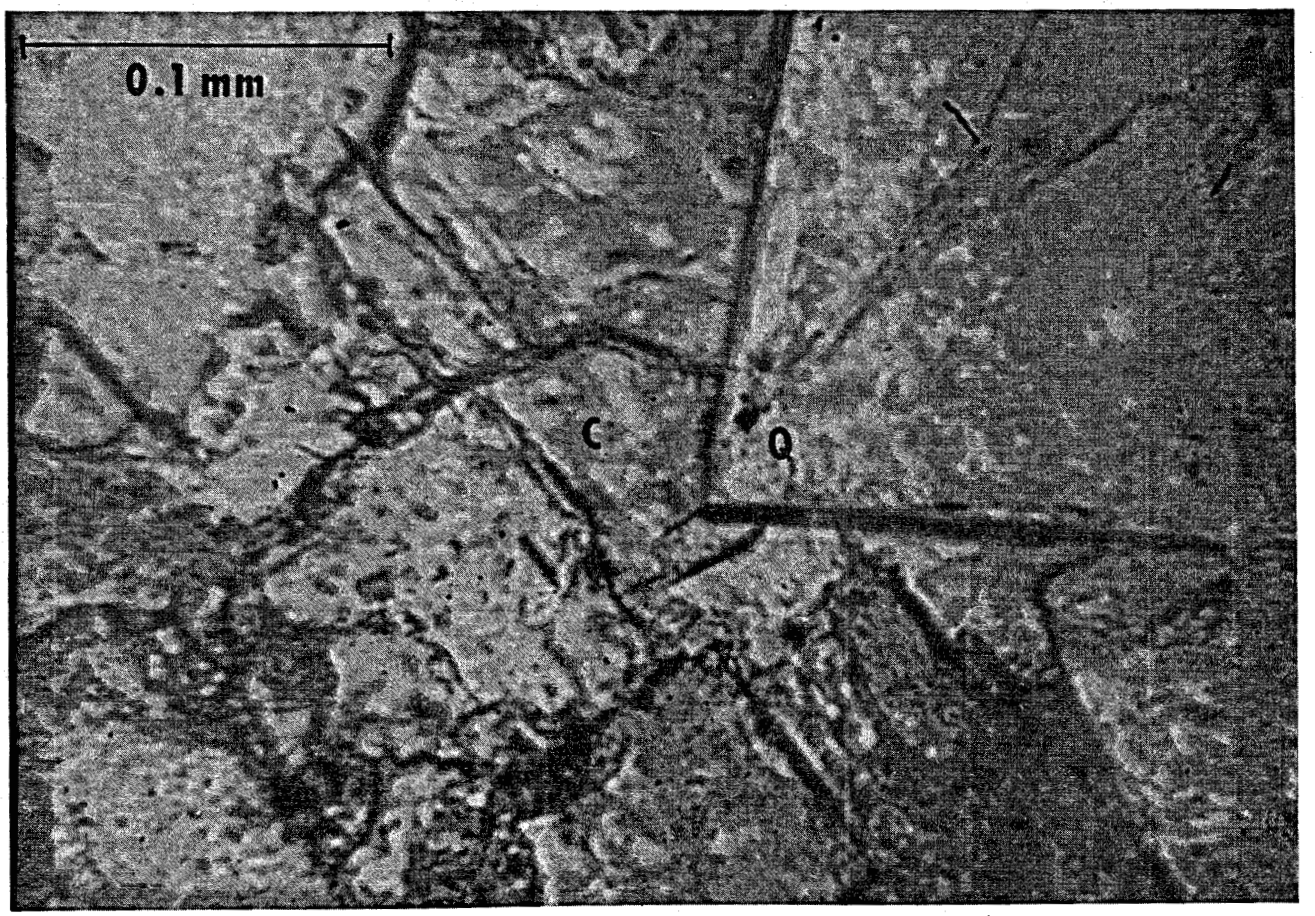

Figure 49. Post-quartz overgrowth (Q) calcite cement (C). Plane polarized light.

preceding calcite, it is ferroan. In samples containing abundant ferroan calcite, most secondary porosity is occluded.

The generalized sequence of diagenetic events occurring in Vicksburg sandstones of McAllen Ranch area is shown in figure 50. The observed sequence agrees well with the general diagenetic sequence developed by Loucks and others (1979) for Tertiary Frio and Vicksburg sandstones of the Texas Gulf Coast, and depths at which we believe specific diagenetic events were initiated are inferred largely from their study.

CONCLUSIONS

Table 3 summarizes the characteristics of the Chocolate Bayou/Danbury Dome area and the McAllen Ranch area. These contrasting characteristics promoted differences in the sequence and intensity of diagenesis, which in turn were responsible for differences in reservoir quality in the two areas. The onset of specific diagenetic events is related to depth to the top of geopressure and the temperature gradient. Intensity of reaction is largely a function of the primary detrital composition of the sandstones and shales. In the Vicksburg sandstones of the McAllen Ranch area, multiple generations of carbonate cement are represented in the sandstone samples examined. Calcite cements formed early in the diagenetic sequence and are present in variable amounts in all depth intervals sampled. Analysis of average interval transit times reveals a significant contrast between depths and intensities of cementation in the two areas. A combined plot for three wells in the McAllen Ranch Field area indicates a higher degree of consolidation than do plots for the Danbury Dome area, Chocolate Bayou area, and the two GCO/DOE Pleasant Bayou test wells (fig. 51). A Frio well in Cameron County, coastward from Hidalgo County, was plotted to show the similarity between lower Vicksburg and Frio Formations in South Texas.

In the McAllen Ranch Field area, Vicksburg sandstones are characterized by a mineralogically immature detrital assemblage. Framework grains are dominantly

feldspars and rock fragments that contribute to the overall chemical and mechanical instability of these sandstones. This instability is enhanced by the higher than normal geothermal gradients, relative to other areas of the Texas Gulf Coast, characterizing McAllen Ranch Field (1.64°F/100 ft above and 2.92°F/100 ft within the hard geopressured zone). Figure 52 graphically depicts the contrasting geothermal gradients in Hidalgo and Brazoria Counties. Therefore, in the McAllen Ranch Field area, diagenetic events tend to happen earlier in the consolidation sequence; early-formed authigenic constituents are developed more extensively and tend to persist to a greater extent than those occurring in the upper Texas coast (Loucks and others, 1979). Precipitation of early calcite cements began as shallowly as 3,000 ft (914 m). Virtually all primary porosity was occluded by these cements by the time the sandstones were buried to 5,000 ft (1,524 m). Apparently, in the Hidalgo County Vicksburg sandstones, post-quartz overgrowth leaching created good reservoirs with abundant secondary porosity, but these reservoirs were subsequently destroyed by the final episode of ferroan calcite cementation which occurred prior to burial of sandstones to 10,600 ft (3,230 m). Similar destruction of secondary porosity by late iron-rich carbonate cement was shown by Loucks and others (1977) to be the major cause of poor quality of deep Frio and Vicksburg sandstones reservoirs in the lower Texas coast.

In the Chocolate Bayou/Danbury Dome area Frio sandstones contain fewer unstable constituents and have been exposed to lower temperatures during burial. These rocks probably never contained authigenic carbonates on the extensive scale found in the South Texas Vicksburg. Secondary porosity was never affected by major late-stage carbonate precipitation. Thus, Frio sandstones of Brazoria County have the greatest potential for deep reservoir quality of all Texas Gulf Coast Tertiary sandstones (Bebout and others, 1978).

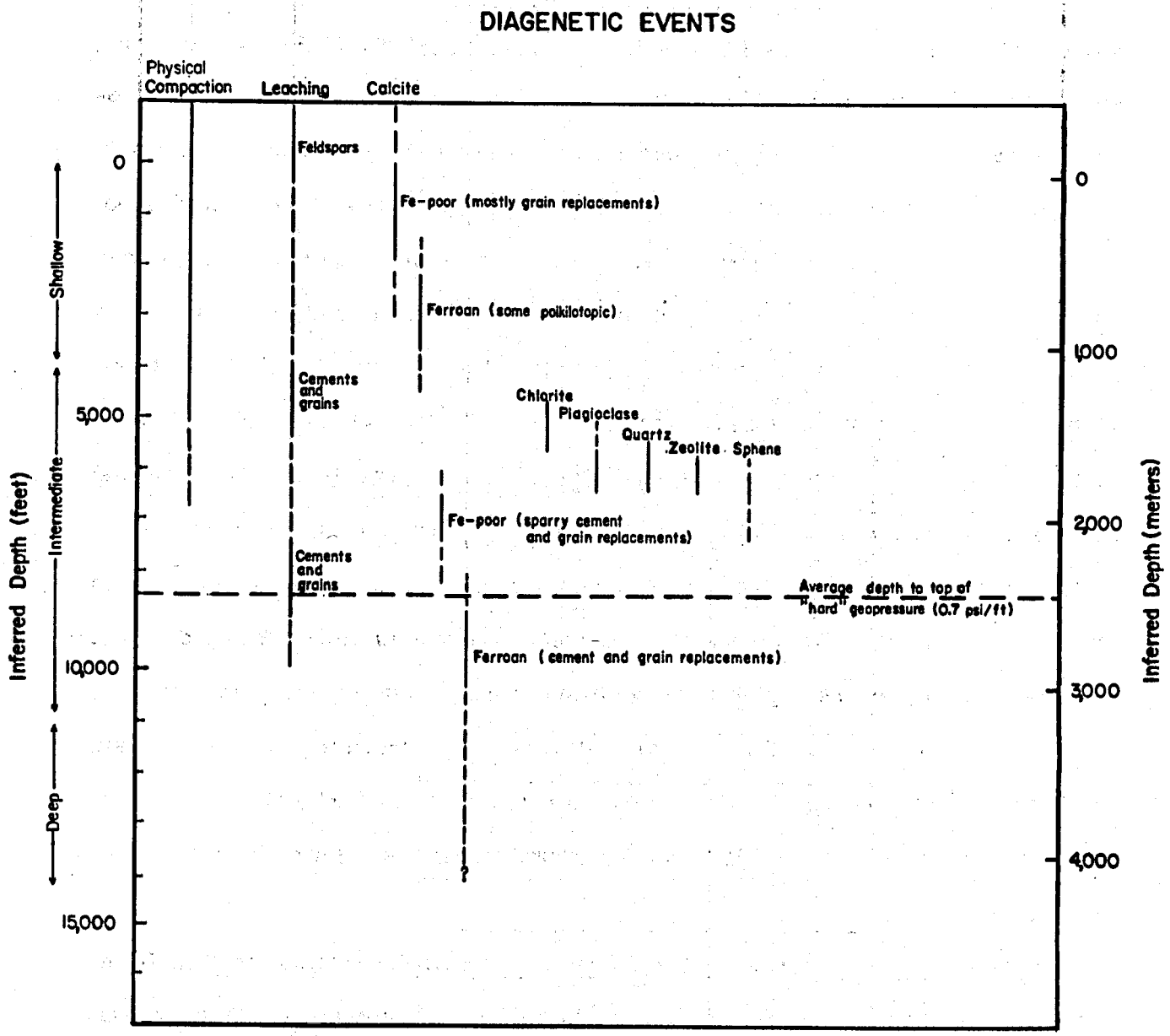

Figure 50. History of diagenetic events, McAllen Ranch area.

TABLE 3.

CHARACTERISTICS OF CHOCOLATE BAYOU/DANBURY AREA VERSUS McALLEN RANCH AREA.

Area	Sediment source	Climate	Chemical and mechanical stability	Carbonate content of shales at depth	Abundance of carbonate cement in sandstones	Depth to top of "hard" geopressure (0.7 psi/ft)	Temperature gradient above/below top of geopressure	Reservoir quality at depth
CHOCOLATE BAYOU/ DANBURY	ROCKY MOUNTAINS: Sedimentary, metamorphic and volcanic WEST TEXAS: Volcanic	Humid	Very stable	Low	Low	Approximately 11,000 ft (3,350m)	1.35°F/100ft / 2.49°F/100ft	Poor to excellent
McALLEN RANCH	WEST TEXAS AND MEXICO: Volcanic LOCAL: Caliche	Arid	Very unstable	Moderate to high	High	Approximately 8,000 ft (2,440m)	1.64°F/100ft / 2.92°F/100ft	Extremely poor

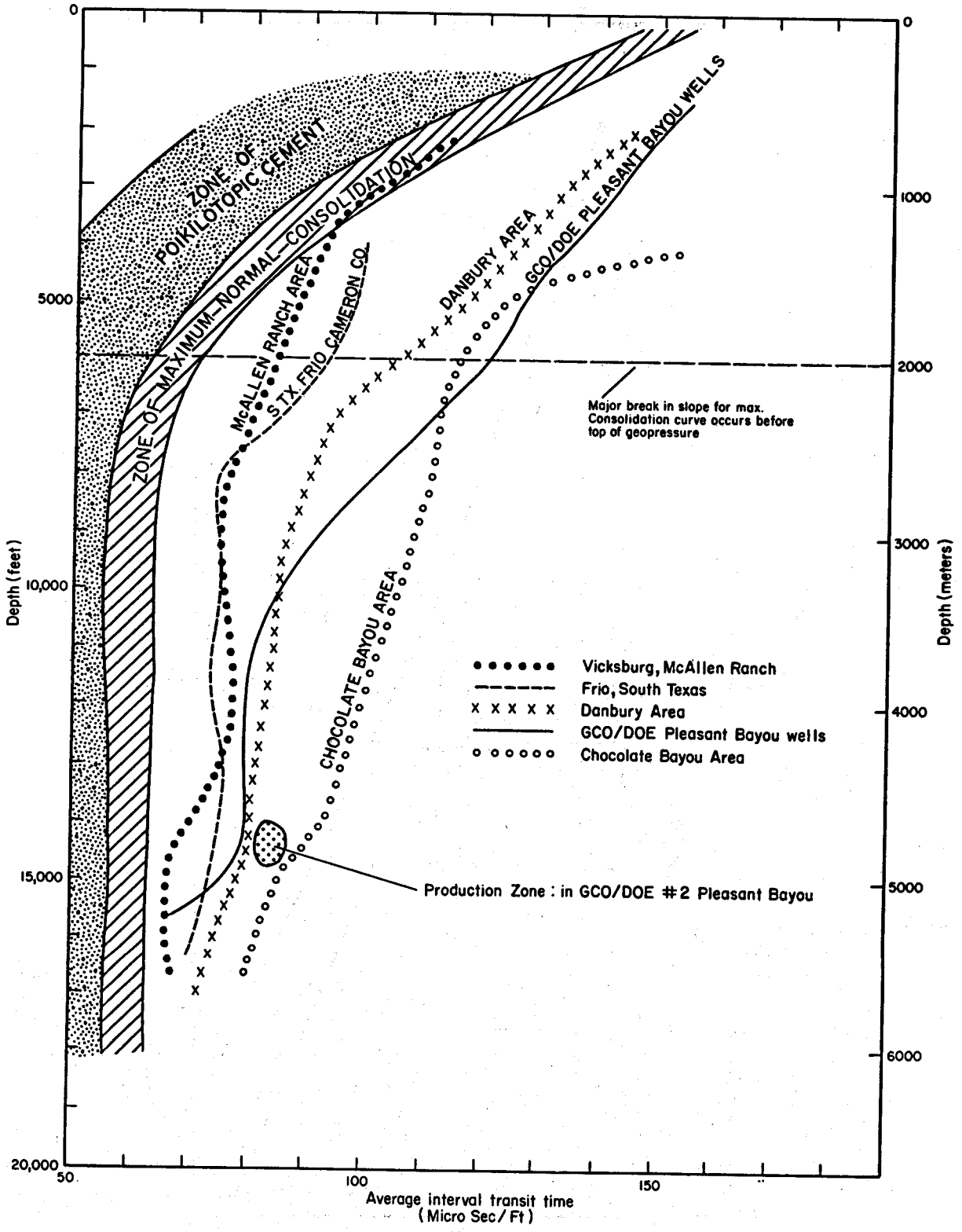

Figure 51. Interval transit time plots for the two study areas.

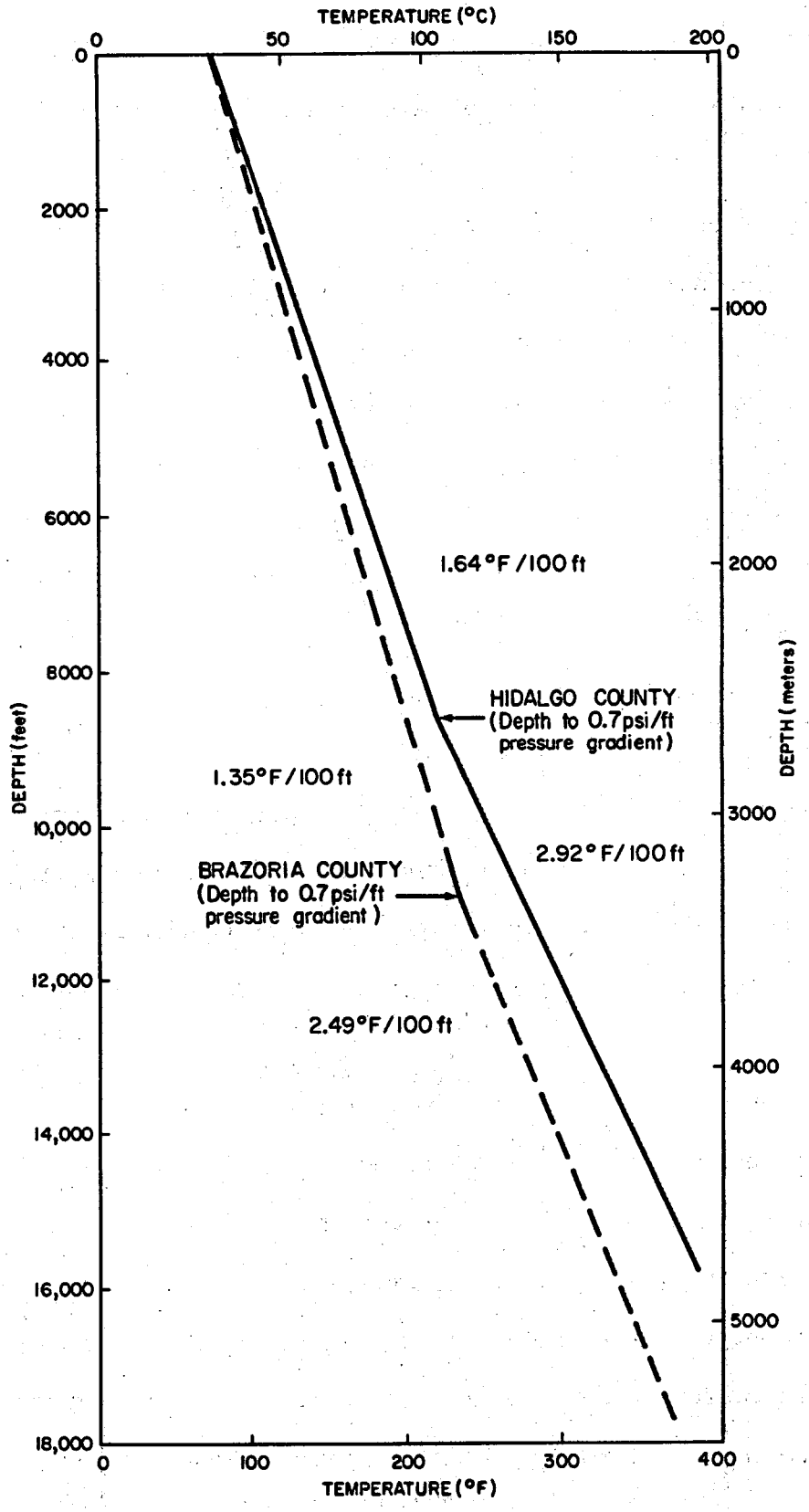

Figure 52. Comparison of temperature versus depth curves for Chocolate Bayou/Danbury Dome area (Brazoria County) and McAllen Ranch area (Hidalgo County).

Frio sandstones from the Pleasant Bayou geothermal test wells exhibit mineralogic trends that are largely consistent with those trends observed in the larger set of all Brazoria County Frio samples; the detrital mineralogies are comparable, as are the diagenetic sequences we have reconstructed. The Pleasant Bayou test sites were selected for the favorable porosities, permeabilities, and sand volumes characterizing the Frio Formation in the geopressured zone of this area, relative to other areas of Brazoria County (Bebout and others, 1978; 1980). Within the geopressured zone, the best reservoir is the medium-grained, bedload fluvial channel deposit occurring from approximately 14,640 to 14,710 ft (4,460 to 4,480 m) in the Pleasant Bayou No. 2 well (Bebout and others, 1980). This unit, by its nature, deviates most from the "typical" Brazoria County Frio sandstones we have described. In 15 of 16 samples from this interval authigenic calcite constitutes no more than 2 percent of the sandstones. These rocks were apparently not subjected to the late-stage calcite cementation that occurred elsewhere along the Gulf Coast, so abundant secondary porosity was preserved. Depositional matrix is a minor constituent in these sandstones; 13 of the samples are matrix-free. The absence of matrix was a major factor controlling the development of secondary porosity by permitting leaching fluids to permeate the sandstones.

Thus, even in a region with broadly favorable reservoir potential, extreme variations in reservoir quality exist on a smaller scale. Factors that determine reservoir quality of individual sandstone units include depositional environment at a local level, relative proportions of porosity types, extent of authigenic mineral development, and pore geometry as related to permeability. Consideration of these regional and local reservoir quality controls can aid in predicting the distribution of reservoirs suitable for geopressured geothermal energy production.

ACKNOWLEDGMENTS

Subsurface data for this project were provided by the following companies: Forest Oil Corporation; Core Laboratories, Incorporated; Shell Oil Company; Exxon Company, U.S.A.; Gulf Oil Company; and Tenneco Oil Company. The help of these organizations is sincerely appreciated.

Numerous individuals have also aided this project with their time and enthusiasm. Robert Berg of Texas A&M University arranged for us to sample Vicksburg cores from the McAllen Ranch Field. Lynton S. Land, The University of Texas at Austin, performed the isotopic analyses and contributed significantly in development of diagenetic models. Marianne Dodge, Gulf Energy Producing Company, helped us with her considerable knowledge of Gulf Coast diagenesis. Kinji Magara and Ray Gregory, Bureau of Economic Geology, improved our understanding of geopressure and geothermal gradients. Thomas Dunn, Amoco Research, arranged for us to use the Amoco SEM, from which we acquired a number of excellent pictures and useful analyses. We thank these individuals for their valuable contributions. We also appreciate the reviews by our colleagues at the Bureau, William R. Kaiser, Marc B. Edwards, and William E. Galloway. Their efforts have contributed noticeably to the clarity of this report. This research was supported by the U.S. Department of Energy under contract number DE-AC08-79ET27111.

REFERENCES

Bebout, D. G., Loucks, R. G., and Gregory, A. R., 1978, Frio sandstone reservoirs: The University of Texas at Austin, Bureau of Economic Geology Report of Investigations No. 91, 92 p.

Berg, R. R. Marshall, W. D. and Shoemaker, P. W., 1979, Structural and depositional history, McAllen Ranch Field, Hidalgo County, Texas: Gulf Coast Association of Geological Societies Transactions, v. 29, p. 24-28.

Boles, J. R., 1979, Active albitization of plagioclase in Gulf Coast Tertiary sandstones: Geological Society of America, Abstracts with Programs, p. 391.

Boles, J. R., 1980, Calcium budget in Frio sandstones, southwest Texas (abs.): American Association of Petroleum Geologists Bulletin, v. 64, no. 5, p. 678.

Boles, J. R., and Franks, S. G., 1979, Clay diagenesis in Wilcox sandstones of southwest Texas: implications of smectite diagenesis on sandstone cementation: Journal of Sedimentary Petrology, v. 49, no. 1, p. 55-70.

Bonham, L. C., 1980, Migration of hydrocarbons in compacting basins: American Association of Petroleum Geologists Bulletin, v. 64, no. 4, p. 549-567.

Bruce, C. H., 1973, Pressured shale and related sediment deformation: mechanism for development of regional contemporaneous faults: American Association of Petroleum Geologists Bulletin, v. 57, no. 5, p. 878-886.

Burst, J. F., 1969, Diagenesis of Gulf Coast clayey sediments and its possible relationship to petroleum migration: American Association of Petroleum Geologists Bulletin, v. 53, no. 1, p. 73-93.

Carothers, W. W., and Kharaka, Y. K., 1980, Stable carbon isotopes of HCO_3^- in oilfield waters--implications for the origin of CO_2: Geochimica et Cosmochimica Acta, v. 44, no. 2, p. 323-332.

Clayton, R. N., Friedman, I., Graf, D. L., Mayeda, T. K., Meents, W. F., and Shimp, N. F., 1972, The origin of saline formation waters, I. isotopic composition: Journal of Geophysical Research, v. 71, p. 3869-3882.

Craig, H., 1966, Isotopic composition and origin of the Red Sea and Salton Sea geothermal brines: Science, v. 154, p. 1544-1548.

Dapples, E. C., 1972, Some concepts of cementation and lithification of sandstones: American Association of Petroleum Geologists Bulletin, v. 56, no. 1, p. 3-25.

Deer, W. A., Howie, R. A., and Zussman, J., 1966, An introduction to the rock forming minerals: New York, John Wiley, p. 17-20.

de Segonzac, C. D., 1970, The transformation of clay minerals during diagenesis and low-grade metamorphism: a review: Sedimentology, v. 15, p. 281-346.

Dickey, P. A., Collins, A. G., Fajardo, I., 1972, Chemical composition of deep formation waters in southwestern Louisiana: American Association of Petroleum Geologists Bulletin, v. 56, no. 8, p. 1530-1533.

Dickinson, W. R., 1970, Interpreting detrital modes of graywacke and arkose: Journal of Sedimentary Petrology, v. 40, no. 2, p. 695-707.

Epstein, S., Graf, D. L., and Degens, E. T., 1963, Oxygen isotope studies on the origin of dolomite, in Craig, H., Miller, S. L. and Wasserburg, G. J., eds., Isotopic and cosmic chemistry: Amsterdam, North Holland Publishing Company, 188 p.

Eslinger, E., 1971, Mineralogy and oxygen isotope ratios of hydrothermal and low-grade metamorphic argillaceous rocks: Cleveland, Ohio, Case Western Reserve University, Ph.D. dissertation, 205 p.

Folk, R. L., 1974, Petrology of sedimentary rocks: Austin, Texas, Hemphill Publishing Company, 182 p.

Folk, R. L., and Assereto, R., 1974, Giant aragonite rays and baroque white dolomite in Tepee fillings, Triassic of Lombardy, Italy (abs.): American Association of Petroleum Geologists, Annual Meeting, p. 34-45.

Foster, W. R., and Custard, H. C., 1980, Smectite-illite transformation--role in generating and maintaining geopressure (abs.): American Association of Petroleum Geologists Bulletin, v. 64, no 5, p. 708.

Friedman, I., and O'Neil, J. R., 1977, Compilation of stable isotope fractionation factors of geochemical interest: U.S. Geological Survey Professional Paper 440-KK.

Garbarini, J. M., and Carpenter, A. B., 1978, Albitization of plagioclase by oil-field waters: Geological Society of America, Abstracts with programs, p. 406.

Galloway, W. E., 1977, Catahoula Formation of the Texas Coastal Plain--depositional systems, mineralogy, structural development, ground-water flow history, and uranium distribution: The University of Texas at Austin, Bureau of Economic Geology Report of Investigations No. 87, 59 p.

Graf, D. L., Friedman, I., and Meents, W. F., 1965, The origin of saline formation waters, II: isotopic fractionation by shale micropore systems: Illinois State Geological Survey Circular 393, 32 p.

Gregory, A. R., and Backus, M. M., 1980, Geopressured formation parameters, geothermal well, Brazoria County, Texas, in Dorfman, M. H., and Fisher, W. L., eds., Fourth Geopressured Geothermal Energy Conference Proceedings: The University of Texas at Austin, Center for Energy Studies, v. 1, p. 235-311.

Han, J. H., 1980, Deltaic systems and associated growth faulting of Vicksburg Formation (Oligocene), South Texas: American Association of Petroleum Geologists and Society of Economic Paleontologists and Mineralogists Abstracts, p. 62.

Hitchon, B., and Friedman, I., 1969, Geochemistry and origin of formation waters in the western Canada sedimentary basin, I: stable isotopes of hydrogen and oxygen: Geochimica et Cosmochimica Acta, v. 33, no. 11, p. 1321-1349.

Hower, J., Eslinger, E. V., Hower, M. E., and Perry, E. A., 1976, Mechanism of burial metamorphism of argillaceous sediment: I. Mineralogical and chemical evidence: Geological Society of America Bulletin, v. 87, no. 5, p. 725-737.

Jones, P. J., 1975, Geothermal and hydrocarbon regimes, northern Gulf of Mexico Basin, in Dorfman, M. H., and Deller, R. W., eds., First Geopressured Geothermal Energy Conference Proceedings: The University of Texas at Austin, Center for Energy Studies, p. 15-97.

Kharaka, Y. K., Callender, E., and Carothers, W. W., 1977a, Geochemistry of geopressured geothermal waters from the Texas Gulf Coast: Third Geopressured Geothermal Energy Conference Proceedings: Lafayette, Louisiana, University of Southwestern Louisiana, v. 1, p. GI-121 - GI-165.

Kharaka, Y. K., Callender, E., and Wallace, R. H., 1977b, Geochemistry of geopressured geothermal waters from the Frio Clay in the Gulf Coast region of Texas: Geology, v. 5, p. 241-244.

Kharaka, Y. K., Lico, M. S., Wright, V. A., and Carothers, W. W., 1980, Geochemistry of formation waters from Pleasant Bayou No. 2 well and adjacent areas in coastal Texas, in Dorfman, M. H., and Fisher, W. L., eds., Fourth Geopressured Geothermal Energy Conference Proceedings: The University of Texas at Austin, Center for Energy Studies, v. 1, p. 168-193.

Land, L. S., in press, The isotopic and trace element chemistry of dolomite: the state of the art: Society of Economic Paleontologists and Mineralogists Special Publication 28.

Land, L. S., and Dutton, S. P., 1978, Cementation of a Pennsylvanian deltaic sandstone: isotopic data: Journal of Sedimentary Petrology, v. 48, no. 4, p. 1167-1176.

Laniz, R. V., Stevens, R. E., and Norman, M. B., 1964, Staining of plagioclase feldspar and other minerals with F, D, and C Red No. 2: U.S. Geological Survey Professional Paper 501-B, p. B152-B153.

Lewis, C. R., and Rose, S. C., 1970, A theory relating high temperatures and overpressures: Journal of Petroleum Technology, v. 22, no. 1, p. 11-16.

Lindholm, R. C. and Finkelman, R. B., 1972, Calcite staining: semiquantitative determination of ferrous iron: Journal of Sedimentary Petrology, v. 42, no. 1, p. 239-242.

Lindquist, S. J., 1977, Secondary porosity development and subsequent reduction, overpressured Frio formation sandstone (Oligocene), South Texas: Gulf Coast Association of Geological Societies Transactions, v. 27, p. 99-107.

Loucks, R. G., 1978, Sandstone distribution and potential for geopressured-geothermal energy production in the Vicksburg Formation along the Texas Gulf Coast: Gulf Coast Association of Geological Societies Transactions, v. 28, p. 109-120.

Loucks, R. G., Bebout, D. G., and Galloway, W. E., 1977, Relationship of porosity formation and preservation to sandstone consolidation history – Gulf Coast Lower Tertiary Frio Formation: Gulf Coast Association of Geological Societies Transactions, v. 27, p. 109-120.

Loucks, R. G., Dodge, M. M., and Galloway, W. E., 1979, Sandstone consolidation analysis to delineate areas of high-quality reservoirs suitable for production of geopressured geothermal energy along the Texas Gulf Coast: U.S. Department of Energy, Division of Geothermal Energy, EG-77-5-05-5554, 97 p.

Loucks, R. G., Richmann, D. L., and Milliken, K. L., 1980, Factors controlling porosity and permeability in geopressured Frio sandstone reservoirs, General Crude Oil/Department of Energy Pleasant Bayou Test Wells, Brazoria County, Texas, in Dorfman, M. H., and Fisher, W. L., eds., Fourth Geopressured Geothermal Energy Conference Proceedings: The University of Texas at Austin, Center for Energy Studies, v. 1, p. 46-82.

McCrea, J. M., 1950, On the isotopic chemistry of carbonates and a paleotemperature scale: Journal of Chemistry and Physics, v. 18, p. 849-857.

Magara, K., 1975, Importance of aquathermal pressuring effect in Gulf Coast: American Association of Petroleum Geologists Bulletin, v. 59, no. 10, p. 2037-2045.

Magara, K , 1978, Compaction and fluid migration, practical petroleum geology: Amsterdam, Elsevier, 311 p.

Murray, G. E., 1960, Geologic framework of Gulf coastal province of United States, in Shepard, F. P., Phleger, F. B., and van Andel, T. H., eds., Recent sediments, Northwest Gulf of Mexico: American Association of Petroleum Geologists, 394 p.

Perry, E. A., and Hower, J., 1970, Burial diagenesis in Gulf Coast sediments: Clays and Clay Minerals, v. 18, no. 3, p. 165-177.

Pittman, E. D. 1979, Porosity, diagenesis, and productive capability of sandstone reservoirs: Society of Economic Paleontologists and Mineralogists Special Publication 26, p. 159-173.

Powers, M. C. 1967, Fluid release mechanisms in compacting marine mudrocks and their importance in oil exploration: American Association of Petroleum Geologists Bulletin, v. 51, no. 7, p. 1240-1253.

Richmann, D. L., Milliken, K. L., Loucks, R. G., and Dodge, M. M., 1980, Mineralogy, diagenesis, and porosity in Vicksburg sandstones, McAllen Ranch Field, Hidalgo County, Texas: Gulf Coast Association of Geological Societies Transactions, v. 30, p. 473-481.

Ritch, H. J., and Kozik, H. G., 1971, Petrophysical study of overpressured sandstone reservoirs, Vicksburg Formation, McAllen Ranch Field, Hidalgo County, Texas: Society of Production Well Log Analysts, 12th Annual Logging Symposium, 14 p.

Schmidt, G. W., 1973, Interstitial water composition and geochemistry of deep Gulf Coast shales and sandstones: American Association of Petroleum Geologists Bulletin, v. 57, no. 2, p. 321-337.

Schmidt, V., and MacDonald, D. A. 1979, The role of secondary porosity in the course of sandstone diagenesis: Society of Economic Paleontologists and Mineralogists, Special Publication 26, p. 175-207.

Sharp, J. M., 1980, Temperature and pressure relations in thick sequences of accumulating sediments (abs.): American Association of Petroleum Geologists Bulletin, v. 64, no. 5, p. 782.

Syers, J. K., Chapman, S. L., Jackson, M. L., Rex, R. W., and Clayton, N. L., 1968, Quartz isolation from rocks, sediments and soils of determination of oxygen isotopic composition: Geochimica et Cosmochimica Acta, v. 32, no. 9, p. 1022-1025.

Thomson, A., 1959, Pressure solution and porosity: Society of Economic Paleontologists and Mineralogists Special Publication 7, p. 92-100.

Towe, K. M., 1962, Diagenesis of clay minerals as a possible source of silica cement in sedimentary rocks: Journal of Sedimentary Petrology, v. 32, no. 1, p. 26-38.

Van Olphen, H., 1963, Compaction of clay sediments in the range of molecular particle distances, in Clays and Clay Minerals: 11th National Clays and Clay Mineral Conference Proceedings, New York, Macmillan, p. 178-187.

Weaver, C. E., 1958, Geologic interpretation of argillaceous sediments: American Association of Petroleum Geologists Bulletin, v. 42, no. 2, p. 254-309.

Weaver, C. E., and Beck, K. C., 1971, Clay water diagenesis during burial: how mud becomes gneiss: Geological Society of America Special Paper 134, 96 p.

Winker, C., 1979, Late Pleistocene fluvial-deltaic deposition, Texas Gulf coastal plain and shelf: The University of Texas at Austin, Master's thesis, 187 p.

Yeh, H.-W., and Savin, S. M., 1977, Mechanism of burial metamorphism of argillaceous sediments: III. Oxygen-isotope evidence: Geological Society of America Bulletin, v. 88, no. 9, p. 1321-1330.

APPENDIX A

Shale Mineralogy and Burial Diagenesis in Four Geopressured Wells, Hidalgo and Brazoria Counties, Texas

Robert L. Freed
Trinity University
San Antonio, Texas

March 1, 1980

Final Report in Partial Fulfillment of a Subcontract Between Trinity University and The University of Texas at Austin

INTRODUCTION

This report is part of a major study of the reservoir parameters for geopressured geothermal energy in the Gulf Coast region, funded by the Department of Energy and administered by the Bureau of Economic Geology, The University of Texas at Austin. This report concentrates on shale mineralogy, using X-ray analysis both to identify and to quantify individual minerals in the shales. Zones of abnormal subsurface pressure receive special attention.

Shale samples from wells in two geopressured geothermal fairways are compared in this study. The Vicksburg Fairway (Loucks, 1978; Loucks and others, 1979) is represented by: (1) 36 samples from Shell Oil Company #1 Dixie Mortgage Loan Company, Hidalgo County, Texas; and (2) 33 samples from Shell Oil Company/Delhi-Taylor Oil Corporation #3 A. A. McAllen, Hidalgo County, Texas. The Brazoria Fairway (Bebout and others, 1976, 1978; Loucks and others, 1977, 1979) is represented by: (1) 23 samples from Gulf Oil Corporation #2 Texas State Lease 53034, Brazoria County, Texas; and (2) 33 samples from General Crude Oil Company/Department of Energy #1 Pleasant Bayou, Brazoria County, Texas.

The purpose of this report is to provide data that will be helpful in answering two fundamental questions. First, what are the mineralogical parameters of geopressured zones in regions with poor reservoir characteristics (Vicksburg Fairway) as compared to regions with good reservoir characteristics (Brazoria Fairway)? Second, what mineralogical evidence is present that will help to determine the extent of interaction between shales and sandstones during diagenesis?

ANALYTICAL METHODS

Sample Preparation

Both selection of sample intervals and sample preparation were performed by the Bureau of Economic Geology. Some of the #1 Pleasant Bayou samples were obtained from full-diameter cores; all other samples were in the form of cuttings. Each sample was sieved and hand-picked under a microscope to remove sand and silt. Samples were then crushed with mortar and pestle and separated into two fractions: (1) approximately two grams with size greater than 4 Ø; and (2) approximately six grams with size greater than 2.5 Ø. Estimates of sample purity are approximately 90% shale in the greater-than-4 Ø samples; approximately 65% shale in the greater-than-2.5 Ø samples. The greater-than-4 Ø (less-than-62-micron) fraction was reserved for X-ray determination of the bulk mineralogy.

The greater-than 2.5 Ø fraction was used for preparation of oriented clay samples as follows:

(1) calcite was removed by treatment with 10% HCl;

(2) organic matter was removed by treatment with 50% H_2O_2;

(3) salts were removed by repeated centrifuging with deionized water until the wash water did not react with $AgNO_3$;

(4) pH was adjusted to 8.5 by addition of 5% NaOH;

(5) sample was dispersed in deionized water and allowed to settle so that a less-than-two-micron fraction could be separated, pipetted onto glass slides, and allowed to dry

X-Ray Analysis -- Bulk Mineralogy

Diffractometer tracings were obtained with a Philips diffractometer utilizing a scintillation detector and pulse height analyzer. CuKα radiation was generated at 35

kilowatts and 15 milliamperes. Each sample was scanned from $4^{\circ}2\theta$ to $70^{\circ}2\theta$ at a rate of 1° per minute with 1° divergence and scatter slits and a 0.1 mm receiving slit.

The method of Schultz (1964) was used to make semiquantitative estimates of the weight percent for total clay, barite, analcime, quartz, potassium feldspar, plagioclase feldspar, calcite, ankerite, dolomite, siderite, pyrite, and hematite. The degrees 2θ, CuKα radiation, for those peak positions used in determining bulk mineralogy (table A-1) are from Schultz (1964) and Chen (1977). The number of mineral constituents present in any one sample (table A-2) ranged from four to nine. The variation in the weight percent sums of each sample's constituents differed for each well (table A-2). These sums have been normalized to 100% in reporting values for individual samples. Although the precision is at best $\pm$ 10% of the amount present and the accuracy is even less reliable (Hower and others, 1976), major changes in individual mineral contents are readily observed, and this method is considered useful for noting mineralogical trends with depth.

X-Ray Analysis -- Oriented Clay Samples

Each of the less-than-two-micron oriented clay samples was scanned from $2^{\circ}2\theta$ to $36^{\circ}2\theta$ three separate times: (1) oriented clay sample with no further treatment; (2) after solvation with ethylene glycol for a minimum of 12 hours in a vacuum desiccator; and (3) after heating to $550^{\circ}C$ ($1022^{\circ}F$) for one hour. Machine settings were the same as those used for the bulk mineralogy samples, with the exception that some samples required different kilovolt and milliampere settings to keep the diffractometer traces within the range of the chart recorder. In these situations, however, the three clay scans for any one sample were produced at identical settings.

The methods of Johns and others (1954) and Perry and Hower (1970) were used to make semiquantitative estimates of the weight percent of illite, kaolinite, chlorite, and mixed-layer illite-smectite. The term "illite" is used in this report to mean

Table A-1. Degrees 2θ (CuKα) peak positions for determining bulk mineralogy (from Schultz, 1964; Chen, 1977). Supplemental peak positions were used as a check for identification.

Mineral	Major Peak Position	Supplemental Peak Position
total clay	19.9	34.6
barite	25.8	42.8
analcime	26.0	30.5
quartz	26.6	
potassium feldspar	27.5	
plagioclase	28.0	
calcite	29.4	
ankerite	30.8	41.0
dolomite	30.9	41.2
siderite	32.1	52.8
pyrite	33.1	56.3
hematite	33.3	35.8

Table A-2. Minimum and maximum number of coexisting mineral constituents; and minimum and maximum weight percent sums of coexisting mineral constituents determined by the method of Schultz (1964).

	#1 Dixie Mortgage Loan Co.	#3 A. A. McAllen	#2 Texas State Lease	#1 Pleasant Bayou
minimum number mineral constituents	4	4	4	4
maximum number mineral constituents	6	6	9	8
minimum sum of mineral constituents	89	91	80	90
maximum sum of mineral constituents	109	110	112	109

discrete illite; that is, illite that is not involved in the mixed-layering of illite and the swelling clay, smectite. The proportions of illite and smectite in the mixed-layer phase were determined by scanning the solvated sample from $15^{\circ}2\theta$ to $18^{\circ}2\theta$ at $\frac{1}{4}^{\circ}2\theta$ per minute (Reynolds and Hower, 1970).

It is well known that a semiquantitative estimate of individual clay minerals is extremely difficult to obtain. The values determined by any of the techniques presently in use are influenced by: the sampling technique; the method of sample preparation; the X-ray instrumentation; the need to solvate and heat the samples between X-ray scans; the resolution of individual peaks as compared to background; degree of crystallinity and size of individual particles; variations in the chemical composition; and the experience and judgment of the investigator. Therefore, individual values reported in this study should be used with great caution. However, because all samples were prepared and examined in the same manner, the relative values in each well can be used to determine mineralogical trends with depth.

RESULTS

General Statement

The data fall into two categories: (1) bulk mineralogy, and (2) clay mineralogy. Bulk mineralogy includes weight percent estimates of quartz, calcite, dolomite, siderite, ankerite, potassium feldspar, plagioclase feldspar, pyrite, hematite, barite, analcime, and all clay constituents grouped together as "total clay." All values were determined from the less-than-62-micron fraction.

Clay mineralogy includes weight percent estimates of kaolinte, discrete illite, chlorite, and mixed-layer illite-smectite. All clay values were determined from the less-than-two-micron fraction. No discrete smectite was observed in any of the samples. The relative proportions of illite and smectite in the mixed-layer phase have

been calculated; these data are presented as both a percentage of the mixed-layer phase and as a weight percent of the total sample. There is some uncertainty in determining the proportion of illite and smectite from the diffractograms. This is due to the difficulty in choosing the maximum peak-height position of a rather broad peak. This range of uncertainty has been included in both tables and figures.

Equilibrium temperatures for each well have been calculated using the relation developed by Kehle (Bebout and others, 1978, p. 74).

Bulk Mineralogy

Hidalgo County, Texas

#1 Dixie Mortgage Loan Company

Quartz and calcite (fig. A-1; table A-3) are both quite similar in weight percent values at all depths. Calcite averages approximately 11 weight percent in shallower samples and about 14 weight percent in deeper samples. Quartz averages about 11 weight percent in samples shallower than 5,500 ft (1,675 m), and about 13 weight percent in deeper samples.

At shallow depths, total clay (fig. A-1; table A-3) averages approximately 68 weight percent. Below 5,500 ft (1,675 m), the trend of total clay weight percent is toward slightly lower values.

Potassium feldspar (fig. A-2; table A-3) is rather constant in amount at all depths, averaging approximately two weight percent. Plagioclase feldspar (fig. A-2; table A-3) averages five weight percent in shallower samples, and gradually increases to an average of about nine weight percent in deeper samples.

Hematite (fig. A-2; table A-3) is found in seven samples shallower than 6,000 ft (1,830 m); pyrite (fig. A-2; table A-3) is present in six deeper samples. Barite (fig. A-2; table A-3) is present in only five samples; it may be authigenic in origin, but most probably it is a contaminant from drilling fluids.

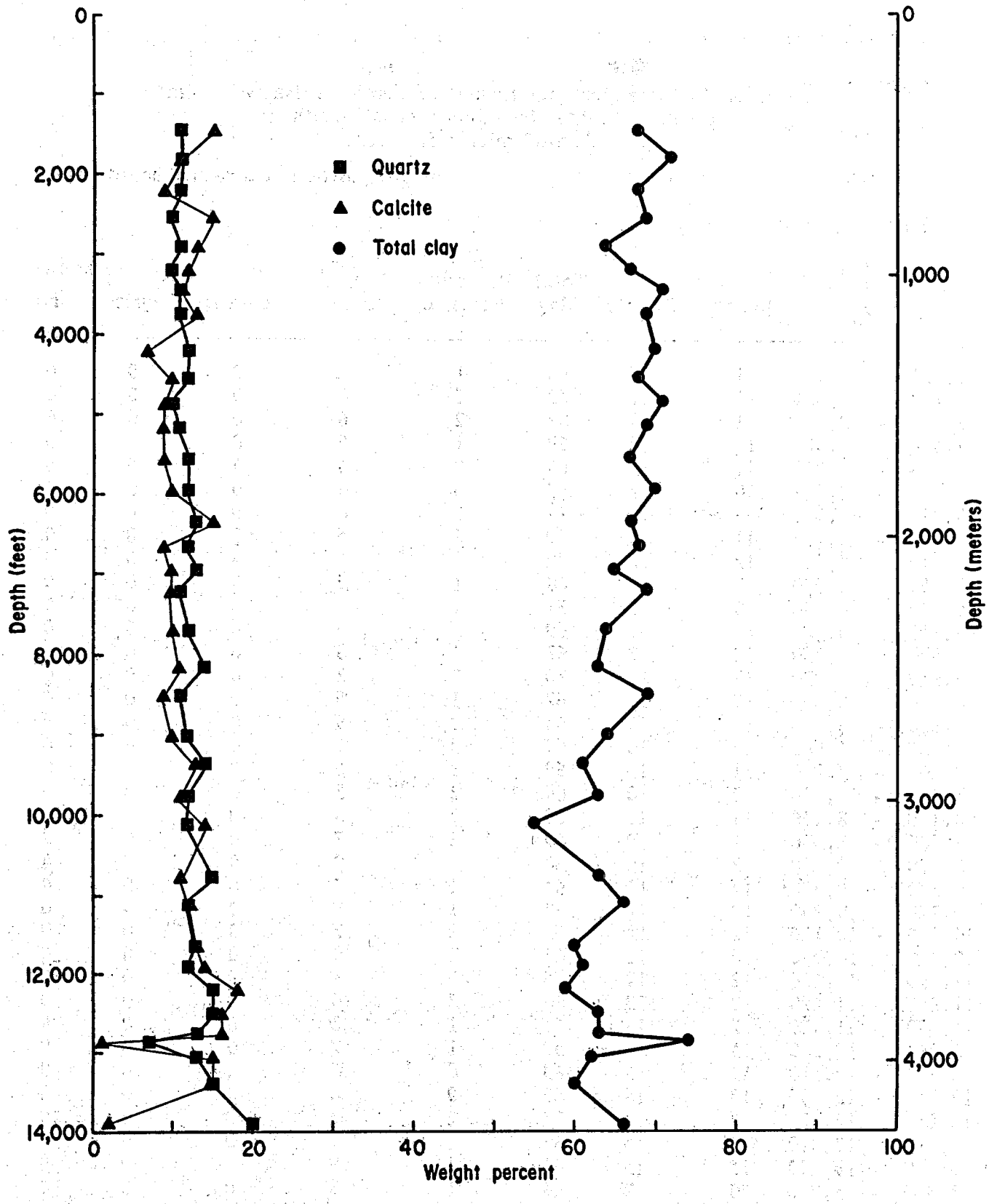

Figure A-1. Shell Oil Company #1 Dixie Mortgage Loan Company, Hidalgo County, Texas: Semiquantitative weight percent estimates for quartz, calcite, and total clay. Data from table A-13.

Table A-3. #1 Dixie Mortgage Loan Co.: Semiquantitative weight percent estimates for mineral constituents in less-than-62-micron fraction.

Sample depth (ft)	Quartz	Calcite	Total Clay	Potassium Feldspar	Plagio-clase	Hematite	Pyrite	Barite
1,454 - 1,485	11	15	68	1	3	2	0	0
1,794 - 1,824	11	11	72	2	4	0	0	0
2,164 - 2,195	11	9	68	2	6	0	0	4
2,534 - 2,575	10	15	69	1	5	0	0	0
2,904 - 2,934	11	13	64	2	6	4	0	0
3,180 - 3,211	10	12	67	3	6	0	0	0
3,421 - 3,451	11	11	71	2	6	0	0	0
3,733 - 3,764	11	13	69	2	5	0	0	0
4,113 - 4,224	12	7	70	3	5	4	0	0
4,550 - 4,580	12	10	68	1	5	4	0	0
4,850 - 4,880	10	9	71	2	5	3	0	0
5,150 - 5,180	11	9	69	2	5	4	0	0
5,550 - 5,580	12	9	67	1	6	6	0	0
5,910 - 5,970	12	10	70	2	7	0	0	0
6,360 - 6,390	13	15	67	1	5	0	0	0
6,630 - 6,660	12	9	68	2	9	0	0	0
6,900 - 6,960	13	10	65	3	5	0	4	0
7,200 - 7,230	11	10	69	3	6	0	0	0
7,670 - 7,730	12	10	64	2	8	0	4	0
8,120 - 8,150	14	11	63	2	6	0	4	0
8,500 - 8,540	11	9	69	2	7	0	0	2
8,990 - 9,000	12	10	64	1	9	0	0	4
9,370 - 9,380	14	13	61	1	7	0	0	4
9,720 - 9,750	12	11	63	1	6	0	4	0
10,100 - 10,120	12	14	55	2	17	0	0	0
10,740 - 10,760	15	11	63	2	9	0	0	0
11,090 - 11,120	12	12	66	3	8	0	0	0
11,640 - 11,670	13	13	60	3	10	0	0	0
11,890 - 11,920	12	14	61	1	8	0	0	4
12,210 - 12,240	15	18	59	1	7	0	0	0
12,490 - 12,510	15	16	63	0	6	0	0	0
12,714 - 12,835	13	16	63	0	8	0	0	0
12,835 - 12,871	7	1	74	2	13	0	4	0
13,010 - 13,040	13	15	62	1	9	0	0	0
13,400 - 13,430	15	15	60	1	9	0	0	0
13,920 - 13,930	20	2	66	1	3	0	8	0

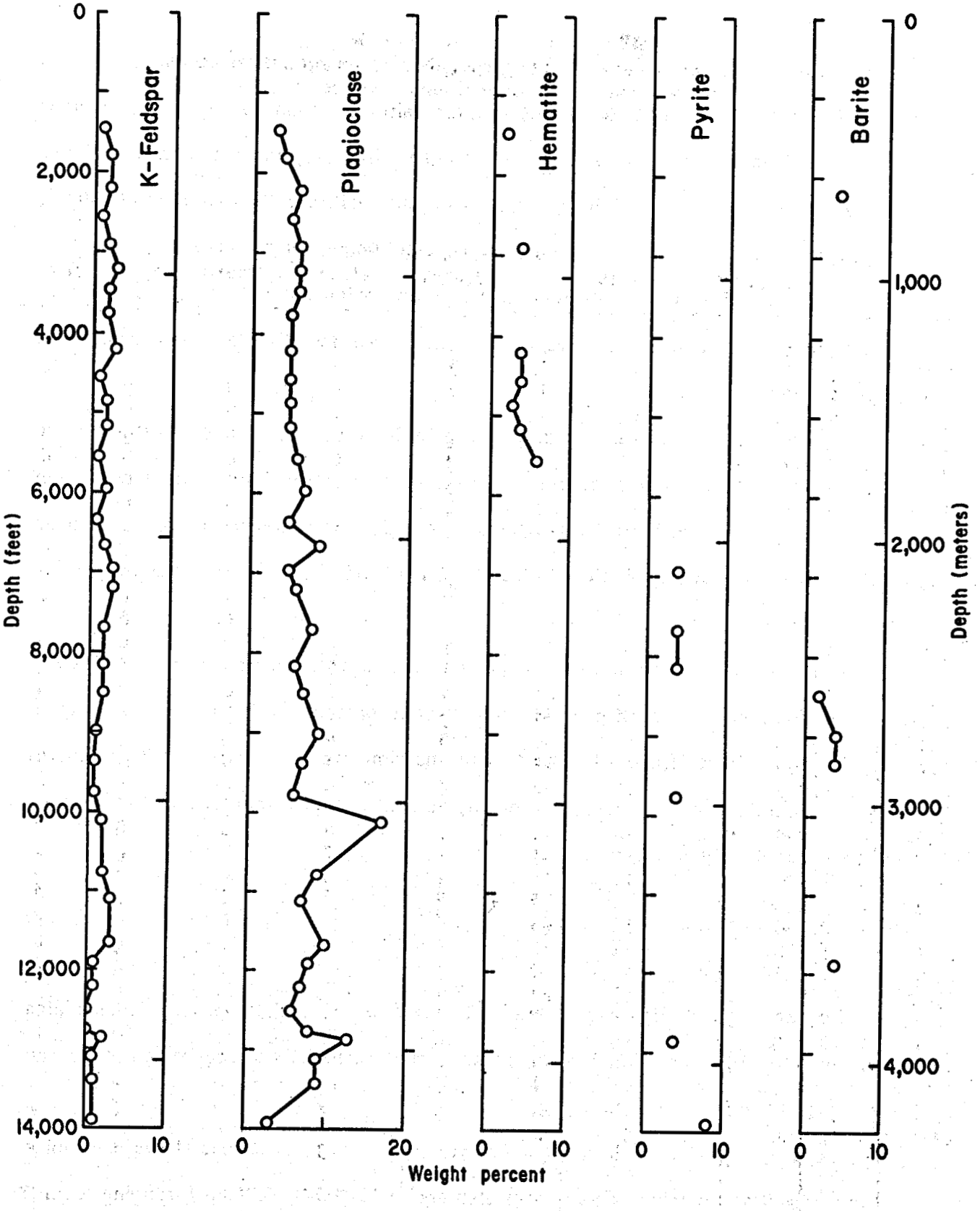

Figure A-2. Shell Oil Company #1 Dixie Mortgage Loan Company, Hidalgo County, Texas: Semiquantitative weight percent estimates for potassium feldspar (K-feldspar), plagioclase feldspar, hematite, pyrite, and barite. Data from table A-3.

#3 A. A. McAllen

Quartz (fig. A-3; table A-4) averages about nine weight percent in samples shallower than 8,000 ft (2,440 m), and increases slightly to an average of 11 weight percent in deeper samples. In contrast, calcite (fig. A-3; table A-4) has a higher average content, about 11 weight percent, at depths shallower than 8,000 ft (2,440 m), and decreases slightly to an average of approximately nine weight percent.

Total clay (fig. A-3; table A-4) average approximately 73 weight percent in samples shallower than 8,000 ft (2,440 m), and decreases slightly to an average of about 71 weight percent.

Both potassium feldspar and plagioclase feldspar (fig. A-4; table A-4) are quite constant in weight percent estimates. Approximately one weight percent potassium feldspar is found throughout all samples. About four weight percent of plagioclase feldspar occurs in samples shallower than 8,000 ft (2,440 m); about five weight percent occurs in deeper samples.

Hematite (fig. A-4; table A-4) is present in four samples from less than 6,000 ft (1,830 m) in depth; pyrite (fig. A-4; table A-4) is present in 12 of the 20 samples deeper than 6,000 ft (1,830 m). Barite and analcime (table A-4) are both present in only one sample each. Barite is probably a contaminant from the drilling fluids; analcime is probably authigenic.

Brazoria County, Texas

#2 Texas State Lease 53034

Quartz content (fig. A-5; table A-5) averages 10 weight percent in samples shallower than 10,500 ft (3,200 m), and then increases slightly in deeper samples to an average of 13 weight percent.

Calcite (fig. A-5; table A-5) is erratic in its distribution but shows a definite trend from higher weight percent estimates above 10,000 ft (3,050 m), ranging from 3 to 19 weight percent, to a more consistent average of three weight percent below 10,000 ft (3,050 m).

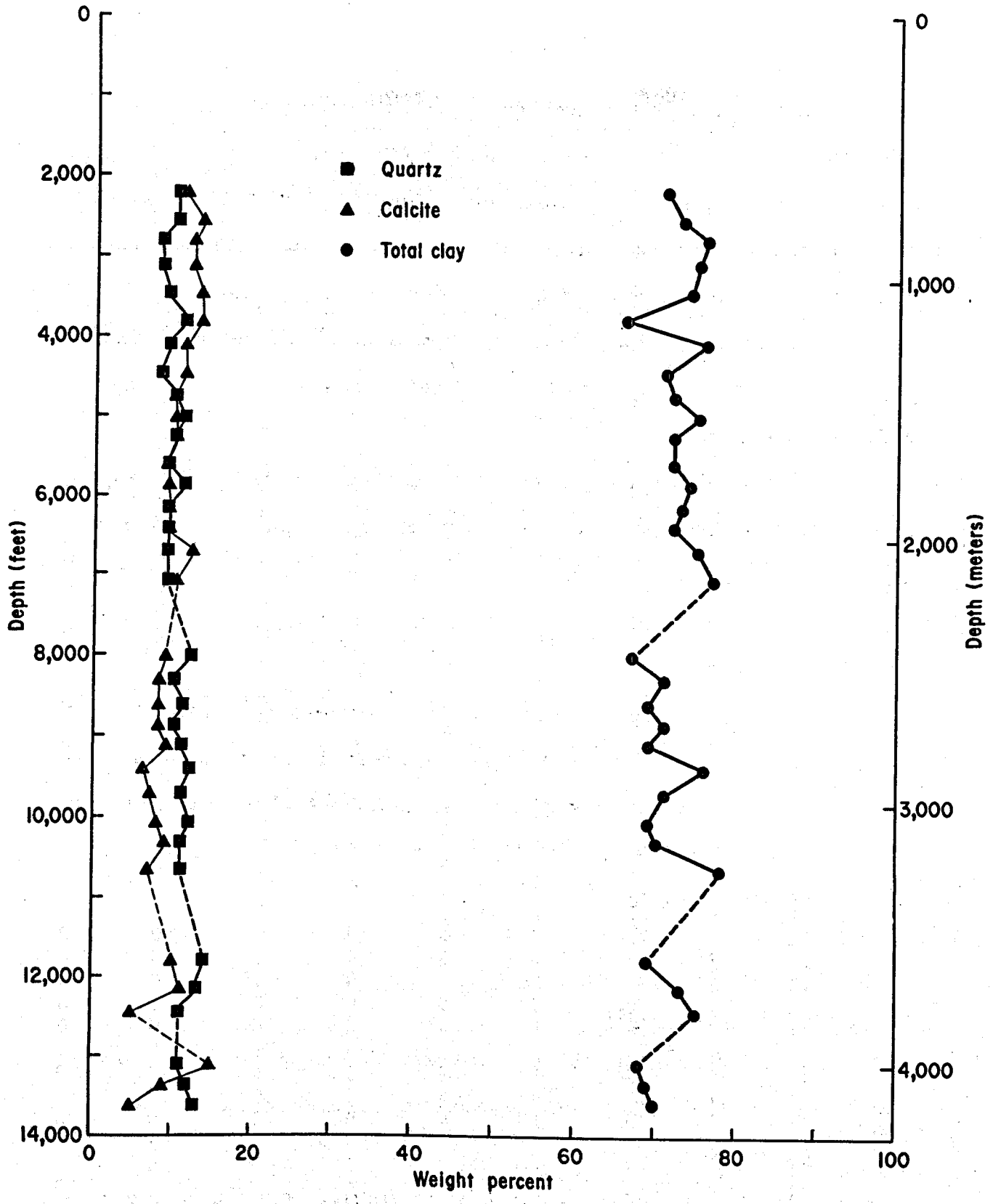

Figure A-3. Shell Oil Company/Delhi-Taylor Oil Corporation #3 A. A. McAllen, Hidalgo County, Texas: Semiquantitative weight percent estimates for quartz, calcite, and total clay. Dashed lines indicate missing less-than-62-micron samples. Data from table A-4.

Table A-4. #3 A. A. McAllen: Semiquantitative weight percent estimates for mineral constituents in less-than-62-micron fraction.

Sample depth (ft)	Quartz	Calcite	Total Clay	Potassium Feldspar	Plagio-clase	Hematite	Pyrite	Barite	Analcime
2,183	10	11	71	1	5	0	0	0	2
2,558	10	13	73	1	3	0	0	0	0
2,809	8	12	76	0	4	0	0	0	0
3,120	8	12	75	1	4	0	0	0	0
3,437	9	13	74	1	3	0	0	0	0
3,780 - 3,797	11	13	66	1	4	4	0	0	0
4,125	9	11	76	1	3	0	0	0	0
4,450	8	11	71	1	4	4	0	0	0
4,720 - 4,751	10	10	72	1	6	0	0	0	0
5,002 - 5,033	11	10	75	0	4	0	0	0	0
5,253 - 5,285	10	10	72	1	4	4	0	0	0
5,569 - 5,600	9	9	72	1	8	0	0	0	0
5,820 - 5,852	11	9	74	1	3	2	0	0	0
6,133 - 6,165	9	9	73	1	3	0	4	0	0
6,385 - 6,417	9	9	72	1	5	0	4	0	0
6,694 - 6,726	9	12	75	1	3	0	0	0	0
7,038 - 7,070	9	10	77	1	3	0	0	0	0
*7,383	—	—	—	-	-	-	-	-	-
*7,727	—	—	—	-	-	-	-	-	-
7,979 - 8,050	12	9	67	2	5	0	4	0	0
8,294 - 8,324	10	8	71	1	5	0	4	0	0
8,595 - 8,600	11	8	69	2	6	0	4	0	0
8,842 - 8,874	10	8	71	2	4	0	4	0	0
9,076 - 9,107	11	9	69	1	5	0	4	0	0
9,395 - 9,427	12	6	76	2	5	0	0	0	0
9,708 - 9,738	11	7	71	1	5	0	4	0	0
10,060 - 10,090	12	8	69	2	5	0	4	0	0
10,302 - 10,333	11	9	70	0	5	0	0	4	0
10,613 - 10,644	11	7	78	1	4	0	0	0	0
*10,926	—	-	—	-	-	-	-	-	-
11,777 - 11,808	14	10	69	1	6	0	0	0	0
12,110 - 12,141	13	11	73	0	4	0	0	0	0
12,460 - 12,491	11	5	75	1	4	0	4	0	0
*12,768	—	—	—	-	-	-	-	-	-
13,077 - 13,107	11	15	68	1	5	0	0	0	0
13,323 - 13,355	12	9	69	0	6	0	4	0	0
13,601 - 13,632	13	5	70	1	7	0	4	0	0

*no less-than-62-micron sample available

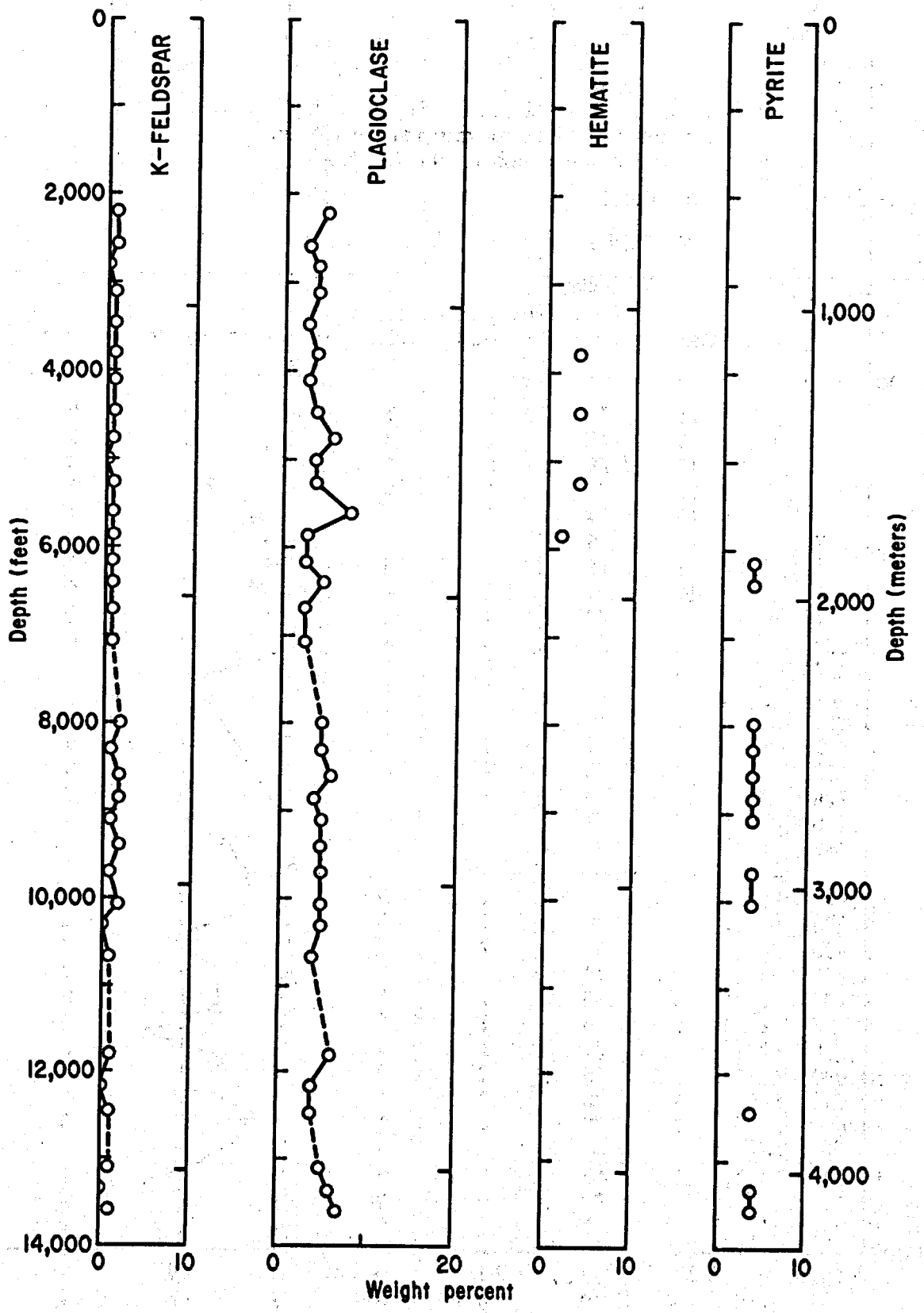

Figure A-4. Shell Oil Company/Delhi-Taylor Oil Corporation #3 A. A. McAllen, Hidalgo County, Texas: Semiquantitative weight percent estimates for potassium feldspar (K-feldspar), plagioclase feldspar, hematite, and pyrite. Dashed lines indicate missing less-than-62-micron samples. Data from table A-4.

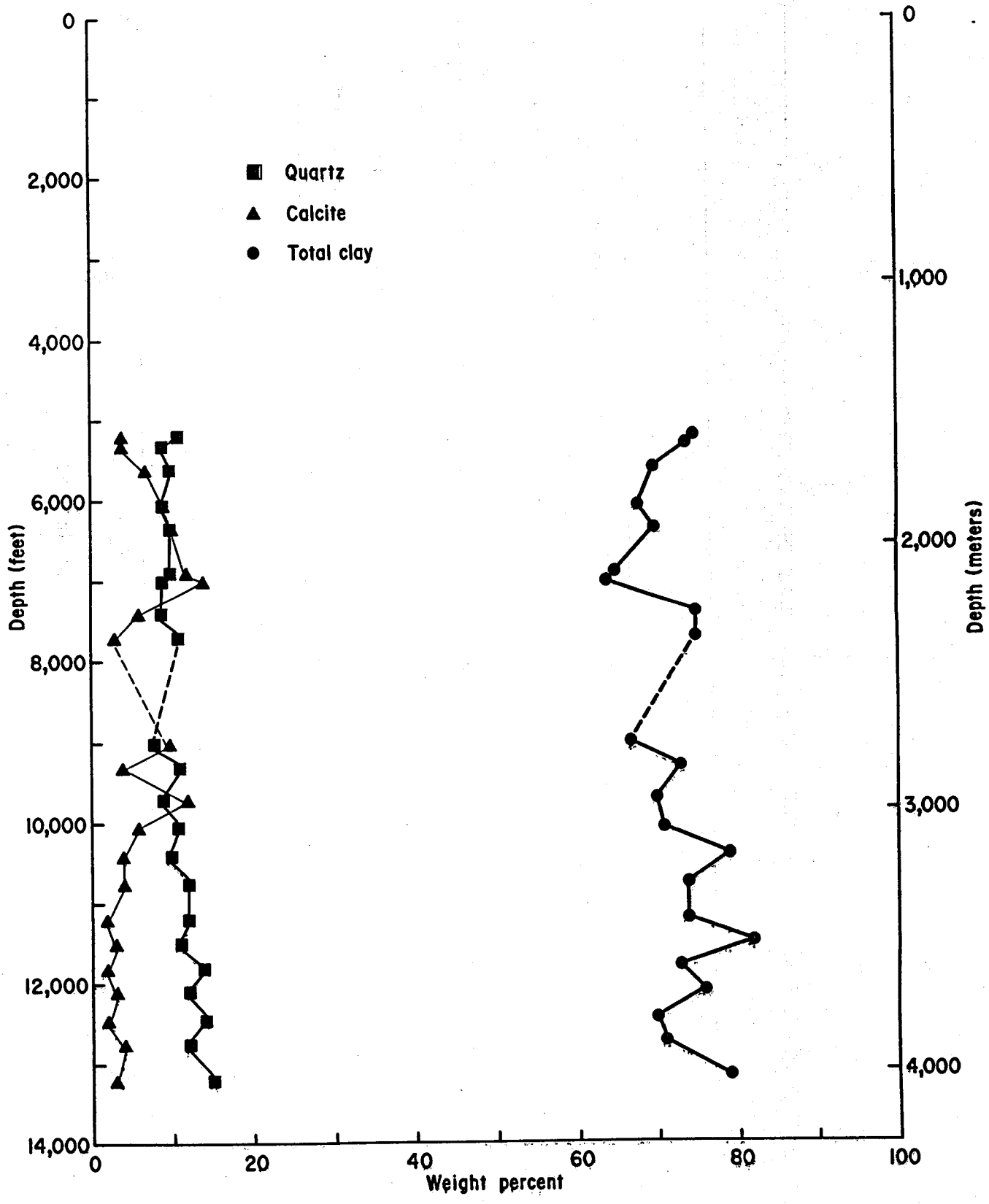

Figure A-5. Gulf Oil Corporation #2 Texas State Lease 53034, Brazoria County, Texas: Semiquantitative weight percent estimates for quartz, calcite, and total clay. Dashed lines indicate a missing less-than-62-micron sample. Data from table A-5.

Table A-5. #2 Texas State Lease 53034: Semiquantitative weight percent estimates for mineral constituents in less-than-62-micron fraction.

Sample depth (ft)	Quartz	Calcite	Total Clay	Potassium Feldspar	Plagio-clase	Pyrite	Siderite	Ankerite	Barite
5,194 - 5,225	11	4	75	2	3	4	1	0	0
5,287 - 5,350	9	4	74	3	2	7	1	0	0
5,598 - 5,630	10	7	70	3	2	4	1	0	4
6,002 - 6,096	9	9	68	3	3	4	0	0	4
6,314 - 6,379	10	10	70	3	2	4	0	0	0
6,848 - 6,911	10	12	65	2	2	4	1	0	4
6,974 - 7,067	9	14	64	3	2	4	1	0	4
7,347 - 7 409	9	6	75	2	3	4	0	1	0
7,641 - 7,734	11	3	75	1	3	6	0	0	0
*8,335 - 8,416	—	—	—	-	-	-	-	-	-
8,989 - 9,114	8	10	67	1	2	5	1	1	5
9,303 - 9,334	11	4	73	1	2	4	0	1	4
9;699 - 9,730	9	12	70	1	3	6	0	0	0
10,011 - 10,060	11	6	71	0	8	4	0	0	0
10,385 - 10,448	10	4	79	1	3	4	0	0	0
10,760 - 10,791	12	4	74	0	6	0	0	0	4
11,197 - 11,269	12	2	74	0	5	2	0	0	5
11,478 - 11,579	11	3	82	0	4	0	0	0	0
11,760 - 11,822	14	2	73	1	5	0	0	0	5
12,041 - 12,135	12	3	76	1	4	4	0	0	0
12,396 - 12,473	14	2	70	0	3	4	0	0	6
12,697 - 12,791	12	4	71	0	2	4	0	2	4
13,133 - 13,246	15	3	79	0	4	0	0	0	0

*no less-than-62-micron sample available

Total clay values (fig. A-5; table A-5) show a gradual increase with depth, changing from an average of 70 weight percent to an average of 75 weight percent.

Potassium feldspar (fig. A-6; table A-5) decreases with depth from an average of three weight percent to less than one weight percent. Potassium feldspar is absent in seven of the 10 samples below 10,000 ft (3,050 m).

Plagioclase feldspar (fig. A-6; table A-5) is constant at an average of two weight percent in samples shallower than 10,000 ft (3,050 m). At that depth the plagioclase content increases to an average of four weight percent.

Pyrite (fig. A-6; table A-5) is present in 18 of the 23 samples examined. Siderite (fig. A-6; table A-5) is present in six samples. Ankerite (fig. A-6; table A-5) is present in four samples and barite (fig. A-6; table A-5) is present in 11 samples. Both the siderite and ankerite are considered authigenic in origin. The barite may be authigenic, but it probably is due to contamination from the drilling mud.

#1 Pleasant Bayou

Quartz content (fig. A-7; table A-6) is variable: beginning at an average of 15 weight percent between 2,000 and 4,000 ft (610 and 1,220 m); decreasing to five weight percent at 6,700 ft (2,040 m); increasing to 14 weight percent at 8,300 ft (2,530 m); and gradually increasing to an average of 16 weight percent in deeper samples.

Calcite (fig. A-7; table A-6) also is variable: beginning at 10 weight percent at 2,200 ft (670 m); increasing to 28 weight percent at 6,700 ft (2,040 m); decreasing rapidly to six weight percent at 7,800 ft (2,380 m). This extreme variation probably is due to the presence of fossil fragments. Below 7,800 ft (2,380 m), the calcite content gradually decreases to zero.

The total clay content (fig. A-7; table A 6) shows a gradual increase with depth in weight percent estimates from approximately 60 weight percent in shallower samples to 75 weight percent in deeper samples.

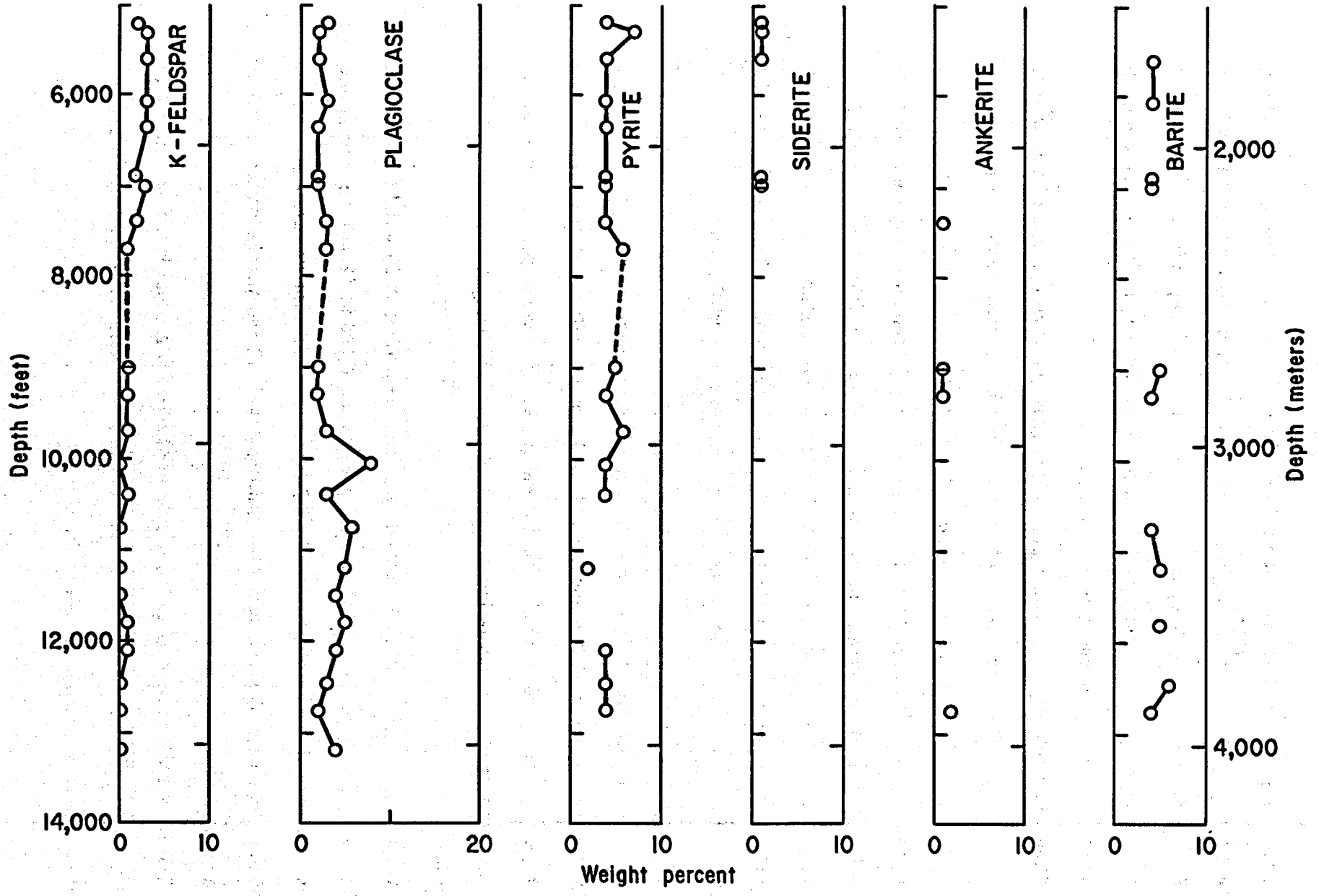

Figure A-6. Gulf Oil Corporation #2 Texas State Lease 53034, Brazoria County, Texas: Semiquantitative weight percent estimates for potassium feldspar (K-feldspar), plagioclase feldspar, pyrite, siderite, ankerite, and barite. Dashed lines indicate a missing less-than-62-micron sample. Data from table A-5.

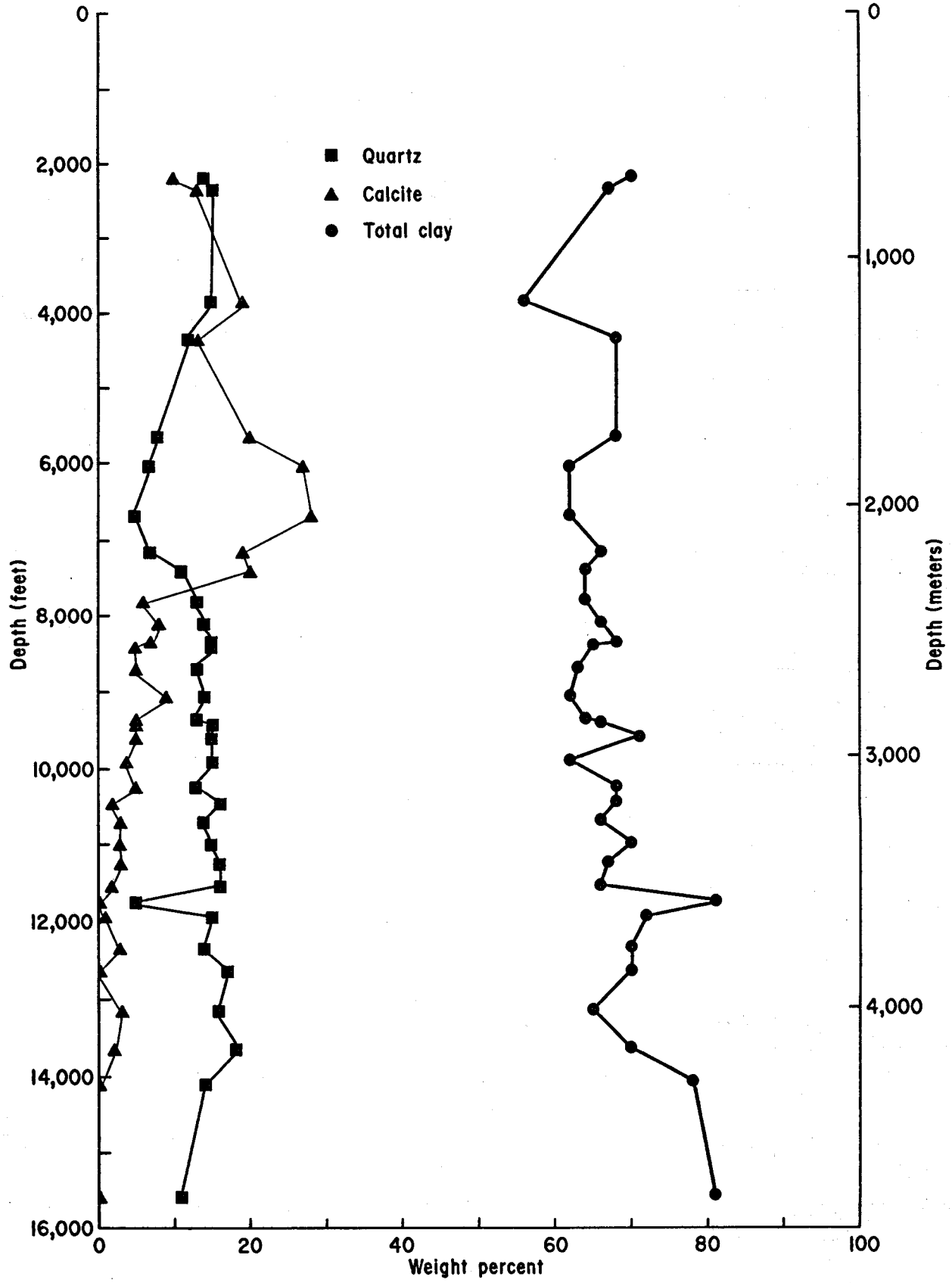

Figure A-7. General Crude Oil Company/Department of Energy #1 Pleasant Bayou, Brazoria County, Texas: Semiquantitative weight percent estimates for quartz, calcite, and total clay. Data from table A-6

Table A-6. #1 Pleasant Bayou: Semiquantitative weight percent estimates for mineral constituents in less-than-62-micron fraction.

Sample depth (ft)	Quartz	Calcite	Total Clay	Potassium Feldspar	Plagioclase	Dolomite	Siderite	Pyrite	Barite
2,185	14	10	70	2	2	1	0	0	0
2,335	15	13	67	2	4	0	0	0	0
3,860	15	19	56	2	4	4	0	0	0
4,347	12	13	68	3	3	1	0	0	0
5,630 - 5,660	8	20	68	2	2	0	0	0	0
6,020 - 6,050	7	27	62	2	2	0	0	0	0
6,703	5	28	62	1	2	2	0	0	0
7,110 - 7,140	7	19	66	2	2	0	0	4	0
7,400 - 7,430	11	20	64	2	3	0	0	0	0
7,800	13	6	64	3	7	0	2	6	0
8,100	14	8	66	3	4	0	1	4	0
8,330 - 8,360	15	7	68	2	3	0	0	4	0
8,400	15	5	65	3	7	0	0	4	0
8,690 - 8,720	13	5	63	1	1	0	1	4	12
9,020 - 9,050	14	9	62	2	2	0	1	4	4
9,320 - 9,350	13	5	64	1	5	0	2	6	4
9,380 - 9,410	15	5	66	2	4	0	2	6	0
9,590 - 9,620	15	5	71	1	3	0	1	4	0
9,890 - 9,920	15	4	62	1	5	0	1	6	7
10,232	13	5	68	3	8	0	0	0	4
10,430 - 10,460	16	2	68	4	5	0	0	0	4
10,700 - 10,730	14	3	66	3	5	0	0	4	6
11,000 - 11,030	15	3	70	4	8	0	0	0	0
11,210 - 11,240	16	3	67	4	5	0	0	0	4
11,540 - 11,570	16	2	66	3	3	0	0	4	6
11,750	5	0	81	4	4	0	0	6	0
11,930 - 11,960	15	1	72	3	4	0	0	4	0
12,320 - 12,350	14	3	70	3	5	0	0	4	0
12,630	17	0	70	3	5	0	0	6	0
13,130 - 13,160	16	3	65	5	5	0	0	4	0
13,610 - 13,640	18	2	70	2	4	0	0	4	0
14,078	14	0	78	2	3	0	0	4	0
15,592	11	0	81	3	4	0	0	0	0

Potassium feldspar (fig. A-8; table A-6) is essentially unchanged with depth at an average of two weight percent. Plagioclase feldspar (fig. A-8; table A-6) increases from an average of three weight percent in samples shallower than 7,500 ft (2,290 m) to an average of nine weight percent in deeper samples.

Dolomite (table A-6) is present in four samples at depths less than 7,000 ft (2,135 m). Siderite and pyrite (fig. A-8; table A-6) are indicators of a reducing environment. Barite (fig. A-8; table A-6) is considered a contaminant from the drilling mud.

Clay Mineralogy

Hidalgo County, Texas

#1 Dixie Mortgage Loan Company

Although individual clay mineral contents vary widely from sample to sample, depth trends can be observed: (1) kaolinite increases (fig. A-9; table A-7); (2) discrete illite decreases (fig. A-9; table A-7); (3) mixed-layer illite-smectite decreases (figs. A-9 and A-10; table A-7); (4) mixed-layer illite increases (fig. A-10; table A-7); and (5) mixed-layer smectite decreases (fig. A-10; table A-7).

The proportions of illite and smectite in mixed-layer illite-smectite (fig. A-11; table A-8) show three distinct zones that characterize the physical arrangement of illite and smectite within the mixed-layer phase:

(1) At depths shallower than 5,750 ft (1,750 m) and proportions of illite layers 40% and less, the illite and smectite are arranged in a random interstratification.

(2) Between 5,750 ft (1,750 m) and 7,450 ft (2,270 m), and with proportions of illite layers of 59 to 70%, the illite and smectite are arranged in a weak order interstratification. This ordering is noted by the presence of a weak superlattice reflection between the illite and smectite peaks on the

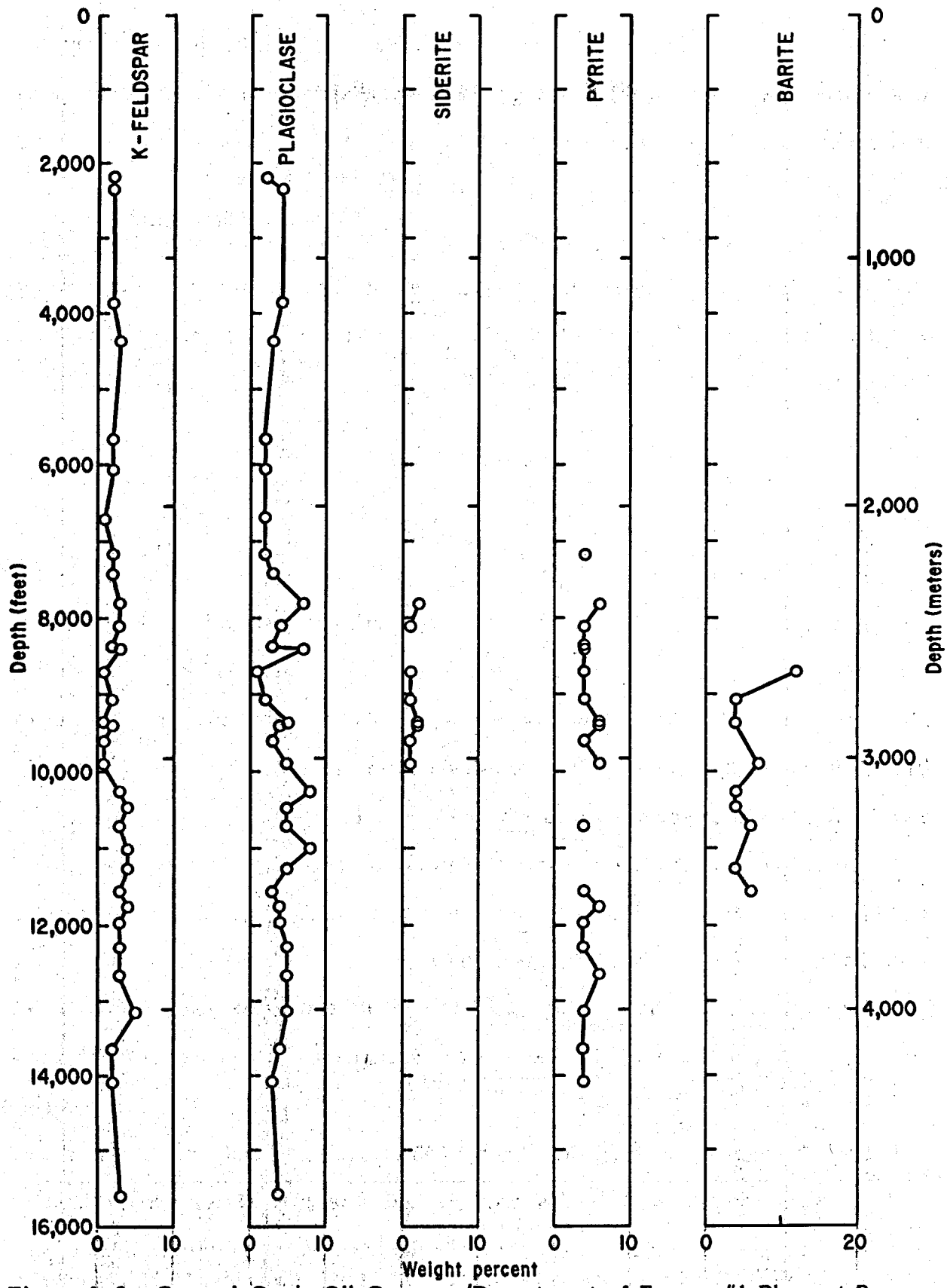

Figure A-8. General Crude Oil Company/Department of Energy #1 Pleasant Bayou, Brazoria County, Texas: Semiquantitative weight percent estimates for potassium feldspar (K-feldspar), plagioclase feldspar, siderite, pyrite, and barite. Data from table A-6.

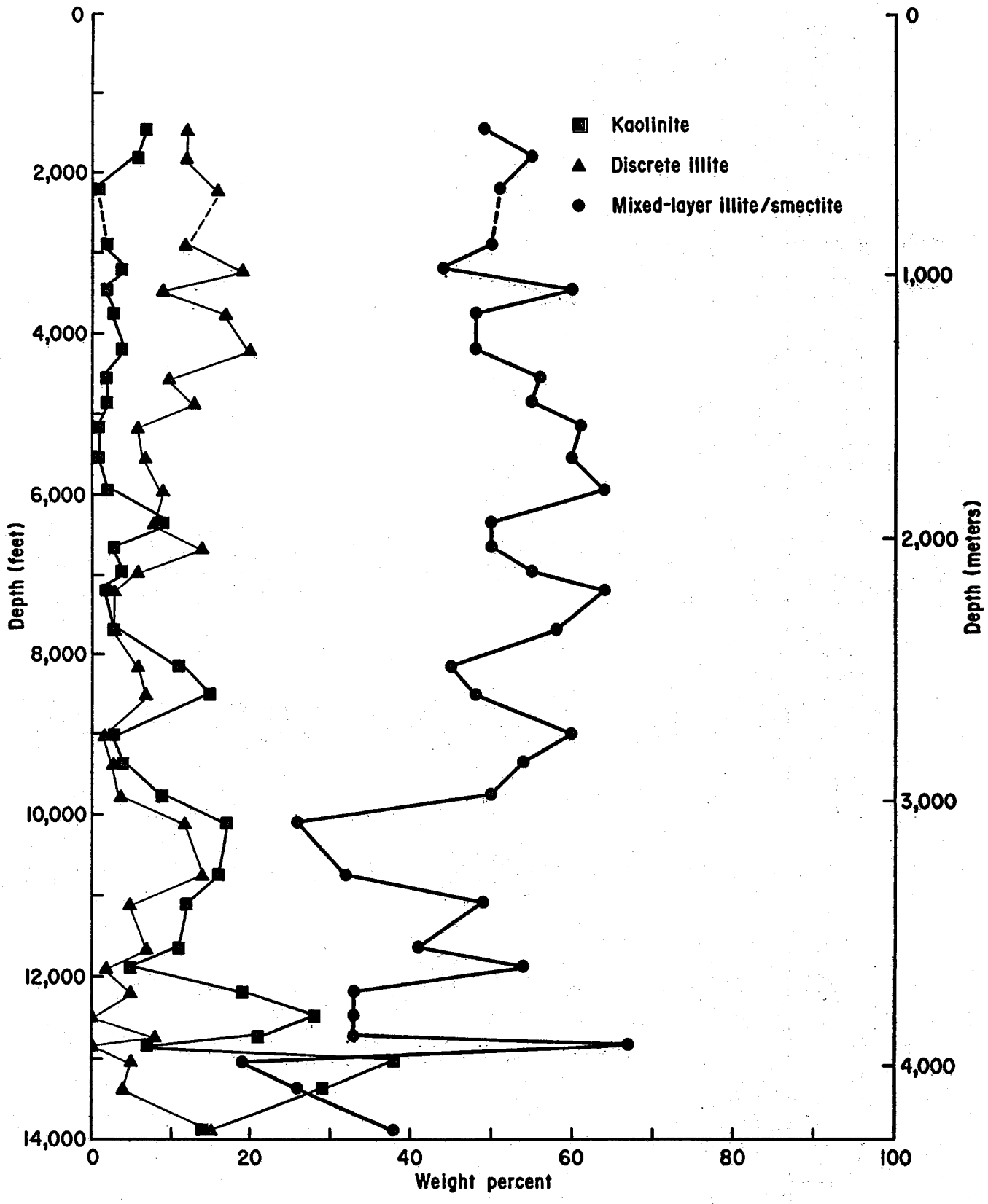

Figure A-9. Shell Oil Company #1 Dixie Mortgage Loan Company, Hidalgo County, Texas: Semiquantitative weight percent estimates for kaolinite, discrete illite, and mixed-layer illite-smectite (mixed-layer I/S). Dashed lines indicate a missing less-than-two-micron sample. Data from table A-7.

Table A-7. #1 Dixie Mortgage Loan Co.: Semiquantitative weight percent estimates of clay constituents in less-than-two-micron fraction.

Sample depth (ft)	Kaolinite	Discrete Illite	Mixed Illite/Smectite	Mixed Illite	Mixed Smectite	Chlorite
1,454 - 1,485	7	12	49	14	35	0
1,794 - 1,824	6	12	55	16	39	0
2,164 - 2,195	1	16	51	17	34	0
*2,534 - 2,575	—	—	—	—	—	-
**2,904 - 2,934	2	12	50	—	—	0
3,180 - 3,211	4	19	44	7	37	0
3,421 - 3,451	2	9	60	13	47	0
3,733 - 3,764	3	17	48	11	37	0
4,113 - 4,224	4	20	48	17	31	0
4,550 - 4,580	2	10	56	12	44	0
4,850 - 4,880	2	13	55	22	33	0
5,150 - 5,180	1	6	61	24	37	0
5,550 - 5,580	1	7	60	24	36	0
5,910 - 5,970	2	9	64	38	26	0
6,360 - 6,390	9	8	50	34	16	0
6,630 - 6,660	3	14	50	31	19	0
6,900 - 6,960	4	6	55	39	16	0
7,200 - 7,230	2	3	64	42	22	0
7,670 - 7,730	3	3	58	45	13	0
8,120 - 8,150	11	6	45	37	8	1
8,500 - 8,540	15	7	48	40	8	0
8,990 - 9,000	3	2	60	50	10	0
9,370 - 9,380	4	3	54	47	7	0
9,720 - 9,750	9	4	50	45	5	1
10,100 - 10,120	17	12	26	23	3	0
10,740 - 10,760	16	14	32	28	4	0
11,090 - 11,120	12	5	49	43	6	0
11,640 - 11,670	11	7	41	36	5	0
11,890 - 11,920	5	2	54	47	7	0
12,210 - 12,240	19	5	33	29	4	1
12,490 - 12,510	28	0	33	30	3	2
12,714 - 12 835	21	8	33	29	4	0
12,835 - 12,871	7	0	67	62	5	0
13,010 - 13,040	38	5	19	16	3	1
13,400 - 13,430	29	4	26	23	3	1
13,920 - 13,930	14	15	38	33	5	0

*no less-than-two-micron sample available
**illite/smectite proportions not determined

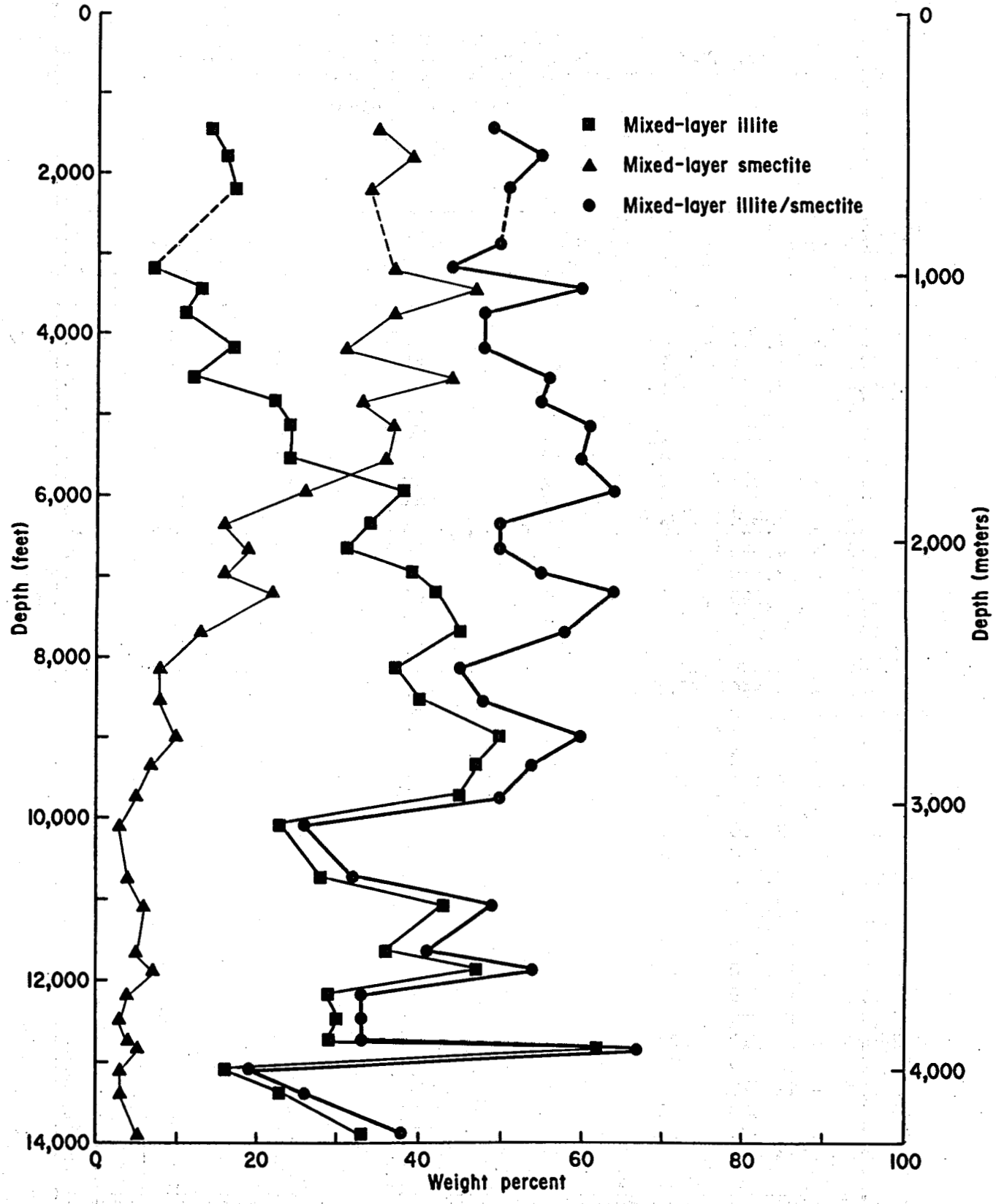

Figure A-10. Shell Oil Company #1 Dixie Mortgage Loan Company, Hidalgo County, Texas: Semiquantitative weight percent estimates of mixed-layer illite, mixed-layer smectite, and total mixed-layer illite-smectite (mixed-layer I/S). Dashed lines indicate either a missing less-than-two-micron sample or no detection of illite and smectite proportions. Data from table A-7.

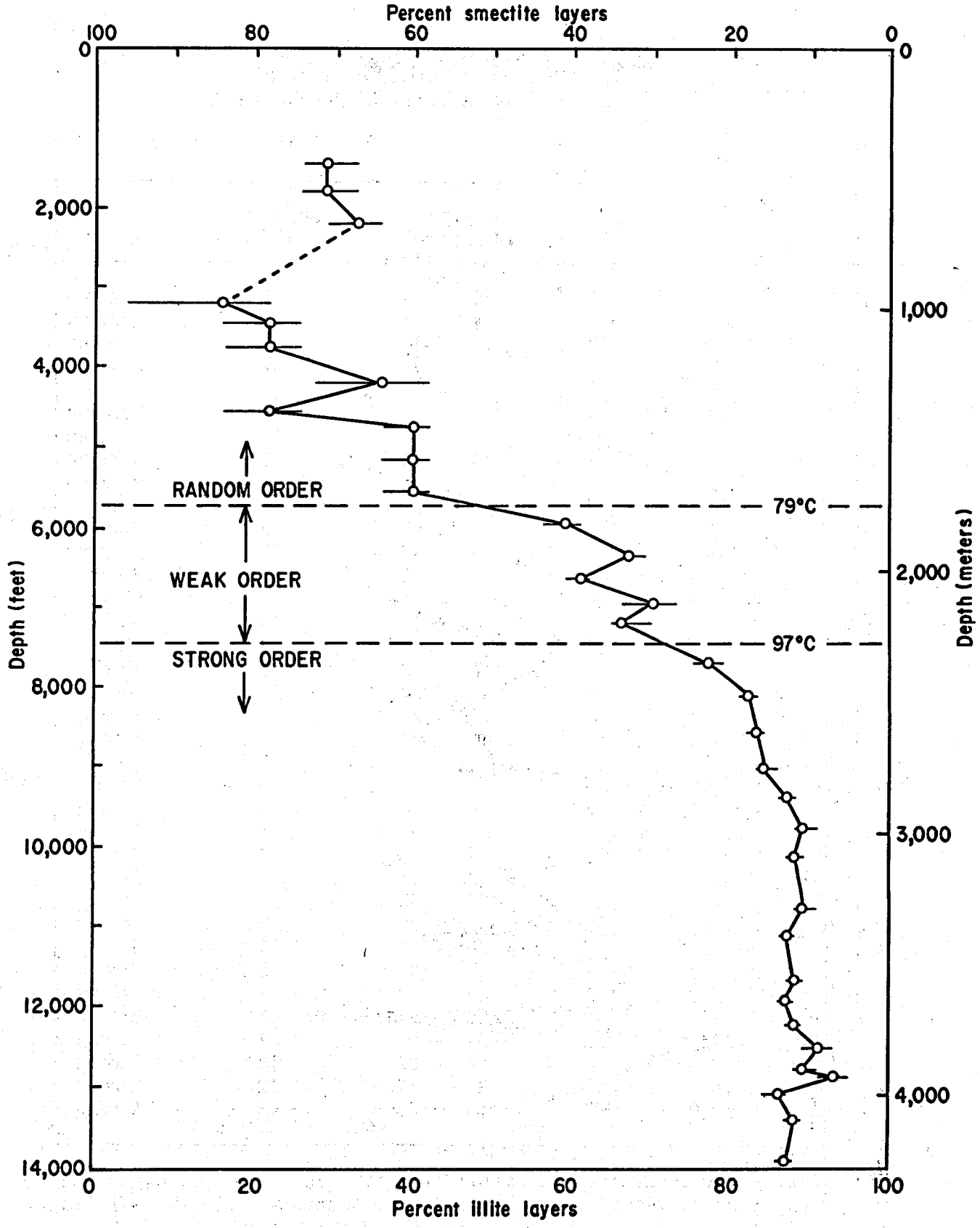

Figure A-11. Shell Oil Company #1 Dixie Mortgage Loan Company, Hidalgo County, Texas: Estimated illite and smectite proportions in mixed-layer illite-smectite. Dashed line indicates no information available. Data from table A-8.

Table A-8. #1 Dixie Mortgage Loan Co.: Proportions of mixed-layer illite and smectite; uncertainty in terms of illite content; type of ordering.

Sample depth (ft)	Illite (%)	Uncertainty (% Illite)	Smectite (%)	Ordering
1,454 - 1,485	29	26 - 33	71	Random
1,794 - 1,824	29	26 - 33	71	Random
2,164 - 2,195	33	29 - 36	67	Random
*2,534 - 2,575	--	----	--	----
**2,904 - 2 934	--	----	--	----
3,180 - 3,211	16	4 - 22	84	Random
3,421 - 3,451	22	16 - 26	78	Random
3,733 - 3,764	22	16 - 26	78	Random
4,113 - 4,224	36	29 - 42	64	Random
4,550 - 4,580	22	16 - 26	78	Random
4,850 - 4,880	40	36 - 42	60	Random
5,150 - 5,180	40	36 - 42	60	Random
5,550 - 5,580	40	36 - 42	60	Random
5,910 - 5,970	59	56 - 61	41	Weak
6,360 - 6,390	67	66 - 69	33	Weak
6,630 - 6,660	61	59 - 62	39	Weak
6,900 - 6,960	70	66 - 73	30	Weak
7,200 - 7,230	66	65 - 70	34	Weak
7,670 - 7,730	77	75 - 79	23	Strong
8,120 - 8,150	82	81 - 83	18	Strong
8,500 - 8,540	83	82 - 84	17	Strong
8,990 - 9,000	84	83 - 86	16	Strong
9,370 - 9,380	87	86 - 88	13	Strong
9,720 - 9,750	89	88 - 91	11	Strong
10,100 - 10,120	88	87 - 89	12	Strong
10,740 - 10,760	89	88 - 91	11	Strong
11,090 - 11,120	87	86 - 88	13	Strong
11,640 - 11,670	88	87 - 89	12	Strong
11,890 - 11,920	87	86 - 88	13	Strong
12,210 - 12,240	88	87 - 89	12	Strong
12,490 - 12,510	91	89 - 93	9	Strong
12,714 - 12,835	89	88 - 91	11	Strong
12,835 - 12,871	93	91 - 95	7	Strong
13,010 - 13,040	86	84 - 87	14	Strong
13,400 - 13,430	88	87 - 89	12	Strong
13,920 - 13,930	87	86 - 88	13	Strong

*no less-than-two-micron sample available
**proportions not determined

diffractogram of the solvated, oriented clay sample. In addition, the shape of the "average" mixed-layer peak for the untreated sample changes significantly. The calculated equilibrium temperature at the boundary between random and weak order zones is 79°C (174°F) (fig. A-11).

(3) Below 7,450 ft (2,270 m), and proportions of illite layers 77% and more, illite and smectite are arranged in a strong order interstratification. This type of ordering is noted by a distinct superlattice reflection between the illite and smectite peaks on the diffractogram of the solvated, oriented sample. The calculated equilibrium temperature at the boundary between weak order and strong order zones is 97°C (207°F) (fig. A-11).

The boundary markers between random, weak, and strong order also are valuable in outlining general relationships between discrete illite and kaolinite (fig. A-9): (1) within the random order zone, more discrete illite than kaolinite is present; (2) within the weak order zone the discrete illite and kaolinite are subequal in content; and (3) within the strong order zone kaolinite dominates over discrete illite.

The depth at which the mixed-layer illite curve (fig. A-10) crosses the mixed-layer smectite curve is on the boundary between random and weak order zones. The boundary between the weak and strong order zones is located between a mixed-layer smectite content of 13 to 16 weight percent.

In samples from depths shallower than 4,700 ft (1,430 m), the weight percent content of discrete illite (fig. A-9) and mixed-layer illite (fig. A-10) are unchanged; in samples deeper than 4,700 ft (1,430 m), definite changes are present. This may be an indication that diagenetic changes begin in the shales at a depth of 4,700 ft (1,430 m). The calculated equilibrium temperature at 4,700 ft (1,430 m) is 69°C (156°F).

Chlorite (table A-7) occurs in six samples, all of which are in the strong order zone.

#3 A. A. McAllen

Clay mineral trends with depth are the same as those observed for #1 Dixie Mortgage Loan: (1) kaolinite increases (fig. A-12; table A-9); (2) discrete illite decreases (fig. A-12; table A-9); (3) mixed-layer illite-smectite decreases (figs. A-12 and A-13; table A-9); (4) mixed-layer illite increases (fig. A-13; table A-9); (5) mixed-layer smectite decreases (fig. A-13; table A-9).

The proportions of illite and smectite in mixed-layer illite smectite (fig. A-14; table A-10) show three distinct ordering zones: (1) at depths shallower than 7,850 ft (2,390 m), and illite proportions of 45% and less, random interstratification is observed; (2) between 7,850 ft (2,390 m) and 9,000 ft (2,740 m), and with illite proportions of 60 to 70%, the interstratification is weak order; and (3) for samples deeper than 9,000 ft (2,740 m), and illite proportions of 75% and greater, the interstratification is strong order. The calculated equilibrium temperatures between the zones are: (1) 86°C (187°F) at the random/weak order boundary; and (2) 106°C (223°F) at the weak/strong order boundary

As observed in the #1 Dixie Mortgage Loan, the content of discrete illite and kaolinite is related to the ordering boundaries. In the random order zone, discrete illite is more abundant than kaolinite (fig. A-12). The values are equivalent in the weak order zone, and kaolinite generally exceeds discrete illite in the strong order zone.

The curve for mixed-layer illite (fig. A-13) crosses the curve for mixed-layer smectite very near the random order/weak order boundary. Unfortunately, no less-than-62-micron sample was available for sample locations of 7,383 ft (2,250 m) or 7,727 ft (2,355 m), so a total clay value could not be determined. Therefore, a more accurate estimate of the "crossover" depth cannot be determined. The boundary between weak and strong order is located between a mixed-layer smectite estimate of 15 to 16 weight percent.

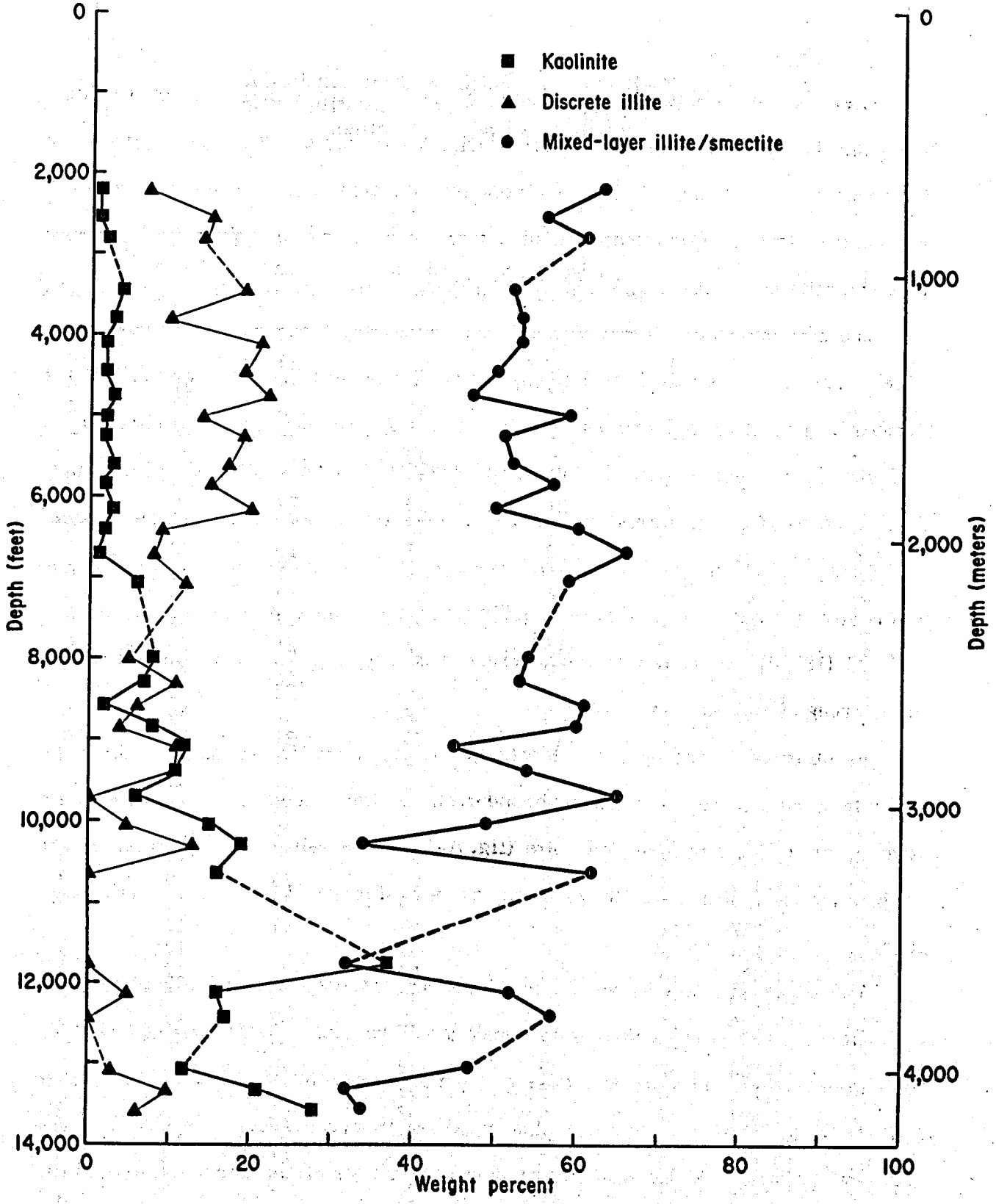

Figure A-12. Shell Oil Company/Delhi-Taylor Oil Corporation #3 A. A. McAllen, Hidalgo County, Texas: Semiquantitative weight percent estimates for kaolinite, discrete illite, and mixed-layer illite-smectite (mixed-layer I/S). Dashed lines indicate either a missing less-than-two-micron sample or no total clay value available. Data from table A-9.

Table A-9. #3 A. A. McAllen: Semiquantitative weight percent estimates of clay constituents in less-than-two-micron fraction.

Sample depth (ft)	Kaolinite	Discrete Illite	Mixed Illite/Smectite	Mixed Illite	Mixed Smectite	Chlorite
2,183	1	7	63	23	40	0
2,558	1	15	56	25	31	0
2,809	2	14	61	16	45	0
* 3,120	—	—	—	—	—	-
3,437	4	19	52	17	35	0
3,780 - 3,797	3	10	53	17	36	0
4,125	2	21	53	24	29	0
4,450	2	19	50	15	35	0
4,720 - 4,751	3	22	47	19	28	0
5,002 - 5 033	2	14	59	21	38	0
5,253 - 5,285	2	19	41	18	33	0
5,569 - 5,600	3	17	52	17	35	0
5,820 - 5,852	2	15	57	21	36	0
6,133 - 6,165	3	20	50	13	37	0
6,385 - 6,417	2	9	60	22	38	0
6,694 - 6,726	1	8	66	22	44	0
7,038 - 7,070	6	12	59	21	38	0
**7,383	—	—	—	—	—	-
**7,727	—	—	—	—	—	-
7 979 - 8,050	8	5	54	38	16	0
8,294 - 8,324	7	11	53	32	21	0
8,595 - 8 600	2	6	61	40	20	0
8,842 - 8,874	8	4	60	36	24	0
9,076 - 9,107	12	11	45	34	11	0
9,395 - 9,427	11	11	54	41	13	0
9 708 - 9,738	6	0	65	53	12	0
10,060 - 10,090	15	5	49	37	12	0
10,302 - 10,333	19	13	34	29	5	4
10,613 - 10,644	16	0	62	47	15	0
**10,926	—	—	—	—	—	-
***11,777 - 11,808	37	0	32	—	—	0
12,110 - 12,141	16	5	52	43	9	0
12,460 - 12,491	17	0	57	52	5	2
**12,768	—	—	—	—	—	-
13,077 - 13,107	12	3	47	44	3	5
13,323 - 13,355	21	10	32	28	4	5
13,601 - 13,632	28	6	34	28	6	1

*no less-than-two-micron sample available
**no total clay value available
***illite/smectite proportions not determined

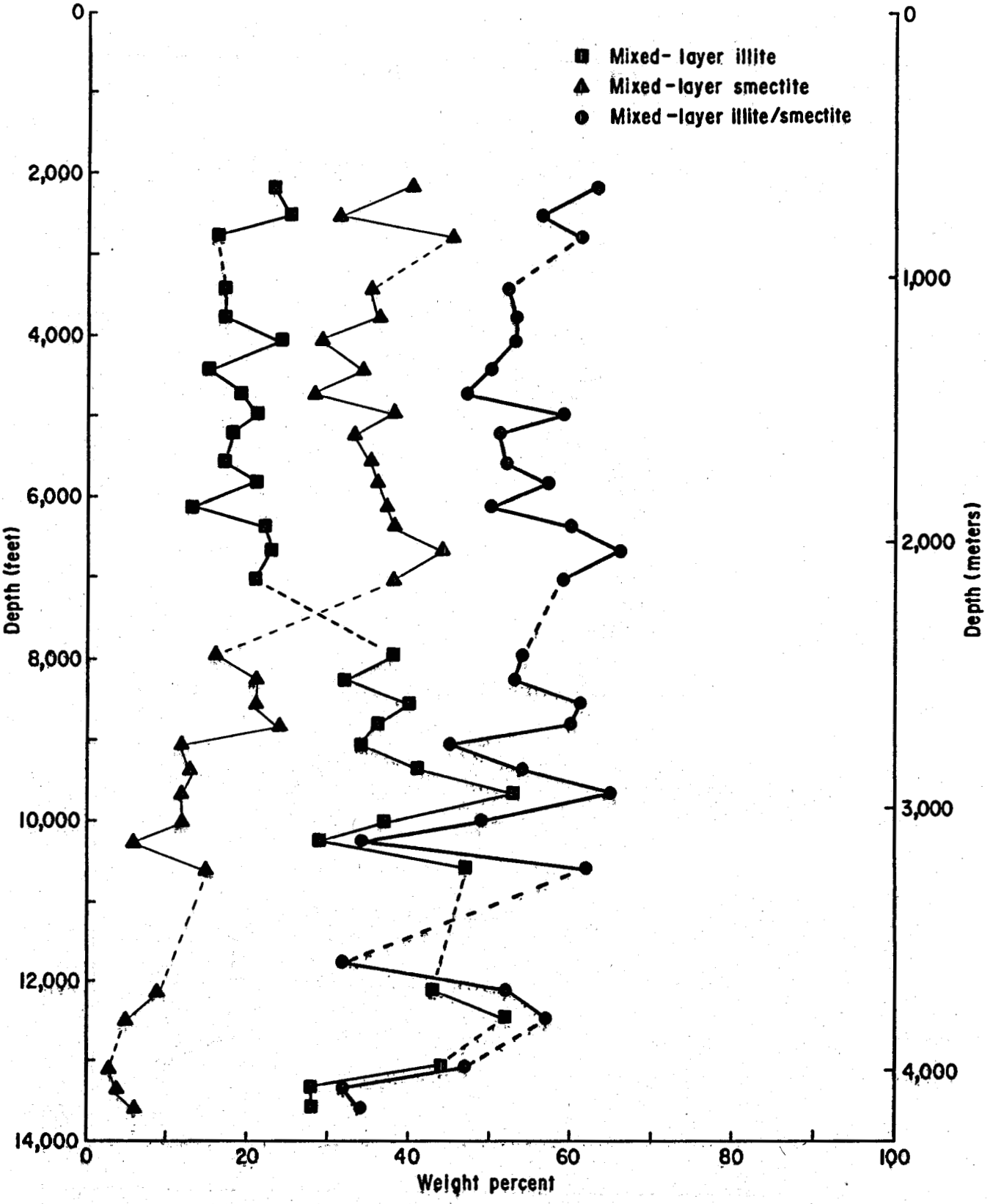

Figure A-13. Shell Oil Company/Delhi-Taylor Oil Corporation #3 A. A. McAllen, Hidalgo County, Texas: Semiquantitative weight percent estimates for mixed-layer illite, mixed-layer smectite, and total mixed-layer illite-smectite (mixed-layer I/S). Dashed lines indicate either a missing less-than-two-micron sample or no total clay value available. Data from table A-9.

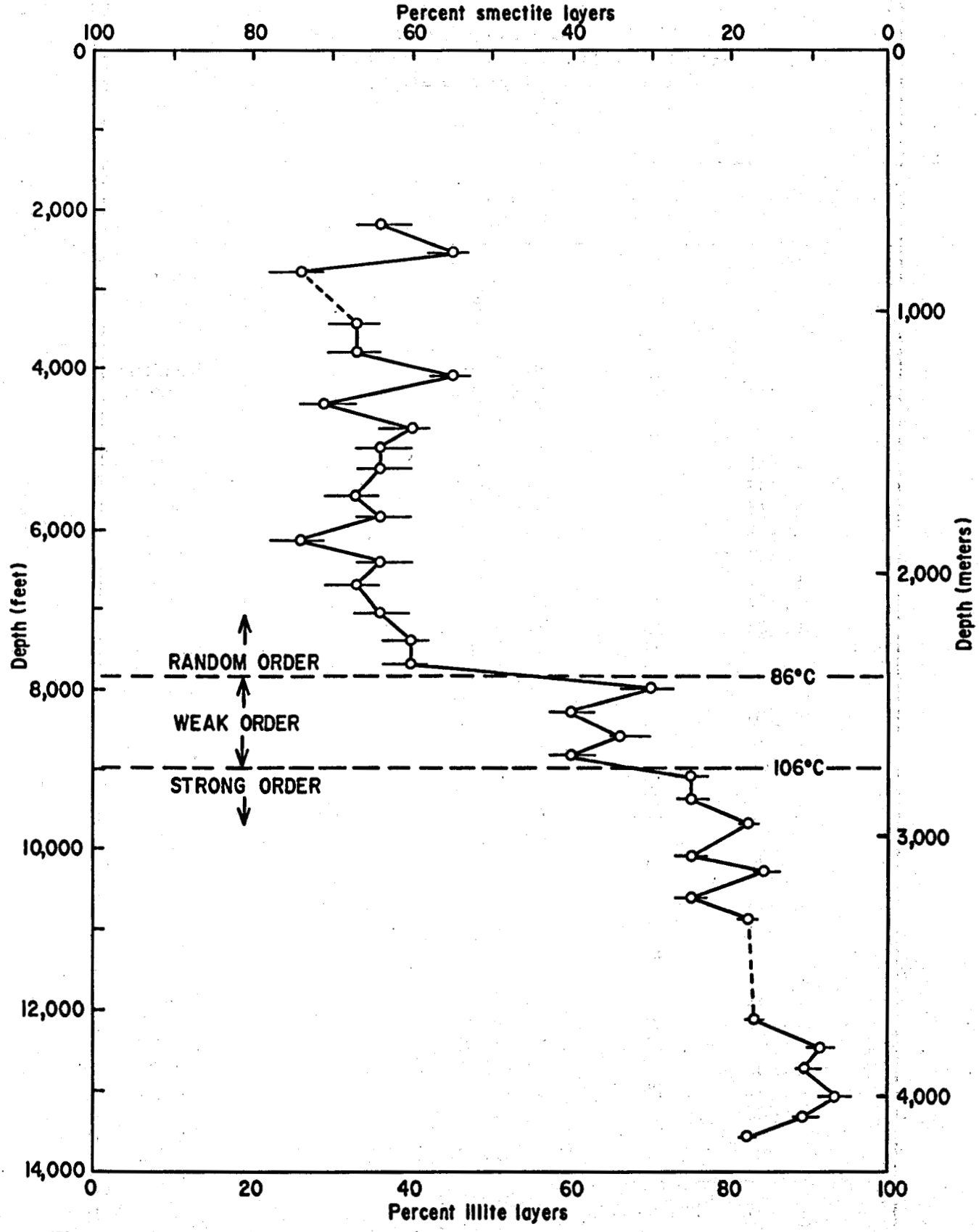

Figure A-14. Shell Oil Company/Delhi-Taylor Oil Corporation #3 A. A. McAllen, Hidalgo County, Texas: Estimated illite and smectite proportions in mixed-layer illite-smectite. Dashed line indicates no information available. Data from table A-10.

Table A-10. #3 A. A. McAllen: Proportions of mixed-layer illite and smectite; uncertainty of illite content; type of ordering.

Sample depth (ft)	Illite (%)	Uncertainty (% Illite)	Smectite (%)	Ordering
2,183	36	33 - 40	64	Random
2,558	45	42 - 47	55	Random
2,809	26	22 - 29	74	Random
*3,120	—	----	—	----
3,437	33	29 - 36	67	Random
3,780 - 3,797	33	29 - 36	67	Random
4,125	45	42 - 47	55	Random
4,450	29	26 - 33	71	Random
4,720 - 4,751	40	36 - 42	60	Random
5,002 - 5,033	36	33 - 40	64	Random
5,253 - 5,285	36	33 - 40	64	Random
5,569 - 5,600	33	29 - 36	67	Random
5,820 - 5,852	36	33 - 40	64	Random
6,133 - 6,165	26	22 - 29	74	Random
6,385 - 6,417	36	33 - 40	64	Random
6,694 - 6,726	33	29 - 36	67	Random
7,038 - 7 070	36	33 - 40	64	Random
7,383	40	36 - 42	60	Random
7,727	40	36 - 42	60	Random
7,979 - 8,050	70	66 - 73	30	Weak
8,294 - 8,324	60	57 - 63	40	Weak
8,595 - 8,600	66	65 - 70	34	Weak
8,842 - 8,874	60	57 - 63	40	Weak
9,076 - 9,107	75	73 - 77	25	Strong
9,375 - 9,427	75	73 - 77	25	Strong
9,708 - 9,738	82	81 - 83	18	Strong
10,060 - 10,090	75	73 - 77	25	Strong
10,302 - 10,333	84	83 - 86	16	Strong
10,613 - 10,644	75	73 - 77	25	Strong
10,926	82	81 - 83	18	Strong
**11 777 - 11,808	—	----	—	----
12,110 - 12,141	83	82 - 84	17	Strong
12,460 - 12,491	91	89 - 93	9	Strong
12,768	89	88 - 91	11	Strong
13,077 - 13,107	93	91 - 95	7	Strong
13,323 - 13,355	89	88 - 91	11	Strong
13,601 - 13,632	82	81 - 83	18	Strong

*no less-than-two-micron sample available
**illite/smectite proportions not determined

The weight percent values for discrete illite (fig. A-12) and mixed-layer illite (fig. A-13) begin to change at 6,300 ft (1,920 m). The calculated equilibrium temperature for this depth is 58°C (136°F).

Chlorite (table A-9) occurs in five samples, all of which are in the strong order zone.

Brazoria County, Texas

#2 Texas State Lease 53034

Clay mineral trends with depth are: (1) kaolinite increases (fig. A-15; table A-11); (2) discrete illite is unchanged (fig. A-15; table A-11); (3) mixed-layer illite-smectite decreases (figs. A-15 and A-16; table A-11); (4) mixed-layer illite increases (fig. A-16; table A-11); (5) mixed-layer smectite decreases (fig. A-16; table A-11).

The proportions of illite and smectite in mixed-layer illite-smectite (fig. A-17; table A-12) show three distinct ordering zones: (1) random interstratification is observed at depths shallower than 9,850 ft (3,000 m) and illite proportions of 52% and less; (2) weak order interstratification occurs between 9,850 ft (3,000 m) and 11,000 ft (3,350 m) and with illite proportions of 57 to 63%; (3) strong order interstratification is noted deeper than 11,000 ft (3,350 m) and illite proportions of 75% and greater. The calculated equilibrium temperatures at zone boundaries are: (1) 116°C (241°F) at the random/weak order boundary and (2) 128°C (272°F) at the weak/strong order boundary. Note that these temperatures are approximately 30°C higher than those in the Hidalgo County wells.

A distinct change occurs in illite-smectite proportions within the random order zone at 7,500 ft (2,290 m) (fig. A-17). This type of change was not observed in the Hidalgo County wells. The calculated equilibrium temperature at 7,500 ft (2,290 m) is 92°C (198°F). This change at 7,500 ft (2,290 m) may mark the top of the geopressured zone.

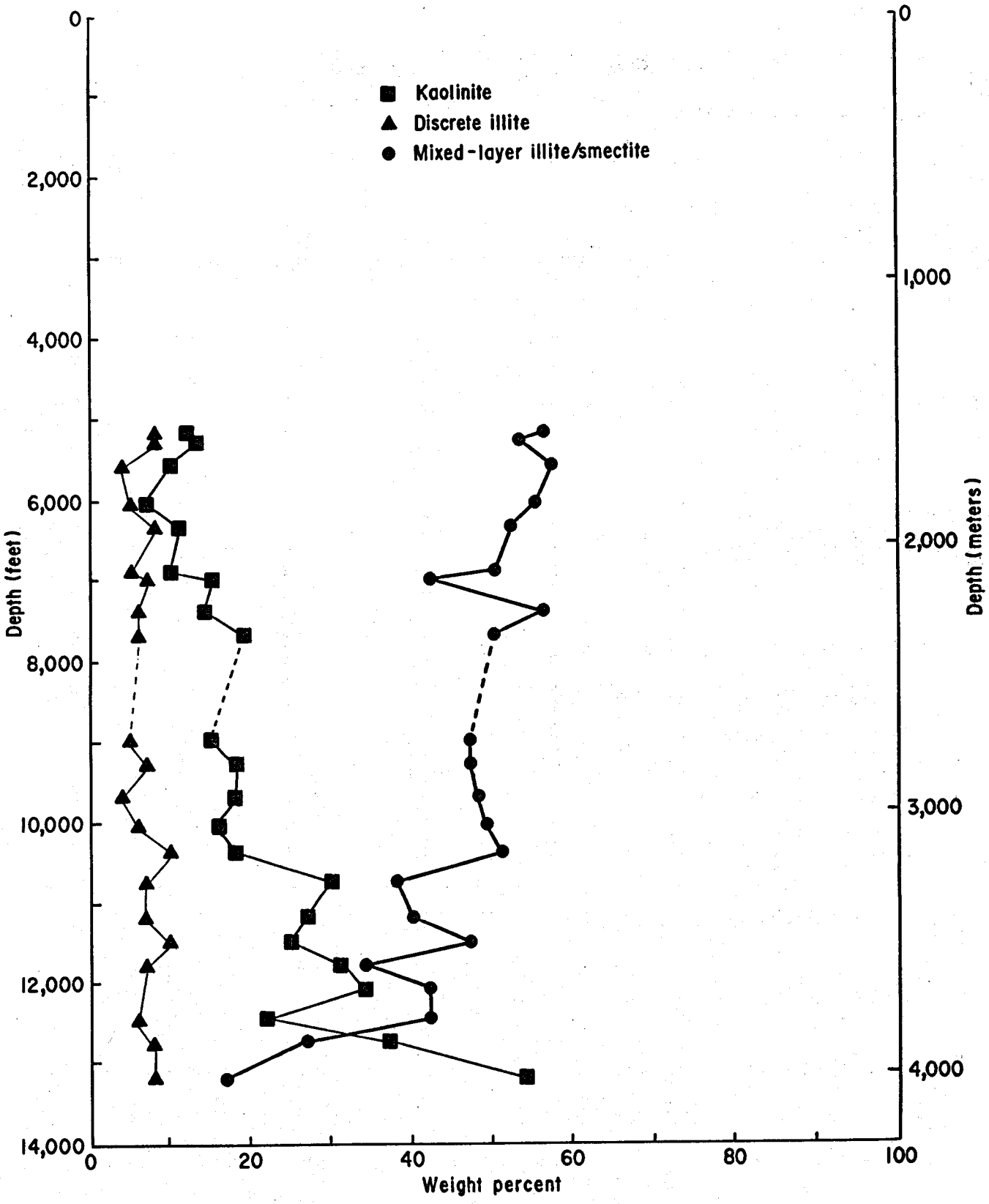

Figure A-15. Gulf Oil Corporation #2 Texas State Lease 53034, Brazoria County, Texas: Semiquantitative weight percent estimates for kaolinite, discrete illite, and mixed-layer illite-smectite (mixed-layer I/S). Dashed lines indicate no total clay value available. Data from table A-11.

Table A-11. #2 Texas State Lease 53034: Semiquantitative weight percent estimates of clay constituents in less-than-two-micron fraction.

Sample depth (ft)	Kaolinite	Discrete Illite	Mixed Illite/Smectite	Mixed Illite	Mixed Smectite	Chlorite
5,194 - 5,225	12	8	56	12	44	0
5,287 - 5,350	14	8	53	12	41	0
5,598 - 5,630	10	4	57	13	44	0
6,002 - 6,096	7	5	55	14	41	0
6,314 - 6,379	11	8	52	11	41	0
6,848 - 6,911	10	5	50	13	37	0
6,974 - 7,067	15	7	42	9	33	0
7,347 - 7,409	14	6	56	15	41	0
7,641 - 7,734	19	6	50	21	29	0
* 8,335 - 8,416	—	—	—	—	—	—
8,989 - 9,114	15	5	47	22	25	0
9,303 - 9,334	18	7	47	24	23	0
9,699 - 9,730	18	4	48	25	23	0
10,011 - 10,060	16	6	49	28	21	0
10,385 - 10,448	18	10	51	32	19	0
10,760 - 10,791	30	7	38	24	14	0
11,197 - 11,269	27	7	40	30	10	0
11,478 - 11,579	25	10	47	37	10	0
11,760 - 11,822	31	7	34	27	7	1
12,041 - 12,135	34	0	42	34	8	0
12,396 - 12,473	22	6	42	34	8	0
12,697 - 12,791	37	8	27	22	5	0
13,133 - 13,246	54	8	17	14	3	0

*no total clay value available

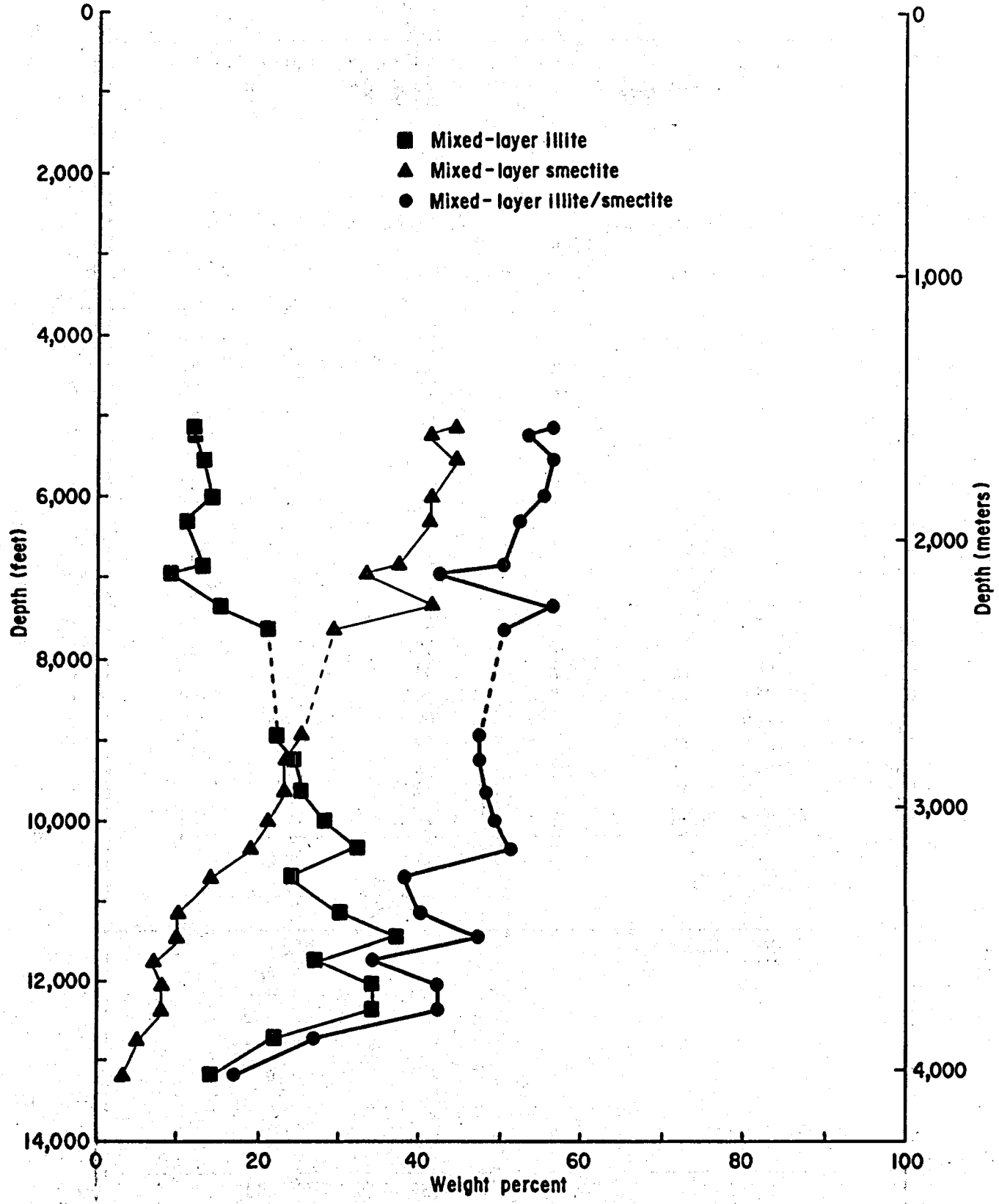

Figure A-16. Gulf Oil Corporation #2 Texas State Lease 53034, Brazoria County, Texas: Semiquantitative weight percent estimates for mixed-layer illite, mixed-layer smectite, and total mixed-layer illite-smectite (mixed-layer I/S). Dashed lines indicate no total clay value available. Data from table A-11.

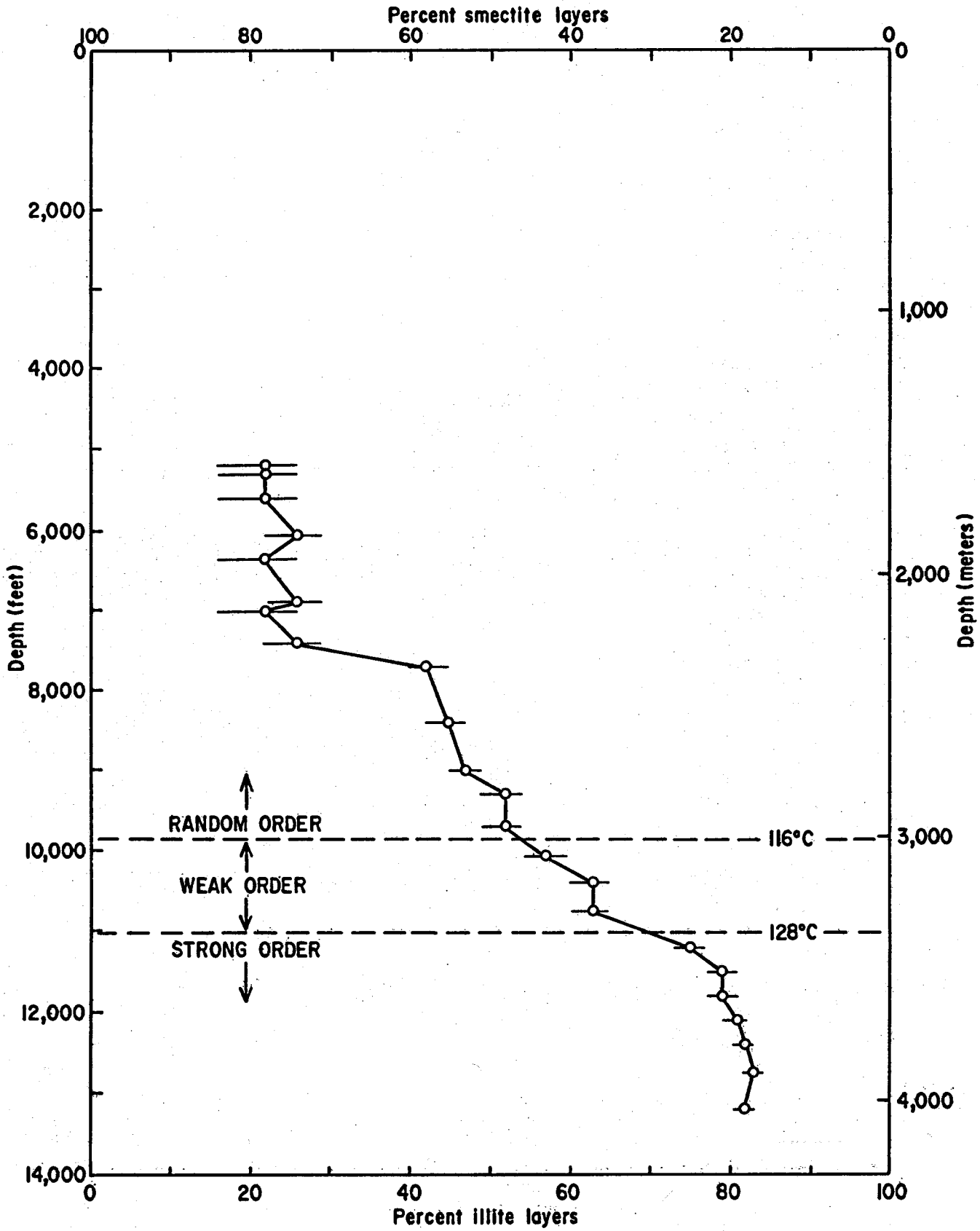

Figure A-17. Gulf Oil Corporation #2 Texas State Lease 53034, Brazoria County, Texas: Estimated illite and smectite proportions in mixed-layer illite-smectite. Data from table A-12.

Table A-12. #2 Texas State Lease 53034: Proportions of mixed-layer illite and smectite; uncertainty of illite content; type of ordering.

Sample depth (ft)	Illite (%)	Uncertainty (% Illite)	Smectite (%)	Ordering
5,194 - 5,225	22	16 - 26	78	Random
5,287 - 5,350	22	16 - 26	78	Random
5,598 - 5,630	22	16 - 26	78	Random
6,002 - 6,090	26	22 - 29	74	Random
6,314 - 6,379	22	16 - 26	78	Random
6,848 - 6,911	26	22 - 29	74	Random
6,974 - 7,067	22	16 - 26	78	Random
7,347 - 7,409	26	22 - 29	74	Random
7,641 - 7,734	42	40 - 45	58	Random
8,335 - 8,416	45	42 - 47	55	Random
8,989 - 9,114	47	45 - 49	53	Random
9,303 - 9,334	52	49 - 54	48	Random
9,699 - 9,730	52	49 - 54	48	Random
10,011 - 10,060	57	54 - 60	43	Weak
10,385 - 10,448	63	60 - 65	37	Weak
10,760 - 10,791	63	60 - 65	37	Weak
11,197 - 11,269	75	73 - 77	25	Strong
11,478 - 11,579	79	77 - 81	21	Strong
11,760 - 11,822	79	77 - 81	21	Strong
12,041 - 12,135	81	79 - 82	19	Strong
12,396 - 12,473	82	81 - 83	18	Strong
12,697 - 12,791	83	82 - 84	17	Strong
13,133 - 13,246	82	81 - 83	18	Strong

Another difference between this well and those in Hidalgo County is the lack of correlation of discrete illite and kaolinite (fig. A-15) as compared to the ordering zones.

The curve for mixed-layer illite (fig. A-16) crosses the curve for mixed-layer smectite very near the boundary between random and weak order. In this well, the boundary is better described as the depth at which the two minerals diverge significantly from each other in weight percent. The boundary between weak order and strong order is between mixed-layer smectite values of 10 to 14 weight percent.

The weight percent estimates of kaolinite (fig. A-15) and mixed-layer illite (fig A-16) begin to change significantly at the same depth, 7,500 ft (2,290 m), as that for the change in illite-smectite proportions noted above.

Chlorite (table A-11) occurs in only one sample, 11,760 ft (3,585 m), which is in the strong order zone.

#1 Pleasant Bayou

Clay mineral trends with depth are quite different compared to trends in the other wells: (1) kaolinite is unchanged (fig. A-18; table A-13); (2) discrete illite decreases (fig. A-18; table A-13); (3) mixed-layer illite-smectite increases (figs. A-18 and A-19; table A-13); (4) mixed-layer illite increases (fig. A-19; table A-13); (5) mixed-layer smectite decreases (fig. A-19; table A-13).

The proportions of illite and smectite in mixed-layer illite-smectite (fig. A-20; table A-14) show ordering zones that are well defined on the basis of illite proportion: (1) random interstratification is observed in samples shallower than 11,400 ft (3,475 m) and illite proportions of 49% and less; (2) weak order interstratification is noted with illite proportions of 63 to 66%, but no depth relationship is present; and (3) strong order interstratification is present at illite proportions of 79% and greater, but again no depth relationship exists. The data from this well indicate that the ordering is more dependent on illite-smectite proportions than on burial depth. The calculated

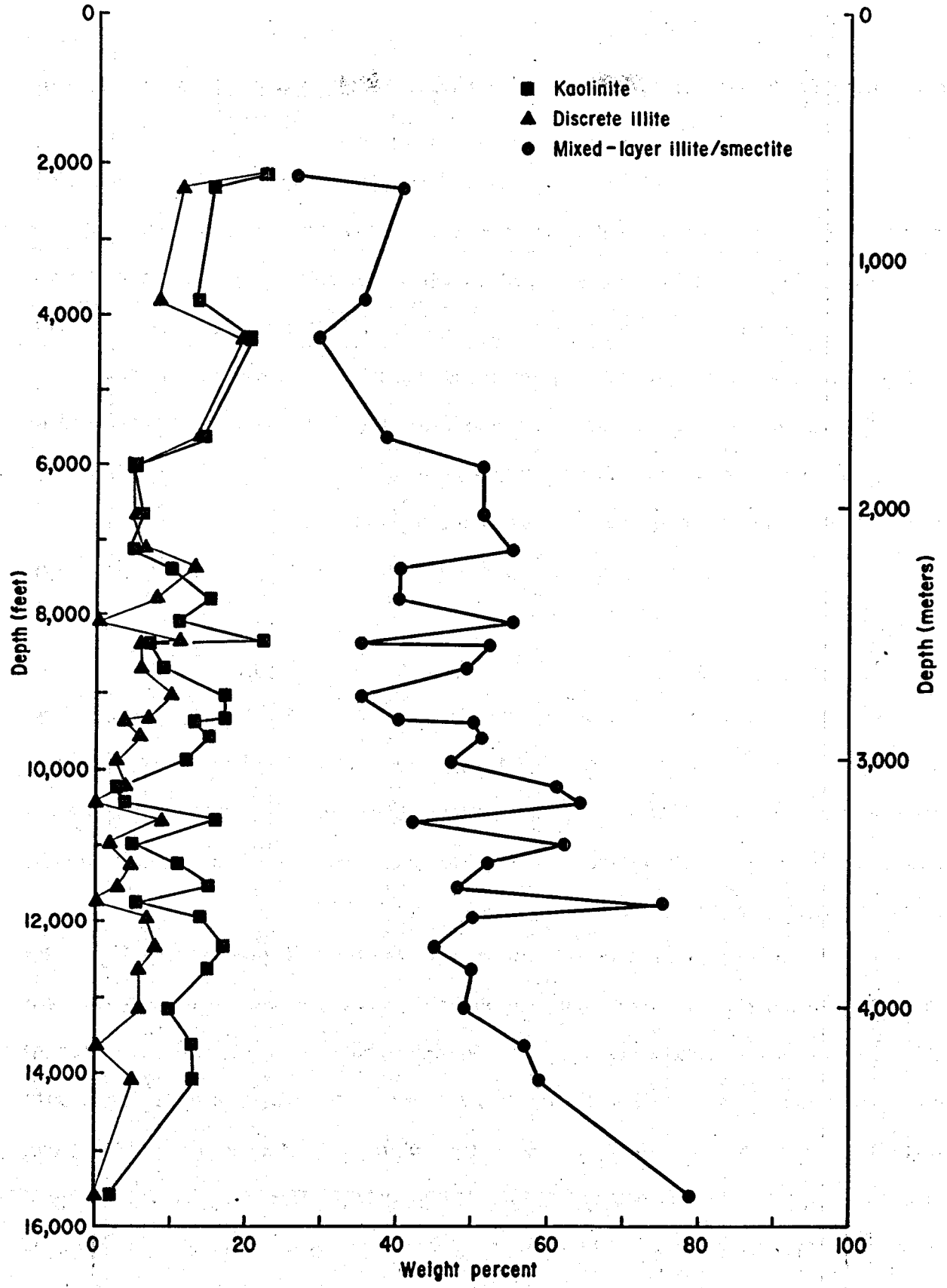

Figure A-18. General Crude Oil Company/Department of Energy #1 Pleasant Bayou, Brazoria County, Texas: Semiquantitative weight percent estimates for kaolinite, discrete illite, and mixed-layer illite-smectite (mixed-layer I/S). Data from table A-13.

Table A-13. #1 Pleasant Bayou: Semiquantitative weight percent estimates of clay constituents in less-than-two-micron fraction.

Sample depth (ft)	Kaolinite	Discrete Illite	Mixed Illite/Smectite	Mixed Illite	Mixed Smectite	Chlorite
2,185	22	22	26	9	17	0
2,335	15	11	40	13	27	0
3,860	13	8	35	6	29	0
4,347	20	19	29	6	23	0
5,630 - 5,660	14	13	38	11	27	3
6,020 - 6,050	5	5	51	11	40	0
6,703	6	5	51	17	34	0
7,110 - 7,140	5	6	55	16	39	0
7,400 - 7,430	10	13	40	12	28	0
7,800	15	8	40	10	30	0
8,100	11	0	55	12	43	0
8,330 - 8,360	22	11	35	8	27	0
8,400	7	6	52	15	37	0
8,690 - 8,720	9	6	49	13	36	0
9,020 - 9,050	17	10	35	12	23	0
9,320 - 9,350	17	7	40	16	24	0
9,380 - 9,410	13	4	50	18	32	0
9,590 - 9,620	15	6	51	18	33	0
9,890 - 9,920	12	3	47	16	31	0
10,232	3	4	61	22	39	0
10,430 - 10,460	4	0	64	30	34	0
10,700 - 10,730	16	9	42	19	23	0
11,000 - 11,030	5	2	62	30	32	0
11,210 - 11,240	11	5	52	24	28	0
11,540 - 11,570	15	3	48	30	18	0
11,750	6	0	75	66	9	0
11,930 - 11,960	14	7	50	33	17	0
12,320 - 12,350	17	8	45	29	16	0
12,630	15	6	50	40	10	0
13,130 - 13,160	10	6	49	32	17	0
13,610 - 13,640	13	0	57	45	12	0
14,078	13	5	59	48	11	0
15,592	2	0	79	68	11	0

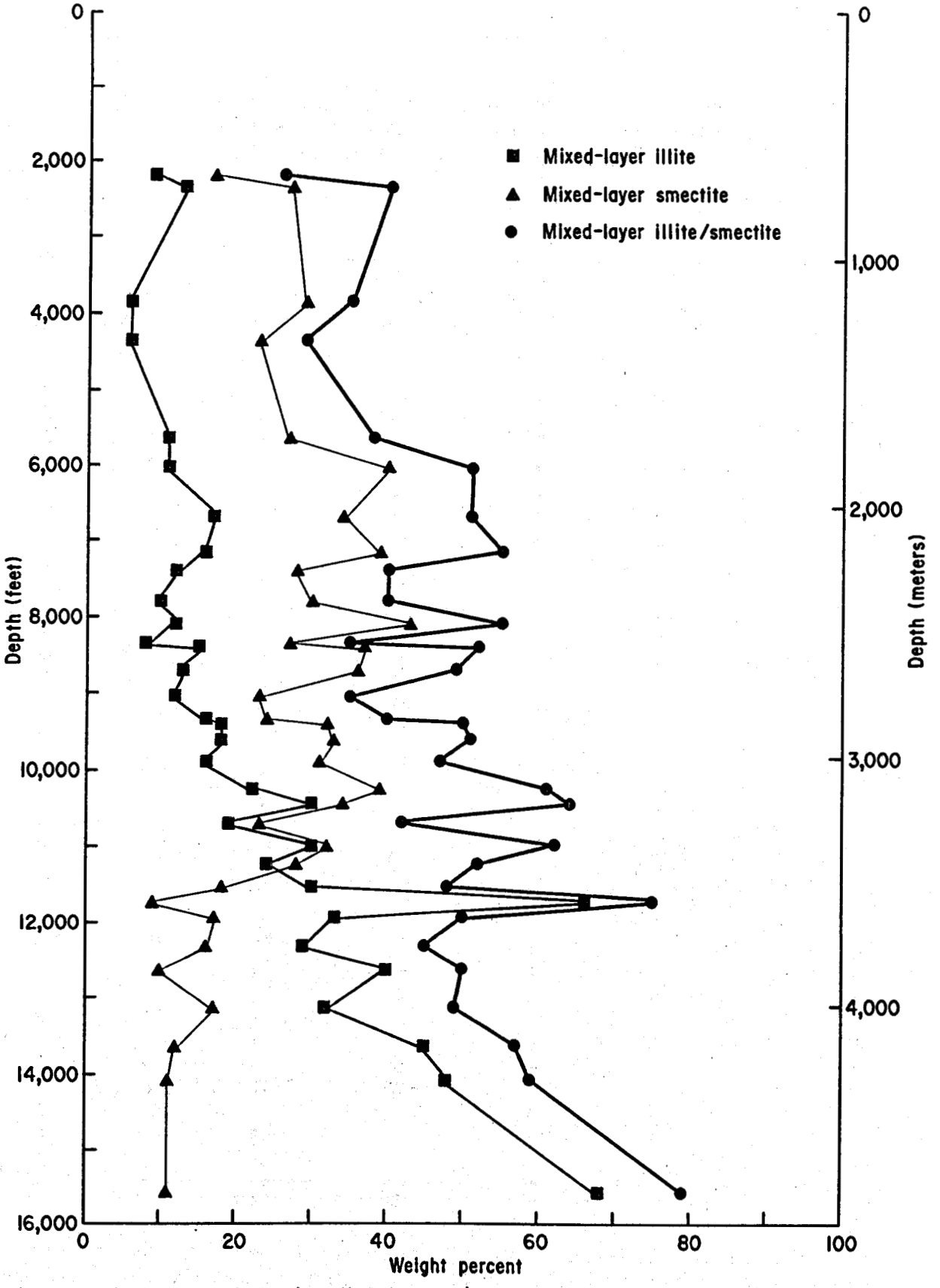

Figure A-19. General Crude Oil Company/Department of Energy #1 Pleasant Bayou, Brazoria County, Texas: Semiquantitative weight percent estimates for mixed-layer illite, mixed-layer smectite, and total mixed-layer illite-smectite (mixed-layer I/S). Data from table A-13

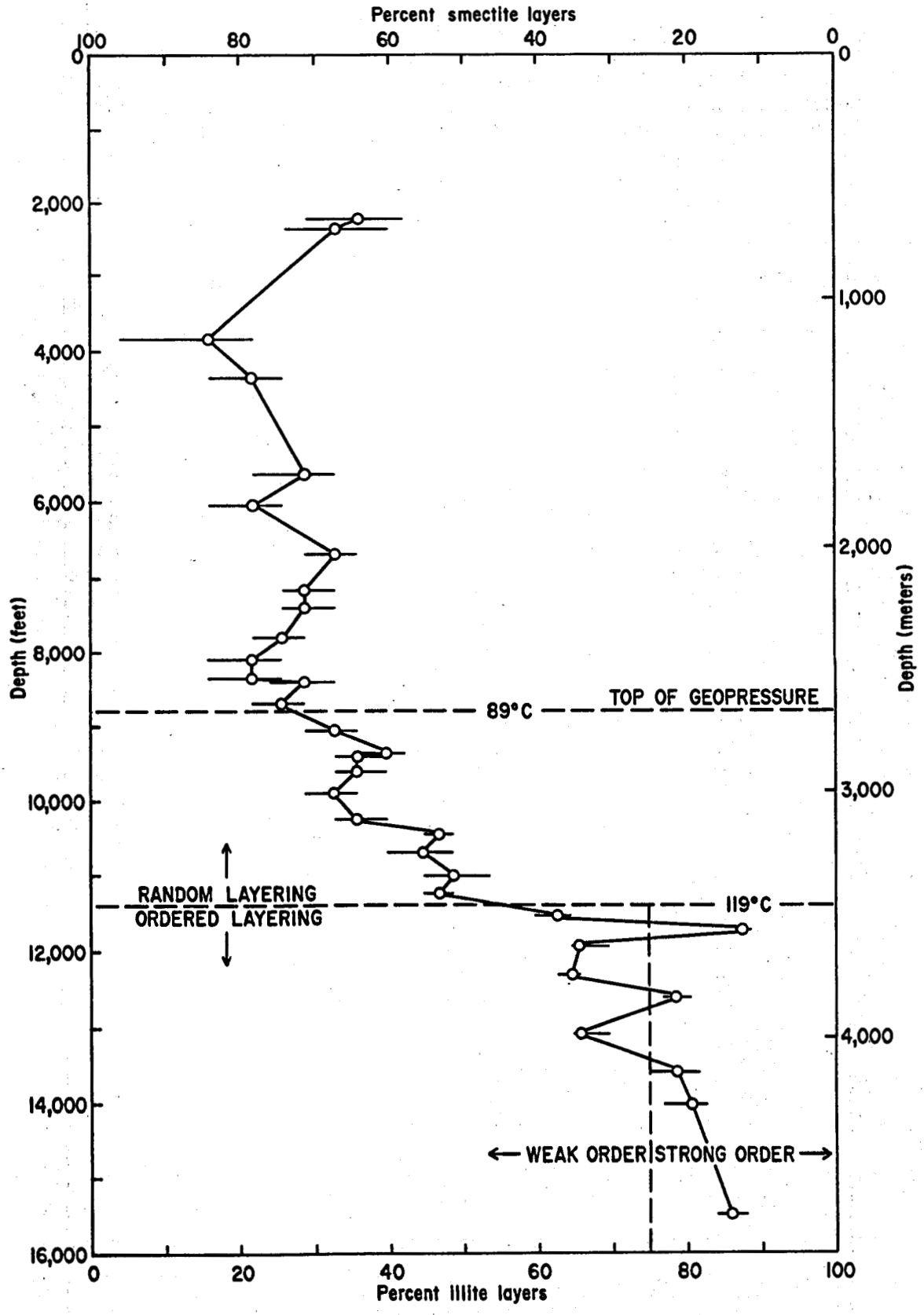

Figure A-20. General Crude Oil Company/Department of Energy #1 Pleasant Bayou, Brazoria County, Texas: Estimated illite and smectite proportions in mixed-layer illite-smectite. Sample sources are both full-diameter core and cuttings. Data from table A-14.

Table A-14. Pleasant Bayou: Proportions of mixed-layer illite and smectite; uncertainty of illite content; type of of ordering. Note: Sample depth with a single number represents a core sample; a range of depth represents a composite sample from cuttings.

Sample depth (ft)	Illite (%)	Uncertainty (% Illite)	Smectite (%)	Ordering
2,185	36	29 - 42	64	Random
2,335	33	26 - 40	67	Random
3,860	16	4 - 22	84	Random
4,347	22	16 - 26	78	Random
5,630 - 5,660	29	22 - 33	71	Random
6,020 - 6,050	22	16 - 26	78	Random
6,703	33	29 - 36	67	Random
7 110 - 7,140	29	26 - 33	71	Random
7,400 - 7,430	29	26 - 33	71	Random
7,800	26	22 - 29	74	Random
8,100	22	16 - 26	78	Random
8,330 - 8,360	22	16 - 26	78	Random
8,400	29	26 - 33	71	Random
8,690 - 8 720	26	22 - 29	74	Random
9,020 - 9,050	33	29 - 36	67	Random
9,320 - 9,350	40	36 - 42	60	Random
9,380 - 9,410	36	33 - 40	64	Random
9,590 - 9,620	36	33 - 40	64	Random
9,890 - 9,920	33	29 - 36	67	Random
10,232	36	33 - 40	64	Random
10,430 - 10,460	47	45 - 49	53	Random
10,700 - 10,730	45	40 - 49	55	Random
11,000 - 11,030	49	45 - 54	51	Random
11,210 - 11,240	47	45 - 49	53	Random
11,540 - 11,570	63	60 - 65	37	Weak
11,750	88	87 - 89	12	Strong
11,930 - 11,960	66	65 - 70	34	Weak
12,320 - 12,350	65	63 - 66	35	Weak
12,630	79	77 - 81	21	Strong
13,130 - 13,160	66	65 - 70	34	Weak
13,610 - 13,640	79	75 - 82	21	Strong
14,078	81	77 - 83	19	Strong
15,592	86	84 - 88	14	Strong

equilibrium temperatures are: (1) 119°C (249°F) between the random order zone and the first sample with weak order interstratification; and (2) 123°C (253°F) at the sample depth, 11,650 ft (3,550 m), for the boundary between weak order and the first sample with strong order interstratification.

The lack of depth correlation for ordering boundaries is due to samples at 11,750 ft (3,580 m) and 12,630 ft (3,850 m). As noted in table A-14, these two samples are from core; the immediately adjacent samples are from cuttings and give values that are averages over a 30-ft interval. The lack of depth correlation may be a function of different sample sources. If only samples from cuttings are considered (fig. A-21), the weak/strong order boundary is at 13,400 ft (4,020 m) and a calculated equilibrium temperature of 142°C (288°F). Mixed-layer illite has a proportion range of 66 to 79% at this alternate weak/strong order boundary.

A distinct change in slope of the graph for illite-smectite proportions at approximately 8,800 ft (2,680 m) (fig. A-20) is interpreted as marking the top of the geopressured zone (Freed, 1979). This change corresponds to a pore fluid pressure gradient of 0.465 psi/ft and a calculated equilibrium temperature of 89°C (192°F).

The rapid change in illite-smectite proportion between 11,200 ft (3,415 m) and 11,750 ft (3,580 m) (fig. A-20) corresponds to a pore fluid pressure gradient of 0.7 psi/ft and a calculated equilibrium temperature of approximately 121°C (251°F).

Discrete illite and kaolinite (fig. A-18) do not have the relationship seen in the Hidalgo County wells.

The curve for mixed-layer illite crosses the curve for mixed-layer smectite at the boundary between random order and the first weak order sample. Note that this "crossover" point consistently has been located in each well at the boundary between random and weak order interstratification. Although the weak to strong order boundary is not defined on the basis of depth, it is distinctly observed between 12 and 16 weight percent smectite (fig. A-19). Note that strong order interstratification is

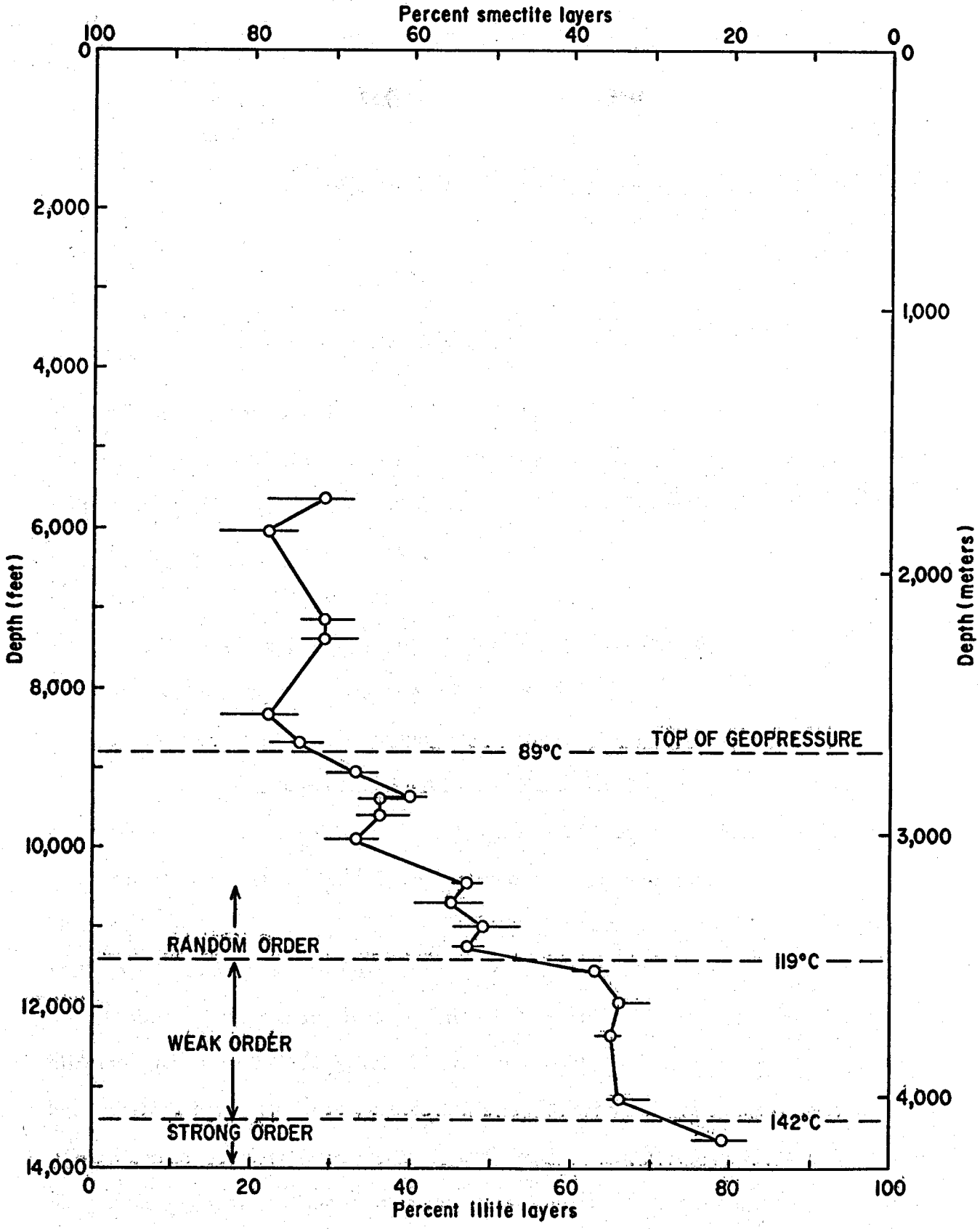

Figure A-21. General Crude Oil Company/Department of Energy #1 Pleasant Bayou, Brazoria County, Texas: Estimated illite and smectite proportions in mixed-layer illite-smectite. Sample sources are only cuttings. Data from table A-14.

consistently found when smectite content is less than approximately 15 weight percent.

Chlorite (table A-13) is present in only one sample, at a depth of 5,630 ft (1,715 m). This chlorite is interpreted as detrital in origin.

DISCUSSION AND CONCLUSIONS

Mixed-Layer Illite-Smectite

Mixed-layer illite-smectite relations have been a focus of interest in the Gulf Coast petroleum industry for over 20 years. Powers (1959, 1967) and Burst (1959) were among the first to discuss the fluid-release mechanism involved in the transformation of smectite to illite. It was the study by Burst (1969) which caught the attention of clay researchers. Since then several field investigations have examined mixed-layer illite-smectite on the Gulf Coast (Boles and Franks, 1979; Hower and others, 1976; Perry and Hower, 1970; Schmidt, 1973; van Moort, 1971). In addition, experimental work has been undertaken to help explain field relationships (Eberl and Hower, 1977; Hiltabrand and others, 1973; Perry and Hower, 1970; Reynolds and Hower, 1970; Velde, 1977). However, only Burst (1969), Powers (1967), and Schmidt (1973) discussed the relationship between abnormal subsurface pressures and the smectite to illite transformation within the mixed-layer phase.

Two different reaction mechanisms for the transformation of smectite to illite have been suggested. The first (Hower and others, 1976) adds both K^+ and Al^{+3} to produce illite. In the second (Boles and Franks, 1979) Al^{+3} acts as an immobile component in the system and only K^+ is added to smectite. As noted by Boles and Franks (1979), the ions released by either reaction are essentially the same, but the quantities given up when Al^{+3} is considered to be immobile are much greater than from the reaction with Al^{+3} as a mobile component.

One important consequence of the reaction with Al^{+3} as an immobile component is a significant weight loss of mixed-layer illite-smectite as the proportion of illite within the mixed-layer phase increases (Boles and Franks, 1979). If the amount of mixed-layer illite-smectite had been initially the same for each clay sample, then this weight loss during the reaction would be approximately 20%, as the illite proportion increases from 30% to 80%. This 20% weight loss in mixed-layer illite-smectite is observed in both Hidalgo County wells (figs. A-9 and A-12) and #2 Texas State Lease 53034 (fig. A-15). If the reaction suggested by Boles and Franks (1979) is adopted as a model for this study, then the supply of mixed-layer illite-smectite was fairly constant during the depositional history for each of these three wells.

Mixed-layer illite-smectite for #1 Pleasant Bayou (fig. A-18) has a weight percent trend which does not conform to the weight loss expected for the reaction of Boles and Franks (1979); in fact, the trend with depth actually increases. Using the model of Boles and Franks (1979), this increase in mixed-layer phase with depth could be explained if the depositional history had an exceptionally high percentage of mixed-layer illite-smectite supplied in early stages, followed by a decreasing supply of mixed-layer phase. The unusually high amount of original mixed-layer phase would more than compensate for the 20% weight loss in deeper mixed-layer illite-smectite samples.

This analysis of change in amount of mixed-layer material through time is also consistent with the reaction suggested by Hower and others (1976). In this case, the weight loss during reaction would be very slight (Boles and Franks, 1979) and the mixed-layer illite-smectite content would not vary significantly if a constant supply of mixed-layer phase had been available initially. An increased amount of mixed-layer illite-smectite during the early stages of deposition would result in more mixed-layer phase in deeper samples, even after diagenesis.

The smectite to illite reaction within the mixed-layer phase requires K^+ from an external source. The source for K^+ in both Hidalgo County wells and in #1 Pleasant Bayou appears to be the breakdown of discrete illite. Potassium feldspar is unchanged in these wells (figs. A-2, A-4, and A-8) and a correlation is suggested by the decrease in discrete illite weight percent (figs. A-9, A-12, and A-18) and a corresponding change in mixed-layer illite and smectite proportions (figs. A-11, A-14, and A-20). In #2 Texas State Lease 53034, a similar correlation is suggested between the decrease in potassium feldspar (fig. A-6) and the change in mixed-layer illite and smectite proportions (fig. A-17). In this case, K^+ is generated by the breakdown of potassium feldspar. Note that discrete illite content is unchanged (fig. A-15).

The chemical reactions within the mixed-layer illite-smectite have been shown by others to be independent of stratigraphic boundaries (Burst, 1969; Hower and others, 1976; Perry and Hower, 1970; van Moort, 1971). The same appears to be true for ordering relationships within the mixed-layer phase. The sample depths for the change from random to weak order interstratification range from 5,750 ft (1,750 m) to 11,400 ft (3,475 m) (table A-15), and range from 7,450 ft (2,270 m) to 11,650 ft (3,550 m) (table A-15) for the change from weak to strong order interstratification. Clearly, depth of burial does not control either change. Temperature seems to be more consistent (table 15) but the 31° to $40^{\circ}C$ (88° to $104^{\circ}F$) difference between the Hidalgo County wells and those from Brazoria County indicates that other factors are involved. Illite proportions are compatible (table A-15) with a range of common values: (1) 52 to 57% in all wells for the random to weak order transformation; (2) 70 to 75% in all wells for the weak to strong order change. A relationship between ordering and the proportions of illite-smectite has been noted by Eberl and Hower (1977), Hower and others (1976) and Reynolds and Hower (1970). However, the ordering was thought to be primarily a function of temperature. This study suggests that the proportions of illite and smectite have a strong influence on ordering.

Table A-15. Comparison of sample depth, equilibrium temperature, and illite proportion range for the random to weak order change and the weak to strong order change for each well.

A. Random to weak order change.

sample source	sample depth (ft)	equilibrium temperature (°C)	range of illite proportion %	figure number
#1 Dixie Mortgage Loan	5,750	79	40 - 59	11
#3 A. A. McAllen	7,850	86	45 - 60	14
#2 Texas State	9,850	116	52 - 57	17
#1 Pleasant Bayou	11,400	119	49 - 63	20

B. Weak to strong order change.

sample source	sample depth (ft)	equilibrium temperature (°C)	range of illite proportion %	figure number
#1 Dixie Mortgage Loan	7,450	97	70 - 77	11
#3 A. A. McAllen	9,000	106	70 - 75	14
#2 Texas State	11,000	128	63 - 75	17
#1 Pleasant Bayou	11,650	123	66 - 79	20
	*(13,400)	(142)	(66 - 79)	(21)

*based only on samples from cuttings

The ordering mechanism suggested by Sawhney (1967) and discussed by Eberl and Hower (1977) may explain the importance of the proportions of illite and smectite. Assume that the diagenetic reactions discussed above have been initiated. As the smectite changes to illite, water is given off and K^+ is fixed in the water-exchangeable cation position. An illite unit (outer tetrahedral layer/octahedral layer/tetrahedral layer/central K^+ layer/tetrahedral layer/octahedral layer/outer tetrahedral layer) would be formed. The distance between the outer tetrahedral layers would be shorter than when water and exchangeable cations were present in the central layer. As suggested by Sawhney (1967) this shortened distance would induce polarization of electron densities toward the central K^+ layer, and the outer tetrahedral layers would become less negative. This would reduce the probability of fixing K^+ in the positions immediately adjacent to these outer tetrahedral layers because there would not be enough negative charge available. This polarization effect assures that each side of the total illite unit would be bounded by water and exchangeable cations. In this manner, ordering is produced by providing smectite layers on each side of an illite unit.

Eberl and Hower (1977) note that multiple groups of illite layers may be needed to provide enough polarizing power to inhibit formation of adjacent illite layers; they suggest groups of two illite layers. The occurrence of strong ordering at an illite proportion of approximately 75% indicates a three-to-one ratio of illite to smectite, which suggests that groups of three illite units are needed to generate enough polarizing power. Once this strength is achieved, the illite-smectite interlayering should be stable until quite high temperatures, at which point thermal energy will force the breakdown of the remaining water interlayers.

The existence of triple-layer illite units in mixed-layer illite-smectite has been noted by Reynolds and Hower (1970). They suggest that this type of order, labeled ISII order, would occur only at illite proportions of 90% or greater. The X-ray patterns for

this report however, clearly show ISII superlattice reflections for the solvated clays from every sample also having strong order interstratification. This ISII superlattice reflection is present in one of the following forms: (1) a dominant single peak; (2) a doublet of superlattice reflections, one from an ISII unit, the other from a single-illite/smectite (IS) unit; (3) a shoulder on a dominant IS peak; or (4) a broad peak incorporating both ISII and IS reflections. Thus, ISII units exist for illite proportions ranging from 75 to 93%.

The occurrence of weak ordering would imply either: (1) that enough ISII groups have formed to generate a superlattice spacing which can be barely detected by X-ray analysis; or (2) that the ordering is IS in nature. The first appearance of weak ordering at approximately 50% illite proportion suggests that IS ordering is achieved first, but is not stable enough to inhibit further production of illite layers. The ordering then proceeds to ISII units.

Other Changes in the Shales

The breakdown of discrete illite in the Hidalgo County wells is compensated for by an increase in kaolinite content (figs. A-9 and A-12). This suggests that kaolinite forms as a result of the discrete illite breakdown. A similar correlation can be seen in #2 Texas State Lease 53034 between potassium feldspar (fig. A-6) and kaolinite (fig. A-15). The trends in #1 Pleasant Bayou for discrete illite and kaolinite (fig. A-18) appear at first glance to have no similar correlation. However, if the depositional history in #1 Pleasant Bayou had an unusually high mixed-layer illite-smectite content in the early stages, the amount of initial kaolinite may have been correspondingly small, or perhaps even nonexistent. If such were the case, the production in deeper samples of authigenic kaolinite from the breakdown of illite would provide most, if not all, of the observed kaolinite. Thus, a constant value for kaolinite throughout the #1 Pleasant Bayou samples would still be consistent with kaolinite forming from discrete illite.

Two reaction systems can be identified: (1) mixed-layer phase/discrete illite/kaolinite; and (2) mixed-layer phase/potassium feldspar/kaolinite. Each of these would supply excess silica, which would explain the increase with depth in quartz content observed in each well (figs. A-1, A-3, A-5, and A-7). The increase in plagioclase feldspar, also observed in each well (figs. A-2, A-4, A-6, and A-8), is probably related to these reaction systems, with Na^{+} and Ca^{+2} supplied during the mixed-layer smectite/illite change, and the remaining components obtained from the breakdown of either discrete illite or potassium feldspar.

The temperatures at which changes take place in the shales are different for the Brazoria and Hidalgo County wells. Changes in the Brazoria County wells take place at approximately 30°C higher than the corresponding changes in the Hidalgo County wells. This is the case for the initiation of mixed-layer smectite/illite changes, the breakdown of discrete illite or potassium feldspar, the formation of kaolinite, the appearance of weak order mixed-layer illite-smectite, and the first appearance of strong order illite-smectite.

Shale/Sandstone Interaction

The sandstones in the wells of Hidalgo County differ from those of Brazoria County in some important characteristics. The sandstones in Hidalgo County (Loucks, 1978; Loucks and others, 1979) are chemically unstable and include feldspar, carbonate rock fragments, and volcanic rock fragments. In contrast, the sandstones in Brazoria County (Bebout and others, 1976; Loucks and others, 1977, 1979) are more stable chemically containing less feldspar and less carbonate and volcanic rock fragments. These differences in the sandstone characteristics of each county appear to have a bearing on the interrelationship between shales and sandstones.

It appears that the shales of the Hidalgo County wells do not provide carbonate to the surrounding sandstones. Calcite content in the Hidalgo County wells is either

unchanged (fig. A 1) or has a minor decrease (fig. A-3). This indicates that carbonate is retained in the shales.

Chlorite in the shales of the Hidalgo County wells (tables A-7 and A-9) appears only in the zone with most diagenetic change, with temperatures in excess of 100°C (212°F). This chlorite is considered authigenic and is thought to form due to the interaction of magnesium and iron, supplied by the mixed-layer smectite/illite change (Boles and Franks, 1979; Hower and others, 1970), with discrete illite. Chlorite formed in this manner would have a high aluminum content. Magnesium and iron are involved in forming aluminous chlorite within the shales; therefore, these elements are restricted to the shales.

The shales in the wells from Brazoria County are quite different. Calcite content (figs. A-5 and A-7) decreases markedly with depth. Also, with the exception of one sample, no iron and magnesium silicates form in the shales. Therefore, it is assumed that carbonate, iron, and magnesium migrate out of the shales. Excess silica is probably also lost.

SUMMARY

(1) Mixed-layer smectite changes to mixed-layer illite according to the reaction suggested by Boles and Franks (1979) with Al^{+3} acting as an immobile component.

(2) The source of K^{+} for the mixed-layer smectite/illite reaction is either discrete illite or potassium feldspar, but not both minerals in the same well.

(3) Ordering in the mixed-layer illite-smectite takes place in two stages, random to weak order and weak to strong order. These changes appear to be related to illite/smectite proportions: (a) random to weak order takes place at an illite proportion of approximately 50%; and (b) weak to strong order takes place at an illite proportion of approximately 75%. Ordering is produced by electron

polarization within illite units, which inhibits formation of other illite units in neighboring positions. Weak order has IS units, but sufficient polarization is not developed for strong order until ISII units are generated.

(4) Increase in quartz with depth is due to silica supplied by the reactions stated in (1) and (2).

(5) Increase of plagioclase feldspar content with depth is due to reaction of Na^{+} and Ca^{+2}, provided by the mixed-layer smectite/illite reaction, with the products of the breakdown of either discrete illite or potassium feldspar.

(6) In Hidalgo County limited materials, perhaps only silica, are supplied by the shale; carbonate content is unchanged, and magnesium and iron are involved in forming aluminous chlorite in the shales. Major diagenetic reactions begin at temperatures of approximately 60° to 70°C (140° to 158°F). Weak order mixed-layer illite-smectite forms at 80° to 85°C (176° to 185°F); the strong order mixed-layer phase forms at 100° to 105°C (212° to 221°F).

(7) In Brazoria County silica, carbonate, iron, and magnesium are supplied by the shales. Major diagenetic reactions begin at approximately 90°C (194°F). Weak order mixed-layer illite-smectite forms at 115° to 120°C (239° to 248°F); the strong order mixed-layer phase forms at approximately 125° to 130°C (257° to 266°F). Note that these temperatures are roughly 25° to 30°C (77° to 86°F) higher than those observed for the same changes in Hidalgo County.

(8) Kaolinite forms from the breakdown of either discrete illite or potassium feldspar, but not both in the same well.

ACKNOWLEDGMENTS

I am grateful to Dr. R. G. Loucks, who initiated this study and has provided valuable support and assistance.

S. Underwood and L. Jirik, both of the Bureau of Economic Geology, The University of Texas at Austin, prepared the samples. P. Mani and J. Mendenhall, both of Trinity University, collected the X-ray data. Funding was provided by the U.S. Department of Energy, under contract number DE-AC08-79ET27111 and by Trinity University.

REFERENCES

Bebout, D. G., Loucks, R. G., Bosch, S. C., and Dorfman, M. H., 1976, Geothermal resources -- Frio Formation, Upper Texas Gulf Coast: The University of Texas at Austin, Bureau of Economic Geology Geological Circular 76-3, 47 p.

Bebout, D. G., Loucks, R. G., and Gregory, A. R., 1978, Frio sandstone reservoirs in the deep subsurface along the Texas Gulf Coast -- their potential for production of geopressured geothermal energy: The University of Texas at Austin, Bureau of Economic Geology Report of Investigations No. 91, 92 p.

Boles, J. E., and Franks, S. G., 1979, Clay diagenesis in Wilcox sandstones of Southwest Texas: implications of smectite diagenesis on sandstone cementation: Journal of Sedimentary Petrology, v. 49, no. 1, p. 55-70.

Burst, J. F., 1957, Post-diagenetic clay mineral environmental relationships in the Gulf Coast Eocene, in Swineford, A., ed., Proceedings of the Sixth National Conference on Clays and Clay Minerals, v. 2, p. 327-341.

Burst, J. F., 1969, Diagenesis of Gulf Coast clayey sediments and its possible relation to petroleum migration: American Association of Petroleum Geologists Bulletin, v. 53, no. 1, p. 73-93

Chen, P.-Y., 1977, Table of key lines in x-ray powder diffraction patterns of minerals in clays and associated rocks: Indiana Geological Survey Occasional Paper 21, 67 p.

Eberl, D., and Hower, J., 1977, The hydrothermal transformation of sodium and potassium smectite into mixed-layer clay: Clays and Clay Minerals, v. 25, no. 3, p. 215-227.

Freed, R. L., 1979, Shale mineralogy of the No. 1 Pleasant Bayou geothermal test well: a progress report (abs.): Fourth United States Gulf Coast Geopressured-Geothermal Conference: Research and Development, p. 9-10.

Hiltabrand, R. R., Ferrell, R. E., and Billings, G. K., 1973, Experimental diagenesis of Gulf Coast argillaceous sediment: American Association of Petroleum Geologists Bulletin, v. 57, no. 2, p. 338-348.

Hower, J., Eslinger, E. V., Hower, M. E., and Perry, E. A., 1976, Mechanism of burial metamorphism of argillaceous sediment: (1) mineralogical and chemical evidence: Geological Society of America Bulletin, v. 87, no. 5, p. 725-737.

Johns, W. D., Grim, R. E., and Bradley, W. F., 1954, Quantitative estimations of clay minerals by diffraction methods: Journal of Sedimentary Petrology, v. 24, no. 4, p. 242-251.

Loucks, R. G., 1978, Sandstone distribution and potential for geopressured geothermal energy production in the Vicksburg Formation along the Texas Gulf Coast: Gulf Coast Association of Geological Societies Transactions, v. 28, p. 239-271.

Loucks, R. G., Bebout, D. G., and Galloway, W. E., 1977, Relationship of porosity formation and preservation to sandstone consolidation history — Gulf Coast lower Tertiary Frio Formation: Gulf Coast Association of Geological Societies Transactions, v. 27, p. 109-120.

Loucks, R. G., Dodge, M. M., and Galloway, W. E., 1979, Sandstone consolidation analysis to delineate areas of high-quality reservoirs suitable for production of geopressured geothermal energy along the Texas Gulf Coast: Division of Geothermal Energy, U.S. Department of Energy Contract No. EG-77-5-05-5554, 97 p.

Perry, E. A., Jr., and Hower, J., 1970, Burial diagenesis in Gulf Coast pelitic sediments: Clays and Clay Minerals, v. 18, no. 3, p. 165-177.

Perry, E. A., Jr., and Hower, J., 1972, Late-stage dehydration in deeply buried pelitic sediments: American Association of Petroleum Geologists Bulletin, v. 56, no. 10, p. 2013-2021.

Powers, M. C., 1957, Adjustment of clays to chemical change and the concept of the equivalence level, in Swineford, A., ed., Proceedings of the Sixth National Conference on Clays and Clay Minerals, v. 2, p. 309-326.

Powers, M. C., 1967, Fluid-release mechanism in compacting marine mudrocks and their importance in oil exploration: American Association of Petroleum Geologists Bulletin, v. 51, no. 7, p. 1240-1254.

Reynolds, R. C., Jr., and Hower, J., 1970, The nature of interlayering in mixed-layer illite montmorillonite: Clays and Clay Minerals, v. 18, no. 1, p. 25-36.

Sawhney, B. L., 1967, Interstratification in vermiculite, in Bailey, S. W., ed., Proceedings of the 15th National Conference on Clays and Clay Minerals, v. 27, p. 75-84.

Schmidt, G. W. 1973, Interstitial water composition and geochemistry of deep Gulf Coast shales and sandstones: American Association of Petroleum Geologists Bulletin, v. 57, no. 2, p. 321-337.

Schultz, L. G., 1964, Quantitative interpretation of mineralogical composition from x-ray and chemical data for the Pierre Shale: U.S. Geological Survey Professional Paper 391-C, p. C1-C31.

van Moort, J. C., 1971, A comparative study of the diagenetic alteration of clay minerals in Mesozoic shales from Papua, New Guinea, and in Tertiary shales from Louisiana, U.S.A.: Clays and Clay Minerals, v. 19, no. 1, p. 1-20.

Velde, B., 1977, A proposed phase diagram for illite, expanding chlorite, corrensite, and illite-montmorillonite mixed layered minerals: Clays and Clay Minerals, v. 25, no. 4, p. 264-270

APPENDIX B

USE OF ISOTOPIC DATA FOR INTERPRETATION OF DIAGENETIC HISTORY

APPENDIX B

USE OF ISOTOPIC DATA FOR INTERPRETATION OF DIAGENETIC HISTORY

Authigenic carbonates, quartz, albite, and kaolinite from sandstones in General Crude Oil/Department of Energy Nos. 1 and 2 Pleasant Bayou and other nearby wells have been analyzed for stable isotopes to gain a better understanding of diagenetic history. Stable isotope ratios of authigenic materials are useful in this regard because they represent a record of the conditions that prevailed at the time precipitation occurred.

Oxygen and carbon isotopic values for both minerals and water are reported in δ-notation:

$$\delta^{18}O‰ = \frac{(^{18}O/^{16}O)\text{sample} - (^{18}O/^{16}O)\text{standard}}{(^{18}O/^{16}O)\text{standard}} \times 1000$$

The standard SMOW (standard mean ocean water; Craig, 1961), the approximate $\delta^{18}O$ for sea water = 0‰, is commonly used to report oxygen isotopic values for water and silicates. The PDB standard (Peedee belemnite; defined by Urey) is often used for oxygen and carbon isotope measurements on carbonates. A mineral or water is said to become "lighter" as the proportion of the light isotope increases, whereas "heavier" samples have relatively greater amounts of the heavier isotope. If $\delta^{18}O$ of sample A is less than $\delta^{18}O$ of sample B, A is said to be "lighter" than B, or B "heavier" than A.

Figure 1 illustrates a typical relationship between the oxygen isotopic composition of a mineral and the temperature and isotopic composition of water ($\delta^{18}O_{H_2O}$) under which the mineral formed. A single $\delta^{18}O_{mineral}$ value can result from a number of $\delta^{18}O_{H_2O}$-temperature combinations. According to the diagram, the

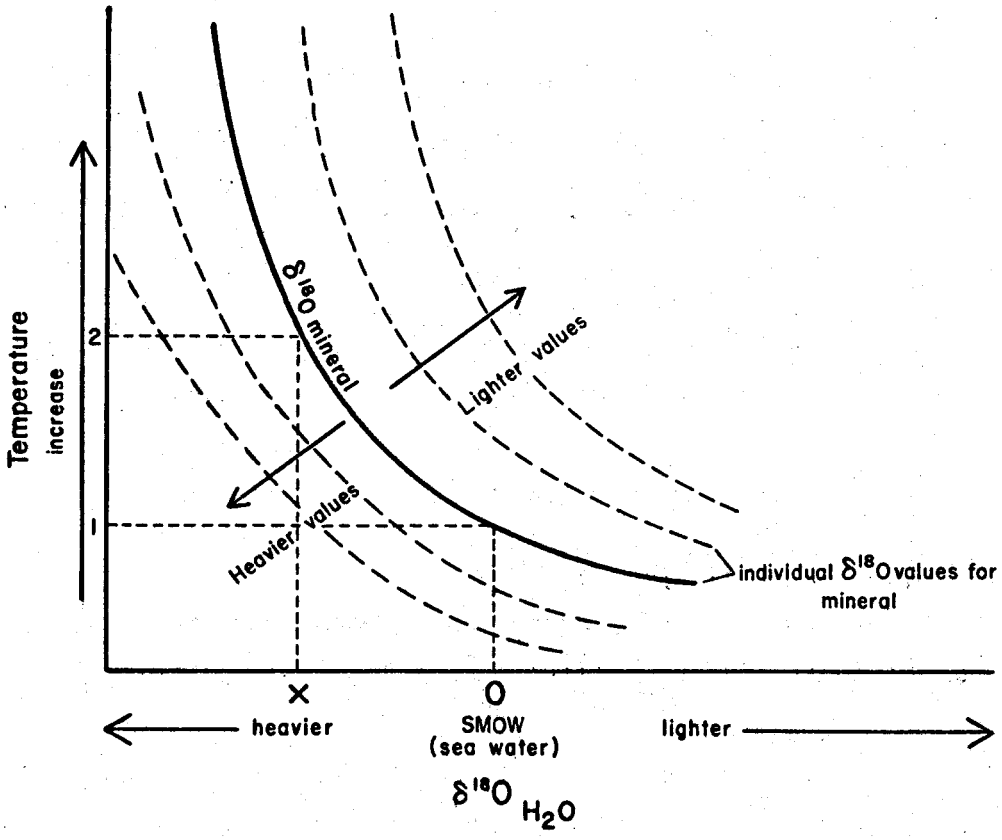

Figure B-1. Schematic diagram showing the relationship between temperatures, $\delta^{18}O_{H_2O}$, and $\delta^{18}O$ of a mineral precipitated from aqueous solution. Each curve represents a single $\delta^{18}O_{mineral}$ value. $\delta^{18}O_{mineral}$ values become progressively "heavier" or "lighter", relative to the solid curve, in the directions of the diagonal arrows. See the text for further explanations.

$\delta^{18}O_{min}$ value shown by the solid curve could have formed equally well from sea water at some low temperature (1) or from a heavier water (x) at some higher temperature (2). Equations relating these three parameters (temperature, $\delta^{18}O_{H_2O}$, $\delta^{18}O_{min}$) for common authigenic minerals are available in numerous publications (Friedman and O'Neil, 1977).

To make interpretations about the temperature at which a mineral formed, it is necessary to know the limits of $\delta^{18}O_{H_2O}$ variations. Likewise, if the limits of temperature variation are known, the $\delta^{18}O_{min}$ value can reveal something about the $\delta^{18}O_{H_2O}$ value in effect at the time of cementation.

REFERENCES

Craig, H., 1961, Standard for reporting concentration of deuterium and oxygen-18 in natural waters: Science, v. 33, p. 1833-1934.

Friedman, I., and O'Neil, J. R., 1977, Compilation of stable isotope fractionation factors of geochemical interest: U.S. Geological Survey Professional Paper, 440-KK, 12 p.

APPENDIX C

OXYGEN AND CARBON ISOTOPIC DATA

Appendix C. Isotopic analyses of carbonate minerals (reported relative to PDB).

Sample Number*	Well Name	Depth (ft)	$\delta^{18}O$ PDB	$\delta^{13}C$ PDB	Petrographic Features
1024	Phillips #1 Houston "Z"	12,858	-10.3	-1.0	Minor grain replacement; mainly cement; post-quartz overgrowth.
1038C	Phillips #2 Gunderson	12,228	-9.7	-2.5	Post-quartz overgrowth; mainly cement; minor grain replacement.
1038D	Phillips #2 Gunderson	12,228	-7.9	-3.5	Post-quartz overgrowth; mainly grain replacement; minor cement.
1045	Phillips #2 Gunderson	12,236	-6.9	+1.3	Pre-quartz overgrowth poikilotopic cement; some grain replacement.
1061A	Phillips #2 Rekdahl	12,371	-7.9	-5.9	Pre-quartz overgrowth nodule; non-ferroan poikilotopic calcite.
1061B-C	Phillips #2 Rekdahl	12,371	-8.1	-5.1	Post-quartz overgrowth (?); mainly grain replacement.
1061B-D	Phillips #2 Rekdahl	12,371	-7.4	-4.5	Post-quartz overgrowth (?); mainly grain replacement, some cement.
1065C	Phillips #2 Rekdahl	12,398	-10.4	-2.15	Poikilotopic non-ferroan cement and grain replacement; post-quartz overgrowth (?).
1065D	Phillips #2 Rekdahl	12,398	-10.0	-2.4	Mainly grain replacement.
1077	Phillips #F-3 Houston	11,951	-5.7	-2.7	Pre-quartz overgrowth; poikilotopic cement with minor grain replacement.
1086	Phillips #F-3 Houston	12,175	-7.6	-3.7	Mainly grain replacement, undulose.

Appendix C continued.

Sample Number*	Well Name	Depth (ft)	$\delta^{18}O$ PDB	$\delta^{13}C$ PDB	Petrographic Features
1091	Phillips #1 Houston "GG"	14,821	-10.3	-2.9	Poikilotopic undulose ferroan calcite; some grain replacement.
1148C	Phillips #1 Houston "JJ"	16,189	-10.9	-3.1	Non-ferroan calcite grain replacement and minor cement; post-quartz overgrowth.
1148D	Phillips #1 Houston "JJ"	16,189	-8.8	-2.3	Ferroan dolomite grain replacement, subhedral.
1161	Phillips #1 Houston "JJ"	16,253	-9.3	-4.7	Poikilotopic cement; post-quartz overgrowth; some grain replacement.
1173C	Phillips #1 Houston "JJ"	16,755	-10.0	-3.2	Approximately 1/3 grain replacement, 2/3 poikilotopic cement; post-quartz overgrowth (?).
1173D	Phillips #1 Houston "JJ"	16,755	-8.5	-2 05	Mostly grain replacement.
1177	Phillips #1 Houston "JJ"	16,779	-8.8	-5.0	Subequal cement and grain replacement; unknown relative timing to quartz.
1200B	Humble #1 Vieman	11,798	-8.5	-9.6	Poikilotopic calcite; pre-quartz overgrowth.
1203	Humble #1 Vieman	11,810	-8.3	-6.4	Poikilotopic calcite; pre-quartz overgrowth.
1205	Humble #1 Vieman	12,172	-8.0	-8.7	Poikilotopic calcite; pre-quartz overgrowth.
1206	Humble #1 Vieman	12,174	-5.4	-25.9	Nodule of strongly undulose poikilotopic calcite; mainly cement but also invades grains; pre-quartz overgrowth.
1208C	Humble #1 Vieman	12,176	-5.4	-22.65	Nodule of strongly undulose poikilotopic calcite; mainly cement but also invades grains; pre-quartz overgrowth.

Appendix C continued.

Sample Number*	Well Name	Depth (ft)	$\delta^{18}O$ PDB	$\delta^{13}C$ PDB	Petrographic Features
1208D	Humble #1 Vieman	12,176	-3.2	-25.6	Some portion of nodule; not seen in thin section.
1221C	Humble #1 Freeport-Sulphur	12,257	-4.6	-3.6	Grain replacement and cement.
1221D	Humble #1 Freeport-Sulphur	12,257	-7.0	-4.4	Grain replacement and cement.
1232C	Humble #1 Skrabanek	17,783	-11.0	-4.8	Mainly grain replacement; some cement; post-quartz overgrowth.
1232D	Humble #1 Skrabanek	17,783	-9.2	-3.0	Undulose grain replacement.
1962	GCO/DOE #1 Pleasant Bayou	4,345	-5.0	-3.4	87.2% poikilotopic ferroan calcite, 8.45% non-ferroan grain replacement, 4.4% forams; pre-quartz overgrowth.
1963	GCO/DOE #1 Pleasant Bayou	6,705	-7.0	-4.0	94.4% sparry ferroan calcite, 2.6% non-ferroan grain replacement; pre-quartz overgrowth.
1964	GCO/DOE #1 Pleasant Bayou	6,707	-4.4	-2.7	Euhedral, pore-filling ferroan dolomite.
1065	GCO/DOE #1 Pleasant Bayou	10,215	-8.3	-10.1	79.7% poikilotopic ferroan calcite, 20.3% non-ferroan grain replacement.
1968	GCO/DOE #1 Pleasant Bayou	10,223	-6.1	-9.5	69.6% poikilotopic ferroan calcite, 30.4% non-ferroan grain replacement.
1969	GCO/DOE #1 Pleasant Bayou	10,225	-7.2	-7.0	41.6% poikilotopic calcite (mostly ferroan), 54.2% non-ferroan grain replacement, 4.2% forams.

Appendix C continued.

Sample Number*	Well Name	Depth (ft)	$\delta^{18}O$ PDB	$\delta^{13}C$ PDB	Petrographic Features
1970	GCO/DOE #1 Pleasant Bayou	10,227	-5.4	-4.7	100% non-ferroan grain replacement.
1976	GCO/DOE #1 Pleasant Bayou	10,259	-8.4	-8.8	90.0% poikilotopic ferroan calcite, 10.0% grain replacement (mostly non-ferroan).
1980	GCO/DOE #1 Pleasant Bayou	10,267	-6.2	-7.8	77.5% poikilotopic ferroan calcite, 22.5% non-ferroan grain replacement.
1981	GCO/DOE #1 Pleasant Bayou	11,733	-8.15	-7.9	95.8% poikilotopic ferroan calcite, 4.2% non-ferroan grain replacement.
1994	GCO/DOE #1 Pleasant Bayou	11,763	-9.3	-6.7	Non-ferroan poikilotopic calcite; minor forams; post-quartz overgrowth.
1999	GCO/DOE #1 Pleasant Bayou	11,773	-9.0	-7.1	Non-ferroan poikilotopic calcite; post-quartz overgrowth.
2010	GCO/DOE #1 Pleasant Bayou	14,061	-11.2	-6.1	Non-ferroan calcite cement.
2011	GCO/DOE #1 Pleasant Bayou	14,080	-11.2	-5.65	Non-ferroan calcite cement.
2028C	GCO/DOE #1 Pleasant Bayou	14,775	-8.7	-2.5	Not recognized in thin section.
2028D	GCO/DOE #1 Pleasant Bayou	14,775	-7.7	-4.6	Ferroan grain replacement.
2029C	GCO/DOE #1 Pleasant Bayou	14,757	-12.8	-4.2	Ferroan (?); post-quartz overgrowth cement.

Appendix C continued.

Sample Number*	Well Name	Depth (ft)	$\delta^{18}O$ PDB	$\delta^{13}C$ PDB	Petrographic Features
2029D	GCO/DOE #1 Pleasant Bayou	14,757	-6.9	-1.5	Mainly grain replacement.
2050	GCO/DOE #1 Pleasant Bayou	15,183	-12.2	-2.4	Post-quartz overgrowth cement; some grain replacement.
2065	GCO/DOE #1 Pleasant Bayou	15,586	-11.7	0.0	Post-quartz overgrowth cement; some grain replacement.
2069	GCO/DOE #2 Pleasant Bayou	14,685	-8.7	-5.3	Poikilotopic ferroan calcite; pre-quartz overgrowth; 91.5% cement, 8.5% grain replacement.
Mollusc	GCO/DOE #1 Pleasant Bayou	4,830	-0.23	+3.25	Unaltered aragonite; from Miocene shale.
Mollusc	GCO/DOE #1 Pleasant Bayou	5,200	-2.3	-0.9	Unaltered aragonite; from Miocene shale.

*D = dolomite; C = calcite associated with dolomite; samples with no letter designation are calcite.

APPENDIX D

ELECTRON MICROPROBE DATA

Appendix D.
Table D-1. Pleasant Bayou Samples.
Carbonate Compositions

Sample #	Depth	Description	%MgO	%SrO	%CaO	%MnO	%FeO
1962	4,345 ft (1,324 m)	Poikilotopic cement	0.41	0.04	57.93	0.28	2.37
			0.53	0.11	56.80	0.15	2.72
			0.49	0.04	52.95	0.20	2.54
			0.48	0.07	52.77	0.23	2.79
			0.57	0.09	50.95	0.25	2.93
			0.56	0.11	51.37	0.13	2.76
			0.45	0.09	52.50	0.30	2.63
			0.38	0.04	52.78	0.30	2.59
			0.28	0.10	54.20	0.18	1.48
			0.32	0.14	54.05	0.13	1.86
		Grain replacement	0.11	0.18	54.86	0.00	0.03
		Foram	0.07	0.12	55.44	0.02	0.00
			0.09	0.13	54.35	0.00	0.03
1999	11,773 ft (3,589 m)	Poikilotopic cement	0.34	0.06	55.33	1.16	0.73
			0.37	0.16	55.49	1.19	0.82
			0.23	0.07	56.38	1.02	0.56
			0.28	0.13	55.18	1.18	0.75
			0.39	0.25	55.48	0.93	0.68
			0.29	0.09	54.75	1.01	0.70
			0.39	0.18	54.32	1.20	0.86
			0.41	0.15	57.29	1.36	0.98
		Grain replacement	0.32	0.19	53.54	1.26	0.85
2040	15,162 ft (4.621 m)	Sparry cement	0.03	0.02	57.19	0.09	0.00
2045	15,173 ft (4,625 m)	Sparry cement	0.33	0.07	57.28	1.12	0.65
			0.21	0.15	57.98	0.86	0.46
			0.21	0.08	57.48	1.12	0.32
		Grain replacement	0.38	0.09	57.02	1.39	0.59
			0.15	0.07	55.61	0.76	0.36
			0.25	0.06	58.55	0.90	0.46
			0.12	0.06	57.72	1.53	0.29
2069	14,285 ft (4,476 m)	Poikilotopic cement	0.59	0.11	55.26	1.25	2.12
			0.54	0.17	53.64	1.28	2.35
			0.60	0.17	54.30	1.39	2.04
			0.57	0.17	52.89	1.32	2.23
			0.44	0.16	54.38	1.18	1.67
			0.51	0.11	54.15	1.39	1.86
			0.53	0.12	54.73	1.33	2.00
			0.51	0.14	53.80	1.23	1.98
			0.45	0.13	54.89	1.23	1.70
			0.51	0.14	54.06	1.28	2.04

Table D-1 continued.

Sample #	Depth	Description	%MgO	%SrO	%CaO	%MnO	%FeO
2069	14,685 ft (4,476 m)	Poikilotopic cement	0.55	0.14	54.59	1.09	2.13
			0.46	0.16	56.62	1.28	1.88
			0.52	0.17	56.73	1.26	1.86
			0.55	0.10	53.94	1.24	1 98
			0.48	0.12	54.66	1.26	1.80
			0.46	0.13	54.14	1.09	1.97
			0.43	0.12	53.07	1.07	1.86
		Grain replacement	0.14	0.16	56.34	1.60	0.71
			0.28	0.13	57.76	1.38	1.02
			0.30	0.12	55.92	1.52	1.00

Appendix D.
Table D-2. McAllen Ranch Field Samples.
Carbonate Compositions

Sample #	Depth	Description	%MgO	%SrO	%CaO	%MnO	%FeO
2136	11,791 ft (3,594 m)	Sparry cement	0.22	0.32	50.59	0.46	0.41
			0.18	0.30	56.19	0.41	0.34
			0.20	0.28	54.47	0.41	0.30
			0.19	0.31	54.80	0.43	0.39
			0.15	0.28	55.32	0.38	0.36
			0.19	0.32	53.95	0.48	0.42
			0.19	0.30	55.18	0.46	0.36
			0.14	0.27	55.78	0.36	0.30
			0.20	0.33	55.46	0.43	0.35
2235	12,500 ft (3,810 m)	Sparry cement	0.14	0.01	55.24	0.04	0.01
			0.00	0.03	56.45	0.05	0.00
		Grain replacement	0.14	0.04	54.12	0.05	0.03
2258	12,656 ft (3,858 m)	Sparry cement	0.05	0.07	55.73	0.30	0.15
		Grain replacement	0.69	0.04	53.92	1.32	0.02

Appendix D.
Table D-3. Pleasant Bayou Samples.
Feldspar Compositions

Sample #	Depth	Na_2O	MgO	Al_2O_3	SiO_2	K_2O	CaO	TiO_2	FeO	Type*
1962	4,345 ft	0.96	0.02	18.66	65.78	15.29	0.07	0.00	0.00	K_1
	(1,324 m)	0.91	0.02	18.49	66.03	15.07	0.03	0.04	0.00	K_2
		0.93	0.02	18.58	65.90	15.18	0.05	0.00	0.00	K_a
1999	11,773 ft	11.93	0.00	20.11	68.60	0.05	0.04	0.00	0.00	P
	(3,589 m)	0.60	0.02	18.99	63.82	15.57	0.06	0.00	0.01	K
		11.71	0.00	20.08	69.18	0.04	0.06	0.00	0.00	P
		11.84	0.02	19.63	67.61	0.06	0.06	0.03	0.00	P
2040	15,162 ft	0.33	0.00	18.89	65.63	16.39	0.00	0.00	0.00	K
	(4,621 m)	0.52	0.00	18.65	64.18	15.70	0.00	0.04	0.00	K_c
		11.37	0.02	19.82	68.71	0.01	0.27	0.07	0.00	P_r
		11.64	0.02	19.73	68.42	0.03	0.18	0.09	0.00	P_r
2045	15,173 ft	11.48	0.02	20.23	68.19	0.07	0.03	0.03	0.00	P
	(4,625 m)	11.85	0.02	19.79	69.43	0.04	0.04	0.00	0.00	P
		11.97	0.02	20.13	69.33	0.04	0.03	0.00	0.00	P
		11.82	0.02	20.00	69.05	0.12	0.02	0.00	0.00	P_c
		11.80	0.02	19.79	67.47	0.10	0.00	0.00	0.00	P_r
		11.49	0.02	19.37	68.54	0.09	0.02	0.00	0.00	P_c
		11.94	0.05	20.41	68.13	0.04	0.01	0.04	0.00	P_r
		12.13	0.03	19.86	70.12	0.02	0.02	0.06	0.00	P_r
2071	14,689 ft	10.21	0.02	21.86	66.11	0.04	2.68	0.07	0.05	P
	(4,477 m)	10.62	0.02	21.73	67.14	0.06	2.04	0.04	0.07	P_c
		11.63	0.00	20.06	72.79	0.02	0.04	0.07	0.02	P_r
		11.62	0.02	20.12	71.84	0.02	0.02	0.04	0.05	P
		11.45	0.02	20.40	71.21	0.00	0.01	0.07	0.02	P
2074	14,695 ft	11.77	0.00	19.22	69.09	0.03	0.02	0.04	0.00	P
	(4,479 m)	11.85	0.00	19.46	69.17	0.04	0.02	0.05	0.00	P_c
		11.78	0.00	19.29	69.06	0.05	0.03	0.00	0.00	P_r
		11.79	0.02	19.21	68.34	0.06	0.02	0.01	0.00	P_c
		11.70	0.00	19.49	68.20	0.03	0.03	0.00	0.00	P_r
		11.71	0.00	19.47	67.29	0.04	0.02	0.04	0.00	P_c
		11.74	0.00	19.25	68.31	0.02	0.02	0.00	0.00	P_r
		11.66	0.00	19.66	67.85	0.04	0.07	0.03	0.01	P_c
		12.01	0.00	19.66	68.43	0.00	0.00	0.05	0.00	P_r
		11.71	0.00	19.70	67.87	0.03	0.02	0.06	0.00	P_r

*$K_{1,2}$ = repeated analyses of potassium feldspar grain

K_a = average of replicate analyses

P or K = single analysis of plagioclase or potassium feldspar grain, respectively

P_c or K_c = analysis of plagioclase or potassium feldspar core

P_r or K_r = analysis of plagioclase or potassium feldspar rim

Appendix D.
Table D-4. McAllen Ranch Field Samples.
Feldspar Compositions

Sample #	Depth	Na_2O	MgO	Al_2O_3	SiO_2	K_2O	CaO	TiO_2	FeO	Type*
2110	10,829 ft (3,301 m)	11.74	0.02	19.60	68.09	0.04	0.17	0.00	0.02	P
2136	11,791 ft	11.72	0.00	19.61	68.83	0.06	0.22	0.00	0.00	P
	(3,594 m)	11.62	0.02	19.72	70.00	0.07	0.11	0.04	0.00	P
		12.02	0.02	20.31	70.13	0.02	0.12	0.01	0.01	P
		11.82	0.02	20.25	69.90	0.04	0.17	0.00	0.00	P
		12.05	0.02	20.15	68.78	0.02	0.18	0.03	0.00	P
		12.07	0.02	20.01	70.13	0.05	0.14	0.00	0.00	P
		11.47	0.00	19.91	68.74	0.03	0.27	0.00	0.00	P
		1.00	0.02	18.80	66.38	15.28	0.04	0.05	0.09	K
2235	12,500 ft	11.80	0.02	20.07	69.00	0.04	0.18	0.01	0.01	o.g.**
	(3,810 m)	11.84	0.02	19.59	69.06	0.04	0.25	0.01	0.00	o.g.
2236	12,519 ft	11.61	0.02	19.86	69.57	0.04	0.04	0.00	0.00	o.g.
	(3,816 m)	11.80	0.00	19.58	69.27	0.06	0.11	0.00	0.00	P
		11.52	0.00	19.75	69.37	0.04	0.16	0.00	0.00	P
		11.43	0.00	19.96	68.92	0.13	0.18	0.04	0.00	P^c
		11.65	0.00	19.58	68.88	0.00	0.14	0.00	0.00	P^r
		11.34	0.02	19.63	68.48	0.06	0.14	0.14	0.00	

*See footnotes under Pleasant Bayou Feldspar Compositions.

**o.g. = plagioclase overgrowth.

*U.S. GOVERNMENT PRINTING OFFICE: 1980-740-145/1065